DEVELOPING NATURAL KILLER T CELL BASED TOOLS AND STRATEGIES FOR TARGETING BREAST CANCER

by

Simon Gebremeskel

Submitted in partial fulfilment of the requirements
for the degree of Doctor of Philosophy

at

Dalhousie University
Halifax, Nova Scotia
February 2018

TABLE OF CONTENT

LIST OF TABLES

LIST OF FIGURES

ABSTRACT

Natural killer T cells are a rare population of immune-regulatory lymphocytes which have been implicated in tumor control. However, the benefit of NKT cell activation therapy in metastatic breast cancer remains poorly understood. The major focus of this work was to examine the potential role of NKT cell activation in a murine model of post-surgical breast cancer metastasis. Following surgical resection of orthotopic 4T1 mammary carcinoma tumors, BALB/c mice were treated with α-GalCer-loaded dendritic cells. This therapeutic approach decreased tumor burden, prolonged survival, and decreased the frequency and activity of myeloid derived suppressor cells. However, survival was not enhanced by additional dendritic cell treatments. This led us to investigate whether we could augment therapeutic outcomes by combining NKT cell activation with chemotherapy or oncolytic virus therapy, both capable of inducing immunogenic cell death. Combining cyclophosphamide or gemcitabine with NKT cell activation therapy significantly enhanced survival, with surviving mice exhibiting attenuated tumor growth following a second tumor challenge. Similarly, combining NKT cell activation therapy with oncolytic vesicular stomatitis virus also significantly enhanced therapeutic outcomes. Collectively, our findings demonstrate that NKT cell activation therapy as a monotherapy, or in combination with chemo- or viro-therapy, can protect mice from post-surgical breast cancer metastasis.

LIST OF ABREVIATIONS USED

α-GalCer	α-galactosylceramide
ANOVA	analysis of variance
APC	allophycocyanin
ATP	adenosine triphosphate
BMDC	bone marrow-derived dendritic cell
CALR	calreticulin
CPX	cyclophosphamide
CTL	cytotoxic T lymphocyte
CTLA-4	cytotoxic T-lymphocyte-associated protein 4
CXCR	CXC chemokine receptor
DC	dendritic cell
DNA	deoxyribonucleic acid
EDTA	ethylenediamine-tetraacetic acid
ELISA	enzyme-linked immunosorbent assay
FasL	Fas ligand
FBS	fetal bovine serum
FITC	fluorescein isothiocyanate
FoxP3	forkhead box P3
GATA-3	GATA binding protein 3
GEM	gemcitabine
GFP	green fluorescent protein
GM-CSF	granulocyte macrophage colony-stimulating factor
HMGB1	high-mobility group box 1
HEPES	4-(2-hydroxyethyl)-1-piperazineethanesulfonic acid
Her-2	human epidermal growth factor receptor 2
ICD	immunogenic cell death
IDO	indoleamine 2,3-dioxygenase
IFN	interferon
IL	interleukin
i.p.	intraperitoneal

i.v.	intravenous
MAF	mafosfamide
MHC	major histocompatibility complex
MyD88	myeloid differentiation primary response gene 88
MDSC	myeloid derived suppressor cell
NLRP3	NOD-like receptor family, pyrin domain-containing protein 3
NK	natural killer
NKG2D	natural killer group 2, member D
NKT	natural killer T
PBS	phosphate buffered saline
PD	programmed cell death protein
PDL-1	programmed death ligand 1
PE	phycoerythrin
PerCP	peridinin chlorophyll protein
PMA	phorbol 12-myristate 13-acetate
RNA	ribonucleic acid
RORγτ	retinoic acid-related orphan receptor γτ
RPMI	Roswell Park Memorial Institute
T-bet	T box expressed in T cells
TCR	T cell receptor
Th1/2/17	T helper type 1/2/17
TGF-β	transforming growth factor β
TLR	Toll-like receptor
TMB	tetramethylbenzidine
TNF	tumor necrosis factor
TRAIL	TNF-related apoptosis-inducing ligand
T-reg	T regulatory cell
VEGF	vascular endothelial growth factor
VSV	vesicular stomatitis virus

ACKNOWLEDGEMENTS

I would like to first and foremost acknowledge my supervisor Dr. Brent Johnston for the opportunity to explore my interests in research and for his expertise, encouragement, patience and input on these research projects. I would also like to extend my gratitude to my committee members Dr. Andy Stadnyk, Dr. Karen Bedard, Dr. Tong-Jun Lin and Dr. David Hoskin for their discussions and guidance through these research projects. I would also like to thank Derek Rowter for his assistance with cell sorting and the Carleton Animal Care Facility for their assistance with animal care studies.

I would also like to thank Dale Corkery, Lynnea Lobert, Kaitlyn Tanner, Daniel Clattenburg, Brynn Walker, Tora Oliphant, Livia Clarke, Terry LeVatte, Drew Slauenwhite, Linnea Veinotte, and Adam Nelson for their assistance with these projects, help with animal colony management, and many good discussions that have made my time in the lab enjoyable and memorable. Thanks to the other past and present member of the Johnston lab for their support, it has truly been a pleasure to work with them. I would also like to thank members of the Bezuhly lab, Hoskin lab, Marshall lab, Lee lab and McCormick lab for many productive collaborations, and sharing their reagents and expertise.

Finally, to my mother, Alganesh, and sisters, Helen and Selam, thank you for your invaluable support throughout my personal and academic journey. Your encouragement and unwavering support has been the foundation from which I have flourished. To all my family and friends who have supported me throughout the years, thank you.

Chapter 1: Introduction

1. Cancer

Cancer remains a leading cause of death in Canada, accounting for 30% of all reported deaths in 2012 [1]. In most developed countries, four key cancers account for greater than 50% of cancer incidence and cancer-related deaths: lung, breast, colorectal and prostate cancer [1]. It is predicted that half of all Canadians will develop cancer in their lifetime and 25% of them will die from the disease [1]. Furthermore, many of the patients who survive a cancer diagnosis will live with many physical, emotional and financial challenges that persist long after the disease is treated [1]. Despite recent progress in our understanding of cancer, development of better diagnostics, and advances in therapeutic approaches, cancer still remains a huge burden on our society.

Tumors can be either benign and self-limiting, or they can be malignant; dividing, invading neighbouring tissues and metastasizing to different parts of the body where they form new tumors [2]. There are more than 200 different types of cancers which can arise in any given organ or tissue in both somatic and germ line cell types [2]. Cancer can broadly be classified into 6 major subtypes based on the histological site of origin, these include: carcinoma, myeloma, sarcoma, leukemia, lymphoma, and mixed tumors arising from multiple tissue types (Table 1) [3]. Carcinoma cells are of epithelial origin and make up 80-90% of all cancer cases. Carcinoma cells can be further divided into adenocarcinoma, which develops in organs or glands capable of secretion, or squamous cell carcinomas which occur in many areas of the body. Myeloma originate from plasma cells of the bone marrow which secrete antibodies. Sarcomas originate from supportive and connective tissues such as fat, bone, tendons, cartilage and muscle. Leukemias are cancers which

affect bone marrow stem cells and they can be myelogenous, lymphocytic or erythremic [3]. Lymphoma is a solid tumor which forms in the glands and nodes of the lymphatic system [4].

Table 1. Cancer Classification

Cancer Subtype	Characteristic
Carcinoma	Epithelial origin, most common (80-90%) type of cancer
Sarcoma	Originates in supportive and connective tissue
Myeloma	Originates in the plasma cells of the bone marrow
Leukemia	Cancers of the bone marrow stem cells
Lymphoma	Originate in the glands and nodes of the lymphatic system

Cancer has traditionally been viewed as a group of diseases that are driven by the accumulation of genetic mutations, which ultimately lead to the progression of normal cells towards a neoplastic state [2,5]. This paradigm has now been expanded to incorporate alterations in the epigenetic regulatory mechanisms which appear to be prevalent in cancer [6,7]. Both genetic mutations and epigenetic alterations that give rise to cancer can arise through hereditary and environmental factors [8]. Genetic and epigenetic alterations can promote cancer progression by: 1) sustaining proliferative signaling, 2) evading growth suppressors, 3) avoiding immune destruction, 4) enabling replicative immortality, 5) promoting tumor associated inflammation, 6) inducing invasion and metastasis, 7) promoting angiogenesis, 8) inducing genome instability, 9) enhancing resistance to cell death, and 10) altering cellular metabolism [5]. Collectively, these 10 features represent the

hallmarks of cancer [5], and present promising therapeutic targets in the fight against cancer.

1.1. Breast cancer

Breast cancer remains the second leading cause of cancer-related deaths and the most prevalent type of cancer amongst Canadian women [1]. While the incidence of breast cancer has remained stable between 2004-2013, the 5-year survival rate has significantly improved over this time [1]. While these results are encouraging, the therapeutic approaches used to treat breast cancer are still associated with harmful side-effects, highlighting the need for improvements.

Breast cancer can be broadly be classified into seven major molecular subtypes; Luminal A, Luminal B, human epidermal growth factor receptor (HER)-2 positive, basal-like, claudin-low, molecular apocrine and normal-breast like [9–11]. Luminal A breast cancers have the best prognosis due to a slow growth profile and high expression of the estrogen receptor [10]. Luminal B tumors show a lower expression of estrogen receptor, are more often high grade with higher Ki67 proliferation index, and often have a poorer outcome compared to luminal A [12]. Luminal A and B subtypes typically express progesterone and estrogen receptor, while HER-2 enriched breast cancer express high levels of the HER-2 receptor. These receptors provide druggable targets using receptor antagonists such as tamoxifen, which targets the estrogen receptor positive tumors [13]. Triple negative breast cancers (lacking HER-2, estrogen and progesterone receptors), are not amenable to hormone or Her-2 therapies and often have the worst prognosis [9–11]. Basal-like and claudin low tumors are primarily triple negative breast cancers. Cluadin-low tumors lack cell-cell junction proteins and have down-regulated epithelial markers such as

E-Cadherin. Molecular apocrine tumors are estrogen receptor negative, but express androgen receptor [9–11]. Normal-like breast cancers tend to be hormone-receptor positive, HER-2 negative, and have low levels of Ki-67 [9–11] (See Table 2) (adapted from [11]).

Table 2. Breast cancer classifications (Adapted from [11])

	IHC markers	**Proliferation cluster**	**Other markers**	**Outcome**
Luminal A	ER+: 91–100% PR+: 70–74% HER2+: 8–11% Ki67: low	Low	*FOXA1* high	Good
Luminal B	ER+: 91–100% PR+: 41–53% HER2+: 15–24% Ki67: high	High	*FGFR1* and *ZIC3* amp	Intermediate or poor
HER2-enriched	ER+: 29–59% PR+: 25–30% HER2+: 66–71% Ki67: high	High	GRB7: high	Poor
Basal-like	ER+: 0–19% PR+: 6–13% HER2+: 9–13% Ki67: high	High	*RB1*:low/- *CDKN2A*: high *BRCA1*: low/- *FGFR2*: amp	Poor
Normal breast-like	ER+: 44–100% PR+: 22–63% HER2+: 0–13% Ki67: low/intermediate	Low / intermediate	--	Intermediate
Claudin-low	ER+: 12–33% PR+: 22–23% HER2+: 6–22% Ki67: intermediate	Intermediate / high	*CDH1*: low/- Claudins: low/-	Intermediate
Molecular apocrine	ER– PR– HER2 +/– Ki67: high	High	Androgen receptor: +	Poor

ER=estrogen receptor. PR=progesterone receptor. FOXA1= Forkhead Box A1. FGFR= Fibroblast growth factor receptor. ZIC3= Zinc finger of the cerebellum 3. GRB7= Growth factor receptor-bound 7. RB1= Retinoblastoma 1. CDKN2A= cyclin-dependent kinase Inhibitor 2A. BRCA1= Breast cancer 1. CDH1= Cadherin 1. + =positive. – =negative.

In addition to molecular subtyping, breast cancer can also be broadly classified into four distinct stages (I-IV), depending on how far the disease has progressed. Stage I includes ductal and lobular carcinoma in situ; ductal carcinoma in situ is restricted to the

milk ducts, whereas lobular carcinoma in situ is restricted to the lobules that produce milk. Stage II includes local spreading and may involve the local lymph nodes, stage III involves spreading of the tumor beyond the immediate region and may have invaded nearby lymph nodes and muscles, stage IV has spread beyond the breast and has invaded other organs [14]. Breast cancer most commonly metastasizes to the lungs, bone, liver and central nervous system [15–17].

The current standard of care for breast cancer involves surgical resection, radiation, chemotherapy, hormonal and targeted therapy, with most patients receiving a combination therapy approach [18]. Surgical resection remains the most effective treatment option for stage I-III breast cancer patients, and recently its use has been expanded to prophylactic treatment of high risk patients [19]. The response to hormonal therapy in breast cancer is associated with the presence and levels of estrogen and progesterone receptor [20–23]. In breast cancers expressing estrogen and progesterone receptors, hormone therapy should be considered. However, patients who do not express these receptors are unlikely to accrue any benefits from the therapy [23].

HER-2 is an oncogene that encodes for the epidermal growth factor ErbB2 and is overexpressed in 25-30% of breast cancers [24,25]. Trastuzumab, a monoclonal antibody targeting the extracellular domain of HER-2, limits tumor growth through antibody-dependent cell-mediated cytotoxicity, inhibition of intracellular signaling, and decreased angiogenesis [26,27]. The combination of trastuzumab and chemotherapy reduced the risk of relapse by 50%, and reduced the risk of death by 30% [26,28]. However, the clinical use of trastuzumab faces several challenges; high cost, cardiotoxicity, and development of drug-resistance [28–31].

Anthracyclines and taxanes remain the most widely used treatments in metastatic breast cancer. Anthracyclines intercalate between DNA/RNA base pairs to prevent synthesis, and inhibit topoisomerase II activity to block transcription and replication of supercoiled DNA [32]. In contrast, taxanes stabilize microtubules to prevent mitosis [32]. Combinations of anthracyclines and taxanes are associated with 40-94% response rate in first line therapy, with 12-41% of the patients achieving complete remission [33,34]. However, the toxicities associated with these therapeutic approaches remain high and patients who relapse often undergo a second line of chemotherapy, highlighting the need for safe and effective therapies. One promising approach is immune modulation therapy.

1.2. Cancer and the immune system

In 1909, Paul Ehrlich hypothesized that the host defense system prevented neoplastic cells from developing into tumors [35,36]. He stated "In the enormously complicated course of fetal and post-fetal development, aberrant cells become unusually common. Fortunately, in the majority of people, they remain latent thanks to the organism's positive mechanism" [35,36]. However, this hypothesis was not experimentally tested at the time. Lewis Thomas and MacFarlane Burnet were the first to use the term "immunological surveillance mechanisms" in the context of tumor control [35]. They suggested that the lymphocytes recognized newly arising tumor specific neo-antigens and eliminated them. The original hypothesis of cancer immunosurveillance only took into account the anti-tumor role of the immune system. This theory has now been expanded to describe a much more dynamic interaction between the immune system and cancer, which takes into consideration both pro- and anti-tumor roles of the immune system [37,38].

Cancer immunoediting can be broken down into three phases: elimination, equilibrium and escape [38]. The elimination phase involves recognition and clearance of transformed cells by the innate and adaptive immune branches. This is thought to occur long before tumours become clinically apparent [37,38]. The elimination phase is interchangeably synonymous with what Thomas and MacFarlane termed as cancer immunosurveillance. If the immune system fails to eliminate the entire tumor, the surviving cells enter the equilibrium phase, where the tumor cells exist in equilibrium with immune system [37,38]. Due to changes in the tumor cell populations as a result of mutations or epigenetic alterations, or changes in the host immune system, the functional dormancy of the tumor may be altered, leading to progression into the escape phase [37,38]. The immune escape phase is now recognized as a hallmark of cancer, and a key target for cancer therapy [5].

1.2.1 Elimination

The innate and adaptive immune systems have both been implicated in cancer immunosurveillance. The innate immune system plays a vital "first line of defense" against cancer, acting in an immediate but non-specific manner. Innate immune cells express germline-encoded receptors, which bind tumor-associated ligands or damage associated molecular patterns. Early recognition of transformed cells and subsequent killing allow for the uptake and presentation of antigens, which can be used to prime the adaptive immune system. Some of the key players in immunosurveillance include natural killer (NK) cells, natural killer T (NKT) cells, $CD4^+$ T cells, $CD8^+$ T cells and dendritic cells. The role of NKT cells in cancer immunity will be discussed in detail on page 16.

1.2.1.1 NK cells

Transformed cells may express cell surface markers that function as recognition targets for direct interaction with innate immune cells. NK cells employ several receptors to recognize and respond to danger signals, including NKG2D (natural killer group 2, member D), NKR-P1A, NKP30, NKP44, NKP46 and NKG2C/CD94 heterodimers [39]. In addition, inhibitory receptors Ly49 (mouse) or killer Ig-related (KIR) (human) that recognize MHC-I on normal cells can detect stressed or transformed cells that downregulate MHC-I, enabling the activation of NK cells via missing-self recognition [37,40]. Furthermore, most NK cells express low-affinity activating receptor FcγRIIIa (CD16) that binds the Fc portion of IgG1 and mediates antibody dependent cellular cytotoxicity [37,40]. Following activation, NK cells can kill tumour cells directly through tumor necrosis factor-alpha-related apoptosis-inducing ligand (TRAIL), FasL, tumor necrosis factor (TNF), perforin and granzymes [41,42]. Mice deficient in these mediators of innate immunity show increased susceptibility to methylcholanthrene (MCA)-induced fibrosarcomas [42].

Transformed cells can express stress ligands which bind to NKG2D on NK cells and a subset of T cells [42–46]. The ligands for NKG2D in humans consist of MHC class I chain-related proteins A and B and UL16 binding proteins, whereas mice express retinoic acid early transcript-1, mouse UL16-binding protein-like transcript 1, and minor histocompatibility complex H-60 in mice [44]. NKG2D ligand expression is low on normal cells, but is upregulated on transformed and infected cells [43,44,46]. This allows for NK cells, $CD8^+$ T cells, γδ T cells and NKT cells to directly lyse the cells [43–46]. Furthermore, IL-12 therapy was shown to mediate protection from MCA-induced sarcomas via an

NKG2D-dependent mechanism [46]. However, some tumor cells can evade NKG2D mediated recognition by releasing soluble NKG2D ligands as a result of metalloprotease cleavage [47], or through exosomes [48].

1.2.1.2. Dendritic cells

Dendritic cells (DCs) are the most potent antigen presenting cells; they can take up, process and present different types of antigens, including tumor antigens [49]. DCs can recognize stress signals on tumor cells and engulf the dying tumor cells, process the antigens and present them to T cells [49]. Immature DCs are recruited to the tumor site and become activated by danger signals and cytokines produced by either the dying tumor cell or tumor infiltrating immune cells [38,46]. Activation and maturation of DCs is required to effectively activate antitumor immunity, and to prevent tolerance [49]. The activated DCs present tumor antigens to $CD4^+$ T cells through MHC-II and provide costimulatory signals and cytokines. Activated $CD4^+$ T cells can directly target MHC-II expressing tumors [50], or indirectly through production of cytokines that activate and support anti-tumor immunity [51,52]. In addition, DCs can also cross present exogenous antigens to $CD8^+$ T cells through MHC-I [53]. Tumor specific $CD4^+$ and $CD8^+$ T cells migrate to the tumor site, where they can target tumors in an antigen-specific manner and produce cytokines that activate other immune cells [38,46].

1.2.1.3. $CD4^+$ T cells

$CD4^+$ T cells are key regulators of the immune system and differentiate into various T helper (Th) cell lineages with distinct biological functions [54]. $CD4^+$ T helper (Th) cells recognize peptides presented by MHC-II molecules on antigen presenting cells. Following activation, $CD4^+$ T cells can differentiate into different lineages based on

transcription and cytokine profiles. $CD4^+$ T cells can be polarized into three major subsets: Th1 cells which produce IFN-γ, Th2 cells which produce IL-4, IL-5 and IL-13, and Th17 cells which primarily produce IL17A/F. The regulatory $FoxP3^+$ $CD4^+$ T cells (T-regs) will be discussed in the immune evasion section.

$CD4^+$ T cells can play a multifaceted role in cancer immunity. $CD4^+$ T cells have been shown to play an important role in protecting against virus-induced sarcomas, eradication of leukemias, and rejection of transplantable tumors [55]. Adoptive transfer of tumor-reactive $CD4^+$ T cells or depletion of $CD4^+$ T cells demonstrated that these cells play an important role in antitumor immunity against tumors [56]. Activated $CD4^+$ T cells were shown to attract macrophages, granulocytes, eosinophils and NK cells to the tumor site [57,58]. Protection is thought to be primarily mediated by Th1 cells secreting IFN-γ [56]. Indeed, IFN-γ has been shown to exert anti-angiogenic effects, improves tumor recognition by upregulating MHC expression, and mediating direct tumor cytotoxicity in the presence of TNF [56]. Adoptive transfer of antigen specific Th1 cells led to anti-tumor cytotoxicity and upregulation of MHC-II on the surface of tumor cells [55,59]. This protection was independent of B cells, NK cells or other T cell subsets. While $CD4^+$ T cells can lyse tumors in an MHC II-restricted manner using perforin or granzyme B, most tumors do not express MHC-II [55,56]. In addition, activated CD4 T cells can also eliminate transformed cells via FAS/FAS-ligand interactions [60].

Th2 effector cell subsets are characterized by the production of IL-4, IL-5, and IL-13 and play an important role in humoral immunity and allergic inflammatory responses. The role of Th2 cells in antitumor immunity remains contradictory. Th2 cells produce IL-4, which can have direct cytotoxic effects and anti-angiogenic properties [61].

IL-4 can also exert antitumor effects through enhancement of infiltrating eosinophils and macrophages, rather than direct Th2 cell activity [62,63]. Similarly, tumor antigen-specific Th2 cells were shown to induce an eosinophil-dependent clearance of metastatic melanoma cells that showed resistance to cytotoxic T lymphocytes [64]. The ability of Th2 cells to mobilize innate immune cells may be the underlying mechanism of this antitumor immune response. In contrast, Th2 type immune responses have also been shown to negatively impact anti-tumor immunity. The induction of antigen-specific Th2 cells was also shown to promote neoplastic transformation and tumor growth in an lipopolysaccharide-accelerated murine model of pancreatic cancer [65]. These contradicting reports on the role of Th2 cells in cancer immunity highlight the need for more studies in this area.

The role of Th17 cells in cancer is also contradictory. Some reports have shown that Th17 cells are capable of inducing tumor rejection, while others reveal that they promote tumor progression [55]. The key signature cytokine of Th17 cells, IL-17A, can promote angiogenesis and tumor growth by upregulating tumor-derived angiogenic factors and proinflammatory cytokines [55]. In contrast, acute exposure to high levels of IL-17A following adoptive transfer of Th17 cells resulted in enhanced tumor immunity [55]. Furthermore, adoptive transfer of Th17 cells enhanced the frequency of tumor-infiltrating DCs and tumor-specific $CD8^+$ T cells, resulting in improved antitumor immunity [66]. These contradicting roles of Th17 cells may be a result of differences in IL-17 dose or duration of exposure: Low level of chronic exposure to IL-17 may facilitate cancer progression, whereas high level of acute exposure may promote tumor immunity.

1.2.1.4. $CD8^+$ T cells

$CD8^+$ T cells are a critical component of the adaptive immune system that play an important role in the control of intracellular pathogens and transformed cells [67]. Generation of effector $CD8^+$ T cells is initiated by DCs that take up antigen within the periphery and cross-present these antigens to naïve $CD8^+$ T cells in the regional lymph nodes [67]. In addition to presentation of antigens on MHC-I, DCs provide key costimulatory signals and cytokines to achieve optimum priming of cytotoxic $CD8^+$ T cells [67]. Cytotoxic $CD8^+$ T cells can recognize specific antigens, undergo clonal expansion, and kill transformed cells. In addition to antigen recognition, activated $CD8^+$ T cells express high levels of NKG2D, which enables them to recognize stressed cells that express NKG2D ligands [67,68]. Both antigen recognition and NKG2D mediated activation of $CD8^+$ T cells can result in lytic (perforin, granzymes, FasL, TRAIL) and nonlytic effector (IFN-γ) mechanisms that are critical in anti-tumor immunity [67,68].

1.2.1.5. Non-cellular mediators of cancer surveillance

Type II interferon (IFN-γ) has been implicated in innate immunosurveillance [46]. Mice deficient in IFN-γ or the IFN-γ receptor were more susceptible to MCA-induced sarcomas and spontaneous tumors compared to wild-type mice [46,51]. Similarly, mice deficient in p53 and either IFN-γ, IFN-γ receptor or signal transducer and activator of transcription (STAT)-1, showed increased incidences and severity of spontaneous tumor formation [51,52]. IFN-γ can also enhance anti-tumor immunity by promoting the generation of T-helper (Th) 1 immunity and cytotoxic $CD8^+$ T cells. Multiple other mechanisms have been implicated in IFN-γ-dependent effects on tumors, including antiproliferative, proapoptotic, and angiostatic properties [46].

Type I IFNs (IFNα/β) are well known for their role in antiviral immunity; however, accumulating evidence implicates type I IFNs in cancer immunosurveillance [69]. The absence of the type I IFN receptor (*Ifnαr1* and *Ifnαr2*) on mouse embryonic fibroblasts predisposed the fibroblasts to cellular transformation [69]. Moreover, MCA-induced *Ifnαr1*$^{-/-}$ fibrosarcoma cells failed to grow in wildtype mice because they were rejected by the IFN competent host [69]. IFNα/β can stimulate NK cell cytotoxicity and cytokine production and promote CD8 T cell and B cell adaptive immune responses via upregulation of antigen presentation [46]. These findings suggest that type I IFNs can act both directly on the cancer cells or on the host immune cells to promote cancer immunosurveillance.

1.2.2. Immune escape

Some tumor cell variants can acquire genetic/epigenetic changes that confer resistance to immune detection and elimination. Tumor escape can be mechanistically broken down into tumor intrinsic mechanisms associated with tumor cells and tumor antigens, or tumor extrinsic mechanisms associated with the host immune system [46]. Some tumor intrinsic mechanisms include: lack of expression of MHC-II and costimulatory molecules, down regulation or loss of MHC-I and genes associated with antigen presentation, low expression of TAA, loss of antigenic epitopes, physical barriers preventing immune infiltration, and loss of response to IFNs [38,46]. In addition, downregulation of glycolipid antigen presentation via MHC-I like CD1d molecule has also been associated with immune evasion [70,71]. Other host immune-avoidance mechanisms mediated by tumours include: expression of molecules that induce tolerance of T cells to tumor antigens (e.g. Program death ligand (PDL)-1), suppression of immune

cells by tumor-derived factors (e.g. TGF-β, IL-10, galectin, indoleamine 2 3-dioxygenase (IDO)) that induce immunosuppressive myeloid or T-regs, defects in maturation of antigen presenting cells, and secretion of soluble ligands that block lymphocyte activation (e.g. NKG2D ligands) [38,46].

1.2.2.1. Myeloid-Derived Suppressor Cells (MDSCs)

Tumor-derived factors disrupt normal myeloid differentiation, leading to the accumulation of heterogeneous populations of undifferentiated myeloid cells referred to collectively as MDSCs [72]. Several cytokines and mediators of inflammation have been implicated in the induction of MDSCs: granulocyte macrophage colony-stimulating factor (GM-CSF), macrophage colony-stimulating factor, IL-1β, IL-6, IL-13, IFN-γ, vascular endothelial growth factor, fms-like tyrosine kinase 3 ligand, and prostaglandin E2 [73,74]. As the tumor burden increases, MDSCs accumulate in a variety of tissues [75], where they act to enhance tumor progression and metastasis by suppressing immune responses. In mice, MDSCs are generally identified as GR-1^+ $CD11b^+$, with monocytic subpopulations $CD11b^+Ly6C^{high}Ly6G^-$ and/or granulocytic subpopulations $CD11b^+Ly6C^-Ly6G^{high}$ accumulating in different models [76]. The granulocytic population is the most prevalent in the 4T1 breast cancer model, which we primarily use in this body of work. In humans, MDSCs are also identified as monocytic $CD11b^+CD33^+CD14^+$HLA-DR^- cells or granulocytic $CD11b^+CD33^+CD15^+$HLA-DR^- cells [73,74].

MDSC contribute to immune suppression through multiple mechanisms (Figure 1). MDSCs can bias towards Th2 immune responses, leading to increased IL-10 and decreased IL-12 production from macrophages [77]. MDSCs inhibit Th1 type immune responses by releasing of nitric oxide species which inhibit STAT1 phosphorylation, a

key signaling event in IFN-γ responsiveness [78]. MDSCs can also express high levels of arginase-1 and IDO, which deplete arginine and tryptophan, two key raw materials required for effective T cell activation [73,74]. MDSCs also produce metalloproteases which cleave L-selectin on T cells, limiting migration of naïve T cells into draining lymph nodes where they are normally activated [79]. MDSCs have also been implicated in supporting angiogenesis, tumour cell invasion and metastasis [72].

Targeting MDSC-induced immune suppression has become a key focus in the development of cancer therapy. In a screen for conventional chemotherapeutic agents that can target MDSCs, 5-Fluorouracil (FU) was found to selectively kill MDSCs and induce a T cell-dependent anti-tumor immunity [80]. Gemcitabine has also been reported to selectively eliminate MDSCs in tumor-bearing mice, resulting in enhanced antitumor activity [77,81]. In contrast, some chemotherapeutic agents such as cyclophosphamide used at high doses can induce MDSCs, potentially limiting their protective capabilities [82,83]. These differences highlight the need to monitor immunosuppressive populations following chemotherapeutic intervention.

1.2.2.2. FoxP3$^+$ T-regs

$CD4^+$ T-regs are characterized by their expression of the Forkhead box P3 (FoxP3) transcription factor and play an important role in maintenance of homeostasis and self-tolerance [84]. Accumulating evidence shows that tumor-derived factors can promote the recruitment and expansion of T-regs, and T-reg infiltration into tumors is often associated with poor outcomes [85,86]. Experimentally, antibody-mediated depletion of T-regs led to spontaneous eradication of inoculated syngeneic tumors in some models

[87]. These mice also exhibited increased tumor-specific CD8 T cell killing activity, and were protected from tumor re-challenge with the same tumor.

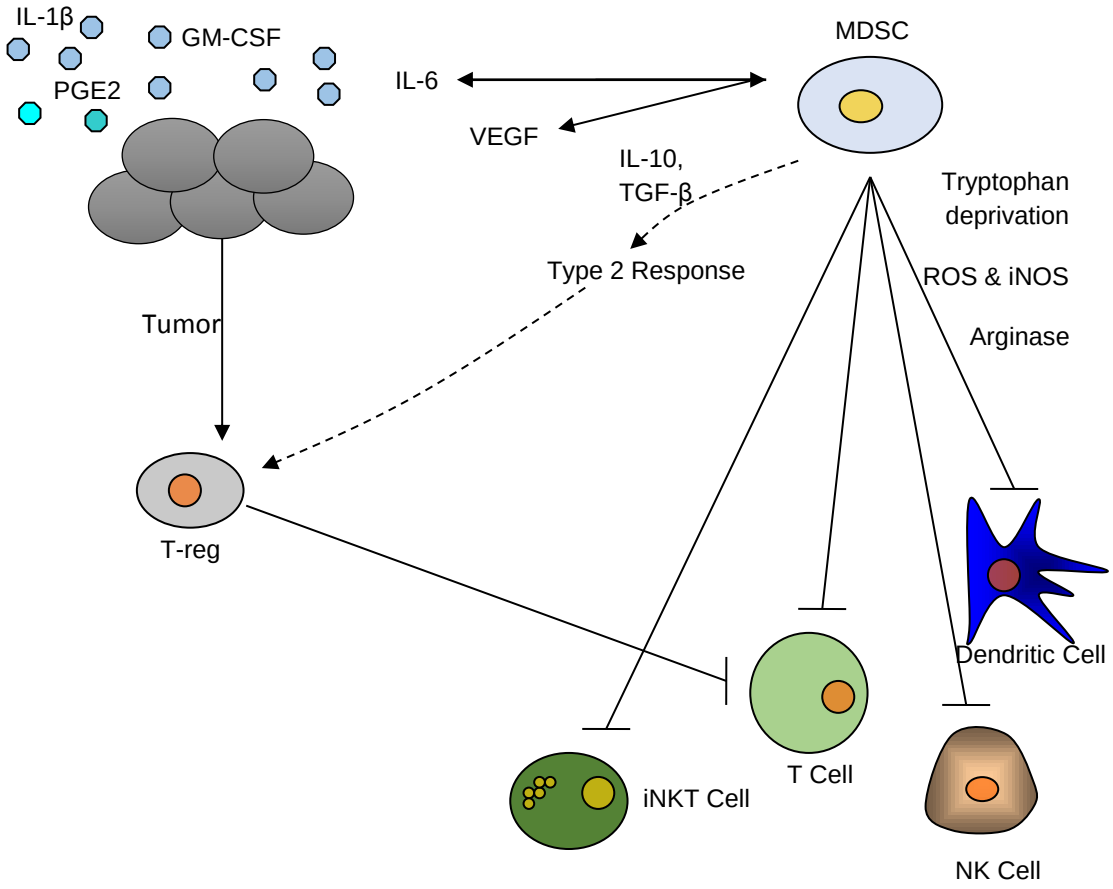

Figure 1. Overview of immune cell activity induced with tumor-associated immune suppression. Tumor-derived factors such as prostaglandin E2 (PGE2), IL-6 and VEGF induce the expansion and accumulation of immunosuppressive cell types such as MDSCs and T-regs. MDSCs promote a pro-tumor environment through suppressing T cell, NK cell, NKT cells and DC function via cysteine deprivation, ROS and RNS production, and arginase activity. MDSCs also induce T-regs and promote a Th2-skewed pro-tumor T cell response. Adapted from [88].

T-regs function to suppress immunity through multiple mechanisms including the production of cytokines like IL-10 and TGF-β, and cell-cell contact-mediated effector T cell inhibition. T-regs secrete IL-10 and TGF-β which promote tolerogenic DCs, by downregulating costimulatory molecules (CD40) and upregulating inhibitory markers

(PDL-1/2) [89,90]. T-regs also express high levels of cytotoxic T lymphocyte-associated antigen-4 (CTLA-4), allowing T-regs to sequester costimulatory CD80/CD86 signals on DCs [89,90]. This results in impaired T cell activation and proliferation. T-regs also constitutively express the high-affinity IL-2 receptor, acting like a sink for IL-2, thus limiting the activation and proliferation of T-cells [89,90]. Accordingly, adding exogenous IL-2 abrogates T-reg suppressive activity *in vitro* [91]. Therapeutically, targeting T-regs in cancer immunotherapy presents a unique opportunity to reinstate anti-tumor immunity and continues to be an active area of research.

2. NKT cells

NKT cells are a population of T cells that express NK cell markers (NK1.1, Ly49, DX5, NKp46) in addition to a lipid-reactive T cell receptor (TCR) [92,93]. There are two major subsets of NKT cells that can be distinguished based on their TCR and lipid reactivity, Type I or invariant NKT cells and Type II NKT cells. Type I NKT cells express an invariant TCRα chain composed of Vα14–Jα18 (Trav11-Traj18) rearrangements paired with Vβ8.2/7/2 in mice, and Vα24–Jα18 (TRAV11-TRAJ18) paired with Vβ11 in humans [94]. Unlike conventional T cells which recognize peptide antigens presented in the context of major histocompatibility complex (MHC), NKT cells recognize lipids presented via CD1d. Type I NKT cells and can be detected through the use of CD1d tetramers loaded with the glycolipid α-galactosylceramide (α-GalCer) (Figure 2) [95,96]. Type II NKT cells are CD1d-restricted cells that have a more diverse repertoire of Vα gene rearrangements (Vα1/3/8), and do not recognize α-GalCer [97,98]. These differences have led to the development of type I NKT cell-deficient Jα18$^{-/-}$ mice and type I/II NKT cell deficient CD1d$^{-/-}$ mice [99,100]. In multiple models using wild-type,

Jα18$^{-/-}$ and CD1d$^{-/-}$ mice, type II NKT cells play a critical role in suppression of anti-tumor immunity, whereas Type I NKT cells exhibit robust anti-tumor activity [99,101,102]. In this body of work, I will refer to Type I NKT cells simply as NKT cells.

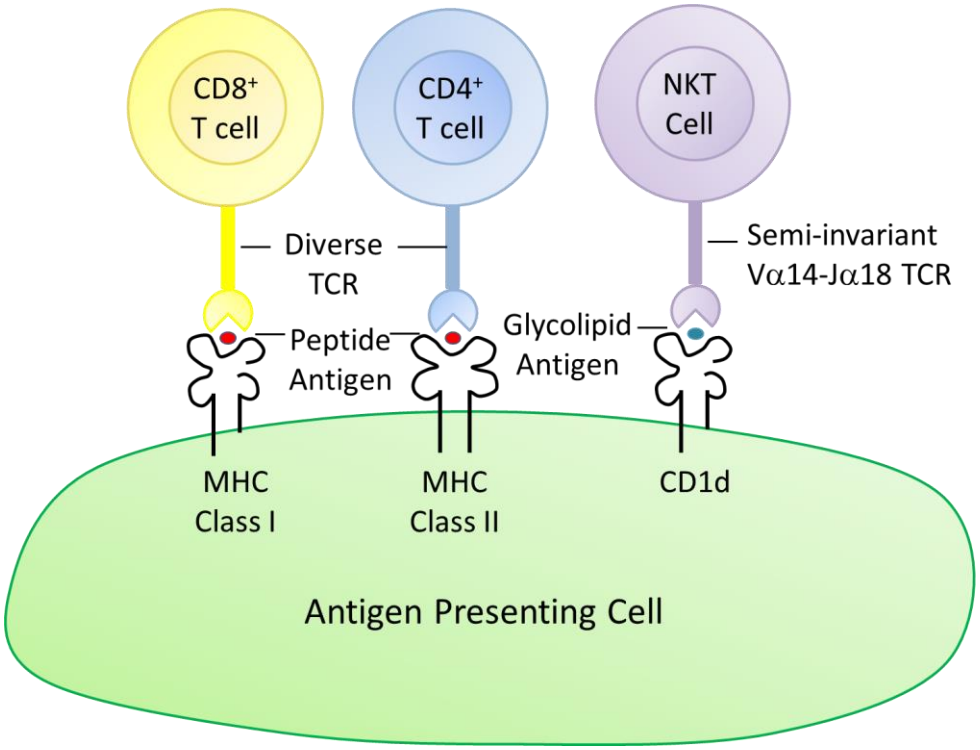

Figure 2. Natural Killer T cells. CD8$^+$ T cells express a diverse T cell receptor (TCR) which recognizes peptide antigens presented by Class I MHC. CD4$^+$ T cells express a diverse TCR which can recognize peptide antigens presented Class II MHC. In contrast, NKT cells recognize glycolipid antigens presented by CD1d on the surface of antigen presenting cells (APCs). In contrast to conventional T cells, NKT cells express an invariant TCR formed by a Vα14-Jα18 rearrangement in mice. Figure was generated by Natasa Zatezalo.

Mature NKT cells from mice and humans can be further broken down into functionally distinct subsets based on the expression of CD4 or CD8 markers; CD4$^+$CD8$^-$ and CD4$^-$CD8$^-$ NKT cells are found in both mice and humans [103,104], whereas CD4$^-$CD8$^+$ NKT cells are only found in humans [105,106]. These subsets of NKT cells have been shown

to express different cytokine profiles [103,104,107], and more recently NKT cells have been classified based on transcription factor profiles into NKT-1, NKT-2, NKT-10, and NKT-17 subsets, analogous to Th1, Th2, Th10, Th17 subsets in conventional T cells [92,108–112].

2.1. NKT cell distribution

Humans and mice have a similar distribution of NKT cells, although mice have ~10 fold higher frequency of NKT cells [92]. Mice have the highest frequency of NKT cells in the liver (12-30%), whereas lower NKT cell frequencies are detected in the spleen (1-3%), lungs (5-10%), bone marrow (0.4-8%), thymus (0.5-1%), intestines (0.05-0.6%), lymph nodes (0.2-1%), and blood (0.2%) [95,96,113–120]. Human NKT cell numbers vary greatly between individuals. The frequency of NKT cells in the liver range from 0.05%-1% [121,122] and blood (0.01- 3%) [104,123–125].

The variation in the frequency of NKT cells between mice and humans has raised concerns about clinical translation of murine based findings. The differences in frequency between human and mouse may be due to differences in affinity of CD1d-lipid complex or due to differences in CD1d trafficking. The human CD1d-lipid complex has a lower affinity for the NKT cell TCR, compared to the murine CD1d-lipid complex [126]. This lower affinity may lead to a lower frequency of NKT cells. The murine CD1d also has a much stronger interaction with clathrin adaptor protein AP-3, which routes the protein into late endosomes and lysosomes [127,128]. This interaction is required for normal NKT cell development and efficient lipid presentation of complex antigens that require enzymatic processing in the late endosomes or lysosome. Recently, a human CD1d knock-in mouse was developed; these mice showed NKT cell frequencies and

distribution that was comparable to that of humans [129]. However, even at these reduced numbers, NKT cell activation protected mice from tumor metastasis [129].

2.2. α-GalCer and analogues

α-GalCer is a glycolipid molecule that was originally identified during a screen for anti-cancer agents derived from marine sponge *Agelas mauritianus* [102,130,131]. The chemical name for α-GalCer is (2S,3S,4R)-1-O-(alpha-D-galactosyl)-N-hexacosanoyl-2-amino-1,3,4-octadecanetriol, and is comprised of a galactose carbohydrate α- linked to a ceramide lipid that has acyl and sphingosine chains (Figure 3) [131,132]. Interestingly, α-GalCer shows cross species reactivity, and can stimulate NKT cells from mice, rats, humans, and macaques [133]. When stimulated with α-GalCer, NKT cells rapidly produce IL-4 (Th2 bias) as early as 2 hours following stimulation, and delayed IFN-γ (Th1) type cytokines peaking at 6-24 hours [134]. Chemical modification of α-GalCer leads to derivatives which can skew NKT cell responses towards either a Th1 or Th2 type immune response, allowing for better immune modulation. Two such analogues are OCH and α-C-GalCer.

Compared to α-GalCer, OCH has a shortened sphingosine chain and is less potent at stimulating NKT cells, but selectively favors the production of IL-4 by NKT cells [135,136]. This makes OCH ideal for treating autoimmune conditions, where a Th2 type response is desired [137]. In contrast, α-C-GalCer, contains a C-glycoside linkage (as opposed to O-glycoside linkage) and skews NKT cells to produce high levels of IFN-γ [138]. These and other derivatives of α-GalCer continue to be an active area of research, with the aim of fine-tuning NKT cell immunotherapy.

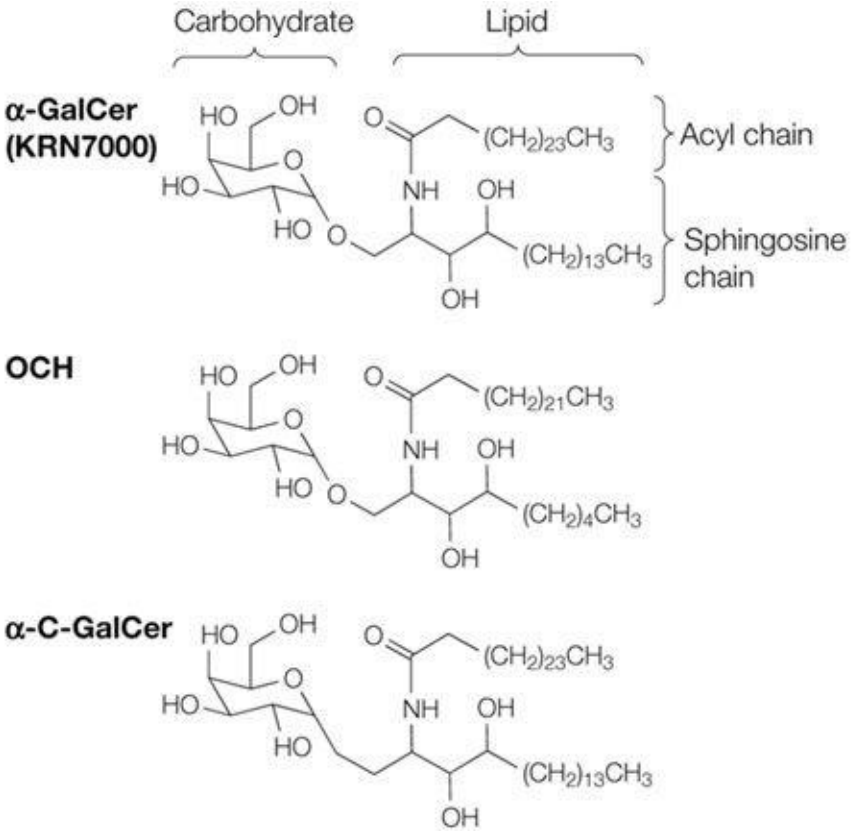

Figure 3. Structure of α-GalCer and analogs. α-GalCer contains galactose carbohydrate attached by an α-linkage to a ceramide lipid. The lipid portion interacts with the antigen-binding groove of CD1d, and carbohydrate portion is accessible to the invariant T cell receptor. OCH has a truncated acyl chain (by 2 carbons) and sphingosine chain (by 9 carbons). α-C-GalCer is a C-glycoside analogue. Adopted from [133].

2.3. NKT cells in cancer

It is well established that NKT cells play important roles in tumor immunosurveillance and anti-tumor immunity in the absence of exogenous stimulation. Mice deficient in NKT cells exhibit enhanced tumour development and metastasis in response to MCA or inactivation of the p53 tumour suppressor [139–141]. Adoptive transfer of NKT cells into NKT cell deficient Jα18$^{-/-}$ mice protected mice against tumors [101,141,142]. Consistent with their role in controlling cancer, NKT cell infiltration into colorectal

carcinomas and neuroblastomas is associated with a favorable prognosis in human patients [143–145]. Low levels of circulating NKT cells are associated with poor survival in patients with acute myeloid leukemia and head and neck cancers [146,147]. Similarly, many human cancers (including breast cancer) have been associated with diminished NKT cell numbers and/or function [148–151]. But the link between these deficiencies in NKT cells and the clinical outcome has not been well established.

NKT cell-mediated tumour immunosurveillance is likely mediated by recognition of tumor-associated glycolipid antigens [152], stress-induced glycolipid self-antigens [153,154], or inflammatory cytokines [155]. Several lines of evidence support the activation of NKT cells by self-lipids displayed on CD1d positive tumors or cross-presented by antigen presenting cells. B-cell lymphomas and other tumours expressing high levels of CD1d are more susceptible to NKT cell-dependent lysis [156]. Similarly, breast cancer cells that downregulate CD1d can evade NKT cell-mediated antitumor immunity and promote metastatic breast cancer progression [70]. Collectively, these studies and others [157,158], implicate direct CD1d-TCR interactions in NKT cell immunosurveillance without exogenous stimulation.

Therapeutic NKT cell activation with exogenous glycolipids provides significant protection from tumor progression [102,134,142,159,160]. Following activation, NKT cells can directly kill transformed or infected cells through perforin, granzyme-B, TRAIL and FasL [161,162]. NKT cells can also rapidly produce immunoregulatory cytokines, including interferon-γ (IFN-γ), tumor necrosis factor (TNF), interleukin-2 (IL-2), IL-4, IL-10, IL-13, IL-17, IL-21, and GM-CSF [106,107,134]. This rapid production of cytokines allows NKT cells to regulate the functions of T cells [141,163–168], NK cells [101,141,165,166,168] and

DCs [163,167,169]. This enables NKT cells to play a pivotal role in regulating immune responses, hence making them a promising therapeutic target for immune modulation therapy.

Following NKT cell activation, NKT cells can produce cytokines such as IL-2 and IFN-γ which activate CD8 T cells and NK cells [158,166]. Activation of both CD8 T cells and NK cells is particularly important because it allows for targeting of both MHC-positive and MHC-negative tumor cells, respectively. NKT cell derived cytokines can also induce the maturation of DCs [163], leading to enhanced stimulation of T cells. CD40/CD40L interactions between DCs and NKT cells can also enhance IL-12 production. In turn, IL-12 stimulates NK cells [166], Th1 and CD8 T cells [170]. Consistent with an important role for NK cells and CD8 T cells, depletion of either NK cells or CD8 T cells attenuates the anti-cancer effects of NKT cell activation [141,168].

NKT cells have also been shown to target some immunosuppressive myeloid populations. NKT cells can directly kill tumor-associated macrophages, resulting in decreased tumor burden [171]. NKT cell deficient mice also had substantially higher levels of MDSCs following influenza virus infection, resulting in decreased immunity and increased mortality [172]. Adoptive transfer of NKT cells abolished the suppressive activity of MDSCs [172]. This effect was CD1d and CD40 dependent, as MDSCs from $CD1d^{-/-}$ or $CD40^{-/-}$ mice were not affected by NKT cells [172]. Given that many cancers upregulate MDSCs, it would be interesting to examine whether NKT cell activation therapy can target these tumor-induced MDSCs.

2.4. NKT cell activation in human clinical trials

In addition to the experimental evidence of NKT cell-mediated tumor control, there have been encouraging outcomes in phase I/II clinical trials [173–175]. In a phase I dose escalation study, 11 non-small cell lung cancer patients were treated with autologous α-GalCer-loaded DCs and showed no adverse events [176]. While this study was not designed to evaluate efficacy, they reported a dramatic increase in circulating NKT cells and 2 out of 11 patients showed stable disease followed out to a year. In a phase I-II study, 17 patients with advanced non-small cell lung cancer were treated with α-GalCer-loaded peripheral blood mononuclear cells [174]. Treatments were administered intravenously four times without adverse effects. Elevated IFN-γ-producing cells were detected in 10 out of 17 patients, and patients showing IFN-γ response had a significantly enhanced median survival time (31.9 months compared to 9.7 months in non-responding patients) [174]. Finally, in a phase II study of 10 head and neck cancer patients, adoptive transfer of NKT cells and α-GalCer-loaded APCs led to 5 cases of objective tumor regression [177]. These clinical findings are preliminary, and larger multicenter trials are required to better understand the role of NKT based immunotherapy.

Collectively, preclinical and clinical data indicate that NKT cell activation therapy is a promising approach to treating cancer. However, we need to develop better tools to study NKT cells and expand our understanding of the potential for NKT cell activation therapy in treating solid tumors. Furthermore, there have been few studies aimed at exploiting the potential of combining NKT cell activation therapies with current standards of care or emerging preclinical approaches. In this body of work, we aim to address some of these gaps in knowledge.

3. Recent progress in cancer immunotherapy

Cancer immunotherapy is now considered a standard of care in leading cancer treatment centres; joining the ranks of surgery, chemotherapy, radiation and targeted therapies [178]. Cancer immunotherapy is broadly aimed at either stimulating an anti-tumor immune response or helping overcome immunosuppressive mechanisms. In this work, I will briefly describe the advances in adoptive cell transfer therapies and immune check-points inhibitors.

3.1. Adoptive cell transfer therapy

Adoptive cell transfer (ACT) primarily involves the isolation and ex-vivo expansion of tumor-specific T cells, NK cells and/or NKT cells, then infusion back into the cancer patient [177,178]. ACT using autologous tumor-infiltrating lymphocytes has been shown to mediate objective tumour regression in 50% of melanoma patients [179]. While this approach is promising, it is a highly personalized and labour intensive treatment that makes it difficult to commercialize.

Lymphocytes can also be engineered to express chimeric antigen receptors (CARs) which target specific antigens on the tumor surface or defined transgenic TCRs that can recognize peptides derived from surface of intracellular antigens presented on MHC [180]. While CAR-NK and CAR-NKT cell therapy is still in the preclinical phase, CAR-T cell therapy is now FDA approved to treat refractory acute B-cell lymphoblastic leukemia [181]. Despite the remarkable results in early clinical studies, TCR-T and CAR-T cell therapies can pose significant safety challenges, including induction of cytokine release syndrome, off target cross-reactivity, and "on-target, off-tumor" toxicity due to

poor control of dose, location and timing of CAR-T cell activity [180,182]. Strategies to avoid the side effects of TCR-T and CAR-T cell therapy include suicide genes, inhibitory CAR, dual-antigen receptors, and the use of small molecules to control CAR-T cell functions [180,182].

3.2. Immune check-point inhibitors

To control the intensity and duration of immune inflammatory responses, the immune system has multiple controls or "check-points". These checkpoints expressed on activated T cells, NK cells, NKT cells and myeloid cells, and provide mechanisms to protect against autoimmune responses. While more than twenty check-points have been identified to date [178], two pairs have received most attention; cytotoxic T lymphocyte-associated antigen-4 (CTLA-4) receptor interactions with B7 ligand, and programmed cell death protein 1 (PD1) receptor interactions with PD-L1 and -L2 ligands. CTLA-4 has a higher binding affinity to B7 than CD28, causing inhibition of proliferation and IL-2 secretion by T-cells [183]. In contrast, PD-1 does not interfere with co-stimulation, but prevents phosphorylation of key signaling molecules involved in T cell activation [184]. Since CTLA-4/B7 interactions act earlier than the PD1/PDL-1, targeting CTLA-4 is likely to influence the initial or priming stage of T-cell activation in the lymph nodes, whereas targeting PD1/PDL-1 is likely to influence the effector phase in the tumor microenvironment [184,185].

In a recent meta-analysis of ipilimumab, a CTLA-4 blocking monoclonal antibody, more than 20% of melanoma patients were alive 10 years later with no evidence of disease [186]. In a head to head comparison between PD-1 and CTLA-4

blocking antibodies, stage III-IV melanoma patients treated with PD-1 blocking antibody (nivolumab) exhibited significantly longer recurrence-free survival and had a better safety profile than ipilimumab [187]. Combination of ipilimumab and nivolumab has shown even greater promise, generating a 50% response rate in metastatic melanoma [188]. These early findings on check-point blocking antibodies mark a significant improvement in how cancer patients are treated.

4. Chemotherapy

Historically, the anti-cancer benefits of chemotherapies were attributed to direct cytotoxicity or permanent arrest of the cell cycle machinery. These therapies were thought to non-specifically target rapidly proliferating cells, leading to the assumption that chemotherapies would inadvertently target proliferating immune cells and result in immunosuppression [189,190]. Furthermore, chemotherapies were thought to induce cell death in an immunologically silent manner. This led many researchers to neglect the role of the immune system in cytotoxic chemotherapy, and the testing guidelines set by regulatory agencies recommended the use of immunodeficient hosts for examination of drug effects on transplanted human cancer cells [191]. Recently, there has been mounting evidence demonstrating that the antitumor activity of many conventional cancer therapies results in part from their ability induce immunogenic tumor cell death and stimulate immune function [192–196].

The most common chemotherapeutics used to target metastatic breast cancer include antimetabolites (e.g. gemcitabine), alkylating agents (e.g. cyclophosphamide), anthracyclins (e.g. doxorubicin) and taxanes (e.g. paclitaxel) [197]. While we have tested

these 4 chemotherapies in our 4T1 model, this thesis will only cover work on gemcitabine and cyclophosphamide in the 4T1 model.

4.1. Gemcitabine

Gemcitabine (GEM; difluorodeoxycytidine) is a chemotherapeutic agent currently approved for the treatment of pancreatic cancer, bladder cancer, ovarian cancer, lung cancer and breast cancer [198–201]. GEM is a pyrimidine analogue that undergoes phospho-activation into difluorodeoxycytidine-triphosphate, which inhibits nucleotide synthesis through inhibition of ribonucleotide reductase, and gets incorporated into DNA, preventing the DNA polymerase from proceeding with DNA replication [202]. This allows GEM to target rapidly proliferating cells. In addition to direct cytotoxic properties, GEM has been shown to reduce MDSCs in tumour models [77]. This reduction in MDSCs was associated with decreased IL-10 levels and increased IL-12 production in the 4T1 mammary tumour model, promoting Th2 to Th1 skewing of the immune response. In addition, GEM treatment decreased the frequency or function of MDSCs [81] and B cells [203], while sparing T cells, NK cells and macrophages [81]. Furthermore, GEM also enhances DC dependent cross presentation of tumor antigens, resulting in increased antitumor immunity [81]. These immune attributes make GEM a good candidate for combination therapy with immunotherapies.

4.2. Cyclophosphamide

Cyclophosphamide (CPX) is an inactive cyclic phosphamide ester which is transformed into its active metabolites via hepatic cytochrome p450 enzymes [204]. CPX prevents cell division primarily by cross-linking DNA and RNA strands. CPX has also been shown to have immunomodulatory effects at low doses. CPX treatment prior to

vaccination dramatically enhanced antigen-specific CD8 T cell responses [205]. CPX treatment also decreased the frequency of T-regs [205]. Recently, CPX was shown to trigger anti-tumor immunity by perturbing the gut microbiome [206]. CPX induced the translocation of Gram-positive bacteria into secondary lymphoid organs, which was associated with a Th1 and Th17 immune response, and an anti-tumor immune response [206]. In this case, Th17 cells express both T-bet and ROR-γt transcription factors which are associated with Th1 and Th17 cells, respectively. Combining DC-based therapy with CPX increased the anti-tumor immune response and improved survival outcomes in tumor bearing mice [207].

5. Oncolytic virus therapy

Anecdotal evidence of viral infection coinciding with tumor regression has existed for more than 150 years ago. Leukemia regression has also been reported in patients infected with influenza or chicken pox [208,209]. This idea of using viruses to treat cancer picked up in the 1950s with the advances in tissue culture systems and rodent cancer models [210]. By the 1960s, hundreds of cancer patients were treated with impure oncolytic virus preparations, with some patients showing beneficial outcomes [210]. Since these early reports, several preclinical studies have confirmed a protective role of viruses in different cancer models [210]. Recently , new approaches of genetically engineering oncolytic viruses have provided promising preclinical and clinical outcomes [208,211]. In 2005, genetically modified oncolytic adenovirus H101 was approved for use in China, and in 2015, a genetically modified herpes virus engineered to generate GM-CSF (Talimogene Laherparepvec (T-VEC)) was approved in the United States [212].

Oncolytic viruses selectively replicate in and kill cancer cells, while having minimal detrimental effects on healthy cells. This selectivity can either occur naturally, or through genetic engineering [213]. Natural virus tropism for cancer cells might be due to presence of entry receptors on the cancer cell or defects in anti-viral defenses [210]. Oncolytic viruses have a unique pharmacokinetic profile, they can navigate through the blood stream and target undiagnosed or inoperable tumors [213]. Furthermore, most oncolytic viruses are amenable to genetic modification, allowing them to deliver desirable immunomodulators to the tumour [210]. For instance, oncolytic viruses can be genetically engineered to express chemokines or cytokines that would recruit or activate immune cells within the tumor microenvironment. Once at the site of the tumor, oncolytic viruses can target tumors through multiple mechanisms. They can directly lyse the cancer cells, target the tumor vasculature, and stimulate anti-tumor immunity [210].

5.1. Vesicular Stomatitis Virus (VSV)

VSV is a negative-strand RNA virus from the rhabdoviridae family with an 11 Kb non-segmented genome encoding 5 viral proteins (glycoprotein, matrix, nucleocapsid, phosphoprotein, and large RNA polymerase) [213]. VSV replication primarily occurs in the cytoplasm and VSV can be rapidly grown to very high titers. VSV primarily infects cattle, swine, horses and insects, but there have been limited reports of human infection. Livestock VSV infections are characterized by vesiculation and ulceration in oral and mucosal cavities, whereas human infection is largely asymptomatic with mild flu-like symptoms [214].

It was initially reported that VSV can cause tumor regression in a human melanoma xenograft in nude mice [215]. VSV is very sensitive to type I interferons,

therefore addition of exogenous IFN-α protected healthy cells from viral infection [216]. Treatment of cancer cells with IFN-α failed to protect against VSV infection, likely due to defects in interferon signaling [216]. VSV is also neurotropic and can cause severe pathogenicity in the central nervous system, which led to safety concerns on VSV's oncolytic use. To improve specificity for cancer cells, Stodjl et al. [213] engineered a mutation in the matrix protein replacing a methionine at position 51 for arginine (VSVΔM51). The wild-type VSV matrix protein binds the host ribonucleic acid export 1, preventing nuclear-cytoplasmic export of host mRNAs, including type I IFNs [217,218]. This mutation in the matrix protein prevents VSVΔM51 from subverting the anti-viral immunity in healthy cells. In contrast, cancer cells have a defective type I IFN response, making them increasingly susceptible to VSVΔM51.

5.2 Reovirus

Mammalian respiratory enteric orphan virus (reovirus) is a non-enveloped, double-stranded segmented RNA virus, which targets human upper respiratory and gastrointestinal tracts and generates relatively benign symptoms [219,220]. Reovirus type 3 Dearing strain has been widely used in preclinical and Phase I/II clinical trials, and is the strain used in this body of work [220]. Cells with an overactive oncogenic Ras pathway are increasingly susceptible to reovirus infection [221]. The Ras signaling pathway can be induced via EGFR signaling and has been shown to be key in sustaining proliferation via p38 MAPK, PI3K and phospholipase C [222]. Constitutive Ras pathway also inhibits the ds RNA-dependent protein kinase R (PKR), making the cells susceptible to reovirus infection. Cancer cells that do not have an overactive Ras pathway are less susceptible to

dsRNA virus replication. Given that more than 30% of tumors have an overactive Ras, there has been a great deal of interest in reovirus oncolytic therapy.

Reovirus demonstrated a marked tumor regression in a xenograft model of HER-2-transformed NIH-3T3 fibroblasts and human U87 glioblastoma cells [223]. While these early studies were performed in immunodeficient mice, similar findings have been reported in immunocompetent mice [224]. Furthermore, reovirus has been shown to induce an antigen specific T cell response in a B16 melanoma model [225] and a murine prostate cancer model [225]. Two disadvantages of this platform are that it is not currently amenable to genetic engineering, and there is a high incidence of neutralizing reovirus immunity within the human population [226].

6. Immunogenic cell death

Regulated cell death is a physiological phenomenon that plays an important role in development and homeostasis [227,228]. These processes were initially characterized based on morphological cell changes, chromatin condensation and membrane blebbing, and were thought to occur in the absence of an inflammatory response. Recently, a consensus has emerged recommending that the nature of cell death should not simply be defined by morphological changes, but rather by distinct molecular, biochemical and metabolic hallmarks [228,229]. This has led to the discovery of new apoptotic cell death modalities and characterization of cell death pathways that elicits antigen specific immune responses against dead-cell antigens [230]. This type of cell death has been termed immunogenic cell death (ICD) and was initially characterized in the context of anticancer chemotherapy [193].

Unlike physiological cell death which induces signals that lead to tolerogenic clearance of cells, ICD generates specific changes in cell surface structures and release of mediators that allow DCs to detect the dying cell and promote an antitumor immune response [231]. DCs engulf parts of the stressed/dying cell and incorporate antigenic peptides into the MHCs. In contrast to tolerogenic cell clearance, it is essential that DCs engulfing dying cells also receive maturation signals from Toll like receptors (TLR) or cytokines so as to be able to optimally activate T cells and prevent the development of tolerance [49,232,233].

While many therapeutics tested (e.g. etoposide, mitomycin C, cisplatin) do not elicit ICD, some therapeutic agents (such as anthracyclines and oxaliplatin) [192–196], radiation therapy [234,235], oncolytic virus therapy [236,237] and photodynamic therapy [238] have been shown to induce ICD. The only way to identify bona fide ICD inducers is through vaccination challenges [239]; tumor cells treated with ICD inducers prior to inoculation into immunocompetent mice vaccinate them against subsequent challenge with the same tumor [192,193,240–242]. After screening for proteins that are upregulated on the surface of cancer cells undergoing ICD, the endoplasmic reticulum (ER) protein calreticulin (CALR) exhibited increased translocation to the plasma membrane of cells undergoing ICD [240,242]. The exposed CALR was found to be critical for ICD, as knockdown of CALR expression significantly hampered development of anti-tumor immunity [235,242]. Following the pre-apoptotic CALR mobilization, cells undergoing ICD release adenosine triphosphate (ATP), which is essential for recruitment of antigen presenting cells (APCs) and the subsequent activation of the inflammasome to promote IL-1β release by DCs [194,241,243–245]. Anthracycline treated cancer cells also upregulate a TLR3/type I IFN/

CXCL10 signaling cascade that is critical for protection from tumor growth [246]. In the late stages of apoptosis (secondary necrosis), cells passively release the chromatin protein high-mobility group box 1 (HMGB1) which acts on TLR4 on DCs to enhance antigen presentation (Figure 4) [192,247,248]. Disruption of any of these ICD pathways impairs generation of anti-tumor responses. Each pathway is described in more detail below.

6.1 ER stress and CALR exposure.

The ER serves as a site for protein folding, modification, and trafficking to their proper cellular compartments. In addition, the ER is also the primary site for lipid biosynthesis and calcium storage [249,250]. Physiologic stress such as increased secretory load, or pathologic stresses such as mutated proteins, can overwhelm the functional capacity of the ER, leading to ER stress [249]. The ER responds to stress by activating an adaptive mechanism called the unfolded protein response [249,250]. The main aim of these processes is to re-establish homeostasis and promote survival. However, when these coping mechanisms are overwhelmed, the pro-survival mechanisms switch to pro-death signals [251]. CALR represents the most abundant protein in the ER lumen and gets translocated to the cell surface of stressed and dying cancer cells [240,242,252]. This translocation of CALR occurs prior to translocation of phosphatidylserine to the outer leaflet of the plasma membrane, hence it is termed a pre-apoptotic event [240,242,252].

CALR functions as a potent "eat me" signal on apoptotic cells through the binding of CD91 on macrophages and DCs [253]. CALR exposure precedes that of phosphatidylserine [242], but both CALR and PS serve as eat me signals on apoptotic cells. However, PS mediates clearance of tumor cells without activating an immune response [254]. PS exposure on cancer cells has also been associated with immunosuppression and

antibody mediated inhibition of PS significantly improved anti-tumor immune responses [255,256]. In contrast to PS, CALR binds CD91 on antigen-presenting cells to promote proinflammatory cytokines (for example IL-6 and tumor necrosis factor) [257,258]. Hence, recognition of CALR on dying cells is an early event that leads to engulfment of dying tumor cells by APCs and priming the adaptive immune response.

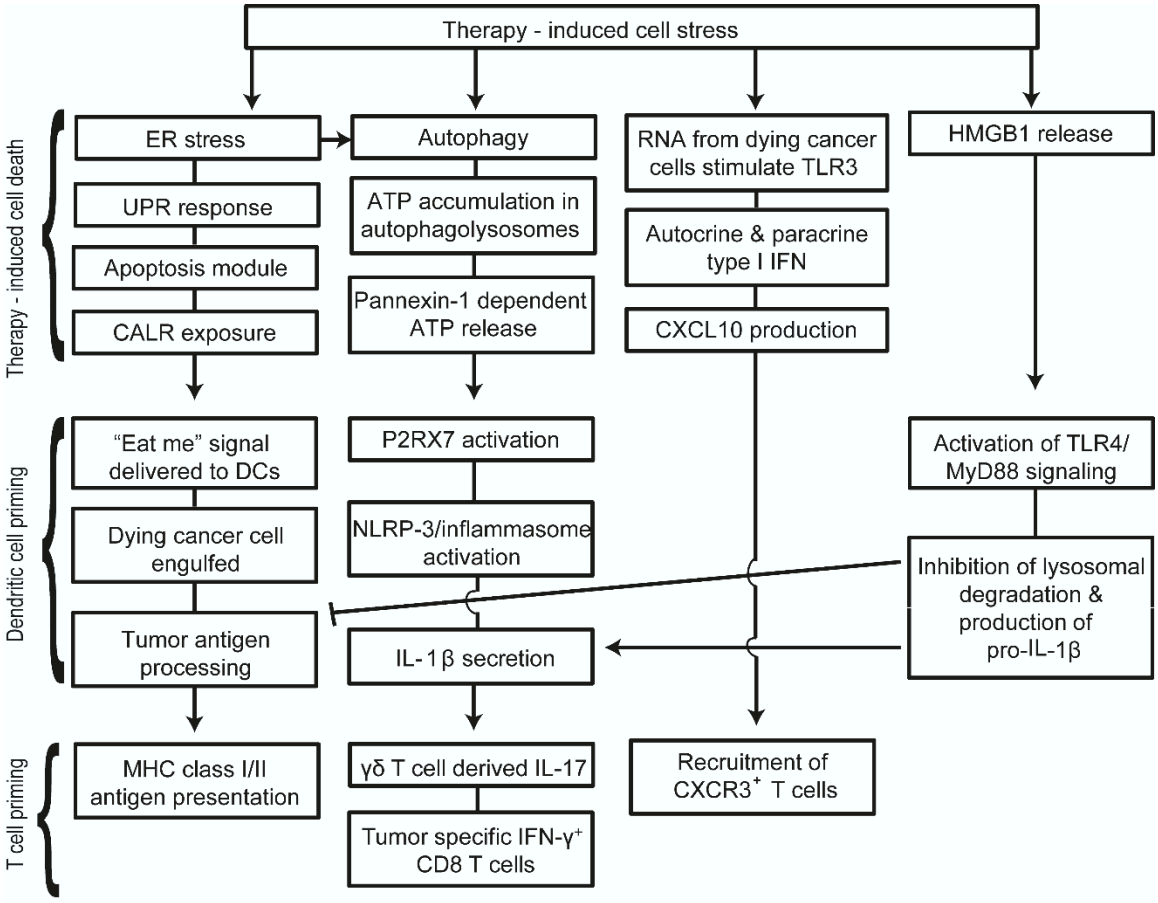

Figure 4. Schematic representation of therapy-induced immunogenic cell death (ICD). Therapy-induced ER stress, autophagy, TLR3 activation and HMGB1 release are key events in immunogenic cell death. Unresolved ER stress leads to the activation of the unfolded protein response, initiation of the pre-apoptotic module and subsequent translocation of CALR. Autophagy plays an important role in accumulation of ATP in phagolysosomes and ATP potently activates the NLRP3/inflammasome pathway in DCs. Following activation of the inflammasome, DCs secrete IL-1β that is essential in the recruitment of γδ T cells and IFN-γ^+ cytotoxic CD8 T cells. Activation of TLR3 in dying cancer cells also leads to autocrine/paracrine type I IFN production and the subsequent production of CXCL10. This is followed by the release of HMGB1 during the late stages of apoptosis. Figure from [259].

6.2 The role of ATP in ICD

ATP has been studied for its role in energy metabolism and autocrine/paracrine cell signaling. Although ATP has a physiologic role in neurotransmission, it can also be released from cells during pathological conditions such as mechanical stress, plasma membrane damage, hypoxia and exposure to cytotoxic agents [260–262]. Multiple distinct ICD inducers (oxaliplatin, mitoxantrone, doxorubicin) can cause ATP release from dying tumor cells [260]. Although ATP release could occur through multiple mechanisms [261,262], autophagy is thought to be the primary mechanism that sustains high ATP levels in cells undergoing ICD [194].

Extracellular ATP has the dual effect of attracting immune cells and activating the inflammasome pathway. ATP signaling via P2Y2 receptors on monocytes and DCs induces their recruitment and activation in the tumor microenvironment [263–265]. Once naïve immune cells are recruited to tumor sites and have been exposed to "eat me" signals, they require activation signals to increase their anti-tumor activities. ATP signaling via P2RX7 receptors is one of the most potent activators of the NLRP3 inflammasome pathway in DCs and macrophages [263,266,267]. Although P2RX7 is expressed on several cell types including DCs and macrophages, ATP primarily acts through P2RX7 on DCs during ICD [241]. The NLRP3 pathway activates the protease caspase-1, which leads to the processing and secretion of pro-IL-1β and pro-IL-18 [267]. Supporting a key role for the ATP/NLRP3 inflammasome in response to chemotherapy, Ghringhelli et al. [241] demonstrated that *P2rx7*$^{-/-}$, *Nlrp3*$^{-/-}$, *Caspase- 1*$^{-/-}$ and *Il1r*$^{-/-}$ mice had significantly decreased chemotherapeutic protection against several transplanted tumour

lines. Furthermore, chemotherapy-induced IL-1β was shown to be required for the recruitment of IL-17 producing γδ T cells [265] and generation of IFN-γ producing tumor specific CD8 T cells [241]. The recruitment of γδ T cells and production of IL-17 occurred prior to tumor specific IFN-γ production by CD8 T cells [265]. Hence ATP release following cytotoxic therapy can mediate activation of the NLRP3 inflammasome, creating a link between the innate and adaptive immune response. In particular, activation of the inflammasome in DCs leads to the production of IL-1β and subsequent recruitment of γδ T cells and priming of CD8 T cells against tumor antigens.

6.3 The role of TLR3 and type-I IFN in ICD

Ligation of TLRs by microbial ligands is known to trigger well characterized signaling cascades that result in anti-microbial immune responses [268], and occasionally, death of the infected cells [269–271]. TLR3 is a key endosomal pathogen recognition receptor for dsRNA and is required for full induction of type I IFN mediated antiviral immune responses [272,273]. While TLR3 agonists have been shown to cause cell death in pancreatic β cells [274,275], endothelial cells [276] and cancer cells [277], a novel role of anthracycline induced TLR3 activation has been recently described in ICD [246]. TIR domain-containing adapter inducing IFN-β (TRIF), the only known adaptor protein of TLR3 signaling, can by itself exhibit proapoptotic tendencies [278–280]. Sistigu *et al.* [246] demonstrated that anthracycline treatments elicited TLR3 signaling in cancer cells, leading to autocrine/paracrine type I IFN signaling and the subsequent secretion of CXCL10 (Figure 5). Genetically knocking out TLR3 on cancer cells ablated this protection, an effect that could be reversed by administering recombinant type I IFN or CXCL10 [246]. This cascade was essential for the successful vaccination of mice against tumor re-challenge.

Consistent with this, a type I IFN signature is a strong prognostic factor for breast cancer patients undergoing anthracycline therapy [246]. Interestingly, this pathway closely mimics the immune response against viral infection, and oncolytic viruses can also induce type I IFN and CXCL10 [225]. Availability of clinical grade TLR3 agonists [281], recombinant type I IFNs [282] and preclinical recombinant CXCL10 [283] provide promising therapeutic avenues.

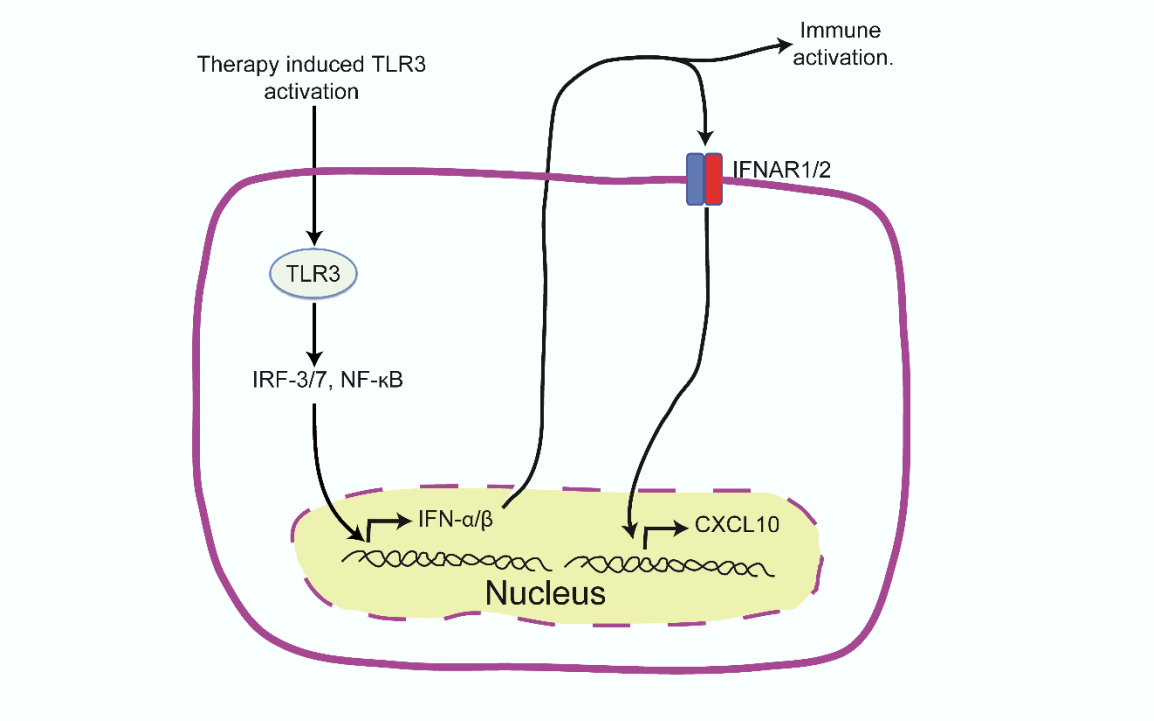

Figure 5. **TLR3/IFN-α/β/CXCL10 axis in ICD**. Schematic representation of the events preceding the release of tumor derived CXCL10 in ICD. Treatment activates TLR3 signaling in cancer cells which leads to the rapid release of IFNα/β by cancer cells. IFNα/β can act in both an autocrine or paracrine manner on neoplastic cells leading to the release of CXCL10. Figure from [259].

6.4 The role of HMGB1 in ICD.

HMGB1 is a ubiquitously expressed protein that plays an important role in stabilizing nucleosomes, regulating gene transcription and DNA repair [284,285]. Besides its role in the nucleus, extracellular HMGB1 is a key driving factor in inflammation, cell

differentiation, cell migration, and tumor metastasis [286]. HMGB1 is actively secreted by macrophages [287], DCs [288] and NK cells [289] in response to infection or injury. Secreted HMGB1 can promote inflammation by binding the receptor for advanced glycation end products (RAGE), TLR2, TLR4 and TLR9, whereas HMGB1 pro-inflammatory activity can be inhibited by binding CD24 [285,290–292]. When bound to nucleosomes, HMGB1 can induce a TLR2 mediated humoral responses against the released DNA/histones [293]. HMGB1 can also associate with the chemokine CXCL12 and recruit immune cells to sites of inflammation [294].

Although early reports suggested that HMGB1 was only released from necrotic cells [291], there is increasing evidence showing that HMGB1 can be released during the late stages of regulated apoptosis, necroptosis, autophagy, and pyroptosis [261,262,292,295]. In particular, the release of HMGB1 was shown to be required for effective induction of ICD [192]. In this study, the authors vaccinated mice with anthracycline or oxaliplatin treated cells one week prior to tumor challenge and demonstrated that antibody mediated blockade of HMGB1 compromised the efficacy of vaccination. Furthermore, protection was compromised in TLR4 deficient (but not other TLRs) and Myd88 deficient mice. These results implicated TLR4 as the receptor for HMGB1 that mediates anti-tumor immune responses. The activation of TLR4 on DCs in culture was shown to enhance the processing of phagocytic cargo, facilitate antigen presentation, upregulate co-stimulatory molecules and increase intracellular levels of pro-IL-1β (a substrate for the inflammasome pathway) [192,231,260]. TLR4 signaling might also prevent the premature lysosomal degradation of engulfed apoptotic debris and potentially preserve tumor associated antigens for presentation [192,296]. This is consistent with the observation that

peptides that are resistant to lysosomal degradation are more antigenic [296]. Tumor cells deficient in HMGB1 exhibit compromised capacity to induce ICD and anti-tumor immune responses; however, TLR4 agonists rescued the chemotherapy-induced anti-tumor immune responses [247]. Similarly, inhibition of lysosomal degradation using chloroquine enhanced the efficacy of chemotherapy in TLR-4$^{-/-}$ mice but not wild type mice [192]. This suggests that TLR-4 signaling in DCs and not the specific TLR4 ligand produced by dying tumor cell is important for inducing ICD.

Collectively, the emerging concepts surrounding ICD have the potential to enhance clinical benefit and should be a consideration when monitoring therapeutic responses. In particular, monitoring the hallmarks of ICD could play an important role in patient-specific therapy selection, tumor-specific therapeutic strategies and combination therapy dose/sequence selection. Important to this body of work, combining immunotherapies with ICD-inducing therapy could potentially lead to enhanced efficacy and diminished toxicities. The therapeutic benefit of combining NKT cell activation therapy with ICD-inducing chemotherapy or oncolytic virus therapy remains poorly understood.

7. Animal models of cancer

Animal models are an important tool in tumor immunology and testing of new therapeutics. In this body of work, we use three syngeneic murine tumour models: 4T1 mammary carcinoma, B16-F10 melanoma, and ID8 ovarian cancer cells. While this work is primarily focused on the 4T1 model, we used the B16-F10 and ID8 model to address certain experiments that could not be done using the 4T1/BALB/c background.

4T1 cells were isolated from a spontaneous mammary carcinoma arising in a BALB/c mouse [297]. This model is aggressive and has many features that resemble advanced human stage IV breast cancer, including spontaneous metastasis from primary orthotopic tumours [298,299]. The primary site of metastasis is to the lungs, and metastasis can occur through both hematogenous and lymphatic routes [297,299]. At later time points, 4T1 cell metastasis can be detected in the liver, lymph nodes, kidneys, bone and brain [299]. One advantage of the 4T1 model is that you can resect the primary tumor, and test different therapeutic approaches to target metastatic burden [165,300]. The 4T1 cells are resistant to the guanine analog 6-thioguanine (6-TG), allowing for quantification of metastasis through clonogenic plating assays [297,299]. In addition, the 4T1 model is highly immunosuppressive and has been shown to induce the accumulation of MDSCs [165,301]. Breast cancer patients have higher levels of circulating MDSCs than healthy individuals, and there is a strong correlation between clinical cancer stage and the levels of circulating MDSCs [302].

The B16 melanoma cell line was derived more than 6 decades ago from a C57BL/6 mouse carrying a chemically induced tumor [303]. There are three subtypes of this cell line, the F1 which is the parental line and is non metastatic, BL6 which is invasive, and F10, which is highly metastatic [303,304]. In this study, we used the B16-F10 cell line (referred to as B16 hereafter). Subcutaneous injection of B16 cells leads to development of a primary tumor, whereas intravenous or intrasplenic injection of B16 cells leads to lung and liver metastasis, respectively [169]. The latter two models are used to test therapeutic strategies against metastatic disease.

ID8 ovarian cancer cells have a capacity to form tumors and hemorrhagic ascetic fluid upon intraperitoneal (i.p) injection into syngeneic to the C57BL/6 mice [305]. The ID8 mouse model was originally developed to study ovarian cancer in mice with an intact immune system. Furthermore, the model exhibits disease behaviors that are similar to the high-grade serous subtype, which accounts for majority of human ovarian cancer cases [306].

8. Thesis overview

While there has been an improvement in the survival outcome for breast cancer patients, the toxicity and disease recurrence associated with the current standards of care remains high. Furthermore, given that most breast cancer associated deaths arise from metastatic disease [1], the development of novel safe and effective therapeutic strategies are of particular interest . Recently, therapeutic approaches that boost the immune system to overcome immunosuppression and target cancer cells have shown promising potential in many cancers [307,308]. Despite promising preclinical and phase I/II clinical data on NKT cell activation therapy, the role of NKT cell activation in targeting breast cancer remains a poorly studied area. *I hypothesize that NKT cell-based therapy could be developed to target breast cancer, especially metastatic disease.*

Chapter 3: Developing novel tools for evaluating the role of NKT cells in cancer control. Despite advances in our understanding of NKT cell biology, many of the molecular mechanisms underlying NKT cell homeostasis and function are still unclear. Tools to dissect these mechanisms are required to support the development of safe and effective NKT cell-based immunotherapies. A major limitation in the study of NKT cells is the ability to generate large numbers of NKT cells for *in vitro* and *in vivo*

experimentation. The objective of this study was to develop a reliable protocol of expanding functional NKT cells and reconstituting them in NKT cell deficient mice. I phenotypically and functionally characterized the expanded NKT cells, and used our reconstitution model to probe the role of NKT cell derived cytokines on anti-tumor immunity.

Chapter 4. Natural killer T cell activation overcomes immunosuppression to enhance clearance of postsurgical breast cancer metastasis in mice. Metastatic lesions are responsible for over 90% of breast cancer associated deaths. Therefore, strategies that target metastasis are of particular interest. This study examined the efficacy of NKT cell activation as a post-surgical immunotherapy in a mouse model of metastatic breast cancer. Following surgical resection of orthotopic 4T1 mammary carcinoma tumors, NKT cells were activated using α-GalCer-loaded DCs. *I hypothesized that NKT cell activation therapy would limit tumor metastasis and prolong survival*. I also examined the effect of NKT cell activation of immunosuppressive MDSC levels and anti-tumor immunity.

Chapter 5. Natural killer T cell immunotherapy in combination with chemotherapy-induced immunogenic cell death targets metastatic breast cancer. Despite advances in chemotherapeutic interventions, the off-target effects and toxicity associated with chemotherapy remain high. Therefore, strategies that reduce off-target toxicity associated with traditional chemotherapy treatments are needed. One promising approach is to combine low doses of chemotherapy with immunotherapies. In this body of work, I wanted to examine whether we could safely and effectively combine NKT cell activation therapy with low doses of cyclophosphamide or gemcitabine to target post-surgical breast

cancer metastasis. *I hypothesized that combining NKT cell activation therapy with chemotherapy would augment therapeutic outcomes*. In addition, I also examined the effect of these chemotherapies on tumor immunogenicity, immunosuppressive populations and anti-tumor immunity.

Chapter 6: Targeting post-surgical breast cancer metastasis with combined NKT cell activation and oncolytic virus therapy. Oncolytic virus therapy is an emerging treatment modality that has shown promising results in preclinical studies and has been recently approved for clinical use. There is emerging evidence to show that oncolytic virus therapy acts in part by stimulating an anti-tumor immune response. Furthermore, oncolytic viruses can safely be combined with immune modulation therapy to improve therapeutic outcomes. However the potential for combining NKT cell activation therapy with oncolytic virus therapy has not been previously described. I wanted to examine whether oncolytic VSV or reovirus could be combined with NKT cell activation therapy to target post-surgical breast cancer metastasis. *I hypothesized that this combination approach would work together to improve anti-tumor immunity and survival.* I also characterized the effect of oncolytic virus infection on tumor immunogenicity.

Chapter 2: Materials and methods.

Mice.

Wild-type C57BL/6, CD45.1 congenic, and IFN-γ $^{-/-}$ mice were purchased from the Jackson Laboratories (Bar Harbor, ME). BALB/c mice were purchased from Charles River Laboratories (Senneville, QC). NKT cell deficient Jα18$^{-/-}$ mice were obtained from Dr. M. Taniguchi (RIKEN Research Center for Allergy and Immunology, Kanagawa, Japan) [309]. Animals were maintained in the Carleton Animal Care Facility at Dalhousie University and used in experiments at 8-12 weeks of age. All experimental protocols were approved by the University Committee on Laboratory Animals in accordance with the guidelines of the Canadian Council on Animal Care.

α-GalCer reconstitution.

Lyophilized α-GalCer (KRN7000), purchased from Toronto Research Chemicals, was reconstituted in sterile 1X PBS containing 0.5% tween 20 to generate a stock concentration of 0.2mg/ml. The reconstituted α-GalCer was sonicated in a 60^{o}C water bath 2-4 hours, and aliquoted in 0.2 ml volumes for storage at -20^{o}C. Aliquots were sonicated in a 60^{o}C water bath prior to use.

Cell lines.

B16-F10 melanoma cells (ATCC; Manassas, VA), 4T1 mammary carcinoma cells (ATCC), ID8 ovarian cancer cells (generated by Dr. K Roby, University of Arkansas) [305], Lewis lung carcinoma (ATCC), mouse fibroblast L-292 cells (ATCC), Pan02 pancreatic cancer cells [310] and Vero kidney epithelial cells (ATCC) were cultured at 37^{o}C, 5% CO_2, in Dulbecco's Modified Eagle Medium (VWR Life Science, Mississauga, ON)

supplemented with 10% fetal bovine serum (FBS) and 100 μg/ml streptomycin, 100 units/ml penicillin (Fisher-HyClone, Ottawa, ON). Cells were harvested in the logarithmic growth phase using trypsin-EDTA (ethylenediamine-tetraacetic acid) treatment (Sigma-Aldrich, Oakville, ON). Washed cells were re-suspended in phosphate buffered saline (PBS) for *in vivo* experiments.

Cell isolation.

Mice were anesthetized using 2-3% isoflurane and euthanized by cervical dislocation. Liver, spleen, thymus, and lymph node lymphocytes were isolated by mechanical dispersion through 70 micron wire mesh. Cells were pelleted by centrifugation at 500g for 10 minutes at 4°C. Liver lymphocytes were separated from hepatocytes by centrifugation through a 33% Percoll gradient (GE Healthcare, Baie d'Urfe, QC). Red blood cells (RBC) were lysed with 5 ml of lysis buffer [150 mM NH_4Cl (Sigma-Aldrich), 10 mM $KHCO_3$ (J.T. Baker, Montreal, QC), and 0.1 mM EDTA (Sigma-Aldrich)] for 5 minutes, followed by addition of an equal volume of phosphate buffered saline (PBS; HyClone, Ottawa, ON) to inhibit further lysis. Cells were centrifuged at 300g for 8 minutes, resuspended in PBS supplemented with 2% FBS and counted using a hemocytometer.

Bone marrow derived dendritic cells culture and glycolipid loading.

Wild type mice were anesthetized with inhaled isoflurane and sacrificed via cervical dislocation. Under sterile conditions, femurs and tibias from mice were harvested and stripped of skin and muscle tissue. A 5ml syringe containing DC medium (RPMI-1640 containing 10% fetal bovine serum, 20μM 2-mercaptoethanol, 2mM L-glutamine, and 100 μg/mL streptomycin, and 100 units/mL penicillin) and a 30 gauge needle were

used to flush bone marrow through a 40 micron cell strainer. The cell suspension was then centrifuged at 300 x g for 8 minutes. The supernatant was aspirated and an RBC lysis was performed using 1 mL lysis buffer for 30 sec. Bone marrow cells were washed and resuspended in 15ml DC medium supplemented with 40 ng/ml GM-CSF and 10 ng/ml IL-4 (PeproTech; Rocky Hill, NJ, USA). The resulting solution was distributed evenly into 3 wells of a 6 well culture plate and incubated at 37^{o}C, 5% CO_2 for 3 days. Fresh medium, supplemented with 40 ng/ml GM-CSF and 10 ng/ml IL-4, was added to cells on day 3. On day 6, non-adherent cells were washed and transferred into new wells containing DC-medium supplemented with 20 ng/ml GM-CSF. DCs were loaded overnight with 0.4 μg/ml α-GalCer (Toronto Research Chemicals, Toronto, ON). Glycolipid loaded DCs were used in NKT cell activation and expansion experiments.

In vivo expansion of NKT cells.

To expand NKT cells for *in vitro* and adoptive transfer experiments, 6 x 10^5 α-GalCer loaded DCs were injected intravenously (i.v.) into C57/BL6 mice and 2x10^5 DCs were used in BALB/c mice. After 72 hours, NKT cells were sorted and used in experiments.

Antibodies and flow cytometry.

The following antibodies were obtained from eBioscience (San Diego, CA), BioLegend (San Diego, CA), or BD Biosciences (Mississauga, ON) unless otherwise specified: Unconjugated anti-CD3ε (clone 145-2C11); Fluorescein isothiocyanate (FITC)-conjugated rat IgG1 (clone eBRG1), FITC-rat IgG2b (clone A95-1), FITC-anti-CD3 (clone 17A2), FITC-anti-CD4 (clone RM4-5), FITC-anti-CD8α (clone 53-6.7), FITC-anti-CD45.1 (A20), FITC-anti-CD49b (DX5), FITC-anti-MHC I (H-2Db; clone

28-14-8), FITC-anti-MHC I (H-2Dd; clone 34-1-2S), FITC-anti-TCRβ (clone H57-597) ; phycoerythrin (PE)-conjugated rat IgG1 (clone eBRG1), PE-rat IgG2b (clone A95-1), PE-anti-CD1d (clone 1B1), PE-anti-CD4 (clone RM4-5), PE-anti-CD8α (clone 53-6.7), PE-anti-CD11b (clone M1/70), PE-anti-CD69 (clone H1.2F3), PE-anti-Gr1 (clone RB6-8C5),PE-anti-IL-17A (clone eBiol7B7), PE-anti-IFN-γ (clone XMG1.2), PE-anti-IL-4 (clone 11B11), PE-NK1.1 (PK136), PE-anti-TCRβ (clone H57-597), PE-anti-TCRvβ2 (clone B20.6), PE-anti-TCRvβ7 (clone TR310), PE-anti-TCRvβ8.2 (clone MR5-2) ; Peridinin chlorophyll protein (PerCP)-conjugated rat IgG2a (clone eBR2a), PerCP-anti-CD3 (clone 145-2C11), PerCP-anti-CD4 (clone RM4-5), PerCP-anti-CD45.2 (clone 104), PerCP-anti-TCRβ (clone H57-597) ; Allophycocyanin (APC)-conjugated anti-CD4 (clone RM4-5), APC-anti-CD8α (clone 53-6.7), APC-anti-CD25 (clone PC61), MHC II (IA/I-E clone M5/114.15.2) and APC-anti-TCRβ (clone H57-597). To examine NKT cells by flow cytometry, cells were stained with APC-labeled or and PE-labeled CD1d tetramers loaded with the glycolipid PBS57 (NIH Tetramer Core Facility, Emory Vaccine Center at Yerkes, Atlanta, GA). Prior to staining, all cell samples were pre-incubated with anti-CD16/32 to block non-specific binding. Flow cytometry was performed using a two laser FACSCalibur with BD CellQuest Pro software (BD Biosciences, Mississauga, ON). Unloaded CD1d tetramers and isotype matched control antibodies were used to establish gating and quadrants. A two-laser FACSAria sorter with BD FACSDiva software (BD Biosciences) was used to sort CD8 T cells ($CD8^+$ $TCR\beta^+$), NK cells ($CD49b^+$ $TCR\beta^-$), and NKT cells (CD1d $tetramer^+$ $TCR\beta^+$) (>96% purity) for *in vitro* assays and adoptive transfer experiments. Intracellular staining for cytokines,

transcription factors or cytotoxic molecules was performed using the Cytofix/Cytoperm Plus kit (eBioscience, San Diego CA).

Intracellular cytokine measurements.

To examine cytokine production following α-GalCer loaded DC treatment, intracellular cytokine staining (IL-4 and IFN-γ) was performed in NK ($TCR\beta^-$ $NK1.1^+$) and NKT (CD1d $tetramer^+$ $TCR\beta^+$) cells 2 hours after treating mice i.p. with 4 μg α-GalCer. Cells were washed with PBS and surface marker staining was performed at room temperature for 20 minutes. Following a wash step, cells were fixed in 4% paraformaldehyde (Fisher Scientific) for 20 minutes, washed with PBS and resuspended in permeabilizing buffer (eBiosciences), and incubated with IL-4 or IFN-γ antibodies. Following a 20 minutes incubation, cells were washed in permeabilizing buffer and resuspended in PBS prior to data acquisition.

***In vitro* T cell activation in anti-CD3ε coated plates.**

To characterize the cytokine production in naïve and expanded NKT cells (72 hours post α-GalCer-loaded DC stimulation) in culture, NKT cells were sorted from naïve and α-GalCer-DC treated mice. Sorted NKT cells ($2x10^5$ cells/well) were incubated at 37°C (5% CO_2) in anti-CD3ε-coated 96-well culture plates containing complete RMPI-1640 supplemented with 2 ng/ml mouse IL-2 (PeproTech, Rocky Hill, NJ). Supernatants were collected at 0.5, 2, 6 and 24 hours for measurement of IFN-γ and IL-4 levels by ELISA according to manufacturer's instructions (eBioscience). Corning Costar 9018 ELISA plates were coated overnight at 4°C with anti-mouse capture antibodies IFN-γ (clone AN-18), or IL-4 (clone 11B11). After coating, the plates were aspirated and washed three times using PBS with 0.05% Tween-20 (Sigma-Aldrich). ELISA plates

were blocked by adding 200 µl of 1X ELISA Diluent (eBioscience), followed by a 1 hour incubation at room temperature. The ELISA plates were washed five times using PBS with 0.05% Tween-20. Serial dilutions of standards for IFN-γ (2000, 1000, 500, 250, 125, 62.5, 31.25, 0 pg/ml) and IL-4 (500, 250, 125, 62.5, 31.25, 15.63, 7.81, 0 pg/ml) were prepared along with 1/20 and 1/50 dilutions of serum samples and supernatant samples. Diluted standards and samples were added to the wells at 100 µl volume and were incubated overnight at 4°C. The plates were then washed five times and 100 µl of biotin-conjugated mouse anti-IFN-γ (clone R4-6A2), and anti-IL-4 (clone BVD6-24G2) were added to the appropriate plates and incubated for 1 hour at room temperature. Plates were aspirated and washed 5 times. Avidin-horseradish peroxidase (HRP) was added at 100 µl per well and incubated for 30 minutes. The plates were aspirated and washed 5 times. The enzymatic substrate tetramethylbenzidine (100 µl/well) was added for 15 minutes, the reaction was stopped by adding 50 µl/well of 2 N H_2SO_4. The absorbance was measured at 405 nm using Epoch Microplate Spectrophotometer (BioTek, Winooski, VT) and cytokine concentrations were calculated using the generated standard curve (Gen 5 software; BioTek).

NK cell transactivation.

To examine whether NKT cell-derived IFN-γ is essential for NK cell transactivation, expanded wild type or IFN-$\gamma^{-/-}$ NKT cells (i.v. $3x10^6$) were adoptively transferred into J$\alpha18^{-/-}$ mice. After 24 hours, mice were treated with α-GalCer (i.p. 4 µg). Six hours after glycolipid stimulation, intracellular IFN-γ staining was examined in NK cells from wild-type mice, J$\alpha18^{-/-}$ mice, and J$\alpha18^{-/-}$ mice receiving either wild-type or

IFN-$\gamma^{-/-}$ NKT cells. Serum cytokine levels were examined at different time points in mice reconstituted with either wild-type or IFN-$\gamma^{-/-}$ NKT cells.

To examine the ability of previously primed DCs to activate naïve NK and NKT cells, splenic DCs ($CD11c^{+}$ $NK1.1^{-}$) were isolated from mice that had received either unloaded DCs or α-GalCer-loaded DCs three days prior. Surface expression of CD1d, CD40, CD80, and CD86 were examined by flow cytometry. Isolated DCs ($5x10^6$) were adoptively transferred into mice 2 hours prior to α-GalCer treatment (i.p. 4ug). Serum and intracellular cytokine levels in NK and NKT cells were examined 2 hours after stimulation.

B16 melanoma liver metastasis model.

Naïve, expanded wild type, or expanded IFN-$\gamma^{-/-}$ NKT cells (i.v. $3x10^6$) were adoptively transferred into J$\alpha18^{-/-}$ mice (C57BL/6 background). Seven days after transfer, $2.5x10^5$ B16-F10 melanoma cells were aseptically inoculated into the spleens of control and NKT cell recipient mice [134]. Mice were anesthetized with 2-3% isoflurane and the left abdominal area was shaved. The shaved area was cleaned with 70% ethanol, followed by 1% iodine (Rougier Pharma, Mirabel, QC). A longitudinal incision was made in the skin, and a small incision was made into the peritoneal wall. The spleen was exteriorized and B16 cells (in 50 µl saline) were injected into the spleen using a 30g needle. The peritoneal cavity was closed using a 4-0 Polysyn suture (Angiotech: Reading, PA). The skin was sutured using a 5-0 polypropylene suture (Ethicon, Somerville, NJ). Mice were treated with 0.05 mg/kg buprenorphine (Temgesic, Schering-Plough, Kenilworth, NJ) as an analgesic and placed in a clean recovery cage.

Fourteen days after tumor cell injection, mice were sacrificed and images of the anterior and posterior surface of each liver were acquired using a QImaging Micropublisher 3.3 digital camera (Surrey, BC) and QCapture (v.2.8.1) software. The relative tumor coverage on the anterior and posterior surfaces was analyzed using Image J software (National Institutes of Health, Bethesda, MD) [134].

NKT cell reconstitution in Jα18$^{-/-}$ mice.

To examine whether expanded NKT cells could be used to reconstitute NKT cell deficient mice, NKT cells were expanded in congenic CD45.1 mice using α-GalCer-loaded DCs. Expanded NKT cells ($10x10^6$) were isolated and injected i.v. into Jα18$^{-/-}$ mice, where CD45.1 could be used to track transferred NKT cells. NKT cell reconstitution was examined at day 7 and day 30. To improve reconstitution, recipient mice were sub-lethally irradiated (750 rads (7.5 Gray); Gammacell 3000 from Nordion, Ottawa, ON) two days prior to adoptive transfer of CD45.1 congenic NKT cells. NKT cell frequency and phenotype were analyzed 7 and 30 days post-transfer. Functional NKT cell responses were examined by measuring serum IL-4 and IFN-γ levels at 2, 6 and 24 hours after α-GalCer treatment (i.p. 4 μg). In other experiments, B16-F10 cells ($2.5x10^5$) were aseptically inoculated into the spleen of age and sex matched wild-type C57BL/6 mice, Jα18$^{-/-}$ mice or irradiated Jα18$^{-/-}$ mice reconstituted 30 days earlier with either wild type or IFN-γ$^{-/-}$ NKT cells. In some groups, α-GalCer (i.p. 4μg) was administered 24 hours post tumor inoculation. Tumor metastasis was examined on day 14.

4T1 primary mammary tumor resection model.

4T1 cells were harvested in the logarithmic growth phase using trypsin-EDTA (Sigma-Aldrich). Cells were resuspended in saline and $2x10^5$ cells (50 μl volume) were

injected subcutaneously (s.c.) into the fourth mammary fat pad of female BALB/c mice. Primary mammary tumors were resected 12 days after tumor cell injection when the primary tumors reached ~200 mm^3 in size [299]. Primary subcutaneous tumor excision was performed aseptically in anesthetized mice (inhaled isoflurane). The abdominal fur around the tumour site was shaved with Oster small animal trimmers with 3 cm margins. The surgical region was wiped with 70% ethanol, followed by iodine and again with 70% ethanol. The tumor and subcutaneous fat tissue were surgically resected and the skin was sutured together using a 5-0 polypropylene suture (Ethicon, Somerville, NJ). Mice received a subcutaneous treatment of 0.05 mg/kg buprenorphine (BCM Corporation; Bloomingdale, NJ) as analgesic. Animals were transferred to clean cages and allowed to recover for 2-4 hours on a 42^oC heating pad.

4T1 post-surgical NKT cell immunotherapy.

To examine whether NKT cell activation using α-GalCer-loaded DCs could protect mice against metastatic disease, mice received α-GalCer-loaded DCs ($2x10^5$) intravenously (i.v.) on day 13 (one day following tumor resection). To examine whether multiple NKT cell activation treatments would further enhance protection, mice received α-GalCer-loaded DCs ($2x10^5$) on day 13 and day 34. To monitor immune activation, serum cytokine levels were collected at various time points following stimulation. IFN-γ and IL-4 levels were determined via ELISA (eBioscience). Lung metastasis was examined using a clonogenic plating assay (details below), and in separate experiments we examined the survival advantage of NKT cell activation therapy.

Clonogenic assay for 4T1 cell metastasis.

The clonogenic assays were performed as previously described [299], with some modifications. To quantify lung metastasis at different time points, the lungs were harvested and dissociated by mechanical dispersion through a sterile 40 micron nylon mesh. Cells were washed, centrifuged at 300g for 8 minutes, and resuspended in 5 ml of clonogenic assay media (RPMI-1640 supplemented with 10% FBS, 100 μg/mL streptomycin, and 100 units/mL penicillin, 20 nM HEPES, 60 μM 6-Thioguanine).

For experiments in Chapter 4, different volumes (1 ml, 500 μl, and 200 μl) of the cell suspension (5 ml total) were plated in 10 ml of clonogenic assay media. Plates were incubated for 10-14 days at 37^{o}C with 5% CO_2. To enumerate 4T1 colonies, plates were fixed with 10 ml 95% methanol for 5 minutes, rinsed twice with 5 ml distilled water, and stained with 0.03% methylene blue for 5 minutes. Plates were rinsed again with 5 ml of distilled water and allowed to dry overnight. Colony forming units (CFU) in whole lung tissue was calculated as: (5 x # colonies in 1 ml plate + 10 x # colonies on 500 μl plate + 25 x # colonies on 200 μl plate)/3.

To reduce the time, cost, and space required for the clonogenic assay, we made some adjustments to the clonogenic assay protocol. For experiments in chapters 5 and 6, the lungs were resuspended in 5ml of media. Different dilutions (100 μl, 50 μl and 25 μl) of the lung cell suspension were added to 24 well plates in a final volume of 500 ul. After 7 days in culture, cell colonies were fixed with 1 ml 95% methanol for 5 minutes, washed twice with 1 ml of distilled water, and stained with 500 μl of 0.03% methylene blue. The number CFU were counted using an automated immunospot colony-counting program (Cellular Technologies Limited).

MDSC isolation and characterization.

To characterize circulating MDSCs in the 4T1 model, blood was obtained at different time points via submandibular venipuncture: 70 µl of blood was collected in 10 µl of heparin (10,000 U/ml; Sigma-Aldrich). RBC lysis was performed by adding 2 ml of lysis buffer for 1 minutes and neutralized by adding an equal volume of PBS. Samples were centrifuged for 5 minutes at 300g, supernatant was discarded and the blood leukocytes were resuspended in 200 ul of HBSS. Blood leukocytes were used for cytospin preparations, flow cytometry ($Gr1^+$ $CD11b^+$), or T cell suppression assays.

Blood leukocyte cytospins.

Cytospins were performed using a Shandon Cytospin III (Bohemia, NY). Silanized slides (Ultident Scientific; St. Laurent, QC) were centrifuged at 500g for 2 minutes with 50 µl HBSS loaded to pre-wet the slides. Prepared blood leukocytes (~ 1 x 10^5 – 3 x 10^5 cells) were centrifuged with low acceleration for 5 minutes at 300g. Slides were dried at room temperature. Samples were fixed for 3 hours in 10% acetate buffered formalin and stained with hematoxylin and eosin (H&E) (Thermo-Scientific). Slides were examined and photographed with a Zeiss Axiovert 200M microscope with a Hamamatsu Orca R2 Camera (Toronto, ON) at 1000x magnification.

Examining the frequency of MDSCs by flow cytometry.

The frequency of MDSCs ($Gr1^+$ $CD11b^+$) populations in the blood were examined by flow cytometry. Submandibular venipuncture was performed once a week and blood leukocytes were isolated and antibody staining was performed as described above.

T cell suppression assay.

To test immunosuppressive activity of blood MDSCs, 70 µl of blood was drawn from naïve mice and tumor-resected mice receiving different treatments (day 35). Blood leukocytes were resuspended in 200 µl RPMI following RBC lysis, and 50 µl was added to each well in a round bottomed 96 well plate. Responder splenocytes were isolated from the spleens of naïve mice by mechanical dispersion through wire mesh followed by RBC lysis. Responder cells were labeled with 5 µM Oregon green (Life Technologies) and resuspended in RPMI-1640 (supplemented with 100 µg/mL streptomycin, and 100 units/mL penicillin, 10% FBS and 1% HEPES). Responder cells ($2x10^5$) were combined in wells with blood leukocytes from tumor-resected animals. Proliferation was induced by adding T-Activator anti-CD3/28 Dynabeads (Life Technologies) in a ratio of 1 bead: 2 splenocytes. Samples were incubated at 37^oC 5% CO_2 for 72 hours. Responder cell proliferation was measured by flow cytometry, gating on $TCR\beta^+$ cells and assessing cell division by Oregon green dilution.

To examine the direct effects of NKT cell activation on MDSC suppressive function and the ability of MDSCs to inhibit proliferation of activated NKT cells, we added $1x10^5$ NKT cells labeled with eFlour 670 (eBioscience) to the T cell suppression assay outlined above. Both T cell and NKT cell proliferation were simultaneously monitored via Oregon Green 488 and eFlour 670 dilution, respectively.

Examining the effect of NKT cell activation on MDSCs in vivo.

To determine whether activated NKT cells directly influence MDSC frequency *in vivo*, mice were inoculated with $2x10^5$ 4T1 cells in the mammary fat pad. Once tumors

were palpable (day 7), α-GalCer-loaded DCs were administered to activate NKT cells. Primary tumor growth and blood MDSC frequency were monitored.

Immune function assays.

To characterize whether NKT cell activation induced $CD8^+$ T cell and/or NK cell mediated anti-tumor immunity, $CD8^+$ $TCR\beta^+$ T cells and $CD49b^+$ $TCR\beta^-$ NK cells were isolated and cultured in a 1:1 ratio with Oregon Green-labelled 4T1 target cells. Cells were cultured in complete RPMI for 4 or 18 hours. Following incubation, supernatants were collected for analysis of IFN-γ levels. Cytotoxicity against 4T1 cells was determined by flow cytometry via staining of Oregon green labeled 4T1 cells with APC-Annexin V and 7-amino-actinomycin D (7-AAD).

VSVΔM51 and reovirus production.

VSVΔM51-expressing luciferase (VSVΔM51-luc) and VSVΔM51-expressing green fluorescence protein (VSVΔM51-GFP) were kindly provided by Dr. Douglas Mahoney (University of Calgary) and were propagated in the lab for experiments. Vero cells were plated in T-175 flasks, grown to 80% confluence and infected with VSVΔM51-luc or VSVΔM51-GFP at a multiplicity of infection (MOI) of 0.1. After 24-48 hours, the supernatant containing VSV was collected and centrifuged at 500g for 5 minutes to pellet cell debris. The supernatant was collected in a 30 ml syringe and filtered through a 0.2 micron filter. The filtrate was gently layered onto a 20% sucrose solution. After ultracentrifugation for 1.5 hours (36 000rpm), the pellet was resuspended in 15% glucose, aliquoted and stored at -80^{o}C. Reovirus (Dearing strain, T3D) was kindly supplied by Dr. Patrick Lee (Professor Emeritus, Dalhousie University) and a fresh batch

was provided every 3 months. VSVΔM51 and reovirus infectivity were determined by standard plaque titration.

Plaque titration assay.

Plaque assays for VSVΔM51 and reovirus were conducted using Vero cells and L-292 cells, respectively. A 10-fold serial dilution (10^{-6} to 10^{-10}) of the virus stock was prepared in cold DMEM. Vero cells or L-292 cells were cultured to confluence in 12-well tissue culture plates, the media was aspirated and 100µl of the serially diluted virus was added to each well in duplicate. Cells were incubated at 37ºC, and 5% CO_2 for 2 hours with gentle shaking every 30 minutes, and unbound viruses were removed by washing two times in DMEM. Following virus infection, 1 ml of 1% agarose overlay (for a 12 well plate make up 3.75 ml of 4% agarose in DMEM, 0.75 ml of FBS, and 10.5 ml of DMEM) was added to each well. Cells were incubated undisturbed for 48 hours at 37ºC, and 5% CO_2. The agarose was removed and the cells fixed in 10% formaldehyde (Fisher Scientific) for 20 minutes and stained with 1% crystal violet (Sigma Aldrich). Plaques were counted for each dilution and virus titer was determined by multiplying the number of plaques by the dilution factor.

Virus titre = (number of plaques in duplicate wells/2)/ (inoculum volume x dilution used)

VSVΔM51 and reovirus infectivity on 4T1 cells.

To determine whether VSVΔM51 or reovirus can infect 4T1 cancer cells, $2x10^5$ cells were cultured in 6 well plates and infected with either VSVΔM51-GFP or reovirus at an MOI of 10. UV irradiated virus was used as control. After 24 hours, cells were fixed in 4% PFA. For reovirus intracellular staining, the cells were washed and resuspended in

intracellular staining buffer (PBS containing 0.5% bovine serum albumin, 0.1% saponin, 20mM NaN_3). Non-specific binding sites were blocked with 10% goat serum for 20 minutes, followed by staining with a rabbit polyclonal anti-reovirus serum (1/2000) (kindly provided by Dr. Patrick Lee, Dalhousie University) for 30 minutes at 4°C. Cells were washed with intracellular staining buffer and incubated for 20 minutes in goat anti-rabbit Alexa Flour 488 (1/4000, Molecular Probes). Cells were washed with intracellular staining buffer and resuspended in 1% PFA prior to data acquisition by flow cytometry (FACSCalibur).

Cell viability assay.

To examine whether gemcitabine (Hospira) or mafosfamide (4-sulfoethylthio-cyclophosphamide, active analog of cyclophosphamide) (Toronto Research Chemicals) had direct cytotoxic effects on 4T1 cells, an MTT assay (Life Technologies) was used. 4T1 carcinoma cells ($5x10^3$ per well) were cultured overnight in 96 well plates, and then treated with different concentrations of gemcitabine or mafosfamide for 24, 48 or 72 hours. In other experiments, the ability of chemotherapeutics to disrupt colony formation was tested. 4T1 cells were plated at $2.5x10^3$ per well in 24 well plates and treated with different concentrations of gemcitabine or mafosfamide for 24, 48 or 72 hours. Tumor colonies were fixed with methanol and stained with 0.03% methylene blue. Colonies were counted using an automated immunospot colony-counting program (Cellular Technologies Limited).

To examine the effect of VSVΔM51 and reovirus on 4T1 cell viability, we used an MTT assay (Life Technologies). MTT solution was prepared in PBS at a stock concentration of 5 mg/ml. 4T1 carcinoma cells were cultured overnight in 96 well plates

at a concentration of $5x10^3$ per well. Cells were treated with varying MOI for 24, 48, and 72 hours. UV irradiated virus (UV-VSVΔM51 or UV-reo) was used as a control. Two hours prior to the endpoint, 20 ul of the MTT reagent was added to each well. At the experimental endpoint, cells were spun down at 1400x g, 4°C for 5 minutes. Supernatant was discarded and 100 ul of DMSO was added to each well, the plate was wrapped in foil and placed on an orbital shaker for 10 minutes. The absorbance reading was performed using an Epoch microplate spectrophotometer (BioTek) at an optical density of 590 nm.

Effect of VSVΔM51 infection on mRNA expression levels.

To examine the effect of VSVΔM51 on tumor-derived cytokines and markers of antigen presentation, 4T1 cells were infected with VSVΔM51 or reovirus (MOI= 1) for 24 hours prior to RNA isolation. Total RNA was isolated using an RNeasy Plus Mini kit (Qiagen) and cDNA was prepared using the advanced cDNA synthesis kit (Wisent Bio). For reverse transcription, 200 ng of RNA was used. Quantitative polymerase chain reactions were performed in duplicate using 1 μl of cDNA and Quantifast SYBR Green (Qiagen). Data were collected on an RG-6000 Rotor-Gene (Corbett Research) and analyzed using the 2−ΔΔCT relative quantification technique and expressed relative to an internal normalizing mRNA [311]. High-stringency primer pairs were used for transporter associated with antigen processing *(tap)-1, tap-2, ccl3, ccl4, ccl5, ccl8, cxcl2, cxcl9, cxcl10, cxcl10, cxcl16, cx3cl1, gapdh, ifn-α, ifn-β, Il-6, tnf* (Table 3). Primer performance was validated using a melting curve analysis.

Expression of MHC I, MHC II, and CD1d on 4T1 cells.

Cancer cells evade detection by the immune system through downregulation of antigen presentation [38,70]. To examine the effect of chemotherapy or oncolytic viruses on

expression of antigen presentation molecules *in vitro*, the expression of CD1d, MHC I, and MHC II on the surface of 4T1 cells was assessed by flow cytometry after treatment with vehicle, gemcitabine, mafosfamide, VSVΔM51 (MOI = 1).

Table 3. List of primers

Gene of interest	Orientation	Sequence
arginase 1	Forward	AGCTGGCTGGTGTGGTGGCAGAGGTCCA
	Reverse	GGGTGGACCCTGGCGTGGCCAGAGATGCT
ccl3	Forward	TGCCTGCTGCTTCTCCTACA
	Reverse	TGGACCCAGGTCTCTTTGGA
ccl4	Forward	CCAGGGTTCTCAGCACCAA
	Reverse	GCTCACTGGGGTTAGCACAGA
ccl5	Forward	CTCACCATATGGCTCGGACA
	Reverse	CTTCTCTGGGTTGGCACACA
ccl6	Forward	GCAGTGCTTCTTTGCCTGCT
	Reverse	ACAGCTTCCATGGGGCACT
cxcl2	Forward	GGCTGTTGTGGCCAGTGAA
	Reverse	GCTTCAGGGTCAAGGCAAAC
cxcl9	Forward	TGGGCATCATCTTCCTGGAG
	Reverse	CCGGATCTAGGCAGGTTTGA
cxcl10	Forward	CCTCATCCTGCTGGGTCTG
	Reverse	CTCAACACGTGGGCAGGA
cxcl11	Forward	CGGGATGAAAGCCGTCAA
	Reverse	TATGAGGCGAGCTTGCTTGG
cxcl16	Forward	CAACCCTGGGAGATGACCAC
	Reverse	CTGTGTCGCTCTCCTGTTGC
cx3cl1	Forward	CCACTGCAGATCCCCAGAAA
	Reverse	GCGGAGGCCTTCTACCATTT
gapdh	Forward	TGCACCACCAACTGCTTAG
	Reverse	GGATGCAGGGATGATGTTC
ifn-α	Forward	GGACTTTGGATTCCCGCAGGAGAAG
	Reverse	GCTGCATCAGACAGCCTTGCAGGTC
ifn-β	Forward	CCCTATGGAGATGACGGAGA
	Reverse	ACTTGAGGTGGTCGTCTGTC
Il-6	Forward	GAGGATACCACTCCCAACAGACC
	Reverse	AAGTGCATCATCGTTGTTCATACA

Table 4. List of primers

Gene of interest	Orientation	Sequence
mcsf	Forward	CATCCAGGCAGAGACTGACA
	Reverse	CTTGCTGATCCTCCTTCCAG
tap 1	Forward	CTGTTCAGGTCCTGCTCTCC
	Reverse	CCACAAGGCCTTTCATGTTT
tap 2	Forward	GCTGTGGGGACTGCTAAAAG
	Reverse	GCAGAAGCCACTCGGACTAC
tgf-β	Forward	TAAAATCGACATGCCGTCCC
	Reverse	GAGACATCAAAGCGGACGAT
tnf-α	Forward	CACGTCGTAGCAAACCACCAAGTGGA
	Reverse	TGGGAGTAGACAAGGTACAACCC

Cell surface CALR translocation.

To examine the effect of chemotherapies or VSVΔM51 on markers of immunogenic cell death (CALR, HMGB1 or ATP), we performed the following experiments. To fluorescently mark the ER, 4T1 cells were stably transduced with a luminal ER marker mCherry-KDEL [312]. Cells were cultured on coverslips overnight prior to treatment with gemcitabine (10 ng/ml) or mafosfamide (5 ug/ml) for 4 hours. To examine the effect of VSVΔM51-GFP on CALR translocation, 4T1 cells were infected with VSVΔM51 at an MOI of 10 and incubated for 8 hours prior to fixation. Cells were fixed with 0.25% paraformaldehyde for 5 minutes, washed in PBS and blocking buffer, and stained with a rabbit anti-CALR antibody (Abcam, Cambridge, MA) for 30 minutes [235]. Cells were washed and reactivity was detected following 30 minutes incubation with an anti-rabbit Alexa Flour 488 conjugated secondary antibody (Invitrogen) in the chemotherapy experiments, or anti-rabbit Alexa Flour 680 for VSVΔM51-GFP experiments. To confirm intracellular expression of CALR, untreated cells were fixed

with 4% PFA for 20 minutes, permeabilized with 0.1% Triton X-100 (BioRad) for 10 min, rinsed three times with PBS, and non-specific binding sites were blocked with 10% FBS for 30 minutes. Primary antibody was added for 1 hour. Subsequently, cells were washed twice with PBS and incubated for 30 minutes in anti-rabbit Alexa Fluor 488. Confocal microscopy (Zeiss LSM 510 Meta) and flow cytometry (FACSCalibur) were used to analyze surface mobilization of CALR.

ATP and HMGB1 release assays.

Supernatants were harvested from chemotherapy treated or VSVΔM51 treated 4T1 cells at 16 hours and 24 hours for measurement of ATP and HMGB1 release, respectively [192,241]. Extracellular ATP levels were measured by the luciferin-based ATP activity assay (Calbiochem). Chemiluminescence was recorded using a Fluoroskan Ascent FL plate reader (Thermo-Scientific). HMGB1 levels were measured by ELISA (IBL international). Absorbance was measured using an Epoch microplate spectrophotometer (BioTek).

Primary 4T1 tumor model to measure *in vivo* CALR exposure and HMGB1 release following chemotherapy treatment.

4T1 cells ($2x10^5$ cells in 50 µl volume) were injected subcutaneously into the fourth mammary fat pad of female BALB/c mice. On day 12, mice received a single intraperitoneal injection of 30 mg/kg gemcitabine or 24 hours of treatment with 20 mg/kg/day cyclophosphamide (Sigma-Aldrich) in their drinking water. The doses for gemcitabine and cyclophosphamide were based on previous low-dose chemotherapy studies [313,314]. The doses and routes of gemcitabine and cyclophosphamide administration were selected based on publications that showed efficacy in cancer models without

negatively impacting the immune system. Cyclophosphamide at 20 mg/kg/day was found to be equivalent to an i.p. 100 mg/kg bolus in a study evaluating combination therapy with a peptide vaccine [315]. The dose of gemcitabine was also chosen from a metronomic study and is one-eighth the maximum tolerated dose in BALB/c mice [313]. Furthermore, this dose was selected to avoid toxicity against immune cells that was reported with i,p. 120 mg/kg [203].

Serum samples were harvested at 24 hours for analysis of HMGB1 and ATP. Primary tumors were also harvested 24 hours following treatment and dissociated into a single cell suspension by mechanical dispersion through a 70-micron sterile wire mesh. CALR expression on 4T1 cells and infiltration of $CD45^+$ $CD11c^+$ DCs were assessed by flow cytometry.

Targeting post-surgical metastasis by combining chemotherapy or oncolytic virus with NKT cell activation therapy.

Primary 4T1 tumors were induced as described above. To study metastasis, tumors were resected 12 days after 4T1 cell inoculation [165]. Mice were allowed to recover for 2 hours prior to receiving intraperitoneal injections of gemcitabine (30 mg/kg on day 12, 14, 16) or cyclophosphamide in their drinking water (20 mg/kg/day from day 12-16). On day 17, NKT cells were activated by i.v. injection of $2x10^5$ α-GalCer-loaded DCs. To examine immune activation, serum IFN-γ and IL-4 levels were determined via ELISA (eBioscience) at 2 and 24 hours following NKT cell stimulation. To examine tumor metastasis and immune phenotyping, lungs and splenocytes were harvested on day 28 for immune phenotyping.

In the oncolytic virus study, mice were allowed to recover for 24 hours following tumor resection. Mice received intravenous injections of $5x10^8$ pfu of VSVΔM51 or reovirus on day 13, 15 and 17. On day 18, NKT cells were activated by i.v. injection of $2x10^5$ α-GalCer-loaded DCs.

ID8 tumor model.

Mice were injected i.p with $3x10^6$ ID8 ovarian cancer cells. Mice received intraperitoneal injections of $5x10^8$ pfu of reovirus on day 9, 11 and 13. Ascites development was monitored.

Immune phenotyping following chemotherapy, NKT cell activation therapy or combination therapy.

In the chemotherapy studies, immune phenotyping was done on day 28 following initial tumor cell inoculation, splenocytes were isolated by mechanical dispersion through wire mesh followed by RBC lysis. The frequencies of $CD4^+$ T cells, $CD8^+$ T cells, and $TCR\beta^+$ $CD4^+$ $CD25^+$ $FoxP3^+$ regulatory T cells (T-regs) were examined, along with expression of the cell surface activation marker CD69. To monitor intracellular cytokine polarization, cells were re-stimulated for 4 hours with 50 ng/ml phorbol 12-myristate 13-acetate (Sigma-Aldrich) and 1 μg/ml ionomycin (Sigma-Aldrich) in the presence of the secretion inhibitor Brefeldin A (BioLegend). Surface stained cells were fixed and stained for intracellular IL-17A, IFN-γ, or granzyme B.

Statistical analysis.

Data are expressed as mean ± standard error of the mean unless otherwise stated. A non-parametric two-tailed Mann-Whitney *U* test was used to compare between two

data groups. Comparisons between more than two data groups were made using a Kruskal-Wallis non-parametric ANOVA with Dunn's post-test. Survival data was analyzed by log-rank (Mantel–Cox) significance test. Statistical significance was set at $p < 0.05$. For survival data comparing multiple pairs of treatment groups, the statistical significance level was set using the Bonferroni corrected threshold ($p < (0.05/K)$, where K is the number of comparisons being performed. Statistical computations were carried out using GraphPad Instat 3.02 and GraphPad Prism 5.

Chapter 3: Developing novel tools for evaluating the role of NKT cells in cancer control.

This work appears in part in the publication:

Gebremeskel S, Slauenwhite D, Johnston B. 2016. Reconstitution models to evaluate natural killer T cell function in tumor control. *Immunology and Cell biology*. 94(1):90-100. doi: 10.1038/icb.2015.67.

Contributions:

SG- designed the study, carried out experiments, analyzed data and prepared the manuscript.

DS- assisted with experimentation and data collection.

BJ- assisted with study design and critical review of the manuscript.

The NKT cell deficient Jα18$^{-/-}$ mouse is a common tool used to study NKT cell involvement in disease processes [309,316,317]. However, it was recently shown that Jα18$^{-/-}$ mice have a 60% reduction in overall TCRα repertoire diversity [318]. This would lead to potential defects in CD4 and CD8 T cells in the Jα18$^{-/-}$ mice. Therefore, concerns have been raised regarding the validity of studies that assess NKT cell function via comparisons of Jα18$^{-/-}$ mice with wild-type animals. One approach to validate these findings would be to reconstitute Jα18$^{-/-}$ mice with wild-type NKT cells. While there are numerous studies describing transient NKT cell reconstitutions by adoptive transfer [103,319–321], there has been little progress in the development of stable long term NKT cell reconstitutions.

One strategy to obtain NKT cells for *in vitro* assays or adoptive transfer studies is through *in vitro* NKT cell expansion [322–325]. However, many of the expansion protocols give rise to NKT cell lines that have altered phenotypes [322,323,325]. In addition, there can be significant variability in the functional responses of NKT cell lines generated in individual cultures [323]. Hence, expansion protocols that reliably generate large numbers of NKT cells that resemble normal NKT cell populations are crucial for mechanistic investigations. In this chapter, we sought to develop reliable protocols of generating functional NKT cells to be used in both *in vitro* and *in vivo* experiments.

Results:

Expansion of NKT cells following treatment with α-GalCer-loaded DCs.

Administration of free glycolipids has been shown to expand NKT cells *in vivo*[326,327]. However, these cells become anergic to further stimulation [328–330], reducing their usefulness for functional assays or adoptive transfer experiments. As NKT cell

activation with glycolipid-loaded DCs can prevent anergy [329,331], we investigated whether α-GalCer-loaded DCs could be used to expand functional NKT cells *in vivo*. Administration of α-GalCer-loaded DCs induced an initial decrease in detectable NKT cells (Fig 6A), consistent with the transient down-regulation of the TCR on glycolipid-activated NKT cells [327,332]. This was followed by a significant expansion of NKT cells in the liver, spleen, bone marrow, and thymus (Fig 6B-D), peaking around day 3 after administration of α-GalCer-loaded DCs. NKT cell numbers in the lymph nodes also increased at day 3 (Fig 6E). NKT cell expansion was followed by a contraction phase, with NKT cell frequency and number returning to near baseline levels by day 10. Administration of unloaded DCs did not alter NKT cell numbers. Thus, α-GalCer-loaded DCs transiently increased NKT cell numbers in peripheral organs, similar to direct administration of free glycolipids [326,332].

Phenotype of expanded NKT cells.

Previous studies have shown that activated NKT cells undergo phenotypic alterations in cell surface receptor expression [323,326,327,332,333], thus we compared the phenotype of naïve and expanded NKT cells. The frequency of $CD4^+$ NKT cells remained unchanged (Fig 7A). However, a sharp reduction in the expression of NK1.1 and CD69 was observed on expanded NKT cells (Fig 7A), which corresponds with an activated phenotype [326,327,332]. Consistent with the ability of α-GalCer-loaded DCs to spare NKT cells from anergy [329,331], the expression of PD-1 was low on expanded NKT cells (Fig 7A).

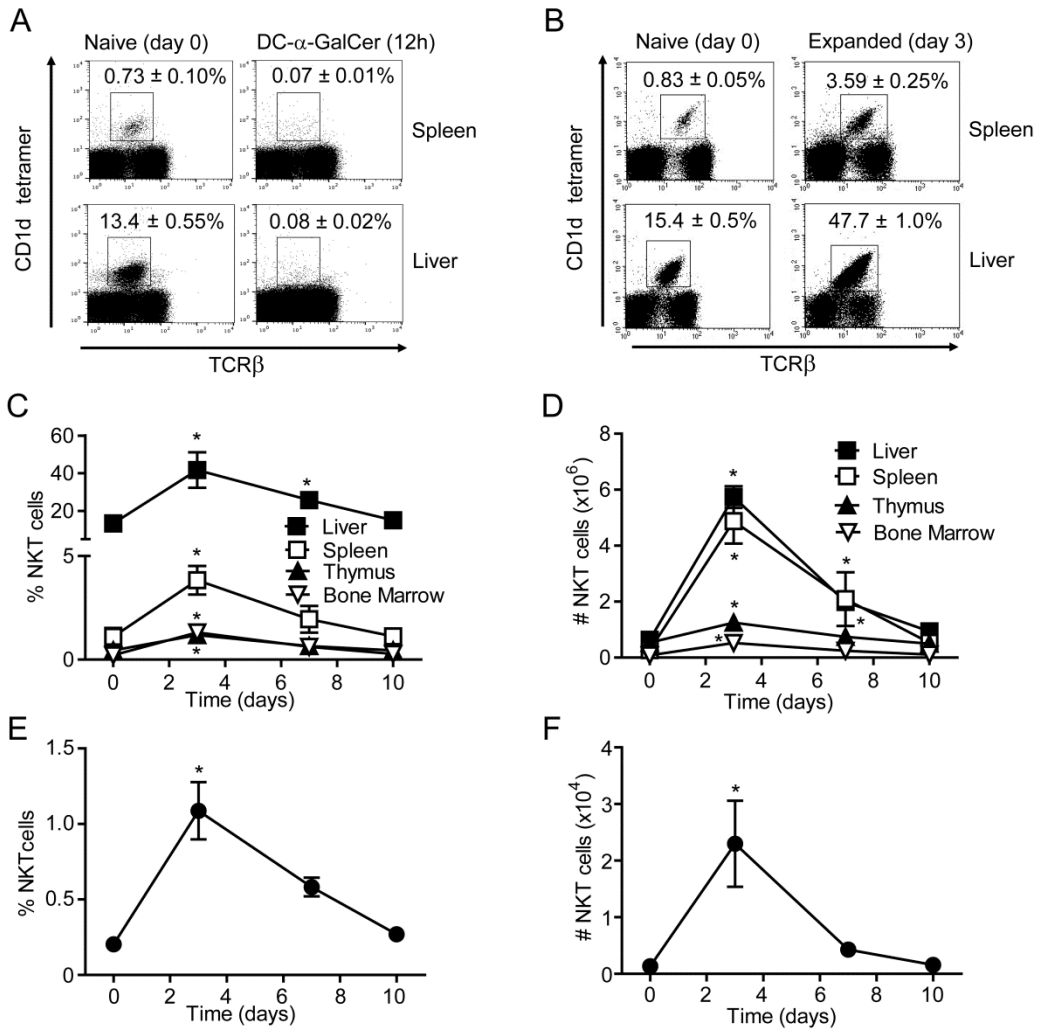

Figure 6. NKT cell expansion following stimulation with α-GalCer-loaded DCs. (A-C) The frequency and (D) number of NKT cells (TCRβ$^+$ CD1d tetramer$^+$) were examined in different tissues by flow cytometry following stimulation with α-GalCer-loaded DCs (i.v. 6x10^5) (n = 3-5 mice per time point). (E) The frequency and (F) number of NKT cells (TCRβ$^+$ CD1d tetramer$^+$) in inguinal lymph nodes were determined using flow cytometry. (n = 4 per group). * $p < 0.05$ compared to naïve mice (Day 0).

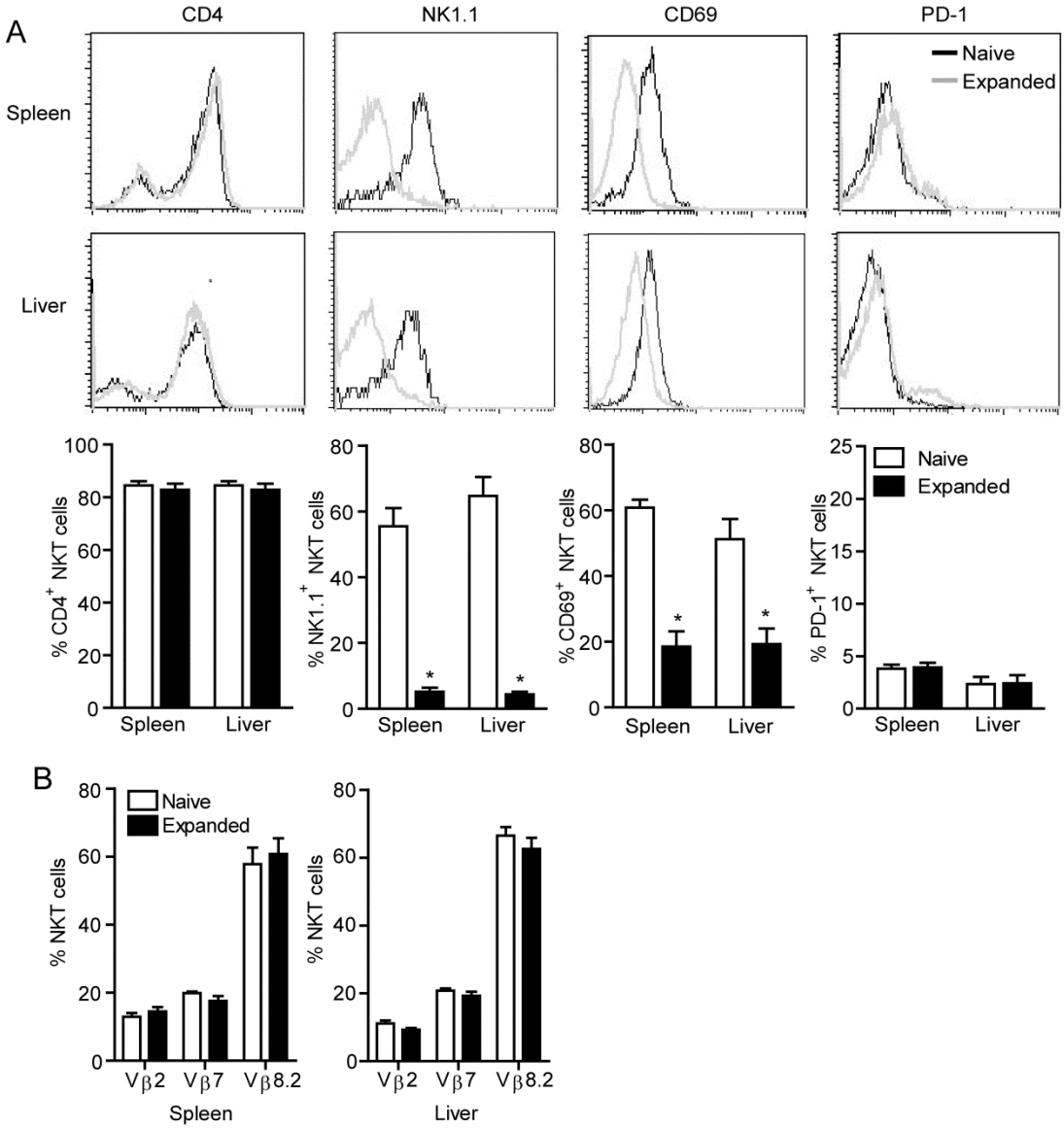

Figure 7. **Surface marker expression and TCR Vβ repertoire of expanded NKT cells.** (A) Spleen and liver lymphocytes were isolated from naïve mice and mice stimulated 72 hours earlier with α-GalCer-loaded DCs (i.v. $6x10^5$). Surface expression of CD4, NK1.1, CD69 and PD-1 were examined on NKT cells ($TCR\beta^+$ CD1d-tetramer$^+$) by flow cytometry (n =5 per group). (B) TCR Vβ chain repertoire was examined on naïve and expanded NKT cells ($CD3^+$ CD1d-tetramer$^+$) from the spleen and liver by flow cytometry (n = 3-4 per group). * $p < 0.05$ compared to NKT cells from naïve mice.

Several studies have demonstrated that the avidity of TCR for glycolipid/CD1d complexes is partly dependent on the variable regions of the TCRβ chain, implicating TCRβ restriction in biological responses of NKT cells [334–336]. *In vitro* expansion of NKT cell lines has been shown to skew the TCR Vβ repertoire [323,325], suggesting that these methods promote the emergence of NKT cell clones with altered affinities. Therefore, we investigated whether *in vivo* expansion of NKT cells caused a skewing of the TCR Vβ repertoire. Compared to naïve NKT cells, the frequencies of Vβ2, Vβ7, and Vβ8.2 usage remained unaltered in *in vivo* expanded NKT cells (Fig 7B), suggesting a potential for conserved ligand affinity.

Expanded NKT cells are hyper-responsive to re-stimulation.

To examine responsiveness of expanded NKT cells to re-stimulation, we examined IFN-γ and IL-4 production following primary (naïve mice) or secondary (expanded mice) *in vivo* activation with free glycolipid (4 μg α-GalCer). A similar frequency of NKT cells exhibited intracellular IFN-γ and IL-4 staining 2 hours after primary or secondary stimulation with α-GalCer (Fig. 8A). Consistent with previous reports [134,165,337], high levels of IL-4 and low levels of IFN-γ were detected in serum of previously unstimulated (naïve) mice 2 hours after primary α-GalCer stimulation (Fig. 8B). However, mice that received a secondary treatment with free glycolipid 3 days after the primary stimulation with α-GalCer-loaded DCs (expanded) exhibited significantly higher levels of serum IL-4 and IFN-γ at the 2 hour time-point (Fig. 8B). Re-stimulated mice became moribund and had to be euthanized 3-5 hours after the secondary α-GalCer administration, precluding examination of later time points. It was not clear whether the early increase in serum cytokines was due to the 20-fold increase in NKT cell number,

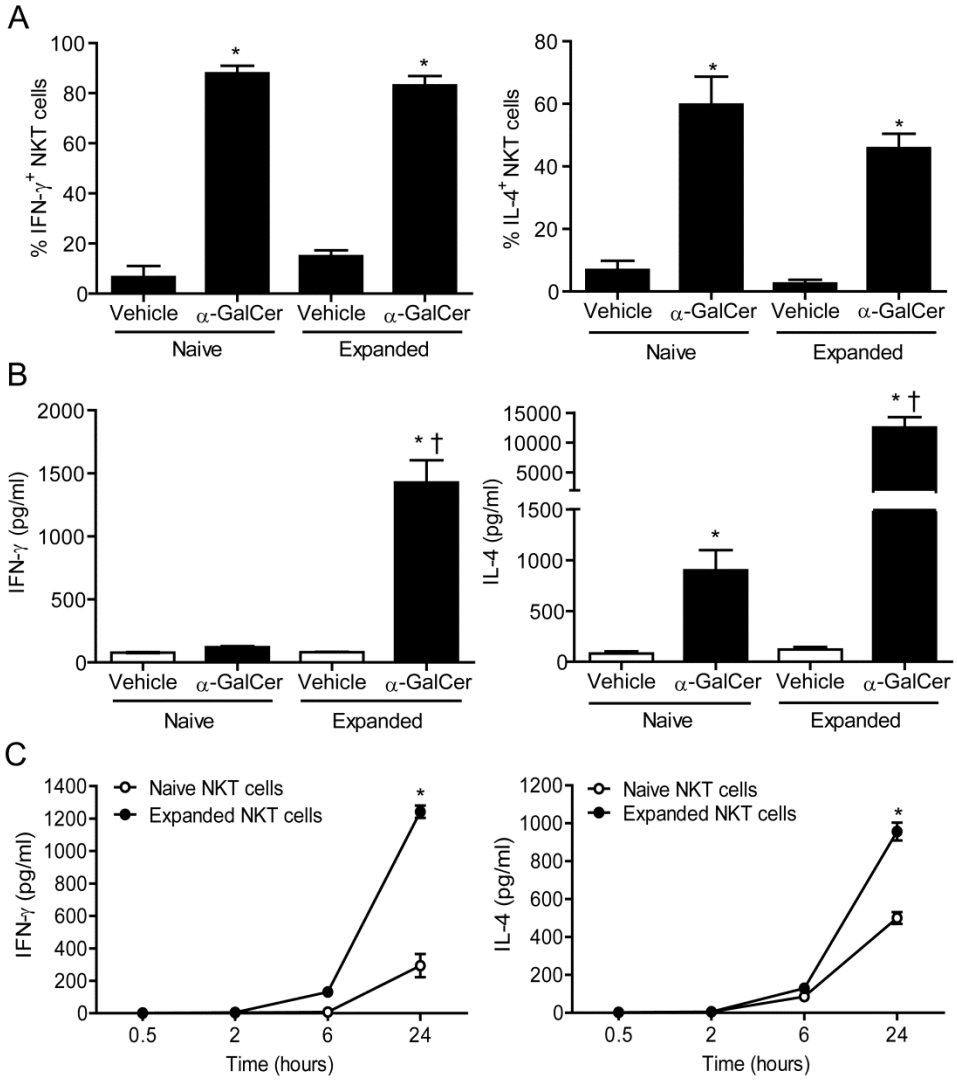

Figure 8. NKT cells expanded with α-GalCer-loaded DCs are hyper-responsive to antigenic re-stimulation. (A) Intracellular cytokine staining in liver NKT cells (TCRβ $^{+}$ CD1d tetramer^{+} cells) was examined 2 hours after stimulation of naïve mice and mice with expanded NKT cells (i.v. $6x10^5$ α-GalCer-loaded DCs 72 hours earlier) with free α-GalCer (i.p. 4 μg) (n = 3-6 per group over 3 independent experiments). * $p < 0.05$ compared to vehicle. (B) Serum cytokine levels 2 hours following free α-GalCer (i.p. 4 μg) administration in naïve mice and mice with expanded NKT cells (i.v. $6x10^5$ α-GalCer-loaded DCs 72 hours earlier) (n = 3-6 per group over 3 independent experiments). * $p < 0.05$ compared to vehicle, † $p < 0.05$ compared to naïve. (C) Cytokine production was measured in cultures containing $2x10^5$ NKT cells sorted from naïve and expanded donors. NKT cells were stimulated on anti-CD3 coated plates in media supplemented with IL-2 (n = 3 per group over 3 independent experiments). * $p < 0.05$ compared to naïve NKT cells.

priming of NKT cell function, or priming of other immune cell populations in response to the first NKT cell stimulation.

To identify whether expanded NKT cells themselves had an enhanced capacity to produce IL-4 and IFN-γ, NKT cells were sorted from naïve mice and mice stimulated 72 hours previously with α-GalCer-loaded DCs. Equal numbers of naïve and expanded NKT cells were cultured in anti-CD3 coated plates supplemented with IL-2, and supernatants were harvested for cytokine quantification. Expanded NKT cells generated more IFN-γ and IL-4 compared to naïve NKT cells (Fig. 8C). This increase in cytokine production was not due to differences in expansion of NKT cells in culture, as similar numbers of cells were harvested at the end of the study. The hyper-responsiveness of NKT cells to secondary stimulation is consistent with a previous study demonstrating that epigenetic modifications allow for enhanced NKT cell responses to re-stimulation [338].

Enhanced NK cell responses in re-stimulated mice.

NK cells did not exhibit increased intracellular IFN-γ 2 hours after primary glycolipid stimulation *in vivo* (Fig. 9A), although IFN-γ staining was observed at 6 hours (see Fig. 10B). However, NK cells in re-stimulated animals exhibited significant IFN-γ staining at 2 hours, suggesting accelerated NK cell transactivation. To determine whether primed NKT cells elicit faster transactivation of NK cells, expanded NKT cells were adoptively transferred into naïve $J\alpha18^{-/-}$ recipients and mice were stimulated with α-GalCer (Fig. 9A). There was no significant IFN-γ staining in NK cells at 2 hours (Fig. 9A), although NK cell transactivation was observed at 6 hours after α-GalCer treatment (see Fig. 10B). This suggests that the rapid NK cell transactivation response elicited by

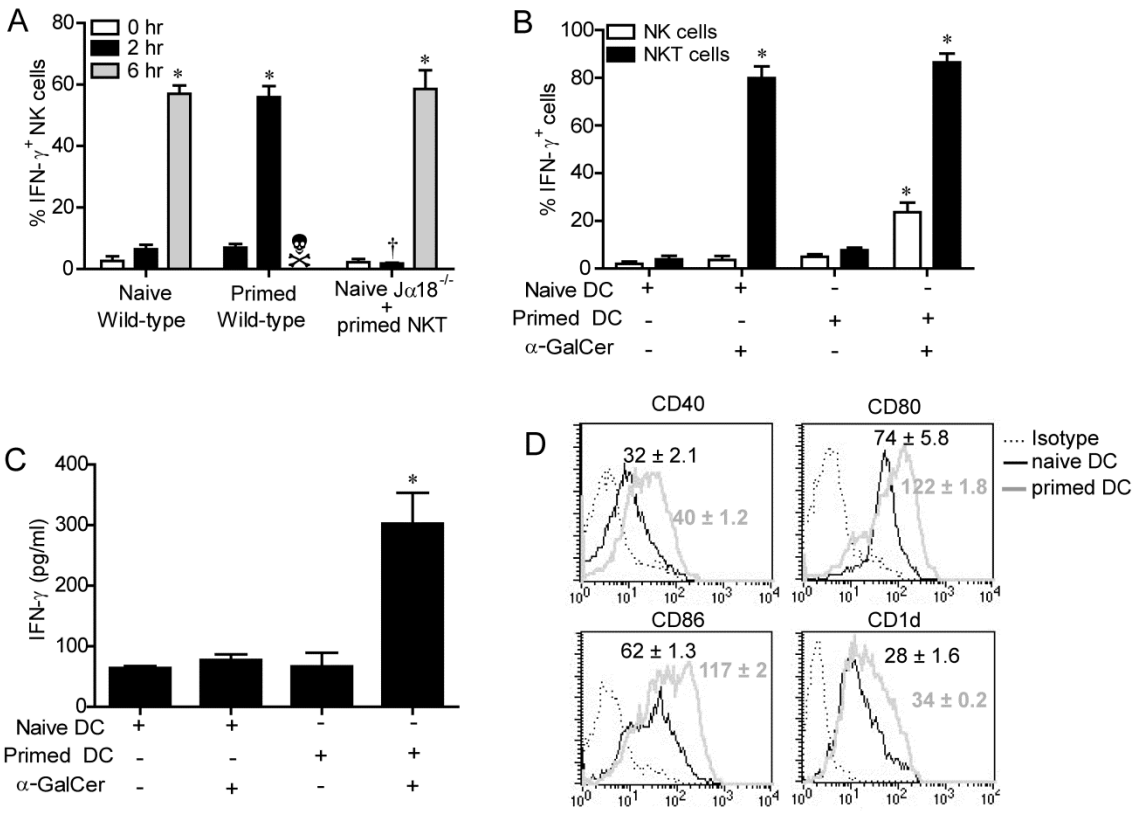

Figure 9. Mechanisms underlying early NK cell transactivation in mice re-stimulated with free α-GalCer. (A). Naïve wild-type mice, wild-type mice primed with α-GalCer-loaded DCs (i.v. $6x10^5$ DCs 72 hours earlier) to expand NKT cells, and naïve $J\alpha18^{-/-}$ mice reconstituted with expanded NKT cells (i.v. $3x10^6$ NKT cells) were stimulated with free α-GalCer (i.p. 4 μg). Intracellular cytokine staining in liver NK cells ($NK1.1^+$ $TCR\beta^-$ cells) was examined 2 hours after glycolipid stimulation (n = 4 per group over 2 independent experiments). Primed mice d Primed mice did not survive to the 6 hours time point. * $p < 0.05$ compared to unstimulated (time 0). † $p < 0.05$ compared to second stimulation in intact wild-type mice. (B, C) Naïve or primed DCs ($CD11c^+$ $NK1.1^-$) were adoptively transferred into wild-type mice 2 hours prior to α-GalCer (i.p. 4 μg) administration. (B) Intracellular cytokine staining in liver NK cells ($NK1.1^+$ $TCR\beta^-$ cells) and NKT cells ($TCR\beta^+CD1d$-$tetramer^+$) (n =4 per group over 2 independent experiments). (C) Serum cytokine levels were quantified 2h following stimulation (n =4 per group over 2 independent experiments). * $p < 0.05$ compared to DC transfer without stimulation. (D) Representative plots showing surface expression of CD40, CD80, CD86 and CD1d on $CD11c^+$ DCs from naïve and primed mice. Values on the plots indicate mean fluorescence intensity ± SEM for naïve DCs (black), and primed DCs (grey) (n =3 per group over 3 independent experiments).

the second glycolipid stimulation in intact mice was not due to NKT cell priming.

Adoptive transfer of naïve or day 3 primed DCs into naïve recipients did not increase NKT cell or NK cell activation on their own, and α-GalCer treatment induced equivalent IFN-γ staining in NKT cells following transfer of naïve or primed DCs (Fig. 9B). However, transfer of primed DCs increased the frequency of IFN-γ-positive NK cells (Fig. 9B) and serum IFN-γ levels at 2 hours after α-GalCer treatment (Fig. 9C). Compared to naïve DCs, DCs isolated from primed mice expressed higher levels of CD40, CD80, CD86, and CD1d (Fig. 9D). This suggests that the elevated serum cytokine levels and early NK cell activation in mice receiving secondary NKT cell activation are at least partly due to the ability of primed DCs to initiate rapid cellular responses. Therefore, re-stimulation of mice with expanded NKT cells resulted in enhanced cytokine production *in vivo* due to increased NKT cell number, increased cytokine production per NKT cell, and enhanced transactivation of NK cells by previously primed DCs.

Control of metastasis by expanded NKT cells.

To determine whether expanded NKT cells could functionally contribute to anti-tumor responses, we examined their effects in a model of B16-F10 liver metastasis [134,309]. Equal numbers of naïve or expanded NKT cells were adoptively transferred into Jα18$^{-/-}$ mice 7 days prior to intrasplenic inoculations with B16-F10 melanoma. Livers were harvested 14 days after tumor cell injection to evaluate metastasis (Fig. 10A). Transfer of naïve NKT cells provided partial protection in Jα18$^{-/-}$ mice, consistent with our

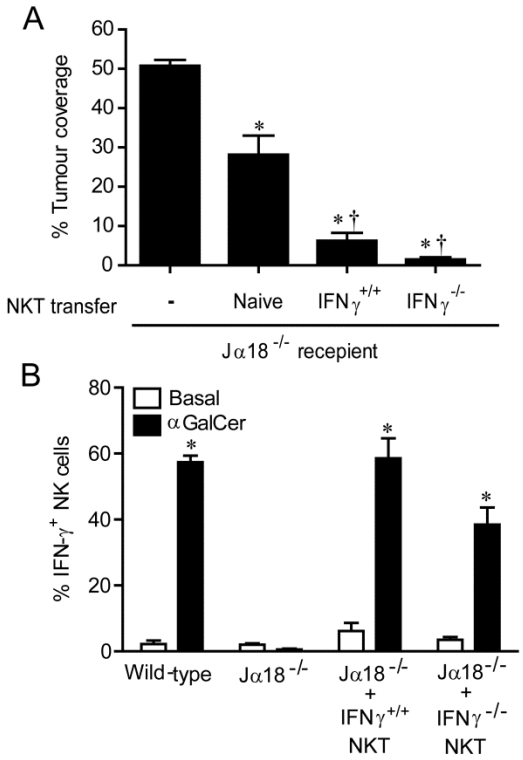

Figure 10. Expanded wild-type and IFN-$\gamma^{-/-}$ NKT cells provide enhanced protection against tumor metastasis. (A) Naïve and expanded IFN-$\gamma^{+/+}$ and IFN-$\gamma^{-/-}$ NKT cells were sorted and adoptively transferred (i.v. $3x10^6$) into NKT cell deficient J$\alpha18^{-/-}$ mice. Seven days after transfer, $2.5x10^5$ B16 melanoma cells were injected into the spleen. Liver metastasis was examined 14 days later using image analysis software to calculate the percent total liver surface area covered by metastatic B16 melanoma. (n= 4-9 per group over 2 independent experiments). * $p < 0.05$ compared to J$\alpha18^{-/-}$ mice without NKT cell transfer, † $p < 0.05$ compared to mice receiving naïve NKT cells. (B) Expanded NKT cells from IFN-$\gamma^{+/+}$ and IFN-$\gamma^{-/-}$ mice were purified and adoptively transferred (i.v. $3x10^6$) into recipient J$\alpha18^{-/-}$ mice. After 24 hours, groups of mice were treated with α-GalCer (i.p. 4 μg). Intracellular IFN-γ staining was examined in NK cells ($NK1.1^+$ $TCR\beta^-$) 6 hours after stimulation (n=5 per group over 2 independent experiments). * $p < 0.05$ compared to basal staining.

previous finding that metastasis is increased in Jα18$^{-/-}$ mice compared to wild-type animals [134]. Surprisingly, transfer of expanded NKT cells provided potent protection from subsequent metastasis without the need for additional glycolipid stimulation. The frequency of expanded NKT cells spontaneously staining for intracellular cytokines at the day of transfer (day 3 post-stimulation) was not significantly different from naïve NKT cells (Fig. 8A), suggesting that basal cytokine production did not mediate protection. However, as transferred NKT cells could have been activated to make cytokines in the recipient, we determined whether NKT cell-derived IFN-γ was required for protection from metastasis. Transfer of expanded NKT cells from wild-type or IFN-γ$^{-/-}$ mice into Jα18$^{-/-}$ mice provided equal protection against metastasis (Fig. 10A), suggesting that expanded NKT cells have enhanced immunosurveillance capacity that is not dependent on NKT cell-derived IFN-γ.

Expanded wild-type and IFN-γ$^{-/-}$ NKT cells were both able to mediate NK cell transactivation in recipient Jα18$^{-/-}$ mice following glycolipid stimulation (Fig. 10B), but did not elicit spontaneous NK cell transactivation that could account for the increased tumor control provided by expanded NKT cells. These data suggest a mechanism of increased immunosurveillance provided by expanded NKT cells that is independent from NKT cell-derived IFN-γ or an altered capacity to transactivate NK cells.

NKT cell reconstitution in Jα18$^{-/-}$ mice.

Despite the potent anti-metastatic effect observed following transfer of expanded NKT cells, there was poor reconstitution of NKT cells in the liver and spleen of recipient Jα18$^{-/-}$ mice (Fig. 11A). While transfer of NKT cells into lymphopenic mice has been previously described [319,320], there have been no objective reports describing effective

reconstitution of NKT cells to wild-type levels. We therefore determined whether non-lethal irradiation could be used to enhance stable reconstitution of NKT cells in Jα18$^{-/-}$ mice. Expanded NKT cells were adoptively transferred into normal and irradiated Jα18$^{-/-}$ mice, and reconstitution was examined 7 and 30 days later (Fig. 11A). Sublethal irradiation of recipients prior to transfer significantly improved the reconstitution of NKT cells. By day 30, the frequency and number of NKT cells, T cells, and NK cells in the livers and spleens of irradiated-reconstituted Jα18$^{-/-}$ mice were equivalent to wild-type mice (Fig. 11A-D). After 30 days, adoptively transferred NKT cells retained a normal distribution of CD4^{+} NKT cells and had reset expression of NK1.1 and CD69 to naive levels (Fig. 12A).

To determine whether the kinetics of NKT cell activation were also restored in reconstituted mice, *in vivo* NKT cell activation experiments were performed using α-GalCer. When stimulated with α-GalCer, the day 30 irradiation-reconstituted Jα18$^{-/-}$ mice exhibited serum IL-4 and IFN-γ responses that were comparable to α-GalCer-stimulated wild-type controls (Fig. 12B). This demonstrates that expanded NKT cells lost their hyper-reactivity by 30 days after stable reconstitution into Jα18$^{-/-}$ mice. In comparison, non-irradiated Jα18$^{-/-}$ mice reconstituted with NKT cells had low serum levels of IL-4 and IFN-γ following α-GalCer-stimulation (Fig. 12B), consistent with ineffective long-term reconstitution (Fig. 12A and B).

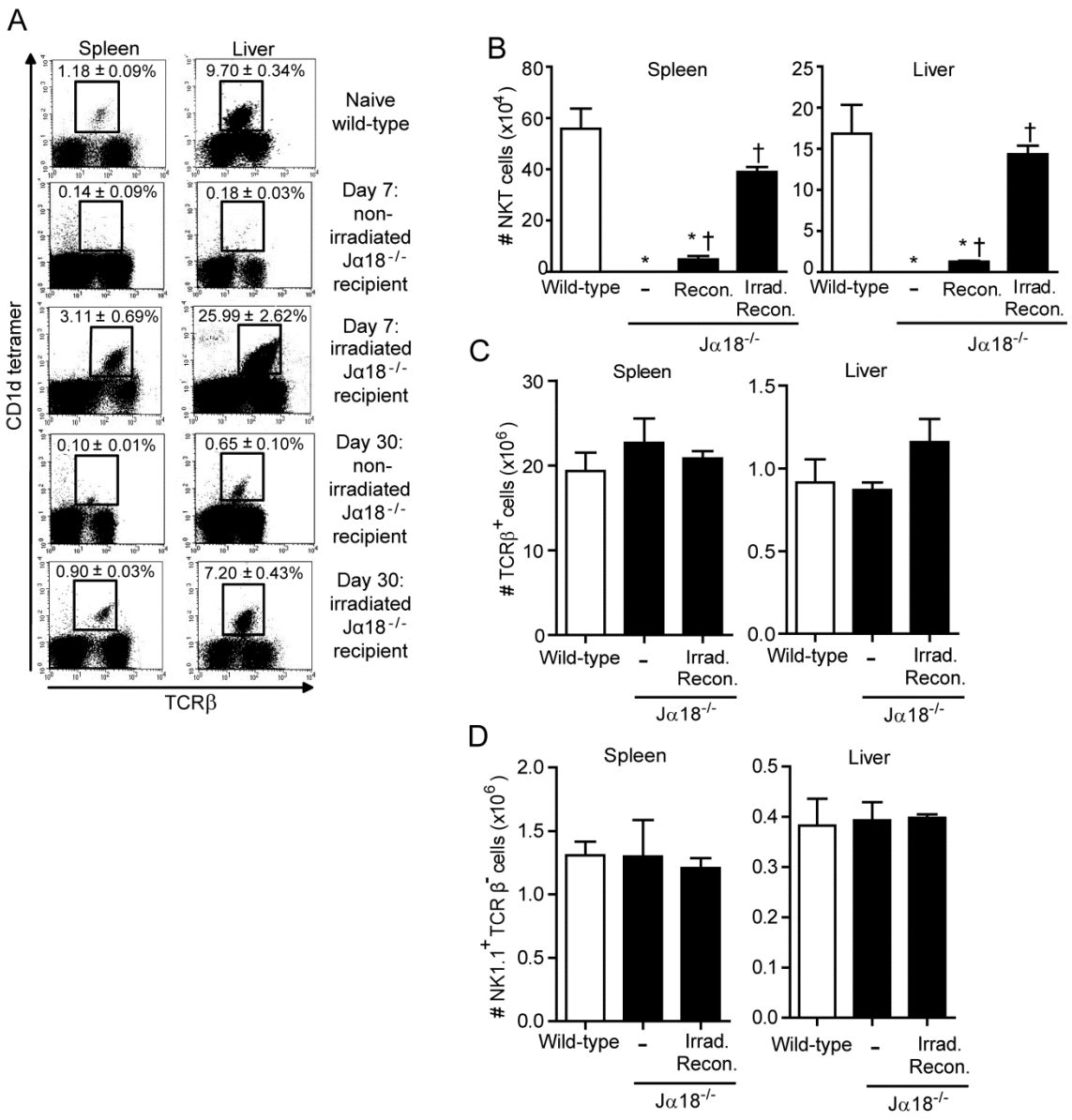

Figure 11. Long term NKT cell reconstitution in NKT cell deficient mice. Expanded NKT cells from CD45.1 congenic donor mice were adoptively transferred into recipient Jα18$^{-/-}$ mice (i.v. 10x10^6). Some groups of Jα18$^{-/-}$ recipients were sub-lethally irradiated (750 rads) 2 days prior to adoptive transfer. (A) Dot plots show the frequency of NKT cells (TCRβ$^+$ CD1d tetramer$^+$) in naïve wild-type mice and reconstituted Jα18$^{-/-}$ mice (7 and 30 days after adoptive transfer). The total number of (B) NKT cells, (C) T cells (TCRβ$^+$ CD1d tetramer$^-$), and (D) NK cells (NK1.1$^+$ TCRβ$^-$) in spleen and liver were examine by flow cytometry 30 days after adoptive transfer of expanded NKT cells (n =5-13 per group over 4 independent experiments). * $p < 0.05$ compared to wild-type (WT) mice, † $p < 0.05$ compared to Jα18$^{-/-}$ mice

.

Effective anti-tumor responses in reconstituted Jα18$^{-/-}$ mice.

To examine the function of reconstituted NKT cells further, we performed tumor metastasis experiments by inoculating B16 melanoma cells into the spleen. Consistent with our previous findings [134], tumor metastasis to the liver was greater in Jα18$^{-/-}$ mice than wild-type animals (Fig. 13A). Despite the altered TCR repertoire among T cells in Jα18$^{-/-}$ mice [318], stable reconstitution of wild-type NKT cells or IFNγ$^{-/-}$ NKT cells in these animals reduced metastasis of B16 melanoma to the levels observed in naïve wild-type mice (Fig. 13A), supporting a role for NKT cells in basal tumor immunosurveillance. The expanded NKT cells had reset from their earlier hyper-reactive state as there was no enhanced clearance of metastases compared to naïve animals. NKT cell activation with α-GalCer protected both reconstituted and wild-type mice to a similar extent, further demonstrating that reconstituted Jα18$^{-/-}$ mice closely resemble wild-type mice, and that the altered TCR repertoire in Jα18$^{-/-}$ mice does not impact the protection provided by NKT cell activation. In addition, stable reconstitution with IFN-γ$^{-/-}$ NKT cells provided equivalent protection against metastasis (Fig. 13A), demonstrating that IFN-γ production by NKT cells is not essential for α-GalCer-induced anti-tumor immunity. NKT cells and NK cells have been reported to produce IFN-γ sequentially following α-GalCer stimulation [142,166,339,340]. Consistent with this, serum IFN-γ levels in mice reconstituted with IFN-γ$^{-/-}$ NKT cells were reduced at 6 hours but not 24 hours after α-GalCer stimulation (Fig. 13B). Importantly, NKT cell derived IFN-γ was not required to elicit IFN-γ production at later time points.

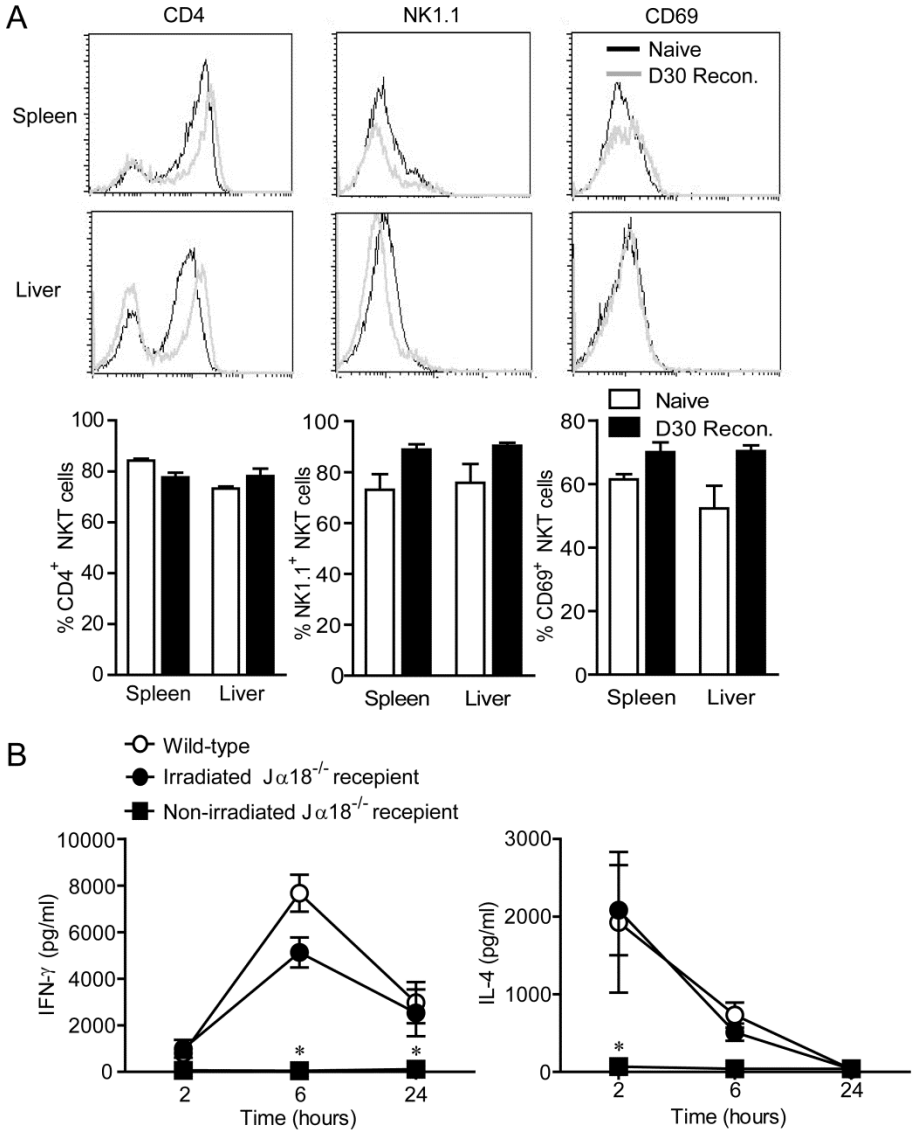

Figure 12. NKT cells in reconstituted Jα18$^{-/-}$ mice resemble naïve NKT cells at day 30. Expanded NKT cells were adoptively transferred (i.v. 10x10^6) into sub-lethally irradiated (750 rads) Jα18$^{-/-}$ mice. (A) Flow cytometry was used to examine surface expression of CD4, NK1.1, and CD69 on naïve and reconstituted NKT cells (TCRβ$^+$CD1d tetramer$^+$) (n =4-5 per group over 2 independent experiments). (B) Serum IFN-γ and IL-4 levels were measured by ELISA after treating wild-type mice and NKT cell reconstituted Jα18$^{-/-}$ mice with α-GalCer (n=5-7 per group over 3 independent experiments). * $p < 0.05$ compared to wild-type mice

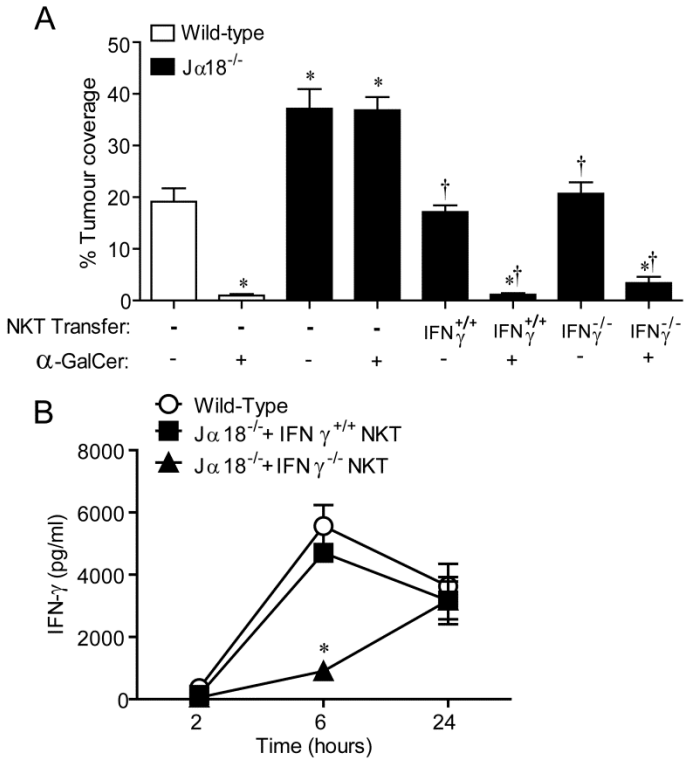

Figure 13. Stable NKT cell-reconstitution protects Jα18$^{-/-}$ mice from B16 melanoma metastasis. (A) Expanded IFN-γ$^{+/+}$ and IFN-γ$^{-/-}$ NKT cells were reconstituted into irradiated Jα18$^{-/-}$ mice for 30 days. Wild-type, Jα18$^{-/-}$, and NKT cell-reconstituted Jα18$^{-/-}$ mice were inoculated in the spleen with 2.5x10^{5} B16 melanoma cells. In the NKT cell activation groups, mice received α-GalCer (i.p. 4 μg) 24 hours after tumor cell inoculation. Liver metastasis was examined at day 14 using image analysis software to calculate the percent total liver surface area covered by metastatic B16 melanoma (n=4-8 per group over 2 independent experiments). * $p < 0.05$ compared to untreated wild-type mice, † $p < 0.05$ compared to untreated Jα18$^{-/-}$ mice. (B) Serum IFN-γ levels were measured 2, 6, and 24 hours after α-GalCer administration in wild-type mice and Jα18$^{-/-}$ mice reconstituted with IFN-γ$^{+/+}$ or IFN-γ$^{-/-}$ NKT cells (n = 4 per group over 2 independent experiments). * $p < 0.05$ compared to wild-type mice.

Discussion

Previous studies have demonstrated that it is possible to expand short lived NKT cell cultures *in vitro* [322–325] or derive long lived NKT cell hybridomas [94,341]. However, expansion and maintenance of functional murine NKT cells *in vitro* is difficult, expensive, and time consuming. Moreover, established protocols result in NKT cell lines that exhibit variable functional responses and altered phenotypes, including reduced $CD4^+$ frequency and a skewed TCR Vβ profile [322,323,325]. In this study, we demonstrate that intravenous administration of α-GalCer-loaded DCs led to the expansion of NKT cells that retained a normal phenotype (CD4 expression and TCR Vβ profile) and could be used to stably and functionally reconstitute NKT cell deficient mice.

Following administration of α-GalCer-loaded DCs, we observed a significant increase in peripheral NKT cell numbers. Expanded NKT cells exhibited reduced surface expression of both NK1.1 and CD69, consistent with the previously described NKT cell activation profile [326,327,332,333]. Some studies have described a return to baseline NK1.1 expression as early as 1 week following activation [342], while others have shown diminished NK1.1 levels up to 6 months following initial activation [329]. In cultured NKT cells, re-expression of NK1.1 and CD69 is suppressed due to the requirement for periodic re-stimulation [323,325]. However, in our adoptive transfer model, NKT cells in reconstituted mice displayed surface levels of NK1.1 and CD69 that were comparable to naive NKT cells by day 30.

In the absence of exogenous glycolipids, antigen presenting cells weakly stimulate NKT cells that express TCR Vβ2, Vβ7 and Vβ8.1/8.2 [334–336]. However, α-GalCer-loaded antigen presenting cells have the capacity to stimulate NKT cells

expressing a broader set of TCR Vβ chains: including Vβ2, Vβ6, Vβ7, Vβ8, Vβ9, Vβ10, and Vβ14 [335]. Consistent with this, Chiba et al. [323] reported outgrowth of NKT cell lines expressing Vβ6, Vβ9, Vβ10, and Vβ14 in their cultures. Others have reported outgrowth of NKT cell lines expressing primarily Vβ7 and Vβ8 [325], which may reflect weaker stimulation via the specific DC line used to expand NKT cells. In our experiments, *in vivo* expanded NKT cells maintained a TCRβ profile that was unchanged from naïve NKT cells (Fig. 7B). As bacterial glycolipids are preferentially recognized by NKT cells with certain Vβ chains [154,336], maintaining a physiological TCR Vβ profile in expanded NKT cells is an asset for studying physiological NKT cell function in culture assays and in reconstituted mice.

NKT cell activation by free α-GalCer has previously been described to generate anergic NKT cells [328–331]. However, priming NKT cells using DCs pulsed with α-GalCer preserves their ability to be re-stimulated via α-GalCer or CD3 ligation [329,331]. Consistent with this, expanded NKT cells displayed robust cytokine responses to glycolipid re-stimulation. Although epigenetic changes have been linked to NKT cell hyper-responsiveness to re-stimulation [338], we found that NKT cell responsiveness returned to normal by 30 days after stable reconstitution into Jα18$^{-/-}$ recipients, suggesting these changes are transient. Indeed, enhanced NKT cell protection against B16 was maintained at 10 days after α-GalCer stimulation [343], a time frame consistent with our transfer experiments with expanded NKT cells (Fig. 10). However, 30 days following adoptive transfer experiments, reconstituted NKT cells required glycolipid stimulation to protect mice from B16 melanoma (Fig. 13).

The generation of Jα18$^{-/-}$ mice marked an important milestone for NKT cell research [309]. However, a reduced TCR repertoire among T cells in Jα18$^{-/-}$ mice has been reported [318], suggesting that immune effects attributed to NKT cells could be the result of altered T cell-dependent antigen recognition in these animals. One way to address this issue is to reconstitute wild-type NKT cells into Jα18$^{-/-}$ mice. However, there have been no previous studies describing the successful long term reconstitution of NKT cells to wild-type levels in Jα18$^{-/-}$ mice. The reconstitution model described here provides a valuable tool to validate immunological functions attributed to NKT cells. Irradiation likely creates a reconstitution niche for NKT cells by temporarily depleting NK cells and CD8^{+} memory cells that compete for survival and expansion factors, such as IL-15 [319,344]. Although sublethal irradiation has been reported to transiently impair NK cell function [345], we found no evidence of this at 30 days after reconstitution as reconstituted mice cleared tumors as well as intact animals. It is possible that glycolipid-induced NKT cell activation overcomes any residual anergy in NK cells as cytokines have been shown to reverse NK cell anergy [346].

Using NKT cell reconstituted Jα18$^{-/-}$ mice, we found that NKT cell stimulation with α-GalCer provides protection from tumor metastasis independent from the restricted TCR repertoire in these mice. It is worth noting that tumor metastasis in the absence of exogenous glycolipid stimulation was reduced in reconstituted animals to the same level observed in wild-type mice. This is consistent with a basal role for NKT cells in immunosurveillance. NKT cells in reconstituted mice had reset to baseline function by day 30 and required glycolipid re-stimulation to induce potent tumor control. In contrast, recently expanded NKT cells elicited potent anti-tumor function 10 days after primary

glycolipid stimulation (3 days in donor plus 7 days in recipient prior to B16 administration) in the absence of additional re-stimulation. As expanded cells did not spontaneously generate more cytokines than naïve cells (Fig. 8), it is likely that they were more sensitive to endogenous activation signals or retained other effector functions that were induced by primary stimulation. For example, it is well established that NKT cells can exert direct anti-tumor immunity through TRAIL [162], perforin [102] and FASL [162], in addition to indirect anti-tumor immunity through cytokine-mediated activation of NK cells [142,166,340] and cytotoxic T lymphocytes [163,164].

Several studies have demonstrated that α-GalCer-mediated anti-tumor responses are impaired in IFN-$\gamma^{-/-}$ mice [142,166,340]. Smyth et al.[142] dissected this further and reported that IFN-$\gamma^{-/-}$ NKT cells were unable to protect recipient J$\alpha18^{-/-}$ mice from metastasis of B16 melanoma cells, suggesting that NKT cell derived IFN-γ was critical for initiating tumor control. In contrast, we demonstrate that NKT cell-derived IFN-γ is not required to provide protection from tumor metastasis. It is unclear whether differences in our findings are related to the number of transferred NKT cells ($2.5x10^5$ vs $3x10^6$ in our study), differences in markers used to isolate cell populations (NK1.1$^+$ TCR$^+$ vs CD1d tetramer$^+$ TCRβ$^+$ in our study), number of tumor cells injected ($5x10^5$ vs $2.5x10^5$ in our study) or differences in route of tumor cell administration (intravenous vs intrasplenic in our study). However, these differences are unlikely due to hyper-reactivity of expanded NKT cells as we also observed protection in stably reconstituted mice where NKT cell function had returned to baseline.

The impact of NKT cell-derived IFN-γ on NK cell transactivation is not clear. Inhibition of early IFN-γ production following α-GalCer stimulation was reported to

reduce subsequent IFN-γ production in NK cells [166,339]. Similarly, wild-type NK cells could not rescue anti-tumor responses following transfer into IFN-$\gamma^{-/-}$ mice [142]. However, neither of these experiments directly implicated NKT cells as the required source of IFN-γ. We found that IFN-$\gamma^{-/-}$ NKT cells can induce potent transactivation of NK cells and late IFN-γ production following α-GalCer treatment. This is consistent with previous reports that NK cell proliferation following α-GalCer treatment is not impacted in IFN-$\gamma^{-/-}$ mice [166,340]. This could be due to α-GalCer-mediated production of IL-12 from DCs [347], leading to IFN-γ independent activation of NK cells. Indeed, blockade of IL-12 receptors has been shown to decrease α-GalCer mediated IFN-γ production [347], implicating IL-12 as an important mediator of α-GalCer induced immune responses.

In conclusion, we have characterized a rapid and reliable method of expanding functional murine NKT cells *in vivo*. The expanded NKT cells can be successfully transferred and reconstituted into irradiated Jα18$^{-/-}$ mice, generating a normal NKT cell population that responds to glycolipid re-stimulation. This expansion and reconstitution model provides a vital tool to study NKT cell biology. For example, reconstitution of NKT cell deficient mice with wild-type NKT cells demonstrated that the altered TCR profile in these mice does not impact NKT cell-mediated tumor control. Furthermore, expanded NKT cells from IFN-$\gamma^{-/-}$ donors revealed that NKT cell-derived IFN-γ is not required for efficient control of tumor metastases or NK cell transactivation. Transfer of NKT cells deficient in other effector molecules will allow for the study of specific mechanisms through which NKT cells exert their biological effector functions in a variety of models. Such studies will ultimately lead to a better understanding of NKT cell function that will aid in the development of improved NKT cell based immunotherapies.

Chapter 4: Natural killer T cell activation overcomes immunosuppression to enhance clearance of postsurgical breast cancer metastasis in mice

This work appears in part in the publication:

Gebremeskel S, Clattenburg DR, Slauenwhite D, Lobert L, Johnston B. 2015. Natural killer T cell activation overcomes immunosuppression to enhance clearance of postsurgical breast cancer metastasis in mice. *Oncoimmunology*. 4:3 e995562. doi: 10.1080/2162402X.2014.995562.

Contributions:

SG- designed the study, carried out experiments, analyzed data and prepared the manuscript.

DC- assisted with study design, carried out experiments and analyzed data.

LL and DS- assisted with experimentation and data collection.

BJ- assisted with study design and critical review of the manuscript.

Preclinical and clinical studies have shown that NKT cell activation with exogenous glycolipids provides significant protection from tumor progression [102,159,160,173,176,348,349]. Although several studies have examined the role of NKT cell activation on primary mammary carcinoma growth [350,351], the potential therapeutic benefits of NKT cell activation in metastatic breast cancer have not been explored in detail. The aim of this work was to examine the role of NKT cell activation in a post-surgical breast cancer metastasis model.

Despite recent advances in the development of cancer vaccines and immunotherapies, tumor tolerance and immune suppression remain formidable obstacles. Tumor-derived factors disrupt normal myeloid differentiation, leading to the accumulation of heterogeneous populations of MDSCs [302,352]. As the tumor burden increases, MDSCs accumulate in a variety of tissues, where they act to enhance tumor progression and metastasis [352]. MDSCs can directly suppress $CD4^+$ and $CD8^+$ T cell responses, and indirectly promote immune suppression through the induction of T-regs [353]. Therefore, immunotherapeutic strategies that target both tumor cells and MDSCs are of particular interest. Given that NKT cells have been shown to regulate MDSC-mediated immune suppression during viral infection [172], the role of NKT cell activation on cancer-associated immunosuppression requires further investigation. In this chapter, I sought to examine the potential benefit of NKT cell activation therapy on metastatic breast cancer and to examine the interactions between activated NKT cells and tumor induced MDSCs.

Free glycolipids have been shown to have protective effects in cancer models [102,134,160]. Previous studies in the lab investigated whether administration of free α-GalCer

would yield optimal protection from tumor metastasis. Although treatment with 4 μg α-GalCer resulted in a significant reduction in tumor metastasis at early time points, this protection was lost by day 28 (Appendix 1A-B). Consistent with this, there was no increase in the survival of mice treated with free glycolipid (Appendix 1C). While dose escalation resulted in increased overall survival at the highest dose of 20 μg, this was also associated with increased mortality (Appendix 1C) and liver toxicity (Appendix 1D). In this study, I wanted to expand on these preliminary studies and examine the potential of using α-GalCer-loaded DCs to activate NKT cells.

Results:

α-GalCer-loaded DCs provide significant protection from tumor metastasis

Compared to free glycolipid administration, transfer of α-GalCer loaded DCs mediates a more Th1 skewed cytokine response and does not induce NKT cell anergy [331]. A single adoptive transfer of α-GalCer-loaded DCs to tumor-resected mice resulted in a significant reduction in tumor metastasis and a significant increase in survival (Fig 14A, B). Mice that survived to day 150 had no detectable tumor cells by clonogenic assay, suggesting they were cured of metastatic disease. Surprisingly, an additional treatment with α-GalCer-loaded DCs on day 34 did not enhance survival compared to the single treatment (Fig 14B). This was not due to anergy as the second administration of α-GalCer-loaded DCs induced serum cytokine responses that were comparable to both the initial stimulation on day 13 and primary cytokine responses in non-tumor bearing mice (Fig 14C, D).

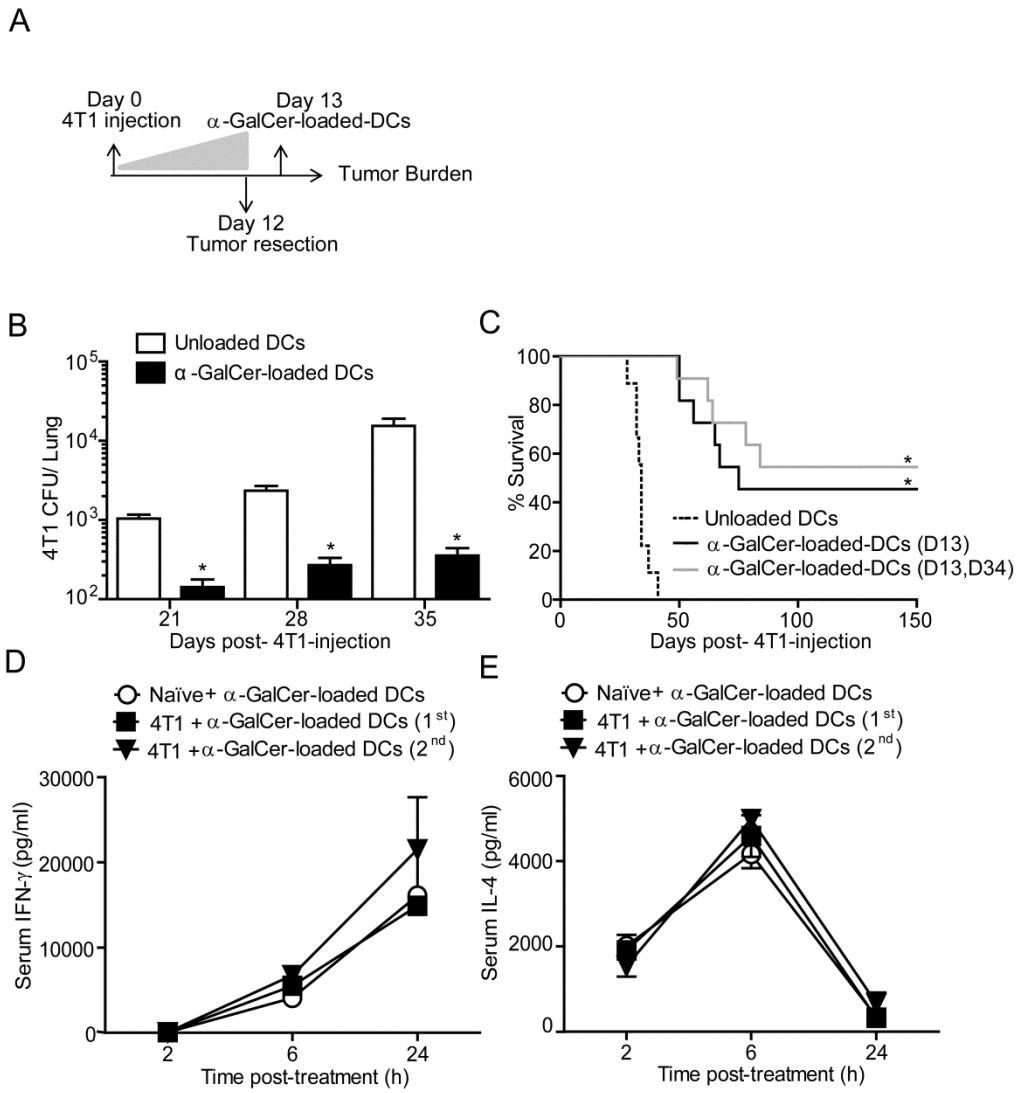

Figure 14. Treatment with α-GalCer-loaded DCs following primary 4T1 tumor resection confers long-term protection from lung metastasis. (A) Schematic of the post-surgical NKT cell activation model. Mice were inoculated with $2x10^5$ 4T1 mammary carcinoma cells and primary tumors were resected on day 12. Mice were treated on day 13, or days 13 and 34 with unloaded DCs or α-GalCer-loaded DCs (i.v. $2x10^5$ cells). (B) Number of 4T1 CFU present in lung cell suspensions isolated at day 21, 28 and 35 post-4T1 injection (n = 6-8 per group). * $p < 0.05$ compared to unloaded DCs. (C) Survival was assessed following treatment with unloaded DCs, a single treatment with α-GalCer-loaded DCs, or two treatments with α-GalCer-loaded DCs (n = 9-11 per group), * $p < 0.016$ via Bonferroni threshold analysis. Serum levels of (D) IFN-γ and (E) IL-4 were measured 2, 6 and 24 hours following the first (day 13) or second (day 34) treatment with α-GalCer-loaded DCs tumor resected mice or naïve mice (n = 3-6 per group).

As NKT cell numbers and function are reduced in many cancer patients [148,150], including breast cancer [150], the effectiveness of endogenous NKT activation could be limited. Therefore, we examined whether adoptive transfer of expanded NKT cells in combination with NKT cell activation would enhance therapeutic outcome in our mice. The adoptive transfer of expanded NKT cells alone or in combination with free α-GalCer did not enhance survival of tumor-resected mice (Table 4). NKT cell adoptive transfer combined with delivery of α-GalCer-loaded DCs also failed to enhance survival compared to treatment with α-GalCer-loaded DCs alone (Table 4).

Blood MDSC levels as a prognostic marker for NKT cell based immunotherapy

Immunosuppressive MDSCs have been shown to accumulate in cancer patients and in the 4T1 tumor model [77,302,352]. However, the relationship between NKT cells and MDSCs is unclear as NKT cells have been shown to suppress and promote MDSC accumulation and activity in different settings [172,354–357]. To begin characterizing leukocyte populations in peripheral blood, we prepared H&E stained cytospins. Compared to naïve controls, tumor bearing mice had significantly higher numbers of granulocytic cells with few lymphocytes and monocytes (Fig 15A). NKT cell activation resulted in a decrease in the accumulation of granulocytic cells. However, there were no morphological distinctions between the granulocytes observed in the naïve and diseased mice. The frequency of $CD11b^+$ $Gr\text{-}1^+$ cells in naïve blood was low (Fig 15B, C), but this population expanded with progressive tumor growth. Following tumor resection, the $CD11b^+$ $Gr\text{-}1^+$ population sharply declined. However, the $CD11b^+$ $Gr\text{-}1^+$ population later surged as metastatic lesions developed in the vehicle treatment group, as well as in the subset of mice that relapsed following NKT cell activation therapy. Mice with circulating

Table 5: Survival outcomes in mice receiving adoptive transfer of NKT cells in combination with free α-GalCer or α-GalCer-loaded DCs

Treatment Group	No Response (≤ 50 Days)[a]	Partial Response (50-150 Days)	Complete Response (150^{+} Days)
Unloaded DCs	9/9[b] (32-37)	0	0
2-5 x 10^5 α-GalCer DCs	6/21 (37 - 50)	7/21 (54, 61, 63, 67, 68, 75, 83)	8/21 (150)
0.5-1 x 10^6 NKT cells + 2-5 x 10^5 α-GalCer DCs	12/21 (32 - 46)	5/21 (53, 56,59, 62, 72)	4/21 (150)
0.5-1 x 10^6 NKT cells + α-GalCer	8/9 (42 - 47)	1/9 (94)	0
0.2-1 x 10^6 NKT cells	8/9 (38 - 41)	1/9 (58)	0

[a] Survival outcomes in mice were stratified into three categories: non-responders survived ≤ 50 days post-4T1 cell injection, partial responders survived > 50 days but < 150 days post-4T1 injection, and complete responders were healthy at 150 days post-4T1 cell injection. [b] The number of mice in each response category out of total number of mice in treatment group. The range or individual day(s) of sacrifice are indicated in brackets. Data was generated in collaboration with Daniel Clattenburg.

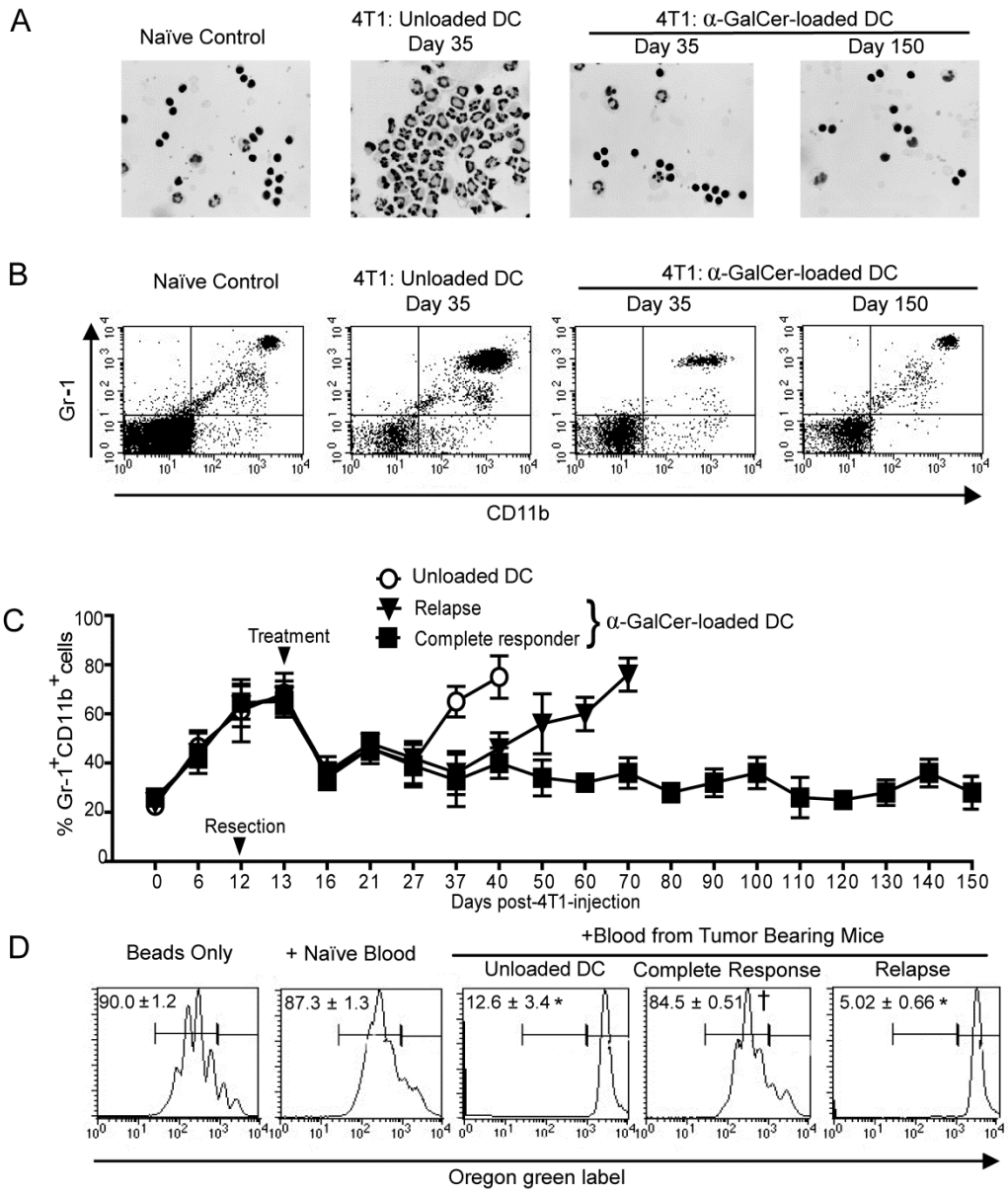

Figure 15. Post-surgical administration of α-GalCer-loaded DCs reduces the frequency and suppressive activity of blood MDSCs. (A) Representative images of H & E-stained cytospins of blood from naïve mice, tumor resected mice receiving treatment with unloaded DCs , or tumor resected mice receiving treatment with α-GalCer-loaded DCs (day 35 and day 150) (n = 3-5 per group) (B) Representative flow cytometry plots of Gr-1 and CD11b staining in peripheral blood cells from naive mice, tumor resected mice treated with unloaded dendritic cells, or α-GalCer-loaded DCs. (C) Frequency of Gr-1+CD11b+ cells in the blood of mice treated with vehicle or α-GalCer-loaded dendritic cells. Treated mice were separated into mice exhibiting transient (relapse) or complete responses to treatment (n = 6). (D) Proliferation of naïve T cells stimulated with anti-CD3/anti-CD28-coated beads was examined by dilution of Oregon Green. Cells were incubated in the absence or presence of peripheral blood leukocytes isolated from naïve mice, tumor resected mice receiving vehicle, tumor resected mice

responding to α-GalCer-loaded DC therapy, or tumor resected mice that relapsed following α-GalCer-loaded DC therapy. Values indicate frequency of proliferating naïve T cells (n = 5-11 per group). * $p < 0.05$ compared to bead stimulation alone, † $p < 0.05$ compared to tumor bearing mice treated with unloaded DCs.

levels of $CD11b^+$ $Gr\text{-}1^+$ cells exceeding 50% succumbed to tumor metastasis. In contrast, mice that responded well to NKT cell activation therapy maintained low levels of $CD11b^+$ $Gr\text{-}1^+$ cells, suggesting that $CD11b^+$ $Gr\text{-}1^+$ levels could be used as a prognostic marker in NKT cell based immunotherapy.

To determine whether the expansion of blood $CD11b^+$ $Gr\text{-}1^+$ cells correlated with immunosuppression, we performed a T cell proliferation assay in the presence of blood from naïve mice, mice treated with unloaded DCs, or mice treated with α-GalCer-loaded DCs. We found that blood isolated from the unloaded DC treatment group or relapsed mice significantly suppressed proliferation of naïve T cells, whereas blood from complete responders did not suppress T cell proliferation (Fig 15D).

Given that the primary tumor is responsible for the elevation in MDSC levels [300], it was not clear whether the sustained reduction in circulating MDSCs following NKT cell activation was due to direct effects of NKT cells on MDSCs or due to maintenance of reduced tumor burden. To determine whether NKT cells directly altered levels of circulating MDSC, we activated NKT cells in unresected mice (day 7 post-tumor inoculation). NKT cell activation resulted in a modest but significant reduction in the levels of circulating MDSCs in tumor bearing mice (Fig 16A). To further support the direct role for NKT cells in reducing MDSC frequency and suppressive activity, we added NKT cells to co-cultures of MDSCs and naïve T cells. MDSCs had no effect on NKT cell proliferation in response to anti-CD3/28-coated activator beads, and NKT cells overcame the suppressive activity of MDSCs to rescue the proliferation of naïve T cells (Fig 16B, C).

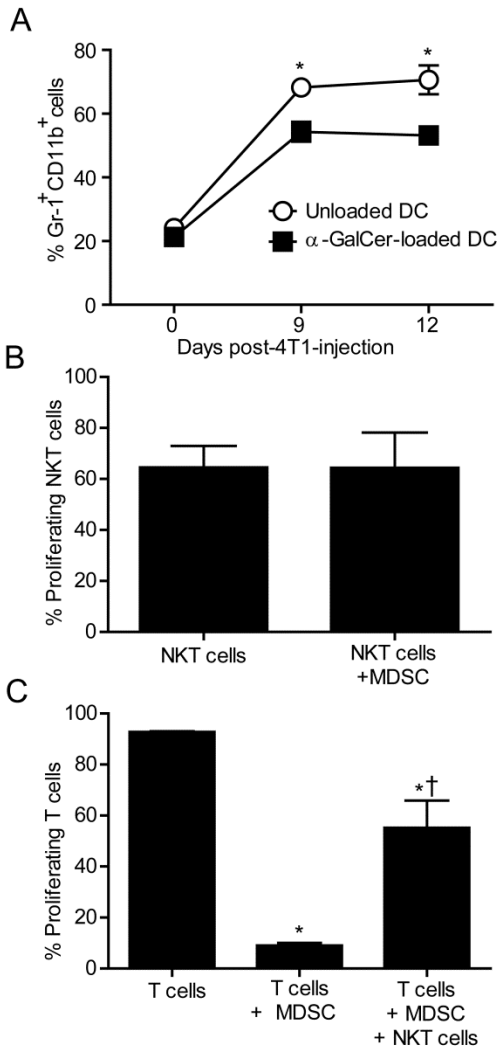

Figure 16. NKT cell activation reduces the frequency and impairs the suppressive activity of MDSCs. (A) Frequency of circulating $Gr1^{+}CD11b^{+}$ cells in 4T1 tumor-bearing mice treated with unloaded or α-GalCer-loaded DCs on day 7 post 4T1 injection. * $p < 0.05$ compared to treatment with unloaded DCs (n = 4 per group) (B) Proliferation of NKT cells was measured by eFluor 670 dilution within NKT cells stimulated with of anti-CD3/anti-CD28 beads alone or in the presence of MDSCs derived from the blood of 4T1 tumor-bearing mice (n = 5 per group). (C) Proliferation of Oregon Green-labeled naive T cells was measured in response to anti-CD3/anti-CD28-coated beads in the absence or presence of NKT cells and MDSCs derived from blood of 4T1 tumor-bearing mice (n = 5 per group). * $p < 0.05$ compared to bead stimulation alone. † $p < 0.05$ compared to bead stimulation in the presence of MDSCs.

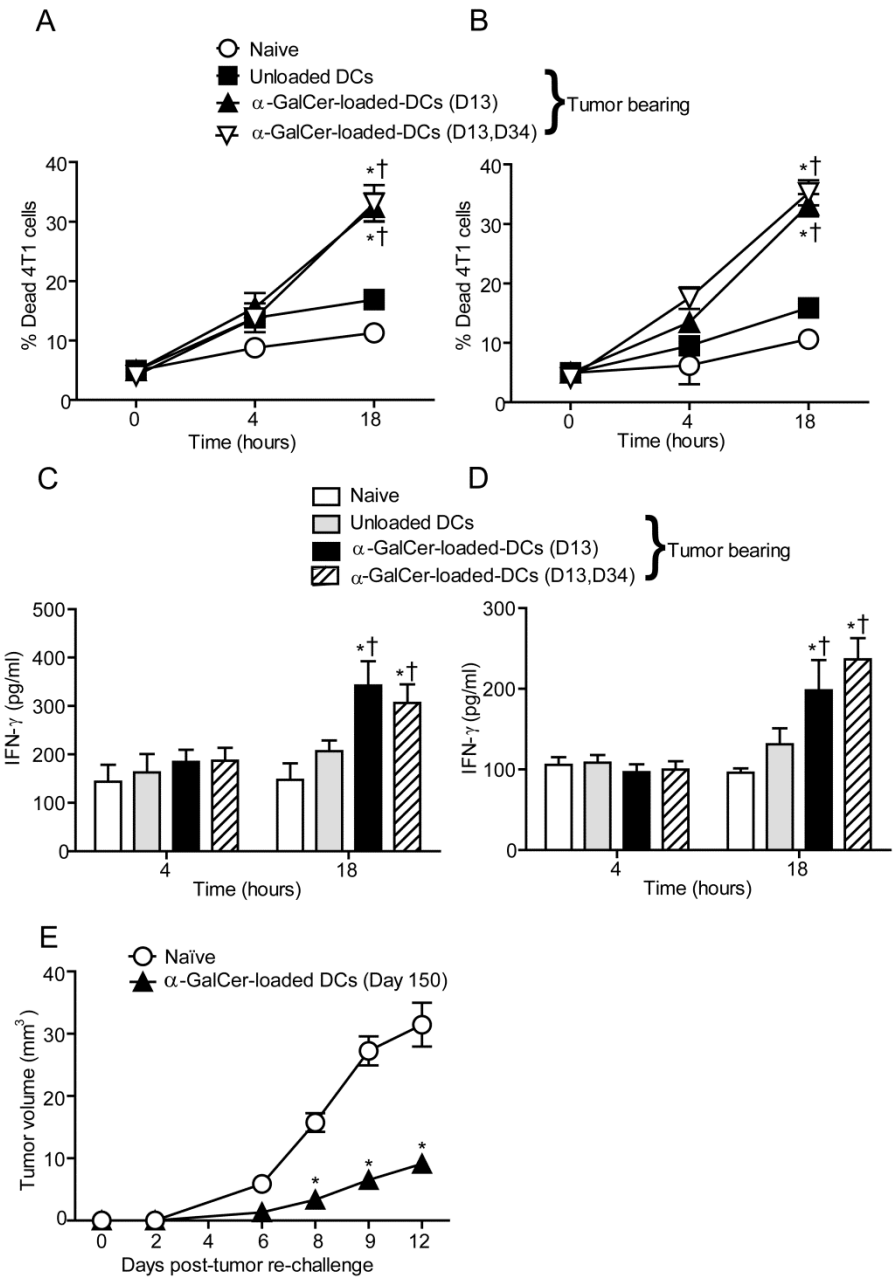

Figure 17. Enhanced tumor-specific responses and protection from tumor re-challenge in mice treated with α-GalCer-loaded DCs. Cell mediated cytotoxicity of sorted (A) NK cells ($CD49b^+$ $TCR\beta^-$) and (B) CD8 T cells ($CD8^+$ $TCR\beta^+$) isolated from the spleens of naïve mice or tumor resected mice treated with unloaded DCs or α-GalCer-loaded DCs (n = 4 per group). Cytotoxicity was measured via annexin V/7-AAD staining of 4T1 cells. Supernatant IFN-γ levels were measured by ELISA from sorted (C) NK cells and (D) $CD8^+$ T cells after 4 or 18 hours in culture (n = 4 per group). (E) Tumor resected mice that survived to day 150 after treatment with α-GalCer-loaded DCs were re-challenged in the flank with 4T1 cells. Tumor volume was compared to tumors grown in naïve mice (n = 5 per group). * $p < 0.05$ compared to naïve mice, † $p < 0.05$ compared to unloaded DCs.

Effect of NKT cell activation on anti-tumor immunity

To examine the effect of NKT cell activation on anti-tumor immunity, we examined IFN-γ production and cytotoxic activity of purified NK cells and $CD8^+$ T cells isolated from the spleens of naïve mice or tumor bearing mice that had received treatment with vehicle- or α-GalCer-loaded DCs. Compared to cells from naïve or vehicle-treated mice, NK cells and $CD8^+$ T cells isolated from mice treated with α-GalCer- loaded DCs exhibited enhanced cytotoxic activity against 4T1 cells (Fig 17A, B). Similarly, NK cells and $CD8^+$ T cells from mice treated with α-GalCer-loaded DCs released greater quantities of IFN-γ into the culture medium (Fig 17C, D). Consistent with the enhanced immune responses in *in vitro* assays, mice surviving to day 150 had significantly decreased tumor growth following re-challenge with 4T1 cells (Fig 17E).

Discussion

Whereas decreases in NKT cell number and/or function have been linked to increased tumor incidence and progression [139,140,150], NKT cell activation has been shown to enhance anti-tumor responses [102,134,138,159,160,350]. Although clinical trials examining NKT cell activation therapies in patients with advanced/recurrent disease have reported few cases of objective tumor regression, tumors tended to remain stable without the appearance of new metastatic foci [159,173,174,176,348,349]. This suggests that NKT cell activation therapy might be more effective at targeting metastatic disease than primary tumors. Since primary breast tumors are effectively treated by surgical resection, and disseminated metastasis remains the primary cause of mortality [358], NKT cell activation therapy presents a promising therapeutic avenue. Using a mouse model of metastatic breast cancer, we found that post-surgical NKT cell activation via α-GalCer-loaded DCs

significantly reduced tumor metastasis, stimulated anti-tumor immune function, and increased survival.

While several studies have examined the role of NKT cells and the therapeutic effects of NKT cell activation in breast cancer models, the findings have been inconsistent. Terabe *et al.* [99] showed that NKT cell deficient Jα18$^{-/-}$ mice had significantly lower metastasis and improved survival in the 4T1 model, implicating an enhanced anti-tumor response in the absence of NKT cells. This finding is consistent with another report showing enhanced anti-tumor CD8^{+} T cell responses were elicited in Jα18$^{-/-}$ mice following treatment with local radiation and CTLA-4 blockade [359]. These studies suggest that NKT cells play suppressive roles in anti-tumor immunity. However, Teng *et al.* [350] showed that NKT cell activation therapy, in combination with antibodies targeting CD262 (DR-5) and CD137, dose-dependently protected mice from primary tumor growth and metastases, suggesting an anti-tumor effect of glycolipid-mediated NKT cell activation . Chen and Ross [360] reported that DCs loaded with α-GalCer and retinoic acid tended to reduce growth and metastasis of orthotopic 4T1 tumors, but their results did not reach statistical significance. Our studies show that NKT cell activation using a larger number of α-GalCer-loaded DCs significantly reduced post-surgical tumor metastasis and increased survival. The differences in the role of NKT cells in these studies may relate to activation of NKT cells by endogenous versus exogenous stimuli. NKT cell activation with α-GalCer-loaded DCs induces a robust IFN-γ response which promotes anti-tumor immunity, while endogenous tumor glycolipids have been shown to induce Th2-polarized responses or suppression [152,361].

Previous studies in the lab showed that free α-GalCer transiently protected mice from metastasis, suggesting that multiple treatments or higher doses would be needed therapeutically (Appendix 1). However, these strategies are limited by the induction of anergy and toxicity, respectively. Anergy is likely induced by glycolipid presentation via B-cells or other CD1d-expressing cells that poorly present the antigen and/or lack appropriate co-stimulatory signals [331,362]. In contrast, glycolipid delivery via DCs induces potent NKT cell activation without induction of anergy [331]. We show that immunotherapy with α-GalCer-loaded DCs protected mice from 4T1 tumor metastasis and significantly increased survival. Importantly, mice surviving to day 150 were free of metastasis, suggesting they had been cured of disease. Despite promising results with a single treatment of α-GalCer-loaded DCs, a second treatment three weeks later did not significantly improve the survival outcome. Similarly, we observed no additional survival benefit by adoptively transferring NKT cells in our model of metastasis. In contrast to our results, co-treatment with expanded NKT cells and glycolipid-loaded DCs has been beneficial in human cancer trials [173]. As mice have a higher frequency of NKT cells, it is possible that additional NKT cells are more useful in human patients where NKT cell number and/or function are limited.

Several clinical studies have reported the use of peripheral blood MDSCs as biomarkers of disease [302,352]. In particular, levels of MDSCs have been directly correlated with clinical stage and metastatic burden in breast cancer patients [302,352]. Furthermore, MDSCs have previously been shown to reduce the efficacy of immunotherapies by impairing antigen presentation and T cell activation [78,363,364]. We found that MDSCs were a good biomarker of metastatic disease and presented a potent prognostic marker for

NKT cell activation therapy. Based on circulating levels of MDSCs, we could track responses to NKT cell activation therapy and identify mice that relapsed. This allows identification of individuals who could benefit from re-treatment or combination therapies with other agents.

The effects of NKT cell stimulation on the frequency and activity of MDSCs remains unclear. NKT cell activation in a mouse model of multiple sclerosis was reported to provide protection via the induction of MDSCs [354], and administration of free α-GalCer has been shown to increase MDSCs in a hepatotoxicity model [357]. In contrast, NKT cells suppresses MDSC accumulation during viral infection [172], and activated NKT cells can induce MDSC differentiation into DCs [172,356,365,366]. An increased number of mouse $CD49b^+$ T cells or human $CD161^+$ T cells in expanded memory T cell cultures were able to overcome the suppressive effects of MDSCs to enhance tumor antigen-specific IFN-γ production [355,366]. Although these studies did not use markers that allow definitive identification of NKT cells, they are consistent with our findings that activated NKT cells rescued T cell proliferation from MDSC mediated suppression. It is likely that the ability of NKT cells to induce or inhibit MDSC function depends on the context of the NKT cell stimulation, the nature of the antigen presenting cell, and stromal signals. Studies have shown that the inhibitory effects of NKT cells on MDSCs are regulated through multiple signaling pathways, involving CD1d, CD40L, and NKG2D [171,172,366].

We show that NKT cell activation resulted in robust $CD8^+$ T cell and NK cell mediated anti-tumor responses. While NKT cells can directly lyse tumor cells, this mechanism of anti-tumor immunity is largely associated with hematological tumors [161,162]. However, cytokine production from activated NKT cells activates and matures

DCs and facilitates downstream effector functions of NK cells, $CD8^+$ cytotoxic T cells, and Th1 $CD4^+$ T cells [92]. Consistent with this, there were increased cytotoxic and IFN-γ responses by NK cell and tumor-specific $CD8^+$ T cells in mice treated with NKT cell activation therapy. Mice that survived long term (150 days) maintained durable immunity that limited growth of 4T1 tumors following re-challenge.

In conclusion, we show that NKT cell activation using α-GalCer-loaded DCs was effective in targeting metastatic breast cancer lesions in mice and significantly enhanced survival. This was associated with reduced expansion of MDSCs and induction of potent anti-tumor responses by NK cells and $CD8^+$ T cells. Our findings provide preclinical evidence supporting the development of therapeutic NKT cell activation strategies to target metastatic breast cancer.

Chapter 5: Natural killer T cell immunotherapy in combination with chemotherapy-induced immunogenic cell death targets metastatic breast cancer

This work appears in part in the publication:

Gebremeskel S, Lobert L, Tanner K, Walker B, Clarke L, Oliphant T, Dellaire G, and Johnston B. Combined chemotherapy and natural killer T cell immunotherapy enhances protection from breast cancer metastasis. *Cancer immunology research.*

Contributions:

SG- designed the study, carried out experiments, analyzed data and prepared the manuscript.

LL, KT, BW, TO, LC and GD- assisted with experimentation and data collection.

BJ- assisted with study design and critical review of the manuscript.

In the previous chapter, we demonstrated that NKT cell activation via a single transfer of glycolipid-loaded DCs significantly enhanced survival in an advanced model of breast cancer metastasis, providing durable 'cures' in 40-50% of mice [165]. As repeated treatment with glycolipid-loaded DCs did not provide an additional survival benefit [165], we investigated whether NKT cell-based immunotherapy can be combined with low dose chemotherapy to enhance survival benefits.

While chemotherapeutic agents are generally selected due to their direct cytotoxic effects, recent studies have demonstrated that many of these drugs also promote immune-mediated recognition of cancer cells [192,194,241,242,259]. This recognition is facilitated by immunogenic cell death (ICD), a process of cell death mediated by a subset of chemotherapeutic agents [367]. Chemotherapy-induced ICD is characterized by cell surface exposure of the CALR [235,242], release of ATP through autophagy-dependent mechanisms [194], and release of chromatin-binding protein high-mobility group box (HMGB)-1 [192]. Collectively, these chemotherapy-induced changes in cell surface composition and release of soluble damage associated molecular patterns (DAMPs), allow DCs to detect the dying cell and initiate an anti-tumor immune response.

Tumor cells treated with chemotherapeutics exhibit increased susceptibility to killing by NKT cells in vitro [368]. Studies examining NKT cell activation in combination with either cisplatin [369] or 5-fluorouracil [370], neither of which are ICD-inducing chemotherapies [367], showed promising results in murine models of mesothelioma and colorectal cancer metastasis, respectively. However, the potential of combining ICD-inducing chemotherapies with NKT cell activation remains undefined. The aim of this

work was to examine the effects of combining NKT cell activation therapy with low doses of ICD-inducing chemotherapy to target metastatic breast cancer.

Results:

Effects of chemotherapeutics on 4T1 cell viability *in vitro*

The cytotoxic effect of gemcitabine and mafosfamide on 4T1 mammary carcinoma cells was investigated by MTT assay at 24, 48 and 72 hours. Gemcitabine, a nucleoside analog, caused a dose dependent cytotoxic response with up to 75% cytotoxicity at 1000ng/ml (Figure 18A). Similarly, gemcitabine and mafosfamide showed a concentration dependent decrease in the number of 4T1 cell colonies in a clonogenic assay (Figure 18B). The alkylating agent mafosfamide also exhibited a dose-dependent effect on 4T1 cells viability and clonogenicity (Figure 18C, D).

Effect of chemotherapeutics on tumor immunogenicity

We also investigated whether gemcitabine or mafosfamide could alter the expression of MHC I, MHC II and CD1d on tumor cells, making them more visible to the immune system. MHC I and MHC II are involved in presentation of peptide antigens to conventional T cells, whereas CD1d is involved in presentation of glycolipid antigens to NKT cells [92]. Gemcitabine and mafosfamide treatments increased the expression of MHC I, MHC II and CD1d in a dose dependent manner (Figure 19A). However, gemcitabine caused a more pronounced increase in expression compared to mafosfamide.

Some chemotherapeutics have been shown to stimulate the immune system by inducing ICD, a process of cell death that increases immune recognition of tumor cells [194,241,242,259]. In order to determine whether gemcitabine and mafosfamide induce ICD in 4T1 cells, we monitored the expression of the classical ICD markers, CALR, ATP and

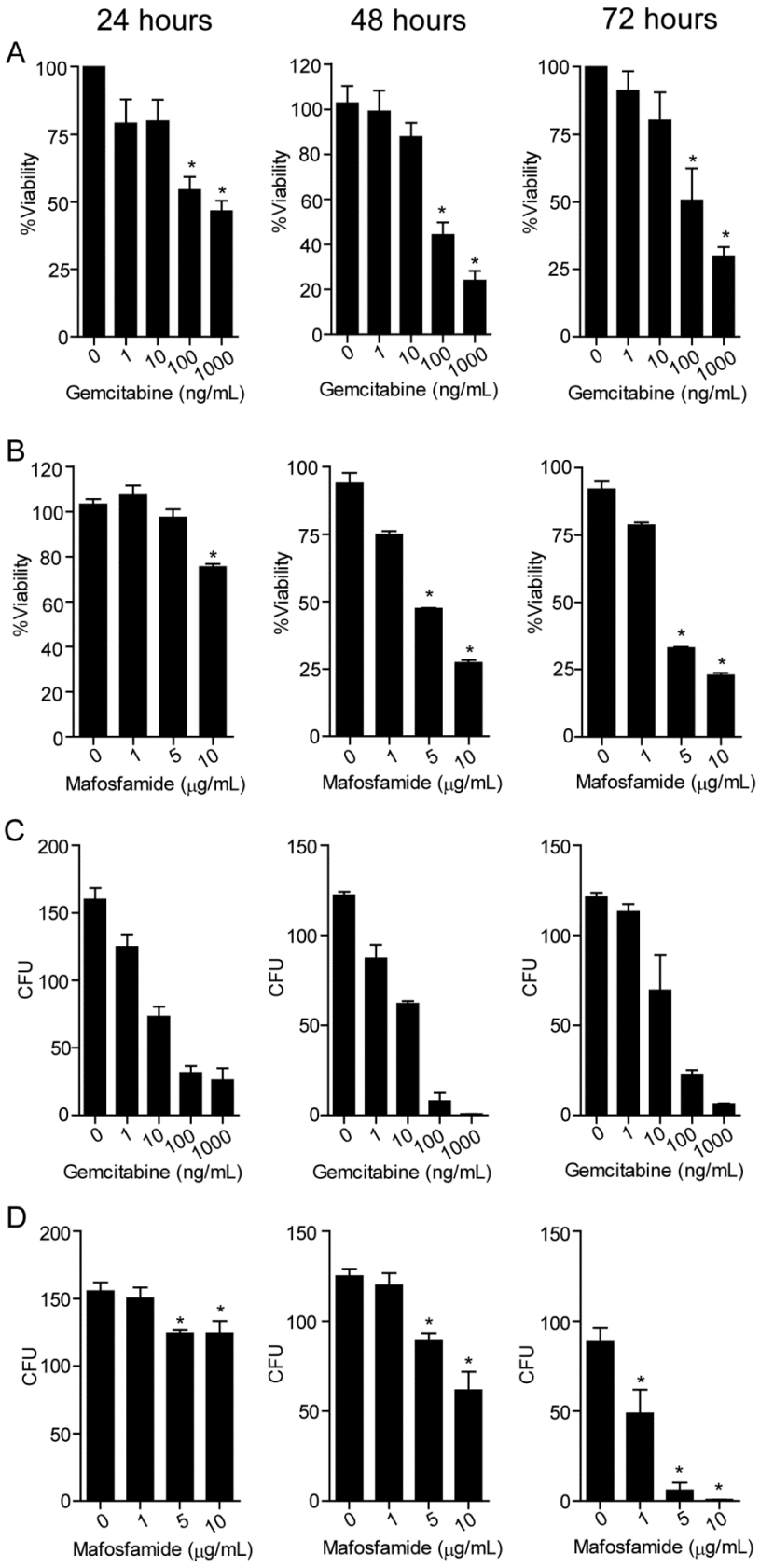
24 hours
48 hours
72 hours
A
%Viability
Gemcitabine (ng/mL)
B
%Viability
Mafosfamide (μg/mL)
C
CFU
Gemcitabine (ng/mL)
D
CFU
Mafosfamide (μg/mL)

Figure 18. Gemcitabine and mafosfamide reduce viability of 4T1 cells. Viability of 4T1 cells treated with A) gemcitabine (0-1000 ng/ml) or B) mafosfamide (0-10 µg/ml) was assessed by MTT assay at 24, 48 and 72 hours following treatment (n= 6 per group). * $p < 0.05$ compared to vehicle. The effect of C) gemcitabine (0-1000 ng/ml) and D) mafosfamide (0-10 µg/ml) on 4T1 cells was also assessed using a clonogenic assay. 4T1 cells were plated in 24 well plates and treated with gemcitabine or mafosfamide for 24, 48 and 72 hours. Colonies were fixed, stained with 0.03% methylene blue, and quantified using an automated immunospot colony-counting program (n= 4 per group). * $p < 0.05$ compared to vehicle.

HMGB1, following treatment *in vitro* and *in vivo*. During ER stress, CALR is mobilized to the plasma membrane [235] and serves as an "eat me" signal to DCs, which promotes the presentation of tumor-derived antigens to T cells [259]. To monitor cell surface localization of CALR, we used both confocal microscopy and flow cytometry on non-permeabilized 4T1 cells. After 4 h of gemcitabine or mafosfamide treatment, we observed a significant increase in CALR translocation to the cell surface (Figure 19B, C). Chemotherapy has also been shown to induce the release of ATP, which recruits DCs to the tumor site and activates the inflammasome in infiltrating DCs [194,241], and HMGB1, which is recognized by toll-like receptor (TLR)-4 to induce DC maturation [192]. We observed significant increases in ATP and HMGB1 release, and an upregulation in the relative expression of *cxcl10* from gemcitabine and mafosfamide treated cells *in vitro* (Figure 19D-H). While gemcitabine also induced increased *ifn-α and ifn-β* levels, the levels in mafosfamide treated cells did not reach statistical significance. The observed increase in *cxcl10* in mafosfamide treated cells may potentially be due to synergistic effects of *ifn-α* and *ifn-β*.

We also observed elevated surface expression of CALR *in vivo* after harvesting primary 4T1 tumors from chemotherapy-treated mice (Figure 19I). Tumor-bearing mice treated with either cyclophosphamide or gemcitabine exhibited increased serum levels of HMGB1 (Figure 19J). While serum ATP levels were below the detection threshold of our assay, we observed an increase in tumor infiltrating $CD11c^+$ DCs in mice receiving either cyclophosphamide or gemcitabine therapy (Figure 19K). Gemcitabine and mafosfamide/cyclophosphamide fulfill the general criteria for ICD by mobilizing CALR to the surface of dying 4T1 cells, and increasing release of ATP and HMGB1.

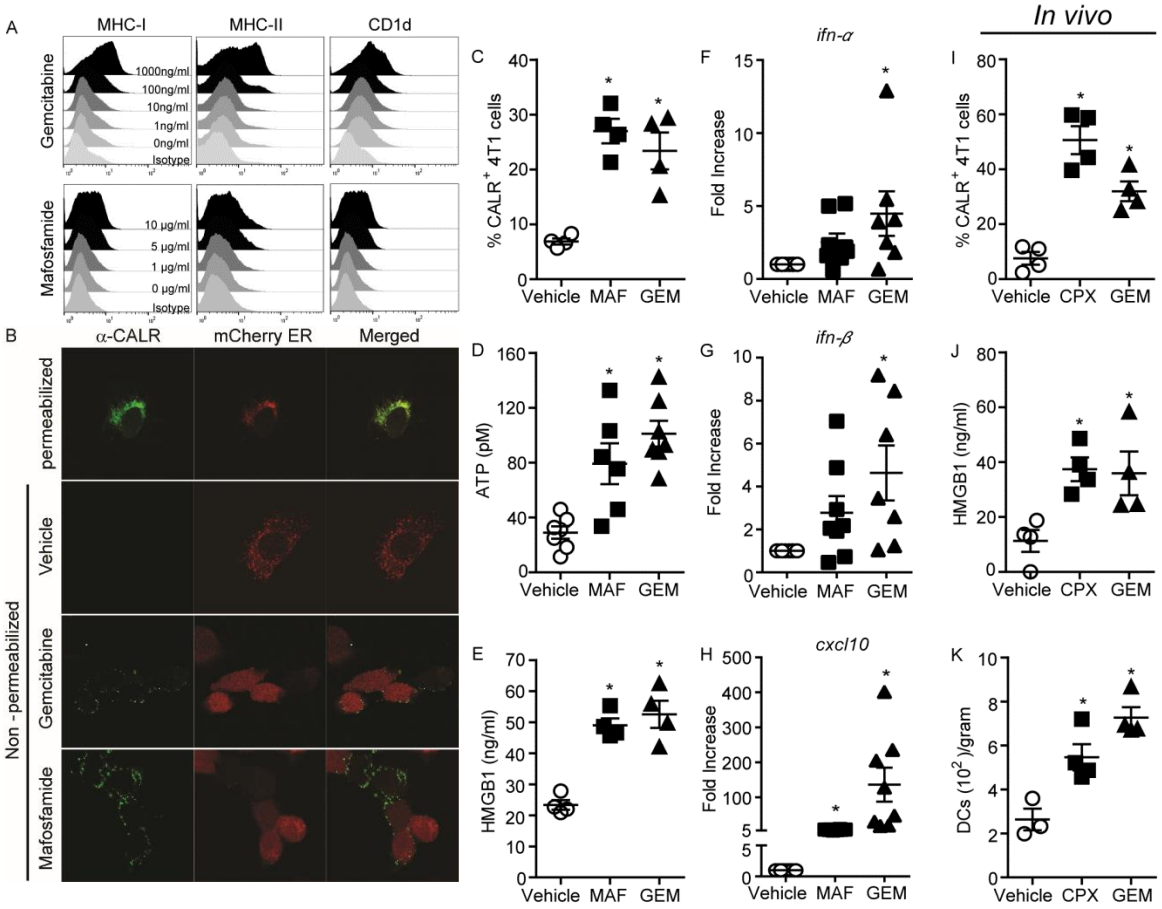

Figure 19.Chemotherapy induced immunogenic changes on 4T1 cells. A) Flow cytometry histograms of MHC I, MHC II and CD1d expression on cultured 4T1 cells 48 hours after gemcitabine (0-1000ng/ml) or mafosfamide (0-10ug/ml) treatment. Plots are representative of n= 5-6 per group. B) Immunofluorescence analysis of CALR (green) localization on 4T1 cells after 4 hours of chemotherapy treatment. ER labelled mCherry-KDEL (red) expressing 4T1 cells were treated with either vehicle, gemcitabine (GEM) (1000ng/ml) or mafosfamide (MAF) (10ug/ml) and cell surface CALR staining was performed on non-permeabilized cells. To confirm ER localization of CALR, vehicle treated 4T1 cells were permeabilized prior to CALR staining and co-localization of CALR staining and ER labelled mCherry was observed via fluorescence microscopy images are representative of n= 4 per group. C) Flow cytometric expression of surface CALR on 4T1 cells 4 hours after treatment (n= 4 per group). * $p < 0.05$ compared to vehicle. D) ATP and E) HMGB1 release into culture supernatants of chemotherapy treated 4T1 cells was examined 16 and 24 hours following treatment, respectively (n= 4 per group). Quantitative PCR (qPCR) examining the expression of F) *ifn-α*, G) *ifn-β* and H) *cxcl10* in 4T1 cells treated with chemotherapy for 24h. qPCR was analyzed using the $2^{-\Delta\Delta CT}$ quantification technique relative to the housekeeping gene GAPDH. I) CALR expression on tumor cells isolated from chemotherapy treated mice. Primary tumors were harvested 24 hours after gemcitabine (GEM) (30mg/kg) or cyclophosphamide (CPX) (20mg/kg) treatment and the cell surface expression of CALR on 4T1 cells was examined using flow cytometry (n= 3-4 per group). * $p < 0.05$ compared to vehicle. J)

Serum HMGB1 levels were examined 24 hours after chemotherapy treatment and K) frequency of tumor infiltrating $CD45^+$ $CD11c^+$ dendritic cells and (n= 3-4 per group). * $p < 0.05$ compared to vehicle.

Combining chemotherapy with NKT cell activation therapy enhances protection from tumor metastasis.

We previously demonstrated that a single adoptive transfer of α-GalCer-loaded DCs into tumor-resected mice significantly reduces tumor metastasis and increases survival [165]. In this study, we aimed to establish whether NKT cells activation therapy could be safely combined with ICD-inducing chemotherapeutics to enhance survival outcomes. Given that some chemotherapies may negatively impact the immune system, we wanted to determine whether gemcitabine or cyclophosphamide would negatively affect NKT cell activation at doses that support ICD. In our post-surgical breast cancer model (Figure 20A), mice received either gemcitabine (Days 12, 14, and 16) or cyclophosphamide (Days 12-16) treatments prior to adoptive transfer of α-GalCer-loaded DCs (Day 17). NKT cell activation by transfer of α-GalCer-loaded DCs significantly increases serum IFN-γ and IL-4 [165]. We did not observe reductions in serum IFN-γ or IL-4 levels when NKT cells were activated following gemcitabine or cyclophosphamide treatments (Figure 20B), suggesting that chemotherapy treatments did not impede NKT cell function. Treatment with cyclophosphamide, gemcitabine, or α-GalCer-loaded DCs alone reduced metastasis of 4T1 cells to the lungs (Figure 20C). This protection was further enhanced when NKT cell activation therapy was combined with gemcitabine or cyclophosphamide. Consistent with these results, we observed enhanced survival when NKT cell activation was combined with cyclophosphamide (Figure 20D) or gemcitabine (Figure 20E) treatments, compared to either drug or NKT cell activation

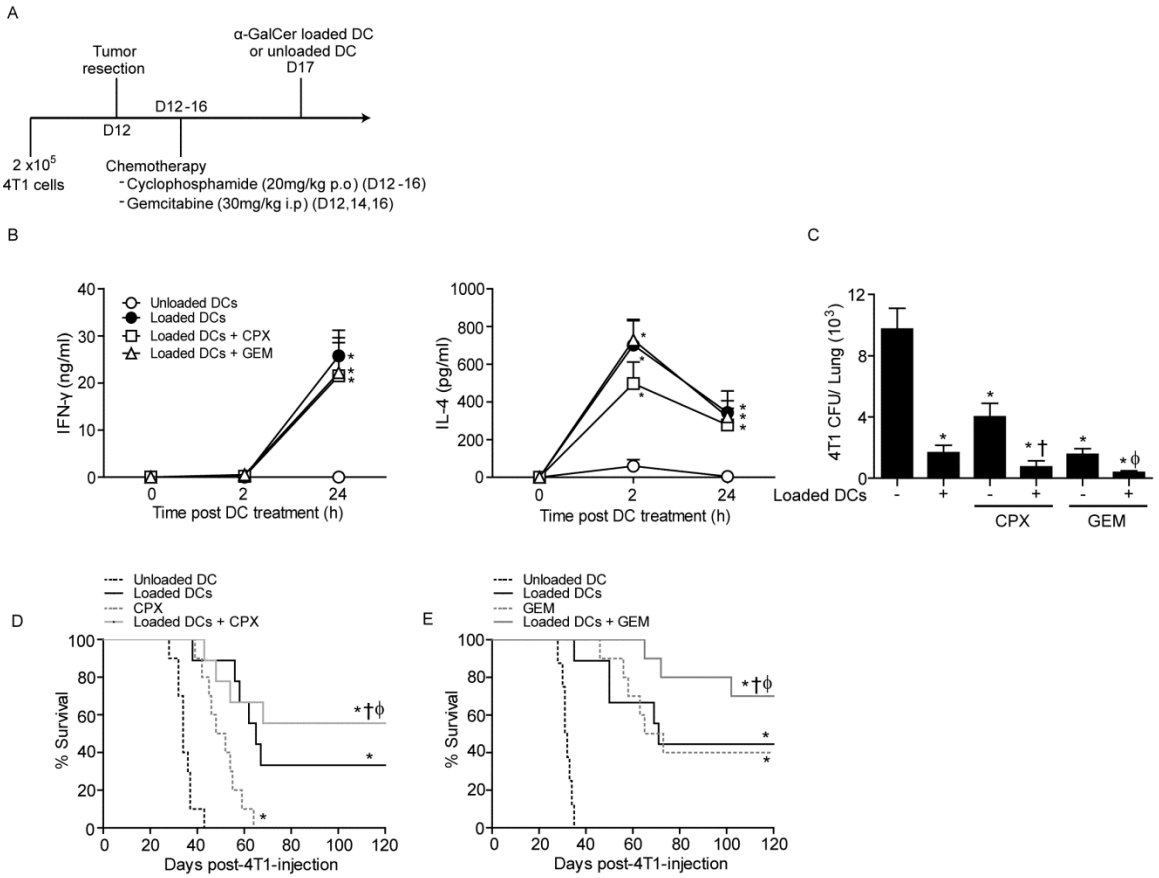

Figure 20. Combining NKT cell activation therapy with low dose chemotherapy to target post-surgical metastatic disease. A) Schematic of treatments in the post-surgical 4T1 metastasis model. Mice were inoculated with $2x10^5$ 4T1 mammary carcinoma cells and primary tumors were resected on day 12. Mice received intraperitoneal injection of gemcitabine (GEM) (30mg/kg on day 12, 14, 16) or perioral cyclophosphamide (CPX) (20mg/kg/day) from day 12-16. On day 17, NKT cells were activated via i.v. injection of $2x10^5$ α-GalCer-loaded DCs. Serum levels of B) IFN-γ and IL-4 were measured 0, 2 and 24 hours after treatment with α-GalCer-loaded DCs (n = 4-5 per group). * $p < 0.05$ compared to unloaded DCs. C) Number of 4T1 CFU present in lung cell suspensions isolated at 28 post-4T1 injection (n = 8-15 per group). * $p < 0.05$ compared to unloaded DCs, † $p < 0.05$ compared to CPX alone, ϕ < 0.05 compared to GEM alone. D) and E) Survival was assessed following treatment with unloaded DCs, α-GalCer-loaded DCs, CPX or combination of CPX with α-GalCer-loaded DCs (n = 9-10 per group), * $p < 0.0167$ compared to unloaded DC, † $p < 0.0167$ compared to CPX alone, ϕ < 0.0167 compared to α-GalCer-loaded DCs.

alone. Mice that survived to day 120 had no detectable tumor cells by clonogenic plating assay, suggesting they were free of metastatic disease.

Effect of monotherapy/combination therapy on anti-tumor immunity

To determine whether mice surviving the initial tumor challenge would have lasting immunological memory against the 4T1 tumor, we re-challenged mice by inoculating 4T1 cells in the contralateral mammary fat pad. Consistent with our previous observation [165], mice that received NKT cell therapy exhibited attenuated tumor growth and metastasis upon re-challenge (Figure 21A, B). Mice that received NKT cell activation in combination with cyclophosphamide or gemcitabine exhibited reduced tumor growth similar to NKT cell activation alone. Interestingly, mice that had been treated with gemcitabine alone exhibited delayed tumor outgrowth but were unable to control the tumors (Figure 21B). These mice also exhibited increased metastatic burden compared to mice that received combination treatments or NKT cell activation alone (Figure 21B).

Effects of therapy on suppressive immune cell populations.

Accumulation of immunosuppressive MDSCs has been associated with cancer progression and poor therapeutic outcomes [371]. We recently demonstrated that NKT cell activation therapy decreases the frequency and suppressive function of $CD11b^+$ $Gr\text{-}1^+$ MDSCs in the 4T1 tumor model (chapter 4) [165]. To determine whether gemcitabine or cyclophosphamide in combination with NKT cell immunotherapy would further impact MDSC levels, we examined the frequency of circulating $CD11b^+$ $Gr\text{-}1^+$ cells (Figure 22A). Primary tumor resection transiently decreased the frequency of $CD11b^+$ $Gr\text{-}1^+$ cells (Figure 22A). We observed delayed post-resection accumulation of $CD11b^+$ $Gr\text{-}1^+$ cells

in mice receiving either gemcitabine or cyclophosphamide alone (Figure 22A). When combined with NKT cell activation, neither cyclophosphamide or gemcitabine treatment reduced the accumulation of $CD11b^+$ $Gr\text{-}1^+$ over what was observed with NKT cell activation alone. To investigate the immunosuppressive activity of $CD11b^+$ $Gr\text{-}1^+$ cells, T cell suppression assays were performed using blood cells isolated from naïve and treated mice (Figure 22B). While blood cells from mice receiving unloaded control DCs exhibited suppressive activity, all therapeutic interventions reduced the suppressive activity of MDSCs at 35 days post tumor inoculation, consistent with the reduced frequency of circulating $CD11b^+$ $Gr\text{-}1^+$ cells.

T-regs have been shown to impede anti-tumour immunity [372]. Consistent with published reports [372], cyclophosphamide treatment reduced the frequency of $FoxP3^+$ T-regs in the spleen of tumor-resected mice (Figure 22C), with or without NKT cell activation therapy. There was no effect of gemcitabine treatment, or NKT cell activation alone, on the frequency of T-regs.

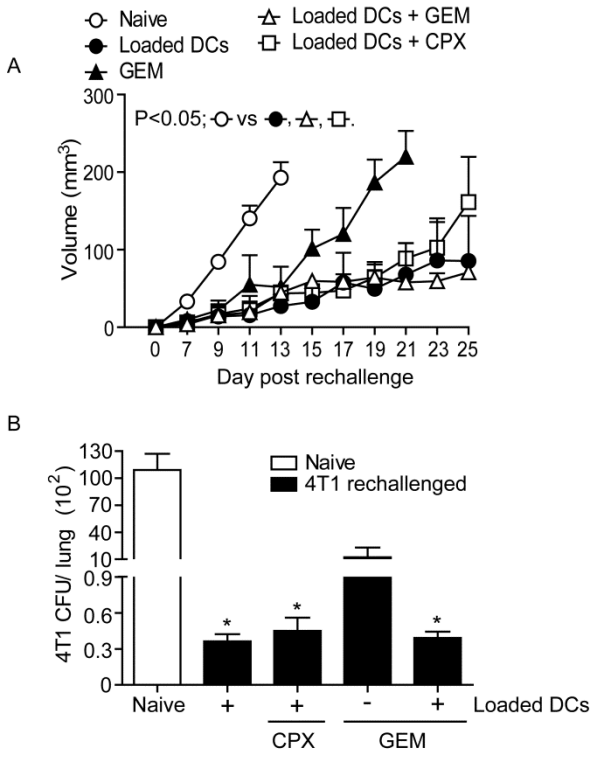

Figure 21. Protection from 4T1 tumor re-challenge in treated mice. A) Tumor resected mice that survived to day 120 after treatment with α-GalCer-loaded DCs, gemcitabine (GEM), GEM plus α-GalCer-loaded DCs, or cyclophosphamide (CPX) plus α-GalCer-loaded DCs were re-challenged in the contralateral mammary fat pad with 4T1 cells. Tumor volume was compared to tumors grown in naïve mice (n = 5-8 per group). B) Metastatic burden was measured by clonogenic assay at Day 25 after 4T1 inoculation (n = 5-8 per group). * $p < 0.05$ compared to naive challenge.

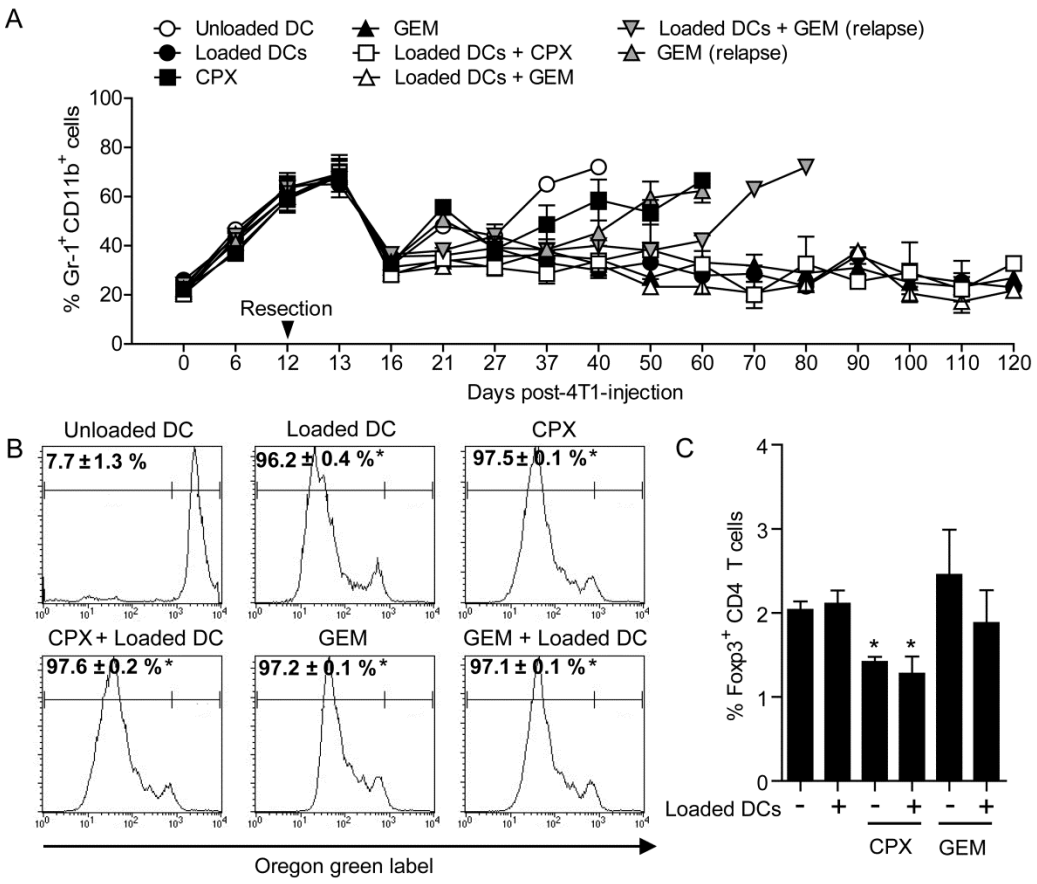

Figure 22. Effect of therapy on immunosuppressive MDSC and T-reg populations in the 4T1 model. A) Frequency of circulating Gr-1$^+$CD11b$^+$ cells in mice treated with unloaded DCs, α-GalCer-loaded DCs, cyclophosphamide (CPX), gemcitabine (GEM) or combined therapies. Treatment groups were further separated to show mice that responded completely to therapy and mice that relapsed (n=7-10 per treatment group). B) Proliferation of naïve Oregon green-labeled responder T cells was examined by dye dilution assay following stimulation with anti-CD3/28 coated beads. Responder cells were incubated in the presence of peripheral blood leukocytes isolated from tumor-bearing/resected mice treated with unloaded DCs, α-GalCer-loaded DCs, CPX, GEM or combination therapies. Histograms are representative, while the values indicate frequency of proliferating T cells ± SEM (n= 4 per group). * $p < 0.05$ compared to unloaded DCs. C) The frequency of TCRβ$^+$ CD4$^+$ CD25$^+$ Foxp3$^+$ regulatory T cells was measured in the spleen by flow cytometry. (n=7-8 per group) * $p < 0.05$ compared to treatment with unloaded DCs.

T cell populations and activation status following NKT cell/chemotherapy treatment.

While chemotherapy can directly induce ICD of 4T1 cells, cells of the immune system are also sensitive to potential cytotoxic or cytostatic effects of chemotherapy. To better understand how chemotherapy alone or in combination with NKT cell activation therapy influences the immune system, we characterized T lymphocyte subsets in the spleen of tumor-resected mice. The total number of $CD4^+$ and $CD8^+$ T lymphocytes in the spleen was not significantly altered by any of the treatments (Figure 23), suggesting that the dose of chemotherapies used were not toxic for these immune cell subsets. The proportions of $CD4^+$ and $CD8^+$ T cells expressing the activation marker CD69 were increased in mice receiving gemcitabine, cyclophosphamide, NKT cell activation, or combination therapies (Figure 23), consistent with reported immunostimulatory activities of chemotherapeutics [205,206,241,373–375] and NKT cell activation therapy [92,163,164]. Overall, we observed a trend towards increased frequencies of $IL17A^+$, IFN-γ^+, and granzyme B^+ CD4 and CD8 T cells in mice receiving either chemotherapy or NKT cell activation therapy. However, only certain groups reached statistical significance. Interestingly, we did not observe additive or synergistic responses when we combined NKT cell activation therapy with chemotherapy. Together these results indicate that NKT cell activation therapy alone or in combination with chemotherapeutic treatments had effects on T cell activation, cytokine profiles, and expression of cytotoxic molecules, but combination therapy failed to further enhance these effects.

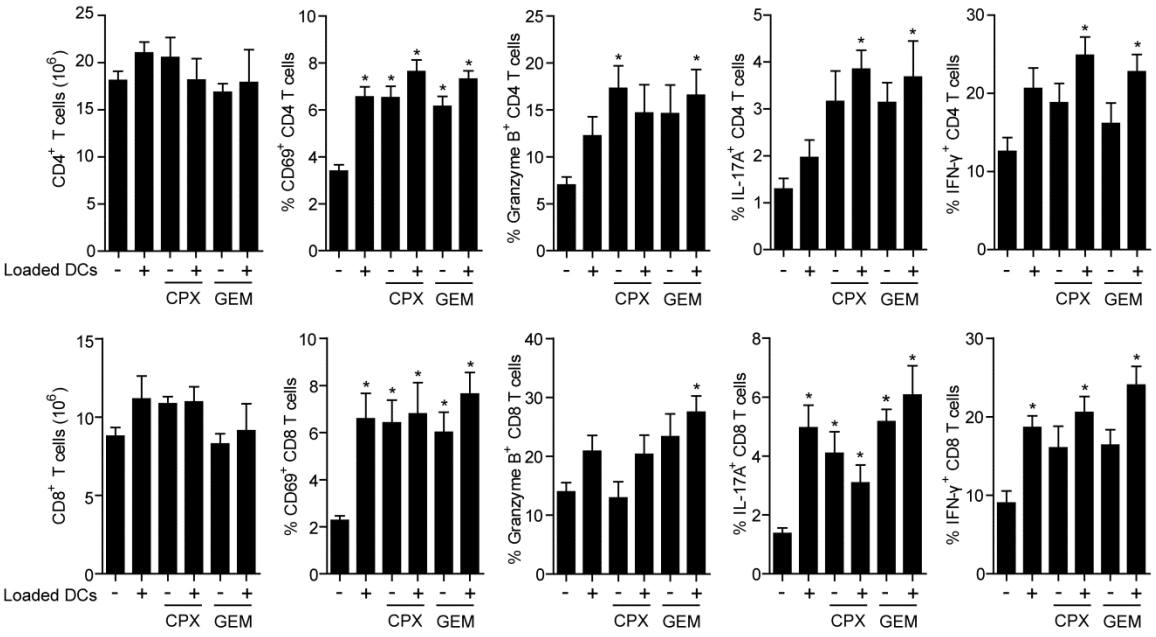

Figure 23. Immune cell phenotype in the 4T1 model following chemo-immunotherapy treatments. Mice were treated as outlined in Fig 20A. The number of CD4 and CD8 T cells in the spleen was examined by flow cytometry at day 28 after initial tumor inoculation. The frequency of $CD69^+$ CD4 and CD8 T cells was assessed (n= 7-8 per group). Cells were re-stimulated in culture with PMA and ionomycin to assess the frequency of granzyme B, IL-17A, and IFN-γ positive CD4 and CD8 T cell subsets. (n=7-8 per group) * $P < 0.05$ compared to treatment with controls.

To further examine the effect of monotherapies or combination therapies on specific anti-tumor immunity, we examined cytotoxic activity and IFN-γ production from NK cells and CD8 T cells isolated from the spleen of tumor-resected mice. Compared to vehicle treated mice, NK cells and CD8 T cells from mice receiving NKT cell activation alone, or NKT cell activation in combination with either gemcitabine or cyclophosphamide exhibited enhanced cytotoxicity against 4T1 cells (Figure 24A, B) and released greater quantities of IFN-γ (Figure 24C, D). Gemcitabine or cyclophosphamide alone did not significantly increase cytotoxicity responses (Figure 24A, B). Gemcitabine and cyclophosphamide treatments trended toward increased IFN-γ release, but only IFN-γ release from CD8 T cells in the gemcitabine group reached statistical significance (Figure 24C, D).

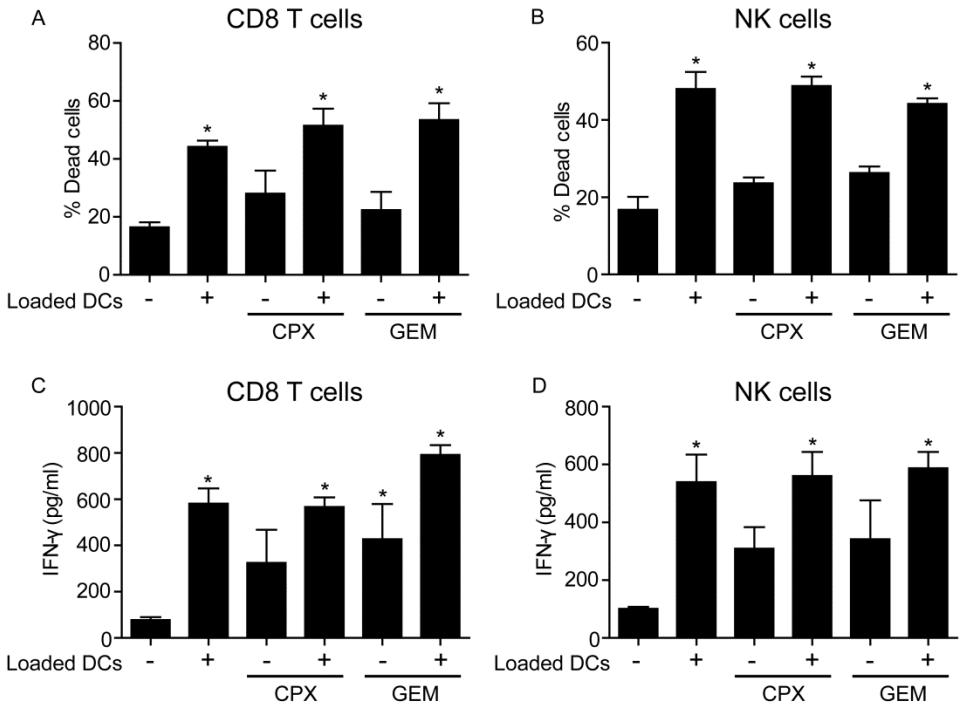

Figure 24. Tumor-specific cytotoxicity and cytokine responses following chemo-immunotherapy treatments. Cell mediated cytotoxicity of purified A) CD8 T cells ($CD8^+$ $TCR\beta^+$) and B) NK cells ($CD49b^+$ $TCR\beta^-$) isolated from the spleen of tumor resected mice treated with unloaded DCs, α-GalCer-loaded DCs, cyclophosphamide (CPX), gemcitabine (GEM) or combination therapies was analyzed via annexin V/7-AAD staining of Oregon Green-labeled 4T1 cells. Supernatant IFN-γ levels were measured by ELISA from sorted C) $CD8^+$ T cells and D) NK cells after 18 hours in culture in 4T1 cells (n = 6 per group). * $p < 0.05$ compared to unloaded DC.

Discussion

Using a mouse model of breast cancer metastasis, we recently demonstrated that NKT cell activation is effective in reducing metastasis, stimulating anti-tumor immunity, and improving survival [165]. However, cures were only achieved in 40-50% of mice, even when NKT cell activation therapy was repeated. This suggests that NKT cell therapy will need to be combined with other therapies to elicit more effective clinical responses. In this study, we demonstrate that NKT cell activation therapy can successfully be combined with moderate doses of gemcitabine or cyclophosphamide to further enhance protection against tumor metastasis and improve survival.

Chemotherapeutic drugs are designed to kill cancer cells, but may do so by different mechanisms [367]. Some chemotherapeutics promote immune responses against the tumor cells by inducing a process of ICD that enhances uptake and presentation of tumor antigens to the immune system [192,194,241,242,259]. This is in part due to the exposure/release of specific DAMPs, which recruit antigen presenting cells, stimulate phagocytosis and induce maturation. While the list of chemotherapy-induced DAMPs continues to increase, the best characterized include the exposure/release of CALR, ATP and HMGB1 [259,367]. CALR exposure is dependent on the induction of a pre-apoptotic ER stress response and the anterograde translocation of CALR to the cell surface [235]. Extracellular and surface-exposed CALR binds to CD91 on macrophages and DCs, leading to the engulfment of dying/stressed cells [253]. This has been shown to stimulate the release of proinflammatory cytokines by APCs and promote the priming of the adaptive immune response [259]. ATP is a chemoattractant for antigen presenting cells [259], and signaling via P2RX7 receptors on DCs and macrophages leads to the activation of

NLRP3/caspase-1 inflammasome pathway, with subsequent release of IL-1β and IL-18 [241]. In particular, IL-1β is required for the hierarchical priming of IL-17$^+$ γδ T cells and IFN-γ$^+$ CD8 T cells [241,373]. HMGB1 released from dying cancer cells is a potent ligand for TLR-4 [192]. HMGB1 binding to TLR-4 on DCs can enhance processing of phagocytic cargo, facilitate antigen presentation, upregulate costimulatory molecules, and increase intracellular levels of pro-IL-1β [192]. Recently, IFN induced CXCL10 release has been shown to be key in the establishment of effective anti-tumor immunity [246]. CXCL10 is a potent ligand for CXCR3, a receptor which is highly expressed on activated/memory T cells, NKT cells and NK cells [376]. Collectively, these DAMPs would promote both the innate and adaptive immune response against the tumor. I observed that treating 4T1 cancer cells with either gemcitabine or mafosfamide significantly increased the exposure/release of CALR, ATP, HMGB1 and *cxcl10*. As NKT cell stimulation enhances T cell polarization and NK and T cell effector responses, I reasoned that coupling NKT cell therapy with increased antigen presentation would enhance anti-tumor immunity and survival.

One of the ways tumor cells escape T cell mediated immunosurveillance is through down regulation of classical MHC I/II-mediated peptide antigen presentation to CD8$^+$ and CD4$^+$ T cells [38], and glycolipid antigen presentation to NKT cells via CD1d [70]. Consequently, chemotherapeutics that restore antigen presentation by cancer cells can help reinstate tumor immunosurveillance and prevent immune escape. Consistent with reports of chemotherapy-induced upregulation of MHC I [377] and MHC II [377,378], I observed an increase in expression of MHC I and MHC II on cancer cells treated with either gemcitabine or mafosfamide. Interestingly, I also observed an increase in CD1d

expression, which has not been reported previously. Collectively, gemcitabine and mafosfamide increased the potential for recognition of cancer cells by the immune system.

Consistent with previous reports, I observed enhanced survival in 4T1-challenged mice receiving cyclophosphamide [379], gemcitabine [77], or glycolipid-loaded DC treatment [165]. Chen *et al* [379] demonstrated a survival rate of ~10% in 4T1 tumor-bearing mice receiving cyclophosphamide treatment; however, their study used a 4-8 fold higher dose of cyclophosphamide delivered intraperitoneally. In our study, while cyclophosphamide therapy prolonged survival, none of the mice survived to the experimental endpoint. Consistent with our observations, others have shown that gemcitabine treatment in a post-surgical 4T1 metastasis model yielded ~28% survival rate [77]. While few studies have examined NKT cell activation therapy in combination with conventional chemotherapy, α-GalCer treatment improved cisplatin-mediated protection in a murine model of mesothelioma, but α-GalCer treatment alone showed no protection from disease progression [369]. Similarly, the combination of α-GalCer and 5-fluorouracil enhanced protection from MC38 colorectal cancer metastasis to the liver compared to either α-GalCer or 5-fluorouracil alone [370]. In our study, combining NKT cell activation with cyclophosphamide or gemcitabine resulted in a significant increase in the survival rate, compared to either therapy alone. Chemotherapy treatment alone did not result in robust $CD8^+$ T cell and NK cell mediated cytotoxicity, despite upregulating the frequency of activated and cytokine-polarized T cells. It is possible that these cells were not specific for tumor antigens as chemotherapy alone did not induce a durable response to tumor re-challenge. However, NKT cell activation therapy alone or in combination with

chemotherapy significantly increased cytotoxic activity and IFN-γ production by $CD8^+$ T and NK cells, and mediated resistance to tumor re-challenge. This implies that the protective effect of gemcitabine or cyclophosphamide monotherapy may be due primarily to direct cytotoxicity. Enhanced antigen presentation, or indirect effects on immune cell populations, such as MDSCs and T-regs, may not be sufficient to overcome immune barriers in the absence of immune activation promoted by NKT cell activation.

The levels of circulating MDSCs have been shown to correlate with disease progression in preclinical [77,165] and clinical studies [371]. MDSCs are of particular interest because they have been shown to inhibit antigen presentation and T cell responses [371]. In the previous chapter, we reported that circulating MDSCs could be used as a prognostic factor in NKT cell based therapy, and that NKT cell activation could overcome MDSC induced immunosuppression [165]. Cytotoxic compounds have been found to deplete MDSCs through mechanisms that remain poorly understood. In particular, gemcitabine treatment of tumor-bearing mice reduces MDSC levels [77,380]. Sinha *et al* [77] demonstrated that gemcitabine-induced reductions in MDSCs resulted in restoration of IL-12 production and decreased IL-10 levels in the 4T1 model, reversing detrimental Th2 immune polarization. In contrast to gemcitabine, cyclophosphamide has been reported to drive expansion of MDSCs at doses ≥100 mg/kg delivered intraperitoneally [82,83]. This is 5-fold higher than the dose used in our work; furthermore, we delivered cyclophosphamide periorally which is likely to decrease bioavailability. In our studies, cyclophosphamide transiently suppressed the accumulation of MDSCs after resection. However, it is possible that this was related to reduced tumor-induced myelopoiesis

resulting from decreased tumor burden, rather than immune stimulation, since all mice in this group ultimately failed to control tumor growth and succumbed to metastatic disease.

The efficacy of chemotherapy-induced ICD is highly dependent on an intact adaptive immune system [192,194] and the ability to promote anti-tumor immunity while decreasing immunosuppression [205,206,373,374]. During chemotherapy-induced ICD, ATP released from dying cells binds to P2RX7 on myeloid cells, induces IL-1β production, and subsequently leads to priming of a T cell-mediated anti-tumor immune response [241]. Cyclophosphamide has been shown to indirectly induce IFN-γ and IL-17A expressing $CD4^+$ T cells by disrupting the integrity of the gut mucosa, and allowing Gram-positive bacteria to colonize the secondary lymphoid organs [206]. In addition, cyclophosphamide transiently decreases the frequency of immunosuppressive T-regs, and enhances T cell priming [205]. In our study, cyclophosphamide increased the frequency of activated T cells and decreased the frequency of T-regs, but failed to induce a Th1 and Th17 polarization. This is likely due to the low dose of cyclophosphamide used in our experiments [206]. Gemcitabine can decrease the frequency and/or function of MDSCs [77,380] and B cells [203], while sparing T cells [203]. Furthermore, gemcitabine has been reported to enhance IFN-γ^+ $CD4^+$ and $CD8^+$ T cells in a murine model of oral cancer [375]. We observed an increase in activated $CD4^+$ and $CD8^+$ T cells in gemcitabine-treated tumor-bearing mice; however, using low doses of gemcitabine, the increase in IFN-γ^+ $CD4^+$ and $CD8^+$ T cells did not reach statistical significance. Interestingly, while combining NKT cell activation with low dose chemotherapy resulted in synergistic improvement in survival outcomes, we did not see a synergistic effect on expression of cytokines or cytotoxic molecules in T cells. It

is possible that the ICD-inducing chemotherapies were able to target immune responses more efficiently to the tumor sites, resulting in increased survival.

In conclusion, we show that NKT cell activation therapy can be safely and effectively combined with ICD-inducing chemotherapy to target metastatic breast cancer. This was associated with the induction of potent anti-tumor responses that protected surviving mice against tumor re-challenge. Our findings provide preclinical evidence supporting the development of therapeutic NKT cell based chemo-immunotherapy to target metastatic breast cancer.

Chapter 6: Targeting post-surgical breast cancer metastasis with combined NKT cell activation and oncolytic virus therapy.

In addition to testing whether NKT cell activation therapy can be successfully combined with current chemotherapeutic interventions, we wanted to investigate whether NKT cell activation therapy could be combined with oncolytic viruses that are currently in clinical trials. One promising approach is to use oncolytic virus therapy. Oncolytic viruses selectively target tumors by exploiting metabolic or signaling pathways that are dysregulated in cancer cells [215,381]. While oncolytic viruses can provide some protection by directly lysing cells, mounting evidence indicates oncolytic viruses can also stimulate a strong anti-tumor immune response [382–385]. Furthermore, strategies that combine oncolytic virus therapy with immune modulation therapy have been shown to further enhance anti-tumor immunity [386–389].

Initial experiments in the lab were focused on examining the potential of combining NKT cell activation with reovirus or VSVΔM51. These viruses have been shown to work synergistically with immune modulation therapy [390,391], *hence I hypothesized that combining them with NKT cell activation therapy would enhance protection in our post-surgical breast cancer model*. To the best of our knowledge, the strategy of combining NKT cell activation with oncolytic virus therapy has not been previously explored. In addition, I investigated the potential antigenic and immunogenic changes that oncolytic viruses can cause on tumor cells.

Results:

Combining reovirus or VSVΔM51 with NKT cell activation therapy to target post-surgical breast cancer metastasis.

We have previously demonstrated that NKT cell activation therapy significantly reduces tumor metastasis and increases survival [165]. In this study, we aimed to investigate whether oncolytic virus therapy could safely and effectively be used in conjunction with NKT cell activation therapy to enhance survival outcomes. Given that some viruses may acutely alter NKT cell responses [392], we wanted to determine whether VSVΔM51 or reovirus would negatively affect NKT cell activation. In our post-surgical breast cancer model (Figure 25A), VSVΔM51 or reovirus treatment did not induce serum IFN-γ or IL-4 levels (Figure 25B-C). NKT cell activation by transfer of α-GalCer-loaded DCs significantly increases serum IFN-γ and IL-4 [165]. We did not observe reductions in serum IFN-γ and IL-4 levels when NKT cells were activated following VSVΔM51 or reovirus treatments, suggesting that virus treatment did not impede NKT cell function. Reovirus treatment alone or in combination with NKT cell activation did not provide any significant protection nor did it enhance the protection by NKT cell activation (Figure 25D-E). These observations were surprising given that reovirus has been shown to be effective against many types of tumors [224,225,393], and the 4T1 model has been shown to have an overactive Ras pathway [394,395], which should make them susceptible to reovirus [221]. Treatment with VSVΔM51 or α-GalCer-loaded DCs alone reduced metastatic burden and improved survival (Figure 25F-G) This protection was further enhanced when VSVΔM51 was combined with NKT cell activation. Mice that survived to the experimental endpoint showed no signs of disease.

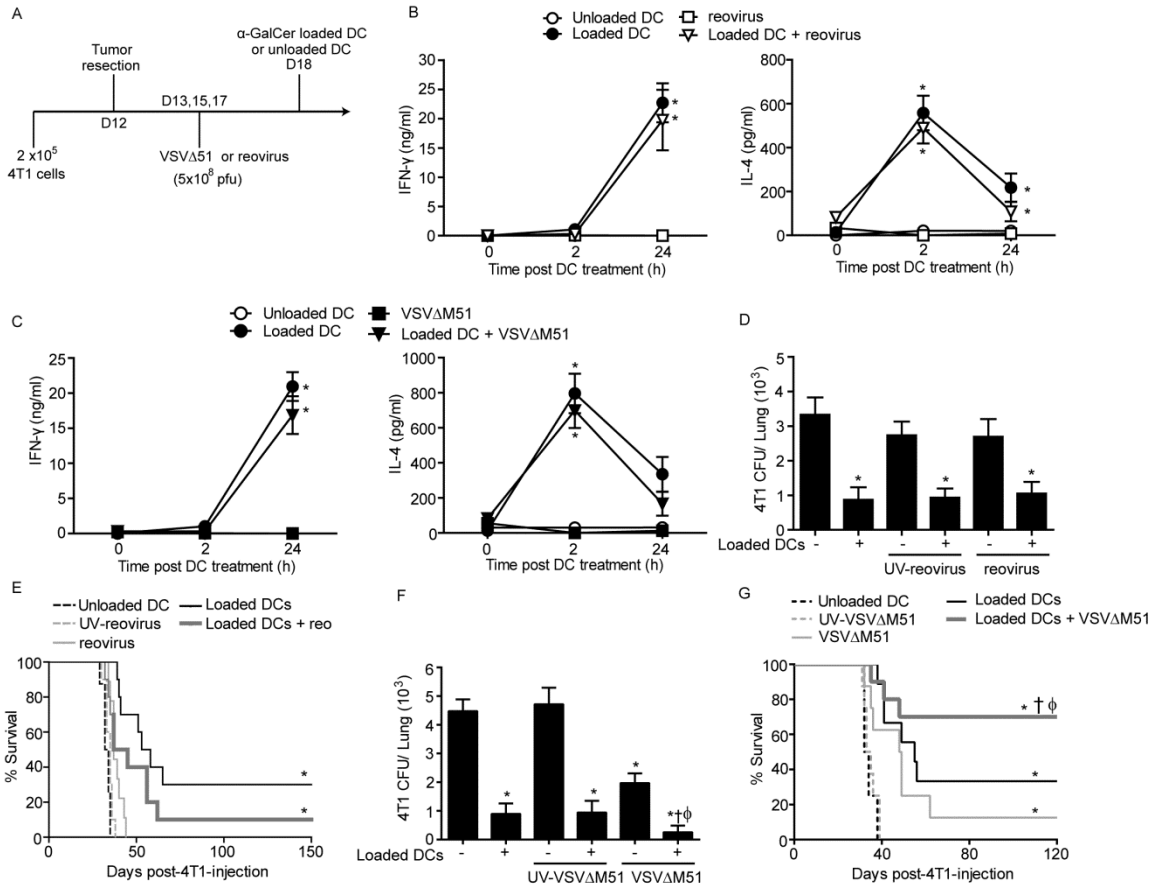

Figure 25. Combining NKT cell activation therapy with oncolytic virus therapy to target post-surgical metastatic disease. A) Schematic of treatments in the post-surgical 4T1 metastasis model. Mice were inoculated with $2x10^5$ 4T1 mammary carcinoma cells and primary tumors were resected on day 12. Mice received i.v. injection of reovirus or VSVΔM51 ($5x10^8$ pfu) on day 13, 15 and 17. On day 18, NKT cells were activated via i.v. injection of $2x10^5$ α-GalCer-loaded DCs. Serum levels of B) and C) IFN-γ and IL-4 were measured 0, 2 and 24 h after treatment with α-GalCer-loaded DCs (n = 3 per group). * $p < 0.05$ compared to unloaded DCs. D) Number of 4T1 CFU present in lung cell suspensions isolated at 28 post-4T1 injection (n = 9-10 per group). * $p < 0.05$ compared to unloaded DCs. E) Survival was assessed following treatment with unloaded DCs, α-GalCer-loaded DCs, UV-reovirus, reovirus, or α-GalCer-loaded DCs in combination with reovirus (n = 10 per group). * $p < 0.01$ compared to unloaded DC. F) Number of 4T1 CFU present in lung cell suspensions isolated at 28 post-4T1 injection (n = 9-10 per group). * $p < 0.05$ compared to unloaded DCs, † $p < 0.05$ compared to VSVΔM51 alone. G) Survival was assessed following treatment with unloaded DCs, α-GalCer-loaded DCs, UV-VSVΔM51, VSVΔM51 or combination of VSVΔM51 with α-GalCer-loaded DCs (n = 10per group). * $p < 0.01$ compared to unloaded DC, † $p < 0.01$ compared to VSVΔM51 alone, ϕ < 0.01 compared to α-GalCer-loaded DCs.

Given that reovirus has been shown to be effective in the ID8 model [224], I wanted to examine whether reovirus would provide better protection as a monotherapy or in combination with NKT cell activation in the ID8 model. We found that reovirus as a monotherapy or in combination with NKT cell activation significantly improved survival outcomes in the ID8 model (Figure 26).

VSVΔM51 can infect and kill 4T1 cells better than reovirus.

We hypothesized that the differences observed in the *in vivo* experiments may in part be due to differences in virus infectivity on different cancer cells. To investigate whether 4T1 cells were susceptible to VSVΔM51 or reovirus infection, cells were synchronously infected at MOI of 10 pfu per cell with VSVΔM51-GFP, reovirus, UV inactivated virus (UV-VSVΔM51-GFP, UV-reo) or medium control. Following 24 hour incubation, ~68% of the 4T1 cells were infected with VSVΔM51, but only ~24% of the 4T1 cells were infected with reovirus (Figure 27A). In line with better ability to infect 4T1 cells, VSVΔM51 also showed a better dose dependent cytotoxic effect on 4T1 cells (Figure 27B). To demonstrate that reovirus did not have a defect in its ability to infect cells, I examined whether reovirus could infect ID8 cells *in vitro*, given that we saw protection in vivo (Figure 27). Reovirus showed a better ability to infect and kill ID8 cells compared to 4T1 cells (Figure 27A-B).

Given that VSVΔM51 was better at infecting and killing 4T1 cells *in vitro*, showed enhanced protection in the post-surgical metastasis model, and is much more amenable to genetic manipulations, we focused the remainder of our studies on VSVΔM51. To further confirm the potential of VSVΔM51 to broadly infect and kill

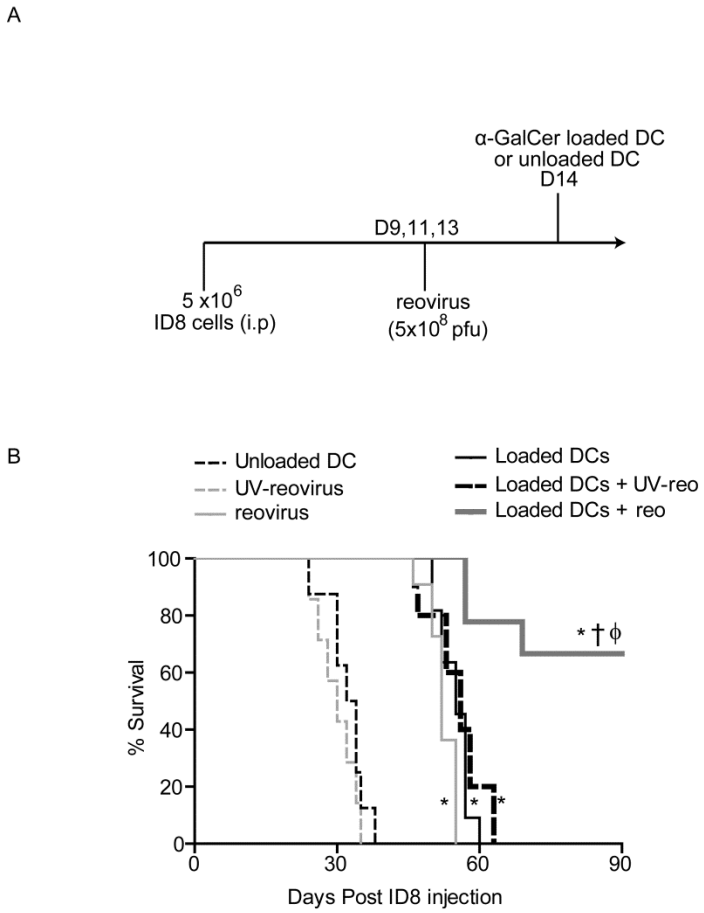

Figure 26. Combining NKT cell activation therapy with reovirus therapy to target ID8 ovarian cancer. A) Schematic of treatment in ID8 ovarian cancer model. Mice were inoculated with $5x10^6$ ID8 ovarian carcinoma cells. Mice received i.p injection of reovirus ($5x10^8$ pfu) on day 11, 13 and 15. On day 14, NKT cells were activated via i.p injection of $2x10^5$ α-GalCer-loaded DCs. B) Survival was assessed following treatment with unloaded DCs, α-GalCer-loaded DCs, UV-reovirus, reovirus, or α-GalCer-loaded DCs in combination with reovirus or UV-reovirus (n = 10 per group). * $p < 0.01$ compared to unloaded DC, † $p < 0.01$ compared to reovirus alone, ϕ < 0.01 compared to α-GalCer-loaded DCs.

cancer cells, I tested whether VSVΔM51 can infect and kill other cell lines available in the lab (Figure 28). We found that VSVΔM51 infected and killed a wide number of mouse cancer cell lines, including B16 melanoma, Lewis lung carcinoma (LLC), and Panc02 pancreatic carcinoma. This demonstrates that VSVΔM51 could potentially be used to target multiple cancer types.

VSVΔM51 enhances antigen presentation.

To examine the effect of VSVΔM51 on antigen presentation, we examined the expression of MHC I, MHC II and CD1d on VSVΔM51-infected 4T1 cells (Figure 29A). MHC-I levels were elevated at 24, 48 and 72 hours following VSVΔM51 infection. In contrast, MHC-II and CD1d levels were upregulated at 48 and 72 hours following VSVΔM51 infection. In addition, we examined the mRNA levels of transporter associated with antigen processing (*tap*) 1 and 2. We also observed an elevation in the *tap1* and *tap2* mRNA levels 24 hours following VSVΔM51 infection (Figure 29B). These results suggest that oncolytic virus infection can enhance tumour cell antigen presentation to the immune system.

VSVΔM51 enhances cytokine production.

VSVΔM51 has been shown to induce cytokine production by infected cancer cells[396]. We examined changes in mRNA expression in 4T1 cells 24 hours following VSVΔM51 infection. VSVΔM51 infection upregulated transcript expression for several inflammatory cytokines:*il-6, ifn-α, ifn-β,* and *tnf;* and chemokines: *ccl3, ccl4, ccl5, cxcl2, cxcl9, cxcl10, cxcl11 and cxcl16* (Figure 30). Interestingly, UV- inactivated VSVΔM51 upregulated *ccl3* mRNA levels, suggesting the possibility of activation through pattern recognition receptors rather than a need for viral replication.

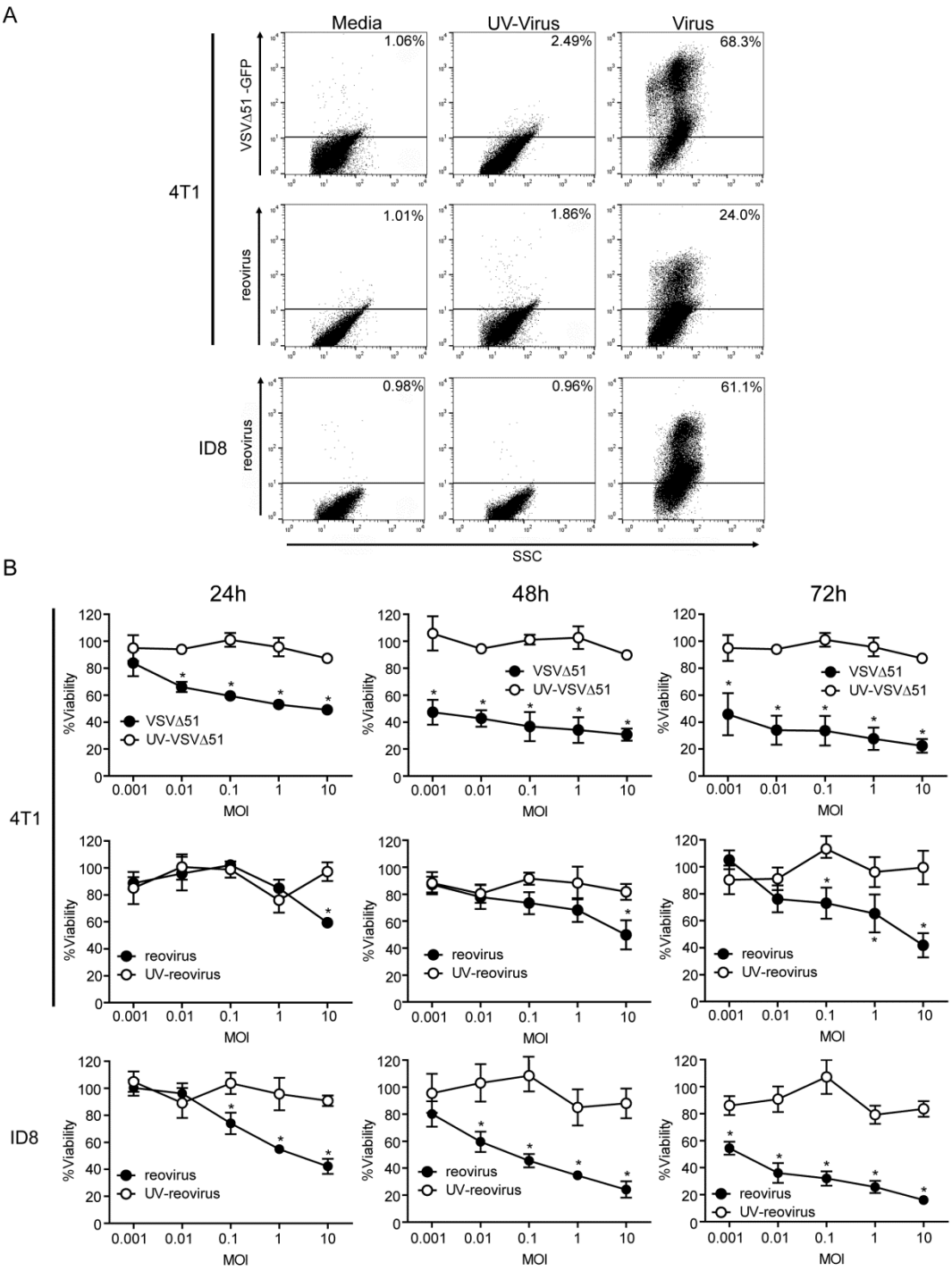

Figure 27. VSVΔM51 infects and kills 4T1 cells better than reovirus. A) 4T1 and ID8 cells were treated with VSVΔM51-GFP, UV-VSVΔM51-GFP, reovirus or UV-reovirus for 24 hours to assess the permissibility of 4T1 cells to productive VSVΔM51 infection by flow cytometry. B) 4T1 and ID8 cell viability was analyzed at different multiplicities of infection (MOI) using an MTT cell viability assay. Cell viability is expressed relative to untreated media conditions for each time point (n=3-4 per group). *P<0.05 compared to UV-VSVΔM51 or UV-reovirus.

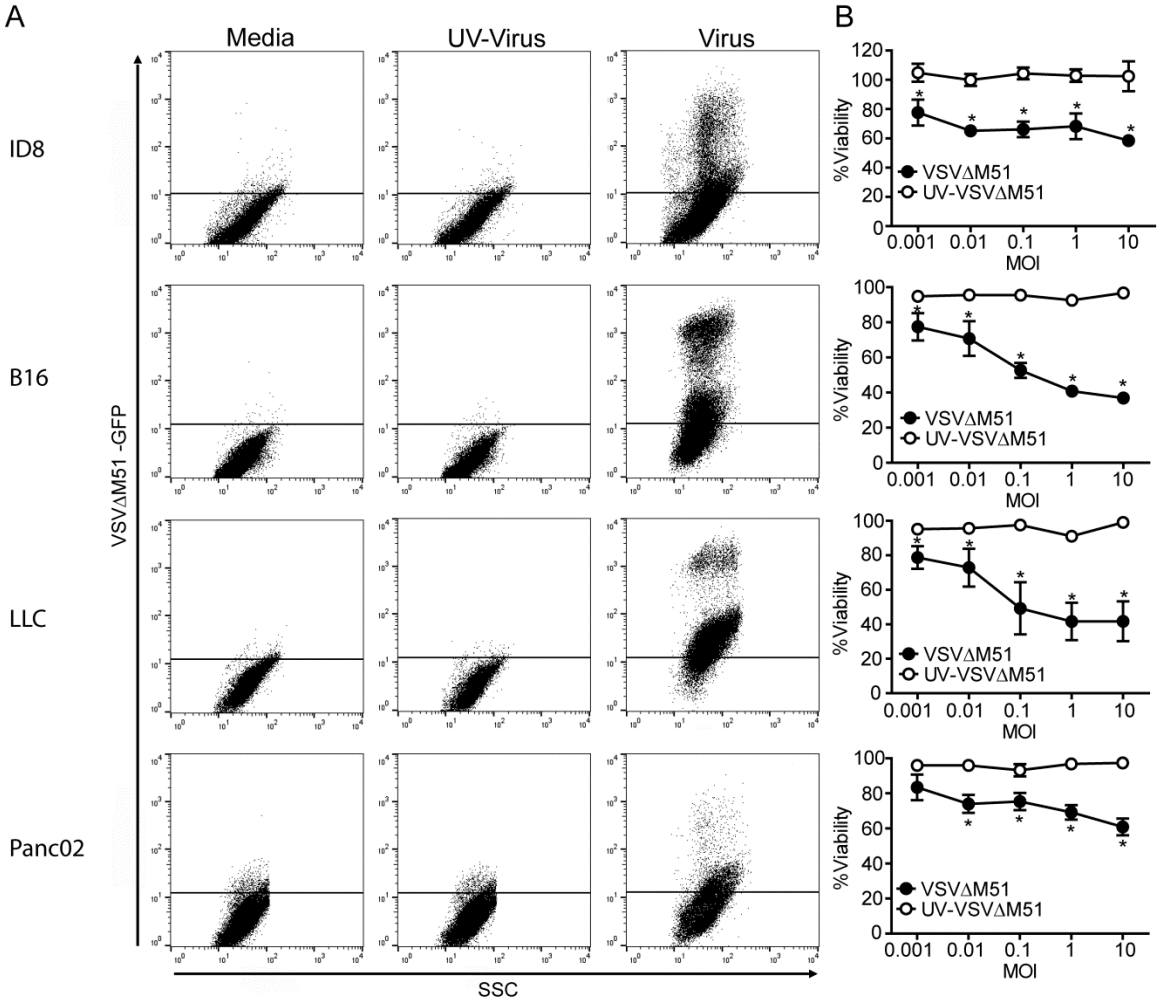

Figure 28. VSVΔM51 infects and kills a broad range of cancer cell types. A) ID8 ovarian carcinoma, B16 melanoma, Lewis lung carcinoma (LLC) and panc02 pancreatic cancer cells were treated with VSVΔM51-GFP or UV-VSVΔM51-GFP for 24 hours to assess the permissibility to productive VSVΔM51 infection by flow cytometry. B) Cell viability was analyzed at different multiplicities of infection (MOI) using an MTT cell viability assay 24 hours following infection. Cell viability is expressed relative to untreated media conditions for each time point (n=3-4 per group). *P<0.05 compared to UV-VSVΔM51.

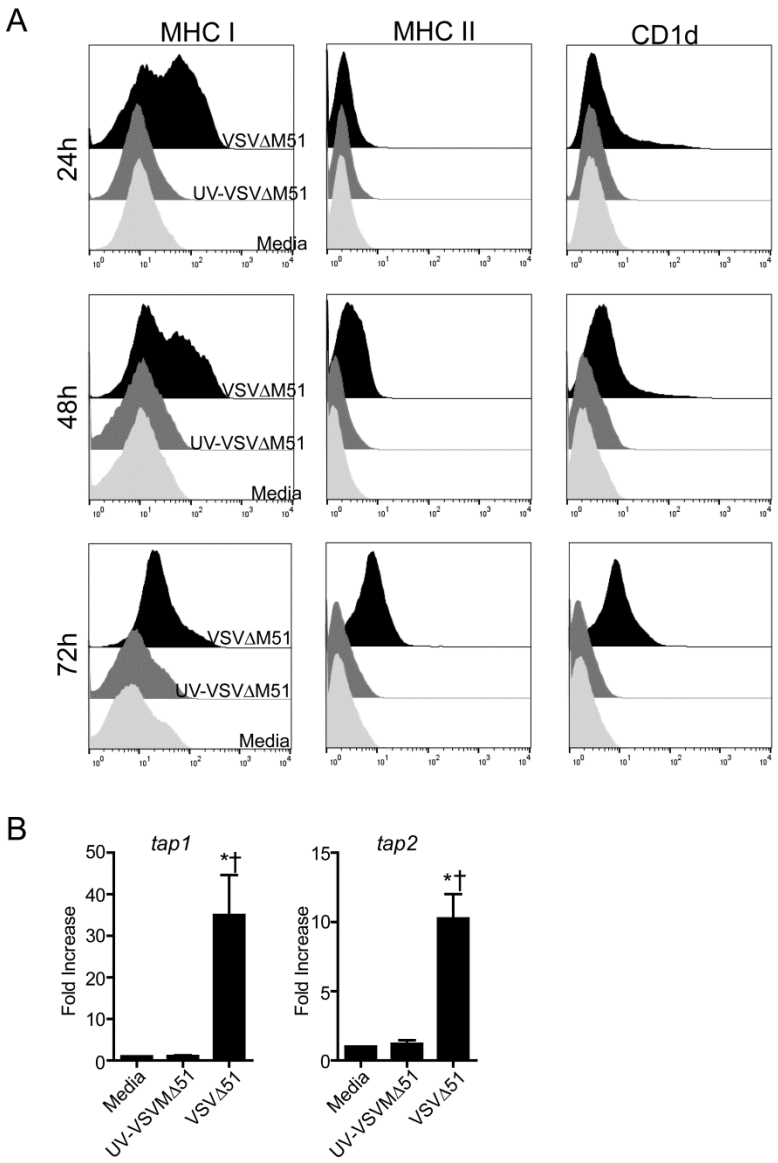

Figure 29. VSVΔM51 enhances antigen presentation on 4T1 cells. A) Flow cytometry histograms of MHC-I, MHC-II and CD1d expression on cultured 4T1 cells 24, 48 and 72 hours after virus infection (MOI 1). Plots are representative of n= 4-6 per group. B) Quantitative PCR (qPCR) examining the expression of *tap1* and *tap2* in 4T1 cells were treated with UV-VSVΔM51 or VSVΔM51 for 24h. qPCR was analyzed using the $2^{-\Delta\Delta CT}$ quantification technique relative to the housekeeping gene GAPDH (n= 6). *P<0.05 compared to Media, † $p < 0.05$ compared to UV-VSVΔM51.

VSVΔM51 enhances tumor immunogenicity.

Some viruses can also stimulate the immune system by inducing ICD, a mechanism of cell death that increases immune recognition of tumor cells [397,398]. To determine whether VSVΔM51 can induce ICD in 4T1 cells, we monitored the expression of CALR, ATP and HMGB1 following virus infection. During ICD, CALR mobilization to the cell surface instructs DCs to engulf the dying tumor cells, enhancing presentation of tumor-derived antigens [235]. To examine the localization of CALR, we used flow cytometry and confocal microscopy on non-permeabilized 4T1 cells. After 8h of VSVΔM51-GFP infection, we observed a significant increase in CALR translocation to the cell surface (Figure 31A-B). However, this was not observed in cells receiving UV-irradiated VSV-GFP, suggesting that viral infection and replication was required. Viruses have also been shown to induce ATP and HMGB1 release [397,398], which recruits DCs to the tumor site and activates the inflammasome in infiltrating DCs [194,241], and induces DC maturation [192], respectively. VSVΔM51 induced a significant increase in ATP and HMGB1 release from 4T1 cells (Figure 31 C-D).

Effect of oncolytic/combination therapy on anti-tumor immunity

To examine whether mice surviving to the experimental endpoint had lasting immunological memory against the 4T1 tumor, we re-challenged mice by inoculating 4T1 cells in the contralateral mammary fat pad. Mice receiving NKT cell activation alone or in combination with VSVΔM51 showed significant protection from tumor growth and metastasis (Figure 32), suggesting immune memory against the 4T1 cells. Whereas mice receiving VSVΔM51 alone were not as effective at delaying tumor growth and metastasis.

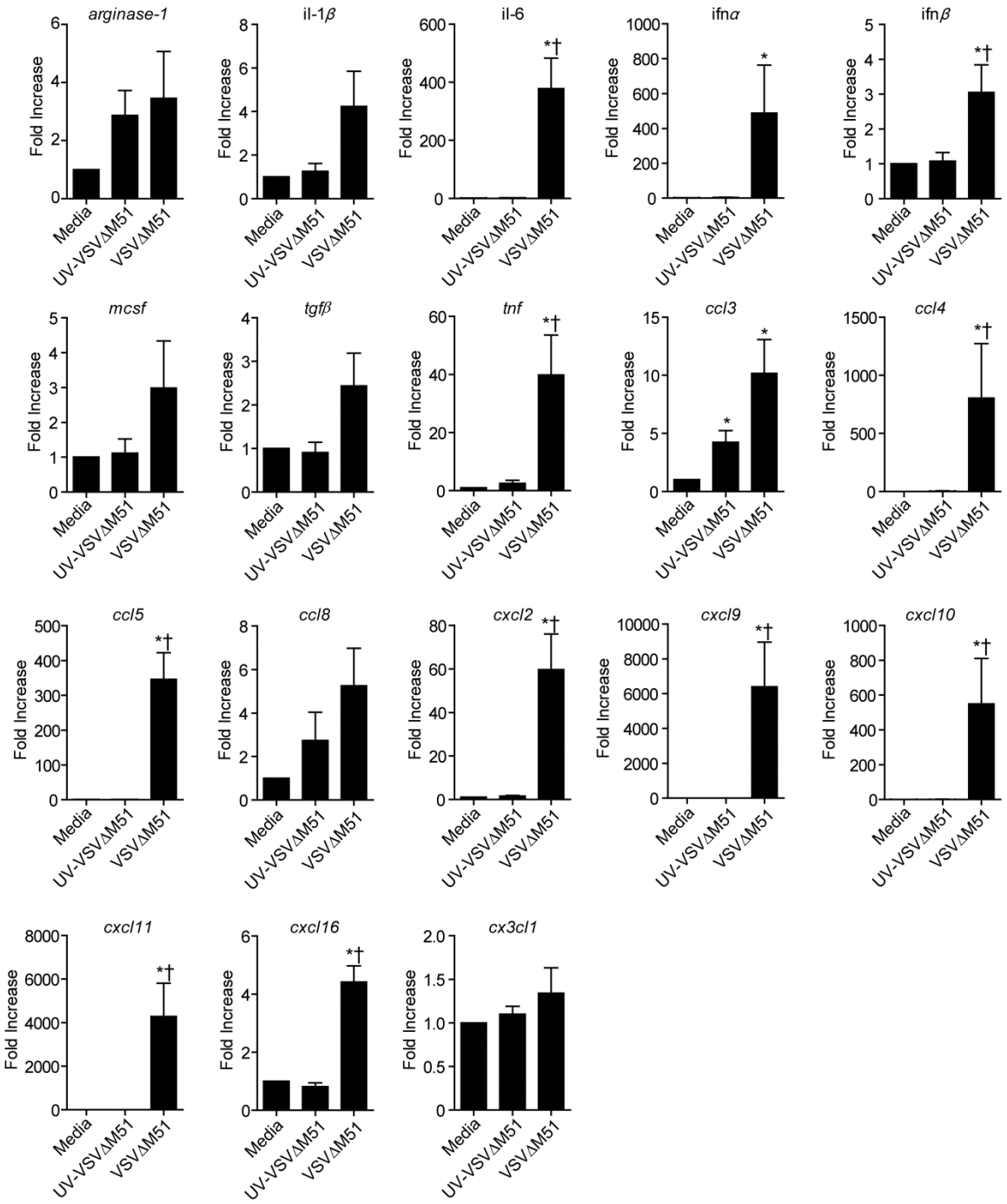

Figure 30. VSVΔM51 alters cytokine and chemokine mRNA levels in 4T1 cells. 4T1 cells were treated with UV-VSVΔM51 or VSVΔM51 for 24 hours. qPCR was analyzed using the $2^{-\Delta\Delta CT}$ quantification technique relative to the housekeeping gene GAPDH (n=6-9). Fold induction was compared to media alone (n= 6-7 per group). P<0.05 compared to Media, † $p < 0.05$ compared to UV-VSVΔM51.

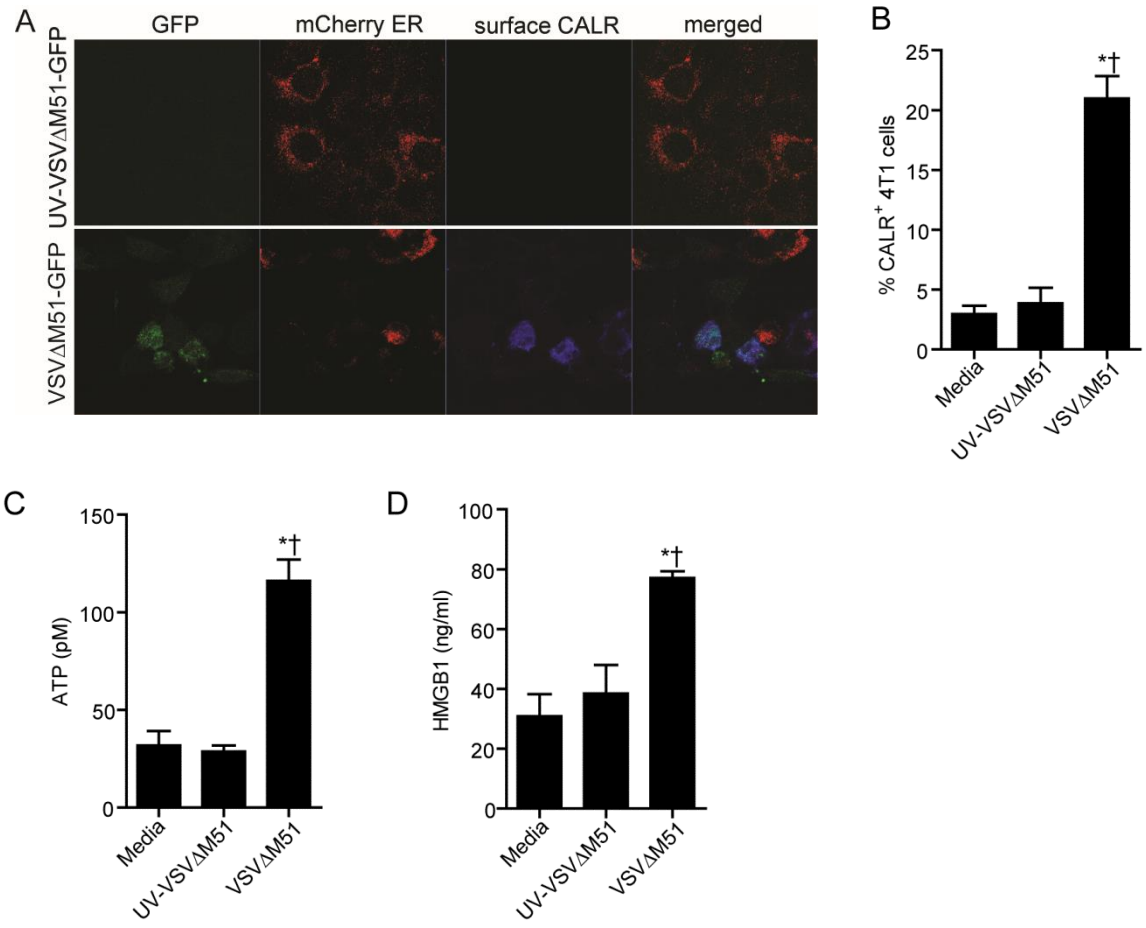

Figure 31. VSVΔM51 induced immunogenic changes on 4T1 cells.
A) Immunofluorescence analysis of CALR (blue) localization on 4T1 cells after 8 hours of VSVΔM51 treatment. ER labelled mCherry-KDEL (red) expressing 4T1 cells were treated with either UV-VSVΔM51-GFP or VSVΔM51-GFP and cell surface CALR staining was performed on non-permeabilized cells. Images are representative of n= 4 per group. B) Flow cytometric expression of surface CALR on 4T1 cells 8 hour after treatment (n= 4 per group). * $p < 0.05$ compared to Media, † $p < 0.05$ compared to UV-VSVΔM51. C) ATP and D) HMGB1 release into culture supernatants of virus treated 4T1 cells was examined 24h following treatment (n= 4 per group). * $p < 0.05$ compared to Media, † $p < 0.05$ compared to UV-VSVΔM51.

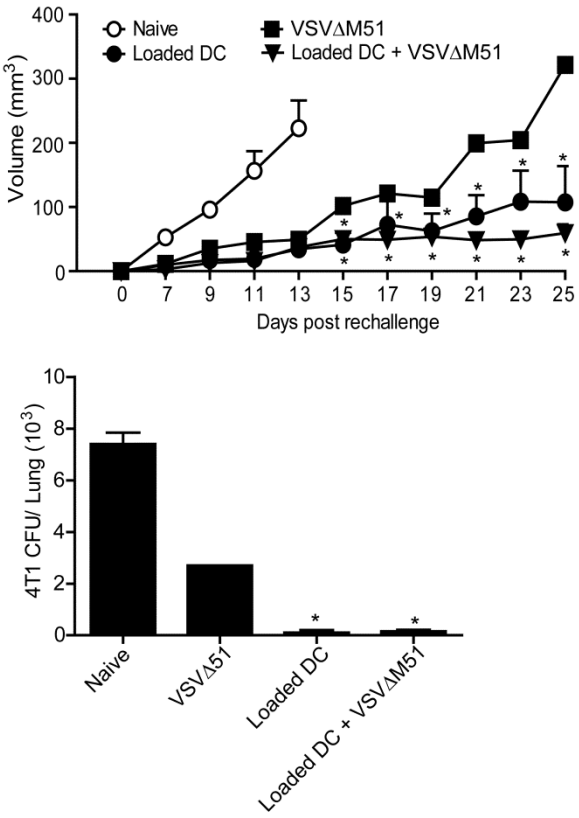

Figure 32. Surviving mice showed delayed tumor growth following re-challenge. Tumor resected mice that survived to day 120 after treatment with α-GalCer-loaded DCs, VSVΔM51, combination of VSVΔM51 and α-GalCer-loaded DCs were re-challenged in the contralateral mammary fat pad with 4T1 cells. A) Tumor volume was compared to tumors grown in naïve mice (n = 4-7 per group, n=1 for VSVΔM51 group). * $p < 0.05$ compared to matched naïve control or naïve control on day 13. (G) Metastatic burden was compared to naïve mice (n = 4-7 per group, n=1 for VSVΔM51 group). * $p < 0.05$ compared to naive control.

Discussion

Oncolytic viruses exert their anti-tumor effect by direct tumor cell lysis, stimulation of the immune response, and/or disruption of tumor vasculature [397,399,400]. To date, there have been a number of oncolytic viruses that are currently undergoing clinical trials, with talimogene laherparepvec (T-VEC) receiving FDA approval in 2015 [211,212]. To enhance efficacy of oncolytic viruses, several studies have attempted to combine oncolytic virus therapy with chemotherapy [401] or immunotherapy [402]. In this study, we investigated whether NKT cell activation therapy can effectively be combined with oncolytic virus therapy to target post-surgical breast cancer metastasis.

Our data demonstrates that reovirus is not effective either as a monotherapy or in combination with NKT cell activation in the 4T1 breast cancer model. In contrast, reovirus was effective as a monotherapy or in combination with NKT cell activation in the ID8 ovarian cancer model. These differences are likely due to the low levels of reovirus infectivity in the 4T1 cells and not likely due to Ras activity, as 4T1 cells have been reported to have high Ras activity [394,395]. Therefore we hypothesize that the defect might be in the ability of reovirus to enter 4T1 cells. The capacity of reovirus to infect cultured cells has been shown to dependent on the reovirus sigma (σ) 1 protein, a fibrous trimer consisting of a tail domain that inserts into the virion and a globular head domain that projects away from the virion surface [403]. The tail domain binds to α-linked sialic acid residues on the cell surface, whereas the head domain binds to junctional adhesion molecule 1 (JAM1) as a cellular receptor, both key interactions in determining cell susceptibility to reovirus infection [403]. Attachment to cell surface α-linked sialic acid residues facilitates binding to JAM1. While 4T1 cells express JAM1 [404], we could not

find any studies comparing the expression levels of both JAM1 and α-linked sialic acid across cell lines, it is possible that 4T1 cells may have lower levels of sialic acid and JAM1, which may negatively impact on the ability of reovirus to infect and kill 4T1 cells.

In contrast, VSVΔM51 can potently infect and kill a broad range of cells in culture, including 4T1 cells [405–407], and this may likely be due to a high expression of a VSVΔM51 entry receptor. VSVΔM51 has been shown to infect cells via multiple ubiquitously expressed cell-surface molecules such as low density lipoprotein receptor, phosphatidylserine, sialoglycolipids and heparin sulfate [408]. In line with better infectivity in the 4T1 cells, VSVΔM51 enhanced survival in the 4T1 breast cancer model [405,409];thus, our study extends these findings to a post-surgical 4T1 model and also demonstrates that combining VSVΔM51 monotherapy in combination with NKT cell activation therapy can further protect against metastatic disease and improve survival (Figure 25G).

Down-regulation of HLA class I (human MHC I), TAP1 and TAP2 has been associated with high-grade breast cancer lesions, whereas low grade lesions showed a strong staining for HLA class I, TAP1 and TAP2 [410]. Consistent with other reports, we observed an increase in transcript levels of *tap1* and *tap2* [411] and MHC-I antigen presentation [389,412] following VSVΔM51 infection. Upregulation of MHC-I expression favors recognition of tumor cells by CD8 T cells, resulting in enhanced antitumor immunity.

VSVΔM51 has also been shown to upregulate MHC-II on microglial cells [413] and dendritic cells [385]. We observed an upregulation of MHC-II on 4T1 cells, potentially making them a target for cytotoxic CD4 T cells [414]. While VSVΔM51 infection did not have an effect on cell surface CD1d levels of CD1d transfected L cells [415] or BMDCs [416],

VSVΔM51 altered intracellular CD1d trafficking [415,416]. It is important to note that these studies only looked at the effect of VSVΔM51 on CD1d 1-4 hours following infection [415,416]. In contrast, mice treated with VSVΔM51 showed reduced CD1d levels on splenic DCs and macrophages 6 days following infection [417]. We observed a slight increase in CD1d expression on 4T1 cells following VSVΔM51 infection 24-72 hours following infection. These differences may be due to the cell types and duration of infection. Future studies will examine the effect of VSVΔM51 on CD1d expression on both cancer and immune cells.

VSVΔM51 infection increased the relative expression of proinflammatory cytokines and chemokines by 4T1 cells. Intratumoral injection of VSVΔM51 in B16 melanoma-bearing mice induced an upregulation in *il-6* and *tnf* mRNA in the primary tumors [418]. Consistent with an anti-viral TLR-mediated response, VSVΔM51 also upregulated *ifn-α* and *ifn-β*. Two recent studies showed IFN-α and IFN-β are required for initiation of anti-tumor responses; they act on $CD8^+CD103^+$ DCs to enhance cross-presentation of tumor antigens to CD8 T cells [419,420]. VSVΔM51 infection in a mouse model of viral encephalitis was also shown to induce the expression of *ccl3, ccl4, ccl5, cxcl2, cxcl10* and *cxcl11* in brain tissues [421]. Chemokine upregulation in the brain was associated with an increase in infiltrating neutrophils, macrophages, NK cells and T cells. This was likely mediated through the actions of CXCL2 on $CXCR2^+$ neutrophils [376]; CCl3, CCl4, CCl5 on $CCR5^+$ macrophages and T cells [376]; CXCL10 and CXCL11 on $CXCR3^+$ T cells and NK cells [376]. While CXCL16 has not been directly implicated in VSV infection, NK cell memory of VSV has been shown to depend on CXCR6 expression [422], a chemokine receptor for CXCL16. Future studies will examine the

chemokine expression patterns in a 4T1 primary tumor model, the tumor-infiltrating immune cells and the potential role of chemokine receptors in oncolytic virus clearance/therapy.

Similar to chemotherapy-induced immunogenic cell death, oncolytic viruses have been shown to induce an immune response against the dying cancer cell [237,397,423,424]. Consistent with our findings using VSVΔM51, oncolytic adenovirus expressing CD40L induced mobilization of CALR to the cell surface, ATP and HMGB1 release from dying cancer cells, resulting in enhanced antitumor immunity [237]. Oncolytic herpes simplex virus 1 has also been shown to induce immunogenic cell death characterized by increased heat shock protein-70, elevated serum HMGB1 and an antigen specific CD8 T cell response [397]. While we have not characterized the anti-tumor immune response, tumor re-challenge experiments suggest VSVΔM51 therapy alone or in combination with NKT cell activation therapy induces a memory response against the 4T1 cells. However additional experiments will be needed to better understand the antitumor immune response.

In conclusion, we show that oncolytic VSVΔM51 can infect 4T1 cells and induce immunogenic cell death. VSVΔM51 can safely and effectively be combined with NKT cell activation therapy to target metastatic 4T1 cells and improve survival outcomes. Further experiments are required to delineate the anti-tumor immune response associated with this therapeutic approach. These preliminary studies perform a proof of principle for the potential of combining NKT cell activation therapy with oncolytic virus therapy.

Chapter 7: Discussion

1. NKT cell expansion and reconstitution model:

We have characterized a rapid and reliable method of expanding functional murine NKT cells *in vivo*, and demonstrated that we can successfully transfer and reconstitute the expanded NKT cells in Jα18$^{-/-}$ mice, generating a normal NKT cell population that responds to glycolipid re-stimulation. This expansion and reconstitution model provides a vital tool to study NKT cell biology. For instance, this tool has allowed us to demonstrate that NKT cell derived IFN-γ is not required for efficient control of tumor metastasis or NK cell transactivation, challenging a longstanding dogma in the field. Transfer of NKT cells deficient in other effector molecules will allow for the study of specific mechanisms through which NKT cells exert their biological effector functions in tumor models. It will be important to expand this work into other disease models and confirm our observations in the B16 melanoma model. There is currently ongoing work in the lab using the expansion and reconstitution model to examine the role of NKT cell derived cytokines in a murine model of rheumatoid arthritis. Such studies will ultimately lead to a better understanding of NKT cell function that will aid in the development of improved NKT cell based immunotherapies.

A second important question that could be addressed using this tool is NKT cell plasticity. Recently, subsets of NKT cells have been identified based on transcription profiles and surface markers [92,108–112]. NKT1 which express T-bet, IFN-γ, TNF-α, granzyme and perforin. NKT2 which express PLZF^{hi}, GATA3, IL-4, IL-13, IL-6. NKT10 express E4BP4, Nur77^{hi}, IL-10 and IL-3. NKT17 express RORγt, IL-17A, IL-21 and IL-22. However, the plasticity of these subsets remains poorly understood. Using the

expansion and reconstitution model, subsets of these NKT cells could be purified, adoptively transferred into NKT cell deficient Jα18$^{-/-}$ and monitored over time. It will be interesting to examine whether over time these cells maintain their profile, or become influenced by their new environments into different subsets of NKT cells.

2. NKT cell in Breast Cancer

We show that NKT cell activation using α-GalCer-loaded DCs was effective in targeting metastatic breast cancer lesions in mice and significantly enhanced survival. This was associated with reduced expansion of MDSCs and induction of potent anti-tumor responses by NK cells and CD8^{+} T cells. Our findings provide preclinical evidence supporting the development of therapeutic NKT cell activation strategies to target metastatic breast cancer. However, there are several hurdles that remain with this strategy. One major hurdle for clinical translation is the need to isolate the patient's own dendritic cells, culture them, and load the DCs with glycolipid for injection back into the patient. This approach limits NKT cell cancer therapy to major academic institutions and cancer centers.

To address this, I would propose several strategies. First, I think it will be important to examine whether the use of checkpoint inhibitors can overcome the anergy associated with direct glycolipid injection [329,331]. There are reports that glycolipid injection with CTLA4 blockade showed some protection in a murine model of 4T1 [359]. Given the increase in the number of checkpoint blocking antibodies (PD1/PDL1, CTLA4, TIM-3, LAG-3), it would be interesting to examine whether combining direct glycolipid with these checkpoint blocking antibodies would provide equivalent protection as glycolipid loaded DCs.

Secondly, anergy is likely induced by glycolipid via other CD1d-expressing cells that poorly present the antigen and/or lack appropriate co-stimulatory signals [331,362]. In contrast, glycolipid delivery via DCs induces potent NKT cell activation without induction of anergy [331]. Therefore, strategies that can directly target glycolipids to DCs, while avoiding other CD1d expressing cells, may allow for glycolipid loading onto DCs without requiring *ex-vivo* loading. Liposomes are vesicles comprising of a phospholipid bilayer and an aqueous core which can be used to carry drugs [425]. Liposomes can be designed to express targeting moieties such as monoclonal antibodies, allowing for specific targeting to certain cell types [425]. A possible mechanism of α-GalCer delivery to DCs would be to incorporate single-chain antibody fragments targeting CD11c and DEC-205 [426]. This would potentially lead to the delivery of α-GalCer to DCs *in vivo*, negating the need for expensive DC isolation procedures in the clinic.

3. Combining NKT cells with oncolytic viruses

We show that oncolytic VSVΔM51 can infect 4T1 cells and induce immunogenic cell death. VSVΔM51 can also induce the expression of cytokines which can activate and recruit immune cells to the site of the tumor. Furthermore, VSVΔM51 can safely and effectively be combined with NKT cell activation therapy to target metastatic breast cancer. Combined treatment significantly enhanced survival compared to individual VSV or NKT cell activation therapies. These preliminary studies perform a proof of principle for the potential of combining NKT cell activation therapy with oncolytic virus therapy. Further experiments are required to better understand the anti-tumor immune response associated with this therapeutic approach.

We have identified several chemokines which are upregulated in infected cancer cells. Of particular interest to our lab are CCR5 ligands (CCL3, CCL4, CCL5), CXCR3 ligands (CXCL10, CXCL11) and CXCR6 ligand (CXCL16). The chemokine receptors CXCR3 and CXCR6 are highly expressed on NKT cells, whereas CCR5 is upregulated on activated NKT cells [120]. It would be interesting to examine whether these chemokine receptors play an important role in our combination therapy strategy. Our lab currently has $CCR5^{-/-}$, $CXCR3^{-/-}$ and $CXCR6^{-/-}$ mice. We will inoculate these chemokine receptor knockout mice and wildtype controls with tumors, treat with oncolytic viruses, then monitor tumor progression and immune infiltration into tumors. It will also be interesting to examine whether combining NKT cell activation with oncolytic virus therapy will provide benefits in the absence of these chemokine receptors. An additional interesting approach would be to knock out these chemokines (CCL3, CCL4, CCL5, CXCL10, CXCL11, CXCL16) in tumor cells and examine what effect this would have on oncolytic virus therapy.

Recent studies have demonstrated that engineering VSV to express immunostimulatory genes including IL-12, IL-15 , IL-23, IFN-γ, IFN-λ and CD40L [427]. We hypothesize that these cytokines/co-stimulatory molecules will potentiate a stronger anti-tumor immune response. Our lab has recently acquired VSV-IL15 and will work towards acquiring the additional constructs. We will examine whether combining these engineered VSV strains with NKT cell activation will provide beneficial effect. Intriguingly, it would be exciting to examine whether we could combine more than one of these viruses during delivery e.g. delivery of VSV-IL12 and VSV-IL15 treatment. Recently, oncolytic viruses have also been engineered to express tumor specific antigens

[428,429]. This work has been further advanced with prime: boost technology, where the first virus is used to prime the immune system to the antigen, and a second virus is used to boost a secondary immune response against the tumor antigen [429]. It would be interesting to examine whether this approach could further be potentiated when combined with NKT cell activation therapy.

Proposed model

NKT cells have been implicated in cancer immunosurveillance, and activation by exogenous glycolipids can further enhance this protection. In these studies, we sought to examine the potential for NKT cell activation therapy as a treatment for targeting post-surgical breast cancer. We found that NKT cell activation using α-GalCer-loaded DCs provided significant protection against post-surgical breast cancer metastasis in mice. This was associated with reduced expansion of MDSCs and induction of potent anti-tumor responses by NK cells and $CD8^+$ T cells. This protection was further enhanced when NKT cell activation therapy was combined with therapies that induce ICD; gemcitabine, cyclophosphamide or VSVΔM51 treatments in combination with NKT cell activation therapy further enhanced survival and induced potent anti-tumor responses (Figure 34). These therapies induced strong memory responses as surviving mice exhibited attenuated tumor growth following tumour re-challenge.

To better understand the mechanisms underlying NKT cell anti-tumor immunity, I also developed tools to study NKT cell biology, establishing a reliable method of expanding functional NKT cells and reconstituting them into $J\alpha18^{-/-}$ mice. This tool has allowed us to demonstrate that NKT cell derived IFN-γ is not required for efficient control of tumor metastasis or NK cell transactivation, challenging a long standing

dogma in the field. While I did not completely elucidate the mechanisms, our work implicates DCs as potential key players in NK cell transactivation.

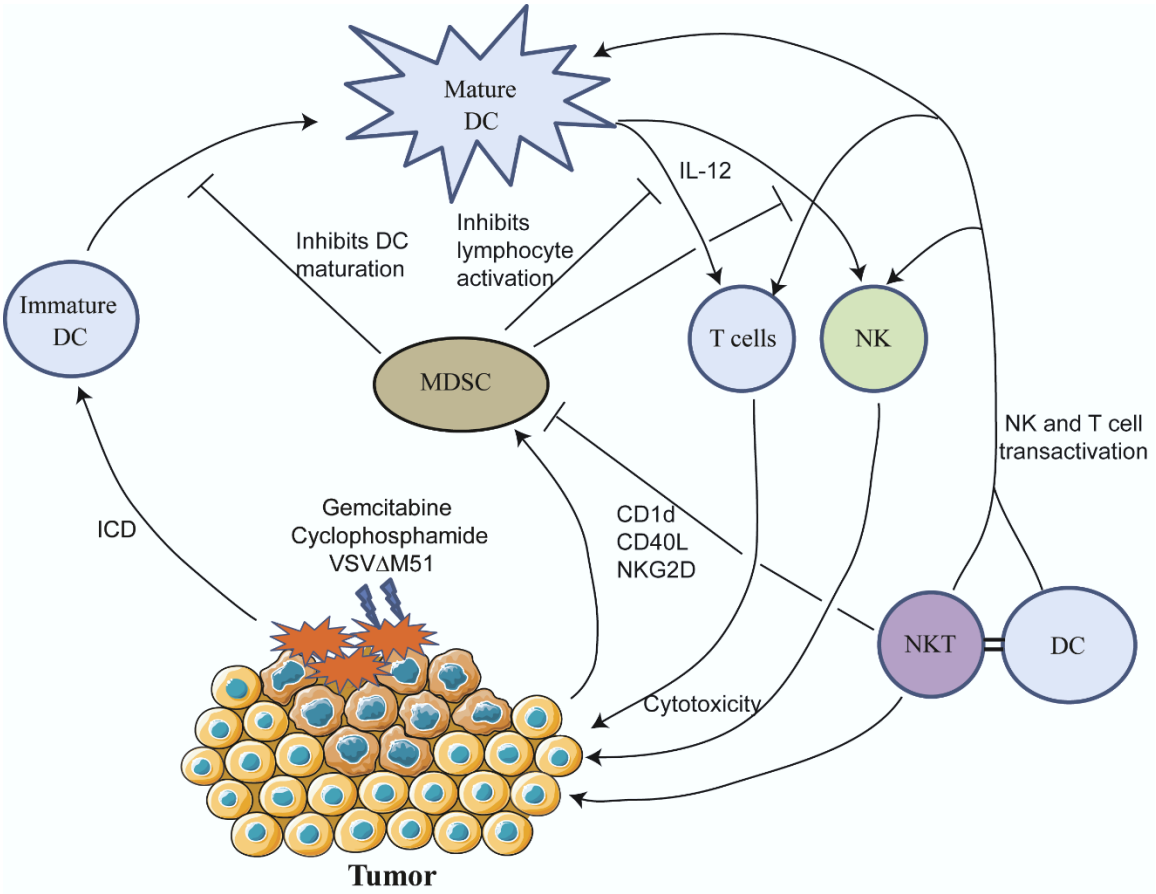

Figure 33. Model outlining mechanisms underlying NKT cell activation therapy in combination with inducers of ICD. Gemcitabine, cyclophosphamide and VSV can upregulate DAMPS. These DAMPS facilitate the recruitment of DCs into the tumor microenvironment, the engulfment of tumor antigens and optimal antigen presentation to T cells. DCs can also produce cytokines that stimulate NK cells and tumour-specific T cells, which target tumor cells for destruction. NKT cells activated using exogenous glycolipids, provide potent support for activation of anti-tumour T cells and NK cells, and can directly kill tumour cells. Activated NKT cells can also overcome tumor-induced suppression mediated by MDSCs.

References

1. Statistics Canada. Canadian cancer statistics. *Can. Cancer Soc.* 1–132 (2017).

2. Hanahan, D. & Weinberg, R. A. The hallmarks of cancer. *Cell* **60,** 319–26 (2000).

3. World Health Organization. International classification of diseases for oncology, 3rd edition (ICD-O-3). *Classification of Diseases* (2015).

4. Siegel, R. S., Pandolfino, T., Guitart, J., Rosen, S. & Kuzel, T. M. Primary cutaneous T-cell lymphoma: review and current concepts. *J. Clin. Oncol.* **18,** 2908–25 (2000).

5. Hanahan, D. & Weinberg, R. A. Hallmarks of cancer: The next generation. *Cell* **144,** 646–74 (2011).

6. Sandoval, J. & Esteller, M. Cancer epigenomics: Beyond genomics. *Curr. Opin. Genetics. Dev.* **22,** 50–55 (2012).

7. Jones, P. A. & Baylin, S. B. The fundamental role of epigenetic events in cancer. *Nat. Rev. Genet. 3 415–428.* **3,** 415–28 (2002).

8. You, J. S. & Jones, P. A. Cancer genetics and epigenetics: Two sides of the same coin? *Cancer Cell* **22,** 9–20 (2012).

9. Herschkowitz, J. I. *et al.* Identification of conserved gene expression features between murine mammary carcinoma models and human breast tumors. *Genome Biol.* **8,** R76 (2007).

10. Cancer, T. & Atlas, G. Comprehensive molecular portraits of human breast tumours. *Nature* **490,** 61–70 (2012).

11. Reis-Filho, J. S. & Pusztai, L. Gene expression profiling in breast cancer: classification, prognostication, and prediction. *Lancet* **378,** 1812–23 (2011).

12. Feeley, L. P., Mulligan, A. M., Pinnaduwage, D., Bull, S. B. & Andrulis, I. L. Distinguishing luminal breast cancer subtypes by Ki67, progesterone receptor or TP53 status provides prognostic information. *Mod. Pathol.* **27,** 554–61 (2014).

13. Gail, M. H. *et al.* Weighing the risks and benefits of tamoxifen treatment for preventing breast cancer. *J. Natl. Cancer Inst.* **91,** 1829–46 (1999).

14. Woodward, W. A. *et al.* Changes in the 2003 American Joint Committee on Cancer staging for breast cancer dramatically affect stage-specific survival. *J Clin Oncol* **21,** 3244–48 (2003).

15. Scully, O. J., Bay, B.-H., Yip, G. & Yu, Y. Breast cancer metastasis. *Cancer Genomics Proteomics* **9,** 311–20 (2012).

16. Barse, P. M. Issues in the treatment of metastatic breast cancer. *Semin. Oncol. Nurs.* **16,** 197–205 (2000).

17. Altundag, K. *et al.* Clinicopathologic characteristics and prognostic factors in 420 metastatic breast cancer patients with central nervous system metastasis. *Cancer* **110,** 2640–47 (2007).

18. Hortobagyi, G. N. Treatment of breast cancer. *N. Engl. J. Med.* **339,** 974–84 (1998).

19. Stucky, C.-C. H., Gray, R. J., Wasif, N., Dueck, A. C. & Pockaj, B. A. Increase in contralateral prophylactic mastectomy: Echoes of a bygone era? *Ann. Surg. Oncol.* **17,** 330–37 (2010).

20. Hawkins, R. A. How best to express oestrogen receptor activity. *Eur. J. Cancer* **36,** S21-23 (2000).

21. Elledge, R. M. *et al.* Estrogen receptor (ER) and progesterone receptor (PgR), by ligand-binding assay compared with ER, PgR and pS2, by immuno-histochemistry in predicting response to tamoxifen in metastatic breast cancer: a Southwest Oncology Group Study. *Int. J. cancer* **89,** 111–17 (2000).

22. Badowska-Kozakiewicz, A. M., Patera, J., Sobol, M. & Przybylski, J. The role of oestrogen and progesterone receptors in breast cancer - immunohistochemical evaluation of oestrogen and progesterone receptor expression in invasive breast cancer in women. *Contemp. Oncol.* **19,** 220–25 (2015).

23. Andrea, N., Paola, F. & Michael, D. J. Prognostic and predictive biomarkers in breast cancer: Past, present and future. *Semin. Cancer Biol.* **17,** 30052–54 (2017).

24. Tandon, A. K., Clark, G. M., Chamness, G. C., Ullrich, A. & McGuire, W. L. HER-2/neu oncogene protein and prognosis in breast cancer. *J. Clin. Oncol.* **7,** 1120–28 (1989).

25. Slamon, D. J. *et al.* Human breast cancer: correlation of relapse and survival with amplification of the HER-2/neu oncogene. *Science (80-.).* **235,** 177–82 (1987).

26. Piccart-Gebhart, M. J. *et al.* Trastuzumab after adjuvant chemotherapy in HER2-positive breast cancer. *N. Engl. J. Med.* **353,** 1659–72 (2005).

27. Spector, N. L. & Blackwell, K. L. Understanding the mechanisms behind trastuzumab therapy for human epidermal growth factor receptor 2-positive breast cancer. *J. Clin. Oncol.* **27,** 5838–47 (2009).

28. Romond, E. H. *et al.* Trastuzumab plus adjuvant chemotherapy for operable HER2-positive breast cancer. *N. Engl. J. Med.* **353,** 1673–84 (2005).

29. Onitilo, A. A., Engel, J. M. & Stankowski, R. V. Cardiovascular toxicity associated with adjuvant trastuzumab therapy: prevalence, patient characteristics, and risk factors. *Ther. Adv. Drug Saf.* **5,** 154–66 (2014).

30. Pohlmann, P. R., Mayer, I. A. & Mernaugh, R. Resistance to trastuzumab in breast cancer. *Clin. Cancer Res.* **15,** 7479–91 (2009).

31. Vu, T. & Claret, F. X. Trastuzumab: Updated mechanisms of action and resistance in breast cancer. *Front. Oncol.* **2,** (2012).

32. Nielsen, D., Kümler, I., Palshof, J. E. & Andersson, M. Efficacy of HER2-targeted therapy in metastatic breast cancer. Monoclonal antibodies and tyrosine kinase inhibitors. *Breast* **22,** 1–12 (2013).

33. Hortobagyi, G. N. & Holmes, F. A. Optimal dosing of paclitaxel and doxorubicin in metastatic breast cancer. *Semin. Oncol.* **24,** 4–7 (1997).

34. Sledge, G. W. *et al.* Phase III Trial ofdoxorubicin, paclitaxel, and the combination of doxorubicin and paclitaxel as front-line chemotherapy for metastatic breast cancer: An intergroup trial (E1193). *J. Clin. Oncol.* **21,** 588–92 (2003).

35. Ribatti, D. The concept of immune surveillance against tumors. The first theories. *Oncotarget* **8,** 7175–80 (2015).

36. Kim, R., Emi, M. & Tanabe, K. Cancer immunoediting from immune surveillance to immune escape. *Immunology* **121,** 1–14 (2007).

37. Vesely, M. D., Kershaw, M. H., Schreiber, R. D. & Smyth, M. J. Natural innate and adaptive immunity to cancer. *Annu. Rev. Immunol.* **29,** 235–71 (2011).

38. Schreiber, R. D., Old, L. J. & Smyth, M. J. Cancer immunoediting: integrating immunity's roles in cancer suppression and promotion. *Science* **331,** 1565–70 (2011).

39. Ryan, J. C. & Seaman, W. E. Divergent functions of lectin-like receptors on NK cells. *Immunol. Rev.* **155,** 79–89 (1997).

40. Bauer, S. *et al.* Activation of NK cells and T cells by NKG2D, a receptor for stress-inducible MICA. *Science (80-.).* **285,** 727–29 (1999).

41. Albertsson, P. a. *et al.* NK cells and the tumour microenvironment: Implications for NK-cell function and anti-tumour activity. *Trends Immunol.* **24,** 603–9 (2003).

42. Smyth, M. J., Swann, J. & Hayakawa, Y. in *Crossroads between innate and adaptive immunity* 103–111 (2007).

43. Diefenbach, A., Jamieson, A. M., Liu, S. D., Shastri, N. & Raulet, D. H. Ligands for the murine NKG2D receptor: expression by tumor cells and activation of NK cells and macrophages. *Nat. Immunol.* **1,** 119–26 (2000).

44. Raulet, D. H. Roles of the NKG2D immunoreceptor and its ligands. *Nat. Rev. Immunol.* **3,** 781–90 (2003).

45. Spear, P., Wu, M.-R., Sentman, M.-L. & Sentman, C. L. NKG2D ligands as therapeutic targets. *Cancer Immun.* **13,** 8–2 (2013).

46. Smyth, M. J., Dunn, G. P. & Schreiber, R. D. Cancer immunosurveillance and immunoediting: The roles of immunity in suppressing tumor development and shaping tumor immunogenicity. *Adv. Immunol.* **90,** 1–50 (2006).

47. Zocchi, M. R. *et al.* ADAM10 new selective inhibitors reduce NKG2D ligand release sensitizing Hodgkin lymphoma cells to NKG2D-mediated killing. *Oncoimmunology* **5,** e1123367 (2016).

48. Clayton, A. *et al.* Human tumor-derived exosomes down-modulate NKG2D expression. *J. Immunol.* **180,** 7249–58 (2008).

49. Steinman, R. M., Hawiger, D. & Nussenzweig, M. C. Tolerogenic dendritic cells. *Annu. Rev. Immunol.* **21,** 685–711 (2003).

50. Quezada, S. A. & Peggs, K. S. Tumor-reactive CD4 + T cells: plasticity beyond helper and regulatory activities. *Immunotherapy* **3,** 915–17 (2011).

51. Shankaran, V. *et al.* IFNγ and lymphocytes prevent primary tumour development and shape tumour immunogenicity. *Nature* **410,** 1107–11 (2001).

52. Street, S. E., Cretney, E. & Smyth, M. J. Perforin and interferon-gamma activities independently control tumor initiation, growth, and metastasis. *Blood* **97,** 192–97 (2001).

53. Fehres, C. M., Unger, W. W. J., Garcia-Vallejo, J. J. & van Kooyk, Y. Understanding the biology of antigen cross-presentation for the design of vaccines against cancer. *Front. Immunol.* **5,** 149 (2014).

54. Muranski, P. & Restifo, N. P. Adoptive immunotherapy of cancer using CD4+ T cells. *Curr. Opin. Immunol.* **21,** 200–208 (2009).

55. Kim, H.-J. & Cantor, H. CD4 T-cell subsets and tumor immunity: The helpful and the not-so-helpful. *Cancer Immunol. Res.* **2,** 91–98 (2014).

56. Zanetti, M. Tapping CD4 T cells for cancer immunotherapy: the choice of personalized genomics. *J. Immunol.* **194,** 2049–56 (2015).

57. Hung, K. *et al.* The central role of CD4(+) T cells in the antitumor immune response. *J. Exp. Med.* **188,** 2357–68 (1998).

58. Greenberg, P. D. Adoptive T cell therapy of tumors: Mechanisms operative in the recognition and elimination of tumor cells. *Adv. Immunol.* **49,** 281–355 (1991).

59. Quezada, S. A. *et al.* Tumor-reactive CD4(+) T cells develop cytotoxic activity and eradicate large established melanoma after transfer into lymphopenic hosts. *J. Exp. Med.* **207,** 637–50 (2010).

60. Peter, M. E. *et al.* The role of CD95 and CD95 ligand in cancer. *Cell Death and Differentiation* **22,** 549–559 (2015).

61. Li, Z., Chen, L. & Qin, Z. Paradoxical roles of IL-4 in tumor immunity. *Cell. Mol. Immunol.* **6,** 415–22 (2009).

62. Tepper, R. I., Coffman, R. L. & Leder, P. An eosinophil-dependent mechanism for the antitumor effect of interleukin-4. *Science* **257,** 548–51 (1992).

63. Tepper, R. I., Pattengale, P. K. & Leder, P. Murine interleukin-4 displays potent anti-tumor activity in vivo. *Cell* **57,** 503–12 (1989).

64. Mattes, J. *et al.* Immunotherapy of cytotoxic T cell-resistant tumors by T helper 2 cells: an eotaxin and STAT6-dependent process. *J. Exp. Med.* **197,** 387–93 (2003).

65. Ochi, A. *et al.* MyD88 inhibition amplifies dendritic cell capacity to promote pancreatic carcinogenesis via Th2 cells. *J. Exp. Med.* **209,** 1671–87 (2012).

66. Martin-Orozco, N. *et al.* T helper 17 cells promote cytotoxic T cell activation in tumor immunity. *Immunity* **31,** 787–98 (2009).

67. Maher, J. & Davies, E. T. Targeting cytotoxic T lymphocytes for cancer immunotherapy. *Br. J. Cancer* **91,** 817–21 (2004).

68. Martínez-Lostao, L., Anel, A. & Pardo, J. How Do Cytotoxic Lymphocytes Kill Cancer Cells? *Clin. Cancer Res.* **21,** 5047–56 (2015).

69. Zitvogel, L., Galluzzi, L., Kepp, O., Smyth, M. J. & Kroemer, G. Type I interferons in anticancer immunity. *Nat. Rev. Immunol.* 5–9 (2015).

70. Hix, L. M. *et al.* CD1d-expressing breast cancer cells modulate NKT cell-mediated antitumor immunity in a murine model of breast cancer metastasis. *PLoS One* **6,** e20702 (2011).

71. Miura, S. *et al.* CD1d, a sentinel molecule bridging innate and adaptive immunity, is downregulated by the human papillomavirus (HPV) E5 protein: a possible mechanism for immune evasion by HPV. *J. Virol.* **84,** 11614–23 (2010).

72. Gabrilovich, D. I., Ostrand-Rosenberg, S. & Bronte, V. Coordinated regulation of myeloid cells by tumours. *Nat. Rev. Immunol.* **12,** 253–68 (2012).

73. Talmadge, J. E. & Gabrilovich, D. I. History of myeloid-derived suppressor cells. *Nat. Rev. Cancer* **13,** 739–52 (2013).

74. Gabrilovich, D. I. & Nagaraj, S. Myeloid-derived suppressor cells as regulators of the immune system. *Nat. Rev.* **9,** 162–74 (2009).

75. Wei, W.-C. *et al.* Inhibiting MDSC differentiation from bone marrow with phytochemical polyacetylenes drastically impairs tumor metastasis. *Sci. Rep.* **6,** 36663 (2016).

76. Youn, J.-I., Collazo, M., Shalova, I. N., Biswas, S. K. & Gabrilovich, D. I. Characterization of the nature of granulocytic myeloid-derived suppressor cells in tumor-bearing mice. *J. Leukoc. Biol.* **91,** 167–81 (2012).

77. Sinha, P., Clements, V. K., Bunt, S. K., Albelda, S. M. & Ostrand-Rosenberg, S. Cross-talk between myeloid-derived suppressor cells and macrophages subverts tumor immunity toward a type 2 response. *J. Immunol.* **179,** 977–83 (2007).

78. Mundy-Bosse, B. L. *et al.* Myeloid-derived suppressor cell inhibition of the IFN response in tumor-bearing mice. *Cancer Res.* **71,** 5101–10 (2011).

79. Hanson, E. M., Clements, V. K., Sinha, P., Ilkovitch, D. & Ostrand-Rosenberg, S. Myeloid-derived suppressor cells down-regulate L-selectin expression on CD4+ and CD8+ T cells. *J. Immunol.* **183,** 937–44 (2009).

80. Vincent, J. *et al.* 5-Fluorouracil selectively kills tumor-associated myeloid-derived suppressor cells resulting in enhanced T cell-dependent antitumor immunity. *Cancer Res.* **70,** 3052–61 (2010).

81. Suzuki, E., Kapoor, V., Jassar, A. S., Kaiser, L. R. & Albelda, S. M. Gemcitabine selectively eliminates splenic Gr-1+/CD11b+ myeloid suppressor cells in tumor-bearing animals and enhances antitumor immune activity. *Clin. Cancer Res.* **11,** 6713–21 (2005).

82. Mikyšková, R. *et al.* Cyclophosphamide-induced myeloid-derived suppressor cell population is immunosuppressive but not identical to myeloid-derived suppressor cells induced by growing TC-1 tumors. *J. Immunother.* **35,** 374–84 (2012).

83. Ding, Z.-C. *et al.* Immunosuppressive myeloid cells induced by chemotherapy attenuate antitumor CD4+ T-cell responses through the PD-1-PD-L1 axis. *Cancer Res.* **74,** 3441–53 (2014).

84. Cava, A. La, Kaer, L. Van & Fu-Dong-Shi. CD4+CD25+ Tregs and NKT cells: regulators regulating regulators. *Trends Immunol.* **27,** 322–27 (2006).

85. Sakaguchi, S., Yamaguchi, T., Nomura, T. & Ono, M. Regulatory T cells and immune tolerance. *Cell* **133,** 775–87 (2008).

86. Tanaka, A. & Sakaguchi, S. Regulatory T cells in cancer immunotherapy. *Cell Res.* **27,** 109–18 (2017).

87. Shimizu, J., Yamazaki, S. & Sakaguchi, S. Induction of tumor immunity by removing CD25+CD4+ T cells: a common basis between tumor immunity and autoimmunity. *J. Immunol.* **163,** 5211–18 (1999).

88. Bunt, S. K., Clements, V. K., Hanson, E. M., Sinha, P. & Ostrand-Rosenberg, S. Inflammation enhances myeloid-derived suppressor cell cross-talk by signaling through Toll-like receptor 4. *J. Leukoc. Biol.* **85,** 996–1004 (2009).

89. Sakaguchi, S., Yamaguchi, T., Nomura, T. & Ono, M. Regulatory T Cells and Immune Tolerance. *Cell* **133,** 775–87 (2008).

90. Tanaka, A. & Sakaguchi, S. Regulatory T cells in cancer immunotherapy. *Cell Res.* **27,** 109–18 (2017).

91. Takahashi, T. *et al.* Immunologic self-tolerance maintained by CD25+CD4+ naturally anergic and suppressive T cells: induction of autoimmune disease by breaking their anergic/suppressive state. *Int. Immunol.* **10,** 1969–80 (1998).

92. Brennan, P. J., Brigl, M. & Brenner, M. B. Invariant natural killer T cells: an innate activation scheme linked to diverse effector functions. *Nat. Rev. Immunol.* **13,** 101–17 (2013).

93. Van Kaer, L., Parekh, V. V & Wu, L. Invariant natural killer T cells: bridging innate and adaptive immunity. *Cell Tissue Res.* **343,** 43–55 (2011).

94. Lantz, O. & Bendelac, A. An invariant T cell receptor α chain is used by a unique subset of major histocompatibility complex class I-specific CD4+ and CD4-8- T cells in mice and humans. *J. Exp. Med.* **180,** 1097–1106 (1994).

95. Benlagha, K., Weiss, A., Beavis, A., Teyton, L. & Bendelac, A. In vivo identification of glycolipid antigen-specific T cells using fluorescent CD1d tetramers. *J. Exp. Med.* **191,** 1895–1903 (2000).

96. Matsuda, J. L. *et al.* Tracking the response of natural killer T cells to a glycolipid antigen using CD1d tetramers. *J. Exp. Med.* **192,** 741–54 (2000).

97. Arrenberg, P., Halder, R., Dai, Y., Maricic, I. & Kumar, V. Oligoclonality and innate-like features in the TCR repertoire of type II NKT cells reactive to a -linked self-glycolipid. *Proc. Natl. Acad. Sci.* **107,** 10984–89 (2010).

98. Patel, O. *et al.* Recognition of CD1d-sulfatide mediated by a type II natural killer T cell antigen receptor. *Nat. Immunol.* **13,** 857–63 (2012).

99. Terabe, M. *et al.* A nonclassical non-Vα14Jα18 CD1d-restricted (type II) NKT cell is sufficient for down-regulation of tumor immunosurveillance. *J. Exp. Med.* **202,** 1627–33 (2005).

100. Ambrosino, E. *et al.* Cross-regulation between type I and type II NKT cells in regulating tumor immunity: a new immunoregulatory axis. *J. Immunol.* **179,** 5126–36 (2007).

101. Gebremeskel, S., Slauenwhite, D. & Johnston, B. Reconstitution models to evaluate natural killer T cell function in tumor control. *Immunol. Cell Biol.* **94,** 90–100 (2016).

102. Kawano, T. *et al.* Natural killer-like nonspecific tumor cell lysis mediated by specific ligand-activated Vα14 NKT cells. *Proc. Natl. Acad. Sci. U. S. A.* **95,** 5690–93 (1998).

103. Crowe, N. Y. *et al.* Differential antitumor immunity mediated by NKT cell subsets in vivo. *J. Exp. Med.* **202,** 1279–88 (2005).

104. Lee, P. T., Benlagha, K., Teyton, L. & Bendelac, A. Distinct functional lineages of human Vα24 natural killer T cells. *J. Exp. Med.* **195,** 637–41 (2002).

105. Kim, C. H., Johnston, B. & Butcher, E. C. Trafficking machinery of NKT cells: Shared and differential chemokine receptor expression among Vα24+Vβ11+ NKT cell subsets with distinct cytokine-producing capacity. *Blood* **100,** 11–16 (2002).

106. Gumperz, J. E., Miyake, S., Yamamura, T. & Brenner, M. B. Functionally distinct subsets of CD1d-restricted natural killer T cells revealed by CD1d tetramer staining. *J. Exp. Med.* **195,** 625–36 (2002).

107. Coquet, J. M. *et al.* Diverse cytokine production by NKT cell subsets and identification of an IL-17-producing CD4-NK1.1- NKT cell population. *Proc. Natl. Acad. Sci. U. S. A.* **105,** 11287–92 (2008).

108. Lynch, L. *et al.* Regulatory iNKT cells lack PLZF expression and control T cell and macrophage homeostasis in adipose tissue. *Nat. Immunol* **16,** 85–95 (2015).

109. Sag, D., Krause, P., Hedrick, C. C., Kronenberg, M. & Wingender, G. IL-10-producing NKT10 cells are a distinct regulatory invariant NKT cell subset. *J. Clin. Invest.* **124,** 3725–40 (2014).

110. Doisne, J.-M. *et al.* Skin and peripheral lymph node invariant NKT cells are mainly retinoic acid receptor-related orphan receptor γt+ and respond preferentially under inflammatory conditions. *J. Immunol.* **183,** 2142–49 (2009).

111. Bai, L. *et al.* Distinct APCs explain the cytokine bias of α-galactosylceramide variants in vivo. *J. Immunol.* **188,** 3053–61 (2012).

112. Constantinides, M. G. & Bendelac, A. Transcriptional regulation of the NKT cell lineage. *Curr. Opin. Immunol.* **25,** 161–67 (2013).

113. Eberl, G. *et al.* Tissue-specific segregation of CD1d-dependent and CD1d-independent NK T cells. *J. Immunol.* **162,** 6410–19 (1999).

114. Hammond, K. J. *et al.* CD1d-restricted NKT cells: an interstrain comparison. *J. Immunol.* **167,** 1164–73 (2001).

115. Laloux, V., Beaudoin, L., Ronet, C. & Lehuen, A. Phenotypic and functional differences between NKT cells colonizing splanchnic and peripheral lymph nodes. *J. Immunol.* **168,** 3251–58 (2002).

116. Scanlon, S. T. *et al.* Airborne lipid antigens mobilize resident intravascular NKT cells to induce allergic airway inflammation. *J. Exp. Med.* **208,** 2113–24 (2011).

117. Kim, J. H., Choi, E. Y. & Chung, D. H. Donor bone marrow type II (non-Vα14Jα18 CD1d-restricted) NKT cells suppress graft-versus-host disease by producing IFN-γ and IL-4. *J. Immunol.* **179,** 6579–87 (2007).

118. Thomas, S. Y. *et al.* PLZF induces an intravascular surveillance program mediated by long-lived LFA-1-ICAM-1 interactions. *J. Exp. Med.* **208,** 1179–88 (2011).

119. Wingender, G. *et al.* Intestinal microbes affect phenotypes and functions of invariant natural killer T cells in mice. *Gastroenterology* **143,** 418–28 (2012).

120. Slauenwhite, D. & Johnston, B. Regulation of NKT cell localization in homeostasis and infection. *Front. Immunol.* **6,** 255 (2015).

121. Kita, H. *et al.* Quantitation and phenotypic analysis of natural killer T cells in primary biliary cirrhosis using a human CD1d tetramer. *Gastroenterology* **123,** 1031–43 (2002).

122. Kenna, T. *et al.* NKT cells from normal and tumor-bearing human livers are phenotypically and functionally distinct from murine NKT cells. *J. Immunol.* **171,** 1775–79 (2003).

123. Berzins, S. P., Cochrane, A. D., Pellicci, D. G., Smyth, M. J. & Godfrey, D. I. Limited correlation between human thymus and blood NKT cell content revealed by an ontogeny study of paired tissue samples. *Eur. J. Immunol.* **35,** 1399–1407 (2005).

124. Chan, A. C. *et al.* Immune characterization of an individual with an exceptionally high natural killer T cell frequency and her immediate family. *Clin. Exp. Immunol.* **156,** 238–45 (2009).

125. Lee, P. T. *et al.* Testing the NKT cell hypothesis of human IDDM pathogenesis. *J. Clin. Invest.* **110,** 793–800 (2002).

126. Pellicci, D. G. *et al.* Differential recognition of CD1d-α-galactosyl ceramide by the Vβ8.2 and Vβ7 semi-invariant NKT T cell receptors. *Immunity* **31,** 47–59 (2009).

127. Sugita, M. *et al.* Failure of trafficking and antigen presentation by CD1 in AP-3-deficient cells. *Immunity* **16,** 697–706 (2002).

128. Elewaut, D. *et al.* The adaptor protein AP-3 is required for CD1d-mediated antigen presentation of glycosphingolipids and development of Vα14i NKT cells. *J. Exp. Med.* **198,** 1133–46 (2003).

129. Wen, X. *et al.* Human CD1d knock-in mouse model demonstrates potent antitumor potential of human CD1d-restricted invariant natural killer T cells. *Proc. Natl. Acad. Sci. U. S. A.* **110,** 2963–68 (2013).

130. Natori, T., Koezuka, Y. & Higa, T. Agelasphins, novel α-galactosylCeramides from the marine sponge agelas-mauritianus. *Tetrahedron Lett.* **34,** 5591–92 (1993).

131. Morita, M. *et al.* Structure-activity relationship of α-galactosylceramides against B16-bearing mice. *J. Med. Chem.* **38,** 2176–87 (1995).

132. Fuji, N. *et al.* Antitumor effect of α-galactosylceramide (KRN7000) on spontaneous hepatic metastases requires endogenous interleukin 12 in the liver. *Clin. Cancer Res.* **6,** 3380–87 (2000).

133. Van Kaer, L. α-Galactosylceramide therapy for autoimmune diseases: prospects and obstacles. *Nat. Rev.* **5,** 31–42 (2005).

134. Cullen, R., Germanov, E., Shimaoka, T. & Johnston, B. Enhanced tumor metastasis in response to blockade of the chemokine receptor CXCR6 is overcome by NKT cell activation. *J. Immunol.* **183,** 5807–15 (2009).

135. Miyamoto, K., Miyake, S. & Yamamura, T. A synthetic glycolipid prevents autoimmune encephalomyelitis by inducing Th2 bias of natural killer T cells. *Nature* **413,** 531–34 (2001).

136. Oki, S., Chiba, A., Yamamura, T. & Miyake, S. The clinical implication and molecular mechanism of preferential IL-4 production by modified glycolipid-stimulated NKT cells. *J. Clin. Invest.* **113,** 1631–40 (2004).

137. Chiba, A. *et al.* Suppression of collagen-induced arthritis by natural killer T cell activation with OCH, a sphingosine-truncated analog of α-galactosylceramide. *Arthritis Rheum.* **50,** 305–13 (2004).

138. Schmieg, J., Yang, G., Franck, R. W. & Tsuji, M. Superior protection against malaria and melanoma metastases by a C-glycoside analogue of the natural killer T cell ligand α-Galactosylceramide. *J. Exp. Med.* **198,** 1631–41 (2003).

139. Smyth, M. J. *et al.* Differential tumor surveillance by natural killer (NK) and NKT cells. *J. Exp. Med.* **191,** 661–68 (2000).

140. Swann, J. B. *et al.* Type I natural killer T cells suppress tumors caused by p53 loss in mice. *Blood* **113,** 6382–85 (2009).

141. Crowe, N. Y., Smyth, M. J. & Godfrey, D. I. A critical role for natural killer T cells in immunosurveillance of methylcholanthrene-induced sarcomas. *J. Exp. Med.* **196,** 119–27 (2002).

142. Smyth, M. J. *et al.* Sequential production of interferon-γ by NK1.1(+) T cells and natural killer cells is essential for the antimetastatic effect of α-galactosylceramide. *Blood* **99,** 1259–66 (2002).

143. Song, L. *et al.* Oncogene MYCN regulates localization of NKT cells to the site of disease in neuroblastoma. *J. Clin. Invest.* **117,** 2702–12 (2007).

144. Tachibana, T. *et al.* Increased intratumor Vα24-positive natural killer T cells: a prognostic factor for primary colorectal carcinomas. *Clin. cancer Res.* **11,** 7322–27 (2005).

145. Metelitsa, L. S. *et al.* Natural killer T cells infiltrate neuroblastomas expressing the chemokine CCL2. *J. Exp. Med.* **199,** 1213–21 (2004).

146. Najera Chuc, A. E., Cervantes, L. A., Retiguin, F. P., Ojeda, J. V & Maldonado, E. R. Low number of invariant NKT cells is associated with poor survival in acute myeloid leukemia. *J. Cancer Res. Clin. Oncol.* **138,** 1427–32 (2012).

147. Molling, J. W. *et al.* Low levels of circulating invariant natural killer T cells predict poor clinical outcome in patients with head and neck squamous cell carcinoma. *J. Clin. Oncol.* **25,** 862–68 (2007).

148. Tahir, S. M. *et al.* Loss of IFN-γ production by invariant NK T cells in advanced cancer. *J. Immunol.* **167,** 4046–50 (2001).

149. Dhodapkar, M. V *et al.* A reversible defect in natural killer T cell function characterizes the progression of premalignant to malignant multiple myeloma. *J. Exp. Med.* **197,** 1667–76 (2003).

150. Molling, J. W. *et al.* Peripheral blood IFN-γ-secreting Vα24+Vβ11+ NKT cell numbers are decreased in cancer patients independent of tumor type or tumor load. *Int. J. cancer.* **116,** 87–93 (2005).

151. Yanagisawa, K. *et al.* Hyporesponsiveness to natural killer T-cell ligand α-galactosylceramide in cancer-bearing state mediated by CD11b+ Gr-1+ cells producing nitric oxide. *Cancer Res.* **66,** 11441–46 (2006).

152. Wu, D. Y., Segal, N. H., Sidobre, S., Kronenberg, M. & Chapman, P. B. Cross-presentation of disialoganglioside GD3 to natural killer T cells. *J. Exp. Med.* **198,** 173–81 (2003).

153. Zhou, D. *et al.* Lysosomal glycosphingolipid recognition by NKT cells. *Science* **306,** 1786–1789 (2004).

154. Mattner, J. *et al.* Exogenous and endogenous glycolipid antigens activate NKT cells during microbial infections. *Nature* **434,** 525–29 (2005).

155. Leite-De-Moraes, M. C. *et al.* A distinct IL-18-induced pathway to fully activate NK T lymphocytes independently from TCR engagement. *J. Immunol.* **163,** 5871–76 (1999).

156. Renukaradhya, G. J. *et al.* Type I NKT cells protect (and type II NKT cells suppress) the host's innate antitumor immune response to a B-cell lymphoma. *Blood* **111,** 5637–45 (2008).

157. Fallarini, S., Paoletti, T., Orsi Battaglini, N. & Lombardi, G. Invariant NKT cells increase drug-induced osteosarcoma cell death. *Br. J. Pharmacol.* **167,** 1533–49 (2012).

158. Metelitsa, L. S. *et al.* Human NKT cells mediate antitumor cytotoxicity directly by recognizing target cell CD1d with bound ligand or indirectly by producing IL-2 to activate NK cells. *J. Immunol.* **167,** 3114–22 (2001).

159. Fujii, S.-I. *et al.* NKT cells as an ideal anti-tumor immunotherapeutic. *Front Immunol* **4,** 409 (2013).

160. Nakagawa, R., Motoki, K. & Ueno, H. Treatment of hepatic metastasis of the Colon26 adenocarcinoma with an α -galactosylceramide, KRN7000. *Cancer Res.* **58,** 1202–7 (1998).

161. Nieda, M. *et al.* TRAIL expression by activated human CD4(+)V alpha 24NKT cells induces in vitro and in vivo apoptosis of human acute myeloid leukemia cells. *Blood* **97,** 2067–74 (2001).

162. Metelitsa, L. S., Weinberg, K. I., Emanuel, P. D. & Seeger, R. C. Expression of CD1d by myelomonocytic leukemias provides a target for cytotoxic NKT cells. *Leukemia* **17,** 1068–77 (2003).

163. Fujii, S., Shimizu, K., Smith, C., Bonifaz, L. & Steinman, R. M. Activation of natural killer T cells by α-galactosylceramide rapidly induces the full maturation of dendritic cells in vivo and thereby acts as an adjuvant for combined CD4 and CD8 T cell immunity to a coadministered protein. *J. Exp. Med.* **198,** 267–79 (2003).

164. Nishimura, T. *et al.* The interface between innate and acquired immunity: glycolipid antigen presentation by CD1d-expressing dendritic cells to NKT cells induces the differentiation of antigen-specific cytotoxic T lymphocytes. *Int. Immunol.* **12,** 987–94 (2000).

165. Gebremeskel, S., Clattenburg, D. R., Slauenwhite, D., Lobert, L. & Johnston, B. Natural killer T cell activation overcomes immunosuppression to enhance clearance of post-surgical breast cancer metastasis in mice. *Oncoimmunology* **4,** e995562 (2015).

166. Eberl, G. & MacDonald, H. R. Selective induction of NK cell proliferation and cytotoxicity by activated NKT cells. *Eur. J. Immunol.* **30,** 985–92 (2000).

167. Hermans, I. F. *et al.* NKT cells enhance CD4+ and CD8+ T cell responses to soluble antigen in vivo through direct interaction with dendritic cells. *J. Immunol.* **171,** 5140–47 (2003).

168. Mattarollo, S. R. *et al.* NKT cell adjuvant-based tumor vaccine for treatment of myc oncogene-driven mouse B-cell lymphoma. *Blood* **120,** 3019–29 (2012).

169. Veinotte, L., Gebremeskel, S. & Johnston, B. CXCL16-positive dendritic cells enhance invariant natural killer T cell-dependent IFNγ production and tumor control. *Oncoimmunology* **5,** e1160979 (2016).

170. Henry, C. J., Ornelles, D., Mitchell, L. M., Brzoza-Lewis, K. & Hiltbold, E. IL-12 produced by dendritic cells augments CD8+ T cell activation through the production of the chemokines CCL1 and CCL17. *J. Immunol.* **181,** 8576–84 (2008).

171. Song, L. *et al.* Vα24-invariant NKT cells mediate antitumor activity via killing of tumor-associated macrophages. *J. Clin. Invest.* **119,** 1524–36 (2009).

172. De Santo, C. *et al.* Invariant NKT cells reduce the immunosuppressive activity of influenza A virus-induced myeloid-derived suppressor cells in mice and humans. *J. Clin. Invest.* **118,** 4036–48 (2008).

173. Kunii, N. *et al.* Combination therapy of in vitro-expanded natural killer T cells and alpha-galactosylceramide-pulsed antigen-presenting cells in patients with recurrent head and neck carcinoma. *Cancer Sci.* **100,** 1092–98 (2009).

174. Motohashi, S. *et al.* A phase I-II study of alpha-galactosylceramide-pulsed IL-2/GM-CSF-cultured peripheral blood mononuclear cells in patients with advanced and recurrent non-small cell lung cancer. *J. Immunol.* **182,** 2492–501 (2009).

175. Uchida, T. *et al.* Phase I study of α-galactosylceramide-pulsed antigen presenting cells administration to the nasal submucosa in unresectable or recurrent head and neck cancer. *Cancer Immunol. Immunother.* **57,** 337–45 (2008).

176. Ishikawa, A. *et al.* A phase I study of α-galactosylceramide (KRN7000)-pulsed dendritic cells in patients with advanced and recurrent non-small cell lung cancer. *Clin. Cancer Res.* **11,** 1910–17 (2005).

177. Yamasaki, K. *et al.* Induction of NKT cell-specific immune responses in cancer tissues after NKT cell-targeted adoptive immunotherapy. *Clin. Immunol.* **138,** 255–65 (2011).

178. Oiseth, S. J. & Aziz, M. S. Cancer immunotherapy : a brief review of the history , possibilities , and challenges ahead. *J. Cancer Metastasis Treat.* **3,** 250–61 (2017).

179. Rosenberg, S. A. & Restifo, N. P. Adoptive cell transfer as personalized immunotherapy for human cancer. *Science* **348,** 62–68 (2015).

180. Morrison, C. CAR-T field booms as next-generation platforms attract big players. *Nat. Biotechnol.* **33,** 571–72 (2015).

181. U.S. Food and Drug Administration. FDA approval brings first gene therapy to the United States. *U.S. Dep. Heal. Hum. Serv.* (2017).

182. Bonifant, C. L., Jackson, H. J., Brentjens, R. J. & Curran, K. J. Toxicity and management in CAR T-cell therapy. *Mol. Ther. Oncolytics* **3,** (2016).

183. Krummel, M. F. & Allison, J. P. CD28 and CTLA-4 have opposing effects on the response of T cells to stimulation. *J. Exp. Med.* **182,** 459–65 (1995).

184. Buchbinder, E. I. & Desai, A. CTLA-4 and PD-1 pathways similarities, differences, and implications of their inhibition. *J. Clin. Oncol.* **39,** 98–106 (2016).

185. Fife, B. T. & Bluestone, J. A. Control of peripheral T-cell tolerance and autoimmunity via the CTLA-4 and PD-1 pathways. *Immunological Reviews* **224,** 166–182 (2008).

186. Schadendorf, D. *et al.* Pooled Analysis of Long-Term Survival Data From Phase II and Phase III Trials of Ipilimumab in Unresectable or Metastatic Melanoma. *J. Clin. Oncol.* **33,** 1889–94 (2015).

187. Weber, J. *et al.* Adjuvant Nivolumab versus Ipilimumab in Resected Stage III or IV Melanoma. *N. Engl. J. Med.* 1824–35 (2017).

188. Postow, M. A. *et al.* Nivolumab and Ipilimumab versus Ipilimumab in Untreated Melanoma. *N. Engl. J. Med.* **372,** 2006–2017 (2015).

189. Zitvogel, L., Apetoh, L., Ghiringhelli, F. & Kroemer, G. Immunological aspects of cancer chemotherapy. *Nat. Rev.* **8,** 59–73 (2008).

190. Zitvogel, L. *et al.* Immunogenic tumor cell death for optimal anticancer therapy: the calreticulin exposure pathway. *Clin. Cancer Res.* **16,** 3100–4 (2010).

191. Johnson, J. I. *et al.* Relationships between drug activity in NCI preclinical in vitro and in vivo models and early clinical trials. *Br. J. Cancer* **84,** 1424–31 (2001).

192. Apetoh, L. *et al.* Toll-like receptor 4-dependent contribution of the immune system to anticancer chemotherapy and radiotherapy. *Nat. Med.* **13,** 1050–59 (2007).

193. Casares, N. *et al.* Caspase-dependent immunogenicity of doxorubicin-induced tumor cell death. *J. Exp. Med.* **202,** 1691–701 (2005).

194. Michaud, M. *et al.* Autophagy-dependent anticancer immune responses induced by chemotherapeutic agents in mice. *Science* **334,** 1573–77 (2011).

195. Zappasodi, R. *et al.* Improved clinical outcome in indolent B-cell lymphoma patients vaccinated with autologous tumor cells experiencing immunogenic death. *Cancer Res.* **70,** 9062–72 (2010).

196. Fucikova, J. *et al.* Human tumor cells killed by anthracyclines induce a tumor-specific immune response. *Cancer Res.* **71,** 4821–33 (2011).

197. Early Breast Cancer Trialists' Collaborative Group *et al.* Comparisons between different polychemotherapy regimens for early breast cancer: meta-analyses of long-term outcome among 100,000 women in 123 randomised trials. *Lancet* **379,** 432–44 (2012).

198. Ferrazzi, D. E. & Stievano, L. Gemcitabine: Monochemotherapy of breast cancer. *Annals of Oncology* **17,** 169–72 (2006).

199. Von Hoff, D. D. *et al.* Increased survival in pancreatic cancer with nab-paclitaxel plus gemcitabine. *N. Engl. J. Med.* **369,** 1691–703 (2013).

200. El Karak, F. & Flechon, A. Gemcitabine in bladder cancer. *Expert Opin. Pharmacother.* **8,** 3251–56 (2007).

201. Hansen, S. W. Gemcitabine in the treatment of ovarian cancer. *Int. J. Gynecol. Cancer* **11,** 39–41 (2001).

202. Galmarini, C. M., Mackey, J. R. & Dumontet, C. Nucleoside analogues: mechanisms of drug resistance and reversal strategies. *Leukemia* **15,** 875–90 (2001).

203. Nowak, A. K., Robinson, B. W. S. & Lake, R. A. Gemcitabine exerts a selective effect on the humoral immune response: implications for combination chemo-immunotherapy. *Cancer Res.* **62,** 2353–58 (2002).

204. McDonald, G. B. *et al.* Cyclophosphamide metabolism, liver toxicity, and mortality following hematopoietic stem cell transplantation. *Blood* **101,** 2043–48 (2003).

205. Salem, M. L. *et al.* Defining the ability of cyclophosphamide preconditioning to enhance the antigen-specific CD8+ T-cell response to peptide vaccination: creation of a beneficial host microenvironment involving type I IFNs and myeloid cells. *J. Immunother.* **30,** 40–53 (2007).

206. Viaud, S. *et al.* The intestinal microbiota modulates the anticancer immune effects of cyclophosphamide. *Science* **342,** 971–76 (2013).

207. Liu, J. Y. *et al.* Single administration of low dose cyclophosphamide augments the antitumor effect of dendritic cell vaccine. *Cancer Immunol. Immunother.* **56,** 1597–1604 (2007).

208. Kelly, E. & Russell, S. J. History of oncolytic viruses: genesis to genetic engineering. *Mol. Ther.* **15,** 651–59 (2007).

209. Bierman, H. R. *et al.* Remissions in leukemia of childhood following acute infectious disease: staphylococcus and streptococcus, varicella, and feline panleukopenia. *Cancer* **6,** 591–605 (1953).

210. Russell, S. J., Peng, K.-W. & Bell, J. C. Oncolytic virotherapy. *Nat. Biotechnol.* **30,** 658–70 (2012).

211. Andtbacka, R. H. I. *et al.* Talimogene laherparepvec improves durable response rate in patients with advanced melanoma. *J. Clin. Oncol.* **33,** 2780–88 (2015).

212. Harrington, K. J. *et al.* Clinical development of talimogene laherparepvec (T-VEC): a modified herpes simplex virus type-1-derived oncolytic immunotherapy. *Expert Rev. Anticancer Ther.* **15,** 1389–403 (2015).

213. Stojdl, D. F. *et al.* VSV strains with defects in their ability to shutdown innate immunity are potent systemic anti-cancer agents. *Cancer Cell* **4,** 263–75 (2003).

214. Lichty, B. D., Power, A. T., Stojdl, D. F. & Bell, J. C. Vesicular stomatitis virus: re-inventing the bullet. *Trends Mol. Med.* **10,** 210–6 (2004).

215. Stojdl, D. F. *et al.* Exploiting tumor-specific defects in the interferon pathway with a previously unknown oncolytic virus. *Nat. Med.* **6,** 821–25 (2000).

216. Stojdl, D. F. *et al.* The murine double-stranded RNA-dependent protein kinase PKR is required for resistance to vesicular stomatitis virus. *J. Virol.* **74,** 9580–85 (2000).

217. von Kobbe C *et al.* Vesicular stomatitis virus matrix protein inhibits host cell gene expression by targeting the nucleoporin Nup98. *Mol. Cell* **6,** 1243–52 (2000).

218. Faria, P. A. *et al.* VSV disrupts the Rae1/mrnp41 mRNA nuclear export pathway. *Mol. Cell* **17,** 93–102 (2005).

219. Sahin, E., Egger, M. E., Mcmasters, K. M. & Zhou, H. S. Development of Oncolytic Reovirus for Cancer Therapy. *J. Cancer Ther.* **4,** 1100–15 (2013).

220. Gong, J., Sachdev, E., Mita, A. C. & Mita, M. M. Clinical development of reovirus for cancer therapy: An oncolytic virus with immune-mediated antitumor activity. *World J. Methodol.* **6,** 25–42 (2016).

221. Shmulevitz, M., Marcato, P. & Lee, P. W. K. Unshackling the links between reovirus oncolysis, Ras signaling, translational control and cancer. *Oncogene* **24,** 7720–28 (2005).

222. Zhao, X., Chester, C., Rajasekaran, N., He, Z. & Kohrt, H. E. Strategic combinations: The future of oncolytic virotherapy with reovirus. *Mol. Cancer Ther.* **15,** 767–73 (2016).

223. Coffey, M. C. Reovirus therapy of tumors with activated Ras pathway. *Science (80-.).* **282,** 1332–1334 (1998).

224. Gujar, S. *et al.* Multifaceted therapeutic targeting of ovarian peritoneal carcinomatosis through virus-induced immunomodulation. *Mol. Ther.* **21,** 338–47 (2013).

225. Gujar, S. A., Pan, D. A., Marcato, P., Garant, K. A. & Lee, P. W. K. Oncolytic virus-initiated protective immunity against prostate cancer. *Mol. Ther.* **19,** 797–804 (2011).

226. Galanis, E. *et al.* Phase II trial of intravenous administration of Reolysin® (Reovirus serotype-3-dearing strain) in patients with metastatic melanoma. *Mol. Ther.* **20,** 1998–2003 (2012).

227. Elmore, S. Apoptosis: a review of programmed cell death. *Toxicol. Pathol.* **35,** 495–516 (2007).

228. Galluzzi, L. *et al.* Essential versus accessory aspects of cell death: recommendations of the NCCD 2015. *Cell Death Differ.* **22,** 58–73 (2014).

229. Galluzzi, L. *et al.* Molecular definitions of cell death subroutines: recommendations of the Nomenclature Committee on Cell Death 2012. *Cell Death Differ.* **19,** 107–20 (2012).

230. Green, D. R., Ferguson, T., Zitvogel, L. & Kroemer, G. Immunogenic and tolerogenic cell death. *Nat. Rev. Immunol.* **9,** 353–63 (2009).

231. Zitvogel, L., Galluzzi, L., Smyth, M. J. & Kroemer, G. Mechanism of action of conventional and targeted anticancer therapies: reinstating immunosurveillance. *Immunity* **39,** 74–88 (2013).

232. Romani, N. *et al.* Generation of mature dendritic cells from human blood. An improved method with special regard to clinical applicability. *J. Immunol. Methods* **196,** 137–51 (1996).

233. Bender, A., Sapp, M., Schuler, G., Steinman, R. M. & Bhardwaj, N. Improved methods for the generation of dendritic cells from nonproliferating progenitors in human blood. *J. Immunol. Methods* **196,** 121–35 (1996).

234. Demaria, S. *et al.* Ionizing radiation inhibition of distant untreated tumors (abscopal effect) is immune mediated. *Int. J. Radiat. Oncol. Biol. Phys.* **58,** 862–70 (2004).

235. Panaretakis, T. *et al.* Mechanisms of pre-apoptotic calreticulin exposure in immunogenic cell death. *EMBO J.* **28,** 578–90 (2009).

236. Miyamoto, S. *et al.* Coxsackievirus B3 is an oncolytic virus with immunostimulatory properties that is active against lung adenocarcinoma. *Cancer Res.* **72,** 2609–21 (2012).

237. Diaconu, I. *et al.* Immune response is an important aspect of the antitumor effect produced by a CD40L-encoding oncolytic adenovirus. *Cancer Res.* **72,** 2327–38 (2012).

238. Garg, A. D. *et al.* A novel pathway combining calreticulin exposure and ATP secretion in immunogenic cancer cell death. *EMBO J.* **31,** 1062–79 (2012).

239. Kepp, O. *et al.* Consensus guidelines for the detection of immunogenic cell death. *Oncoimmunology* 1–19 (2014).

240. Obeid, M. *et al.* Ecto-calreticulin in immunogenic chemotherapy. *Immunol. Rev.* **220,** 22–34 (2007).

241. Ghiringhelli, F. *et al.* Activation of the NLRP3 inflammasome in dendritic cells induces IL-1β-dependent adaptive immunity against tumors. *Nat. Med.* **15,** 1170–78 (2009).

242. Obeid, M. *et al.* Calreticulin exposure dictates the immunogenicity of cancer cell death. *Nat. Med.* **13,** 54–61 (2007).

243. Aymeric, L. *et al.* Tumor cell death and ATP release prime dendritic cells and efficient anticancer immunity. *Cancer Res.* **70,** 855–58 (2010).

244. Seki, S. *et al.* Anti-angiogenic effect of P2X7 receptor antagonist oxidized ATP as a mechanism of anti-tumor growth. *Pharm. Anal Acta* **3,** 190 (2012).

245. Sukkurwala, A. Q. *et al.* Immunogenic calreticulin exposure occurs through a phylogenetically conserved stress pathway involving the chemokine CXCL8. *Cell Death Differ.* **21,** 59–68 (2014).

246. Sistigu, A. *et al.* Cancer cell–autonomous contribution of type I interferon signaling to the efficacy of chemotherapy. *Nat. Med.* **20,** 1301–9 (2014).

247. Yamazaki, T. *et al.* Defective immunogenic cell death of HMGB1-deficient tumors: compensatory therapy with TLR4 agonists. *Cell Death Differ.* **21,** 69–78 (2014).

248. Tesniere, A. *et al.* Immunogenic death of colon cancer cells treated with oxaliplatin. *Oncogene* **29,** 482–91 (2010).

249. Diehl, J. A., Fuchs, S. Y. & Koumenis, C. The cell biology of the unfolded protein response. *Gastroenterology* **141,** 38–41. (2011).

250. Schroder, M. & Kaufman, R. J. The mammalian unfolded protein response. *Annu Rev Biochem* **74,** 739–89 (2005).

251. Hetz, C. The unfolded protein response: controlling cell fate decisions under ER stress and beyond. *Nat. Rev. Mol. Cell Biol.* **13,** 89–102 (2012).

252. Obeid, M. *et al.* Calreticulin exposure is required for the immunogenicity of gamma-irradiation and UVC light-induced apoptosis. *Cell Death Differ.* **14,** 1848–50 (2007).

253. Gardai, S. J. *et al.* Cell-surface calreticulin initiates clearance of viable or apoptotic cells through trans-activation of LRP on the phagocyte. *Cell* **123,** 321–34 (2005).

254. Li, M. O., Sarkisian, M. R., Mehal, W. Z., Rakic, P. & Flavell, R. A. Phosphatidylserine receptor is required for clearance of apoptotic cells. *Science* **302,** 1560–63 (2003).

255. Yin, Y., Huang, X., Lynn, K. D. & Thorpe, P. E. Phosphatidylserine-targeting antibody induces M1 macrophage polarization and promotes myeloid-derived suppressor cell differentiation. *Cancer Immunol. Res.* **1,** 256–68 (2013).

256. Ran, S. *et al.* Antitumor effects of a monoclonal antibody that binds anionic phospholipids on the surface of tumor blood vessels in mice. *Clin. Cancer Res.* **11,** 1551–62 (2005).

257. Pawaria, S. & Binder, R. J. CD91-dependent programming of T-helper cell responses following heat shock protein immunization. *Nat. Commun.* **2,** 521 (2011).

258. Yeom, M. *et al.* Phosphatidylserine inhibits inflammatory responses in interleukin-1β-stimulated fibroblast-like synoviocytes and alleviates carrageenan-induced arthritis in rat. *Nutr. Res.* **33,** 242–50 (2013).

259. Gebremeskel, S. & Johnston, B. Concepts and mechanisms underlying chemotherapy induced immunogenic cell death: impact on clinical studies and considerations for combined therapies. *Oncotarget* **6,** 41600–19 (2015).

260. Kroemer, G., Galluzzi, L., Kepp, O. & Zitvogel, L. Immunogenic cell death in cancer therapy. *Annu. Rev. Immunol.* **31,** 51–72 (2013).

261. Inoue, H. & Tani, K. Multimodal immunogenic cancer cell death as a consequence of anticancer cytotoxic treatments. *Cell Death Differ.* **21,** 39–49 (2014).

262. Yang, H. *et al.* Contribution of RIP3 and MLKL to immunogenic cell death signaling in cancer chemotherapy. *Oncoimmunology* **5,** e1149673 (2016).

263. Elliott, M. R. *et al.* Nucleotides released by apoptotic cells act as a find-me signal to promote phagocytic clearance. *Nature* **461,** 282–86 (2009).

264. Müller, T. *et al.* The purinergic receptor P2Y2 receptor mediates chemotaxis of dendritic cells and eosinophils in allergic lung inflammation. *Allergy* **65,** 1545–53 (2010).

265. Ma, Y. *et al.* Anticancer chemotherapy-induced intratumoral recruitment and differentiation of antigen-presenting cells. *Immunity* **38,** 729–41 (2013).

266. Petrovski, G. *et al.* Phagocytosis of cells dying through autophagy induces inflammasome activation and IL-1β release in human macrophages. *Autophagy* **7,** 321–30 (2011).

267. Gombault, A., Baron, L. & Couillin, I. ATP release and purinergic signaling in NLRP3 inflammasome activation. *Front. Immunol.* **3,** 414 (2012).

268. Takeda, K. & Akira, S. TLR signaling pathways. *Semin Immunol* **16,** 3–9 (2004).

269. Aliprantis, A. O., Yang, R. B., Weiss, D. S., Godowski, P. & Zychlinsky, A. The apoptotic signaling pathway activated by Toll-like receptor-2. *EMBO J.* **19,** 3325–36 (2000).

270. Everett, H. & McFadden, G. Apoptosis: an innate immune response to virus infection. *Trends Microbiol.* **7,** 160–65 (1999).

271. López, M. *et al.* The 19-kDa Mycobacterium tuberculosis protein induces macrophage apoptosis through Toll-like receptor-2. *J. Immunol.* **170,** 2409–16 (2003).

272. Alexopoulou, L., Holt, A. C., Medzhitov, R. & Flavell, R. Recognition of double-stranded RNA and activation of NF-kB by Toll-like receptor 3. *Nature* **413,** 732–38 (2001).

273. Matsumoto, M. *et al.* Subcellular localization of toll-like receptor 3 in human dendritic cells. *J Immunol* **171,** 3154–62 (2003).

274. Scarim, A. L. *et al.* Mechanisms of beta-cell death in response to double-stranded (ds) RNA and interferon-gamma: dsRNA-dependent protein kinase apoptosis and nitric oxide-dependent necrosis. *Am. J. Pathol.* **159,** 273–83 (2001).

275. Robbins, M. A., Maksumova, L., Pocock, E. & Chantler, J. K. Nuclear factor-kappaB translocation mediates double-stranded ribonucleic acid-induced NIT-1 beta-cell apoptosis and up-regulates caspase-12 and tumor necrosis factor receptor-associated ligand (TRAIL). *Endocrinology* **144,** 4616–25 (2003).

276. Kaiser, W. J., Kaufman, J. L. & Offermann, M. K. IFN-α sensitizes human umbilical vein endothelial cells to apoptosis induced by double-stranded RNA. *J. Immunol.* **172,** 1699–1710 (2004).

277. Salaun, B., Coste, I., Rissoan, M.-C., Lebecque, S. J. & Renno, T. TLR3 can directly trigger apoptosis in human cancer cells. *J. Immunol.* **176,** 4894–4901 (2006).

278. Kaiser, W. J. & Offermann, M. K. Apoptosis induced by the toll-like receptor adaptor TRIF is dependent on its receptor interacting protein homotypic interaction motif. *J. Immunol.* **174,** 4942–52 (2005).

279. Ruckdeschel, K. *et al.* Signaling of apoptosis through TLRs critically involves toll/IL-1 receptor domain-containing adapter inducing IFN-beta, but not MyD88, in bacteria-infected murine macrophages. *J. Immunol.* **173,** 3320–28 (2004).

280. Zhang, J., Xu, L.-G., Han, K.-J., Wei, X. & Shu, H.-B. PIASy represses TRIF-induced ISRE and NF-kappaB activation but not apoptosis. *FEBS Lett.* **570,** 97–101 (2004).

281. Aranda, F. *et al.* Trial Watch: Toll-like receptor agonists in oncological indications. *Oncoimmunology* **3,** e29179 (2014).

282. Friedman, R. M. Clinical uses of interferons. *Br. J. Clin. Pharmacol.* **65,** 158–62 (2008).

283. Li, G. *et al.* Improved therapeutic effectiveness by combining recombinant CXC chemokine ligand 10 with Cisplatin in solid tumors. *Clin. Cancer Res.* **11,** 4217–24 (2005).

284. Park, J. S. *et al.* Activation of gene expression in human neutrophils by high mobility group box 1 protein. *Am. J. Physiol. Cell Physiol.* **284,** C870-9 (2003).

285. Lotze, M. T. & Tracey, K. J. High-mobility group box 1 protein (HMGB1): nuclear weapon in the immune arsenal. *Nat. Rev. Immunol.* **5,** 331–42 (2005).

286. Tang, D., Kang, R., Zeh, H. J. & Lotze, M. T. High-mobility group box 1 and cancer. *Biochim. Biophys. Acta* **1799,** 131–40 (2010).

287. Bonaldi, T. *et al.* Monocytic cells hyperacetylate chromatin protein HMGB1 to redirect it towards secretion. *EMBO J.* **22,** 5551–60 (2003).

288. Dumitriu, I. E., Bianchi, M. E., Bacci, M., Manfredi, A. A. & Rovere-Querini, P. The secretion of HMGB1 is required for the migration of maturing dendritic cells. *J. Leukoc. Biol.* **81,** 84–91 (2007).

289. Semino, C., Angelini, G., Poggi, A. & Rubartelli, A. NK/iDC interaction results in IL-18 secretion by DCs at the synaptic cleft followed by NK cell activation and release of the DC maturation factor HMGB1. *Blood* **106,** 609–16 (2005).

290. Dong, X. D. E. *et al.* High mobility group box I (HMGB1) release from tumor cells after treatment: implications for development of targeted chemoimmunotherapy. *J. Immunother.* **30,** 596–606 (2007).

291. Scaffidi, P., Misteli, T. & Bianchi, M. E. Release of chromatin protein HMGB1 by necrotic cells triggers inflammation. *Nature* **418,** 191–95 (2002).

292. Tian, J. *et al.* Toll-like receptor 9-dependent activation by DNA-containing immune complexes is mediated by HMGB1 and RAGE. *Nat. Immunol.* **8,** 487–96 (2007).

293. Urbonaviciute, V. *et al.* Induction of inflammatory and immune responses by HMGB1-nucleosome complexes: implications for the pathogenesis of SLE. *J. Exp. Med.* **205,** 3007–18 (2008).

294. Schiraldi, M. *et al.* HMGB1 promotes recruitment of inflammatory cells to damaged tissues by forming a complex with CXCL12 and signaling via CXCR4. *J. Exp. Med.* **209,** 551–63 (2012).

295. Bell, C. W., Jiang, W., Reich, C. F. & Pisetsky, D. S. The extracellular release of HMGB1 during apoptotic cell death. *Am. J. Physiol. Cell Physiol.* **291,** C1318-25 (2006).

296. Delamarre, L., Couture, R., Mellman, I. & Trombetta, E. S. Enhancing immunogenicity by limiting susceptibility to lysosomal proteolysis. *J. Exp. Med.* **203,** 2049–55 (2006).

297. Aslakson, C. J. & Miller, F. R. Selective events in the metastatic process defined by analysis of the sequential dissemination of subpopulations of a mouse mammary tumor. *Cancer Res.* **52,** 1399–1405 (1992).

298. Pulaski, B. A. & Ostrand-Rosenberg, S. Mouse 4T1 breast tumor model. *Curr. Protoc. Immunol.* **Chapter 20,** Unit 20.2 (2001).

299. Pulaski, B. A. & Ostrand-Rosenberg, S. Reduction of established spontaneous mammary carcinoma metastases following immunotherapy with major histocompatibility complex class II and B7.1 cell-based tumor vaccines. *Cancer Res.* **58,** 1486–93 (1998).

300. Ghochikyan, A. *et al.* Primary 4T1 tumor resection provides critical 'window of opportunity' for immunotherapy. *Clin. Exp. Metastasis* **31,** 185–98 (2014).

301. Ostrand-Rosenberg, S. & Sinha, P. Myeloid-derived suppressor cells: linking inflammation and cancer. *J. Immunol.* **182,** 4499–506 (2009).

302. Diaz-Montero, C. M. *et al.* Increased circulating myeloid-derived suppressor cells correlate with clinical cancer stage, metastatic tumor burden, and doxorubicin-cyclophosphamide chemotherapy. *Cancer Immunol. Immunother.* **58,** 49–59 (2009).

303. Fidler, I. J. Biological behavior of malignant melanoma cells correlated to their survival in vivo. *Cancer Res.* **35,** 218–24 (1975).

304. Hart, D. A. & Smith, R. Differences between the F10, BL6 and F1 sublines of the B16 melanoma in the enhancement of plasminogen activator and plasminogen activator inhibitor secretion by phorbol myristate acetate. *Cancer Lett.* **35,** 27–38 (1987).

305. Roby, K. F. *et al.* Development of a syngeneic mouse model for events related to ovarian cancer. *Carcinogenesis* **21,** 585–91 (2000).

306. Vang, R., Shih, I.-M. & Kurman, R. J. Ovarian low-grade and high-grade serous carcinoma: pathogenesis, clinicopathologic and molecular biologic features, and diagnostic problems. *Adv. Anat. Pathol.* **16,** 267–82 (2009).

307. Restifo, N. P., Dudley, M. E. & Rosenberg, S. A. Adoptive immunotherapy for cancer: harnessing the T cell response. *Nature Reviews Immunology* **12,** 269–81 (2012).

308. Topalian, S. L., Drake, C. G. & Pardoll, D. M. Targeting the PD-1/B7-H1(PD-L1) pathway to activate anti-tumor immunity. *Curr. Opin. Immunol.* **24,** 207–12 (2012).

309. Cui, J. *et al.* Requirement for Vα14 NKT cells in IL-12-mediated rejection of tumors. *Science* **278,** 1623–26 (1997).

310. Corbett, T. H. *et al.* Induction and chemotherapeutic response of two transplantable ductal adenocarcinomas of the pancreas in C57BL/6 mice. *Cancer Res.* **44,** 717–26 (1984).

311. Livak, K. J. & Schmittgen, T. D. Analysis of relative gene expression data using real-time quantitative PCR and the 2-ΔΔCT method. *Methods* **25,** 402–8 (2001).

312. Kim, Y.-M., Brinkmann, M. M., Paquet, M.-E. & Ploegh, H. L. UNC93B1 delivers nucleotide-sensing toll-like receptors to endolysosomes. *Nature* **452,** 234–38 (2008).

313. Cham, K. K. Y. *et al.* Metronomic gemcitabine suppresses tumour growth, improves perfusion, and reduces hypoxia in human pancreatic ductal adenocarcinoma. *Br. J. Cancer* **103,** 52–60 (2010).

314. Emmenegger, U. *et al.* Tumors that acquire resistance to low-dose metronomic cyclophosphamide retain sensitivity to maximum tolerated dose cyclophosphamide. *Neoplasia* **13,** 40–48 (2011).

315. Weir, G. M. *et al.* Metronomic cyclophosphamide enhances HPV16E7 peptide vaccine induced antigen-specific and cytotoxic T-cell mediated antitumor immune response. *Oncoimmunology* **3,** e953407 (2014).

316. Paget, C. *et al.* Potential role of invariant NKT cells in the control of pulmonary inflammation and CD8+ T cell response during acute influenza A virus H3N2 pneumonia. *J. Immunol.* **186,** 5590–602 (2011).

317. Salio, M., Silk, J. D., Jones, E. Y. & Cerundolo, V. Biology of CD1- and MR1-restricted T cells. *Annu. Rev. Immunol.* **32,** 323–66 (2014).

318. Bedel, R. *et al.* Lower TCR repertoire diversity in Traj18-deficient mice. *Nat. Immunol.* **13,** 705–6 (2012).

319. Matsuda, J. L. *et al.* Homeostasis of Vα14i NKT cells. *Nat. Immunol.* **3,** 966–74 (2002).

320. Mempel, M. *et al.* Natural killer T cells restricted by the monomorphic MHC class 1b CD1d1 molecules behave like inflammatory cells. *J. Immunol.* **168,** 365–71 (2002).

321. Akbari, O. *et al.* ICOS/ICOSL interaction is required for CD4+ invariant NKT cell function and homeostatic survival. *J. Immunol.* **180,** 5448–56 (2008).

322. Maeda, M., Lohwasser, S., Yamamura, T. & Takei, F. Regulation of NKT cells by Ly49: analysis of primary NKT cells and generation of NKT cell line. *J. Immunol.* **167,** 4180–86 (2001).

323. Chiba, A. *et al.* Rapid and reliable generation of invariant natural killer T-cell lines in vitro. *Immunology* **128,** 324–33 (2009).

324. Chamoto, K. *et al.* NKT cells act as regulatory cells rather than killer cells during activation of NK cell-mediated cytotoxicity by α-galactosylceramide in vivo. *Immunol. Lett.* **95,** 5–11 (2004).

325. Molling, J. W. *et al.* Generation and sustained expansion of mouse spleen invariant NKT cell lines with preserved cytokine releasing capacity. *J. Immunol. Methods* **322,** 70–81 (2007).

326. Ikarashi, Y. *et al.* Phenotypical and functional alterations during the expansion phase of invariant Vα14 natural killer T (Vα14i NKT) cells in mice primed with α-galactosylceramide. *Immunology* **116,** 30–37 (2005).

327. Crowe, N. Y. *et al.* Glycolipid antigen drives rapid expansion and sustained cytokine production by NK T cells. *J. Immunol.* **171,** 4020–27 (2003).

328. Chang, W. S. *et al.* Programmed death-1/programmed death ligand 1 interaction regulates the induction and maintenance of invariant NKT cell anergy. *J. Immunol.* **181,** 6707–10 (2008).

329. Parekh, V. V *et al.* Glycolipid antigen induces long-term natural killer T cell anergy in mice. *J. Clin. Invest.* **115,** 2572–83 (2005).

330. Uldrich, A. P. *et al.* NKT cell stimulation with glycolipid antigen in vivo: costimulation-dependent expansion, Bim-dependent contraction, and hyporesponsiveness to further antigenic challenge. *J. Immunol.* **175,** 3092–101 (2005).

331. Fujii, S., Shimizu, K., Kronenberg, M. & Steinman, R. M. Prolonged IFN-γ-producing NKT response induced with α-galactosylceramide-loaded DCs. *Nat. Immunol.* **3,** 867–74 (2002).

332. Wilson, M. T. *et al.* The response of natural killer T cells to glycolipid antigens is characterized by surface receptor down-modulation and expansion. *Proc. Natl. Acad. Sci. U. S. A.* **100,** 10913–18 (2003).

333. Harada, M. *et al.* Down-regulation of the invariant Vα14 antigen receptor in NKT cells upon activation. *Int. Immunol.* **16,** 241–47 (2004).

334. Schumann, J., Mycko, M. P., Dellabona, P., Casorati, G. & MacDonald, H. R. Influence of the TCR Vβ domain on the selection of semi-invariant NKT cells by endogenous ligands. *J. Immunol.* **176,** 2064–68 (2006).

335. Wei, D. G., Curran, S. A., Savage, P. B., Teyton, L. & Bendelac, A. Mechanisms imposing the Vbeta bias of Valpha14 natural killer T cells and consequences for microbial glycolipid recognition. *J. Exp. Med.* **203,** 1197–207 (2006).

336. Mallevaey, T. *et al.* T cell receptor CDR2β and CDR3β loops collaborate functionally to shape the iNKT cell repertoire. *Immunity* **31,** 60–71 (2009).

337. Matsuda, J. L. *et al.* Mouse Vα14i natural killer T cells are resistant to cytokine polarization in vivo. *Proc. Natl. Acad. Sci. U. S. A.* **100,** 8395–400 (2003).

338. Wang, X. *et al.* Human invariant natural killer T cells acquire transient innate responsiveness via histone H4 acetylation induced by weak TCR stimulation. *J. Exp. Med.* **209,** 987–1000 (2012).

339. Carnaud, C. *et al.* Cross-talk between cells of the innate immune system: NKT cells rapidly activate NK cells. *J. Immunol.* **163,** 4647–50 (1999).

340. Smyth, M. J. *et al.* Sequential activation of NKT cells and NK cells provides effective innate immunotherapy of cancer. *J. Exp. Med.* **201,** 1973–85 (2005).

341. Gumperz, J. E. *et al.* Murine CD1d-restricted T cell recognition of cellular lipids. *Immunity* **12,** 211–21 (2000).

342. Ota, T. *et al.* IFN-gamma-mediated negative feedback regulation of NKT-cell function by CD94/NKG2. *Blood* **106,** 184–92 (2005).

343. Nakagawa, R. *et al.* Mechanisms of the antimetastatic effect in the liver and of the hepatocyte injury induced by alpha-Galactosylceramide in mice. *J. Immunol.* **166,** 6578–84 (2001).

344. Ranson, T. *et al.* IL-15 availability conditions homeostasis of peripheral natural killer T cells. *Proc. Natl. Acad. Sci. U. S. A.* **100,** 2663–68 (2003).

345. Parkinson, D. R., Brightman, R. P. & Waksal, S. D. Altered natural killer cell biology in C57BL/6 mice after leukemogenic split-dose irradiation. *J. Immunol.* **126,** 1460–64 (1981).

346. Ardolino, M. *et al.* Cytokine therapy reverses NK cell anergy in MHC-deficient tumors. *J. Clin. Invest.* **124,** 4781–94 (2014).

347. Kitamura, H. *et al.* The natural killer T (NKT) cell ligand α-galactosylceramide demonstrates its immunopotentiating effect by inducing interleukin (IL)-12 production by dendritic cells and IL-12 receptor expression on NKT cells. *J. Exp. Med.* **189,** 1121–28 (1999).

348. Motohashi, S. *et al.* A phase I study of in vitro expanded natural killer T cells in patients with advanced and recurrent non-small cell lung cancer. *Clin. Cancer Res.* **12,** 6079–86 (2006).

349. Motohashi, S., Okamoto, Y., Yoshino, I. & Nakayama, T. Anti-tumor immune responses induced by iNKT cell-based immunotherapy for lung cancer and head and neck cancer. *Clin. Immunol.* **140,** 167–76 (2011).

350. Teng, M. W. L. *et al.* Combined natural killer T-cell based immunotherapy eradicates established tumors in mice. *Cancer Res.* **67,** 7495–504 (2007).

351. Hayakawa, Y., Rovero, S., Forni, G. & Smyth, M. J. α-galactosylceramide (KRN7000) suppression of chemical- and oncogene-dependent carcinogenesis. *Proc. Natl. Acad. Sci. U. S. A.* **100,** 9464–69 (2003).

352. Almand, B. *et al.* Increased production of immature myeloid cells in cancer patients: a mechanism of immunosuppression in cancer. *J. Immunol.* **166,** 678–89 (2001).

353. Gabrilovich, D. I. & Nagaraj, S. Myeloid-derived suppressor cells as regulators of the immune system. *Nat. Rev.* **9,** 162–74 (2009).

354. Parekh, V. V, Wu, L., Olivares-Villagómez, D., Wilson, K. T. & Van Kaer, L. Activated invariant NKT cells control central nervous system autoimmunity in a mechanism that involves myeloid-derived suppressor cells. *J. Immunol.* **190,** 1948–60 (2013).

355. Kmieciak, M. *et al.* Activated NKT cells and NK cells render T cells resistant to myeloid-derived suppressor cells and result in an effective adoptive cellular therapy against breast cancer in the FVBN202 transgenic mouse. *J. Immunol.* **187,** 708–17 (2011).

356. Ko, H. J., Lee, J. M., Kim, Y. J., Lee, K. A. & Kang, C. Y. Immunosuppressive myeloid-derived suppressor cells can be converted into immunogenic APCs with the help of activated NKT cells: an alternative cell-based antitumor vaccine. *J. Immunol.* **182,** 1818–28 (2009).

357. Huang, J.-R. *et al.* α-galactosylceramide but not phenyl-glycolipids induced NKT cell anergy and IL-33-mediated myeloid-derived suppressor cell accumulation via upregulation of egr2/3. *J. Immunol.* **192,** 1972–81 (2014).

358. Weigelt, B., Peterse, J. L. & van 't Veer, L. J. Breast cancer metastasis: markers and models. *Nat. Rev. Cancer* **5,** 591–602 (2005).

359. Pilones, K. A. *et al.* Invariant natural killer T cells regulate breast cancer response to radiation and CTLA-4 blockade. *Clin. Cancer Res.* **15,** 597–606 (2009).

360. Chen, Q. & Ross, A. C. All-trans-retinoic acid and the glycolipid α-galactosylceramide combined reduce breast tumor growth and lung metastasis in a 4T1 murine breast tumor model. *Nutr. Cancer* **64,** 1219–27 (2012).

361. Webb, T. J. *et al.* Molecular identification of GD3 as a suppressor of the innate immune response in ovarian cancer. *Cancer Res.* **72,** 3744–52 (2012).

362. Bezbradica, J. S. *et al.* Distinct roles of dendritic cells and B cells in Va14Ja18 natural T cell activation in vivo. *J. Immunol.* **174,** 4696–705 (2005).

363. Wesolowski, R., Markowitz, J. & Carson, W. E. Myeloid derived suppressor cells – a new therapeutic target in the treatment of cancer. *J. Immunother. Cancer* **1,** 10 (2013).

364. Alizadeh, D. & Larmonier, N. Chemotherapeutic targeting of cancer-induced immunosuppressive cells. *Cancer Res.* **74,** 2663–68 (2014).

365. Kim, Y.-S. *et al.* Functional changes in myeloid-derived suppressor cells (MDSCs) during tumor growth: FKBP51 contributes to the regulation of the immunosuppressive function of MDSCs. *J. Immunol.* **188,** 4226–34 (2012).

366. Payne, K. K. *et al.* Peripheral blood mononuclear cells of patients with breast cancer can be reprogrammed to enhance anti-HER-2/neu reactivity and overcome myeloid-derived suppressor cells. *Breast Cancer Res. Treat.* **142,** 45–57 (2013).

367. Bezu, L. *et al.* Combinatorial strategies for the induction of immunogenic cell death. *Front. Immunol.* **6,** 1–11 (2015).

368. Mattarollo, S. R., Kenna, T., Nieda, M. & Nicol, A. J. Chemotherapy pretreatment sensitizes solid tumor-derived cell lines to Vα24+ NKT cell-mediated cytotoxicity. *Int. J. Cancer* **119,** 1630–37 (2006).

369. Wu, L. *et al.* Activation of CD1d-restricted natural killer T cells can inhibit cancer cell proliferation during chemotherapy by promoting the immune responses in murine mesothelioma. *Cancer Immunol. Immunother.* **63,** 1285–96 (2014).

370. Aketa, H. *et al.* The combination therapy of α-galactosylceramide and 5-fluorouracil showed antitumor effect synergistically against liver tumor in mice. *Int. J. Cancer* **133,** 1126–34 (2013).

371. Diaz-Montero, C. M., Finke, J. & Montero, A. J. Myeloid-derived suppressor cells in cancer: therapeutic, predictive, and prognostic implications. *Semin. Oncol.* **41,** 174–84 (2014).

372. Ghiringhelli, F. *et al.* Metronomic cyclophosphamide regimen selectively depletes CD4+CD25+ regulatory T cells and restores T and NK effector functions in end stage cancer patients. *Cancer Immunol. Immunother.* **56,** 641–48 (2007).

373. Ma, Y. *et al.* Contribution of IL-17-producing γδ T cells to the efficacy of anticancer chemotherapy. *J. Exp. Med.* **208,** 491–503 (2011).

374. Viaud, S. *et al.* Cyclophosphamide induces differentiation of Th17 cells in cancer patients. *Cancer Res.* **71,** 661–65 (2011).

375. Tomihara, K. *et al.* Gemcitabine chemotherapy induces phenotypic alterations of tumor cells that facilitate antitumor T cell responses in a mouse model of oral cancer. *Oral Oncol.* **50,** 457–67 (2014).

376. Griffith, J. W., Sokol, C. L. & Luster, A. D. Chemokines and chemokine receptors: positioning cells for host defense and immunity. *Annu. Rev. Immunol.* **32,** 659–702 (2014).

377. Liu, W. M., Fowler, D. W., Smith, P. & Dalgleish, A. G. Pre-treatment with chemotherapy can enhance the antigenicity and immunogenicity of tumours by promoting adaptive immune responses. *Br. J. Cancer* **102,** 115–23 (2010).

378. Leung, J. & Suh, W.-K. Host B7-H4 regulates antitumor T cell responses through inhibition of myeloid-derived suppressor cells in a 4T1 tumor transplantation model. *J. Immunol.* **190,** 6651–61 (2013).

379. Chen, X. *et al.* Effective chemoimmunotherapy with anti-TGFβ antibody and cyclophosphamide in a mouse model of breast cancer. *PLoS One* **9,** 1–10 (2014).

380. Le, H. K. *et al.* Gemcitabine directly inhibits myeloid derived suppressor cells in BALB/c mice bearing 4T1 mammary carcinoma and augments expansion of T cells from tumor-bearing mice. *Int. Immunopharmacol.* **9,** 900–9 (2009).

381. Kaufman, H. L., Kohlhapp, F. J. & Zloza, A. Oncolytic viruses: a new class of immunotherapy drugs. *Nat. Rev. Drug Discov.* **14,** 642–62 (2015).

382. Diaz, R. M. *et al.* Oncolytic immunovirotherapy for melanoma using vesicular stomatitis virus. *Cancer Res.* **67,** 2840–48 (2007).

383. Prestwich, R. J. *et al.* Tumor infection by oncolytic reovirus primes adaptive antitumor immunity. *Clin. Cancer Res.* **14,** 7358–66 (2008).

384. Zhang, J. *et al.* Maraba MG1 virus enhances natural killer cell function via conventional dendritic cells to reduce postoperative metastatic disease. *Mol. Ther.* **22,** 1320–32 (2014).

385. Boudreau, J. E. *et al.* Recombinant vesicular stomatitis virus transduction of dendritic cells enhances their ability to prime innate and adaptive antitumor immunity. *Mol. Ther.* **17,** 1465–72 (2009).

386. Gujar, S. a & Lee, P. W. K. Oncolytic virus-mediated reversal of impaired tumor antigen presentation. *Front. Oncol.* **4,** 77–84 (2014).

387. Guan, M., Romano, G., Coroniti, R. & Henderson, E. E. Progress in oncolytic virotherapy for the treatment of thyroid malignant neoplasm. *J. Exp. Clin. Cancer Res.* **33,** 91–98 (2014).

388. Alkayyal, A. A. *et al.* NK-cell recruitment necessary for eradication of peritoneal carcinomatosis with an IL12-expressing Maraba virus cellular vaccine. *Cancer Immunol. Res.* 211–221 (2017).

389. Bourgeois-Daigneault, M.-C. *et al.* Oncolytic vesicular stomatitis virus expressing interferon-γ has enhanced therapeutic activity. *Mol. Ther. — Oncolytics* **3,** 16001–12 (2016).

390. Rajani, K. *et al.* Combination therapy with Reovirus and anti-PD-1 blockade controls tumor growth through innate and adaptive immune responses. *Mol. Ther.* **24,** 166–74 (2016).

391. Shen, W., Patnaik, M. M., Ruiz, A., Russell, S. J. & Peng, K.-W. Immunovirotherapy with vesicular stomatitis virus and PD-L1 blockade enhances therapeutic outcome in murine acute myeloid leukemia. *Blood* **127,** 1449–58 (2016).

392. Horst, D., Geerdink, R. J., Gram, A. M., Stoppelenburg, A. J. & Ressing, M. E. Hiding lipid presentation: viral interference with CD1d-restricted invariant natural killer T (iNKT) cell activation. *Viruses* **4,** 2379–99 (2012).

393. Gujar, S. A., Marcato, P., Pan, D. & Lee, P. W. K. Reovirus virotherapy overrides tumor antigen presentation evasion and promotes protective antitumor immunity. *Mol. Cancer Ther.* **9,** 2924–33 (2010).

394. Kim, R.-J. *et al.* Ras activation contributes to the maintenance and expansion of Sca-1pos cells in a mouse model of breast cancer. *Cancer Lett.* **287,** 172–81 (2010).

395. Phan, V. T. *et al.* Oncogenic RAS pathway activation promotes resistance to anti-VEGF therapy through G-CSF-induced neutrophil recruitment. *Proc. Natl. Acad. Sci.* **110,** 6079–84 (2013).

396. Bourgeois-Daigneault, M. C. *et al.* Neoadjuvant oncolytic virotherapy before surgery sensitizes triple-negative breast cancer to immune checkpoint therapy. *Sci. Transl. Med.* **10,** (2018).

397. Workenhe, S. T. & Mossman, K. L. Oncolytic virotherapy and immunogenic cancer cell death: sharpening the sword for improved cancer treatment strategies. *Mol. Ther.* **22,** 251–56 (2014).

398. Takasu, A. *et al.* Immunogenic cell death by oncolytic herpes simplex virus type 1 in squamous cell carcinoma cells. *Cancer Gene Ther.* **23,** 107–13 (2016).

399. Sobol, P. T. *et al.* Adaptive antiviral immunity is a determinant of the therapeutic success of oncolytic virotherapy. *Mol. Ther.* **19,** 335–44 (2011).

400. Breitbach, C. J. *et al.* Oncolytic vaccinia virus disrupts tumor-associated vasculature in humans. *Cancer Res.* **73,** 1265–75 (2013).

401. Nguyen, A., Ho, L. & Wan, Y. Chemotherapy and Oncolytic Virotherapy: Advanced Tactics in the War against Cancer. *Front. Oncol.* **4,** 145 (2014).

402. Rojas, J. J., Sampath, P., Hou, W. & Thorne, S. H. Defining effective combinations of immune checkpoint blockade and oncolytic virotherapy. *Clin. Cancer Res.* **21,** 5543–51 (2015).

403. Forrest, J. C. & Dermody, T. S. Reovirus receptors and pathogenesis. *J. Virol.* **77,** 9109–15 (2003).

404. Murakami, M. *et al.* Abrogation of junctional adhesion molecule-A expression induces cell apoptosis and reduces breast cancer progression. *PLoS One* **6,** e21242 (2011).

405. Ebert, O., Harbaran, S., Shinozaki, K. & Woo, S. L. C. Systemic therapy of experimental breast cancer metastases by mutant vesicular stomatitis virus in immune-competent mice. *Cancer Gene Ther.* **12,** 350–58 (2005).

406. Murphy, A. M. *et al.* Vesicular stomatitis virus as an oncolytic agent against pancreatic ductal adenocarcinoma. *J. Virol.* **86,** 3073–87 (2012).

407. Shah, N. R., Sunderland, A., Grdzelishvili, V. Z., Govindarajan, R. & Choi, D. Cell type mediated resistance of vesicular stomatitis virus and sendai virus to ribavirin. *PLoS One* **5,** e11265 (2010).

408. Felt, S. A. & Grdzelishvili, V. Z. Recent advances in vesicular stomatitis virus-based oncolytic virotherapy: a 5-year update. *J. Gen. Virol.* [ahead of print] (2017).

409. Le Boeuf, F. *et al.* Reovirus FAST protein enhances vesicular stomatitis virus oncolytic virotherapy in primary and metastatic tumor models. *Mol. Ther. - Oncolytics* **6,** 80–89 (2017).

410. Vitale, M. *et al.* HLA class I antigen and transporter associated with antigen processing (TAP1 and TAP2) down-regulation in high-grade primary breast carcinoma lesions. *Cancer Res.* **58,** 737–42 (1998).

411. Zuo, Q. *et al.* Inducible TAP1 negatively regulates the antiviral innate immune response by targeting the TAK1 complex. *J Immunol* **198,** 3690–704 (2017).

412. Janelle, V. *et al.* The strength of the T cell response against a surrogate tumor antigen induced by oncolytic VSV therapy does not correlate with tumor control. *Mol. Ther.* **22,** 1198–210 (2014).

413. Steel, C. D., Hahto, S. M. & Ciavarra, R. P. Peripheral dendritic cells are essential for both the innate and adaptive antiviral immune responses in the central nervous system. *Virology* **387,** 117–26 (2009).

414. Haabeth, O. A. W. *et al.* How do CD4(+) T cells detect and eliminate tumor cells that either lack or express MHC class II molecules? *Front. Immunol.* **5,** 174 (2014).

415. Renukaradhya, G. J. *et al.* Virus-induced inhibition of CD1d1-mediated antigen presentation: reciprocal regulation by p38 and ERK. *J. Immunol.* **175,** 4301–308 (2005).

416. Renukaradhya, G. J., Khan, M. A., Shaji, D. & Brutkiewicz, R. R. Vesicular stomatitis virus matrix protein impairs CD1d-mediated antigen presentation through activation of the p38 MAPK pathway. *J. Virol.* **82,** 12535–42 (2008).

417. Lin, Y., Roberts, T. J., Spence, P. M. & Brutkiewicz, R. R. Reduction in CD1d expression on dendritic cells and macrophages by an acute virus infection. *J. Leukoc. Biol.* **77,** 151–58 (2005).

418. Galivo, F. *et al.* Single-cycle viral gene expression, rather than progressive replication and oncolysis, is required for VSV therapy of B16 melanoma. *Gene Ther.* **17,** 158–70 (2010).

419. Fuertes, M. B. *et al.* Host type I IFN signals are required for antitumor CD8 + T cell responses through CD8α + dendritic cells. *J. Exp. Med.* **208,** 2005–16 (2011).

420. Diamond, M. S. *et al.* Type I interferon is selectively required by dendritic cells for immune rejection of tumors. *J. Exp. Med.* **208,** 1989–2003 (2011).

421. Ireland, D. D. C. & Reiss, C. S. Gene expression contributing to recruitment of circulating cells in response to vesicular stomatitis virus infection of the CNS. *Viral Immunol.* **19,** 536–45 (2006).

422. Paust, S. *et al.* Critical role for the chemokine receptor CXCR6 in NK cell-mediated antigen-specific memory of haptens and viruses. *Nat. Immunol.* **11,** 1127–35 (2010).

423. Donnelly, O. G. *et al.* Measles virus causes immunogenic cell death in human melanoma. *Gene Ther.* **20,** 7–15 (2013).

424. Workenhe, S. T., Pol, J. G., Lichty, B. D., Cummings, D. T. & Mossman, K. L. Combining oncolytic HSV-1 with immunogenic cell death-inducing drug mitoxantrone breaks cancer immune tolerance and improves therapeutic efficacy. *Cancer Immunol. Res.* **1,** 309–19 (2013).

425. Deshpande, P. P., Biswas, S. & Torchilin, V. P. Current trends in the use of liposomes for tumor targeting. *Nanomedicine (Lond).* **8,** 1509–28 (2013).

426. Altin, J. G., van Broekhoven, C. L. & Parish, C. R. Targeting dendritic cells with antigen-containing liposomes: antitumour immunity. *Expert Opin. Biol. Ther.* **4,** 1735–47 (2004).

427. Hastie, E. & Grdzelishvili, V. Z. Vesicular stomatitis virus as a flexible platform for oncolytic virotherapy against cancer. *J. Gen. Virol.* **93,** 2529–45 (2012).

428. Lu, S. Heterologous prime-boost vaccination. *Current Opinion in Immunology* **21,** 346–51 (2009).

429. Pol, J. G. *et al.* Maraba virus as a potent oncolytic vaccine vector. *Mol. Ther.* **22,** 420–29 (2014).

Appendix

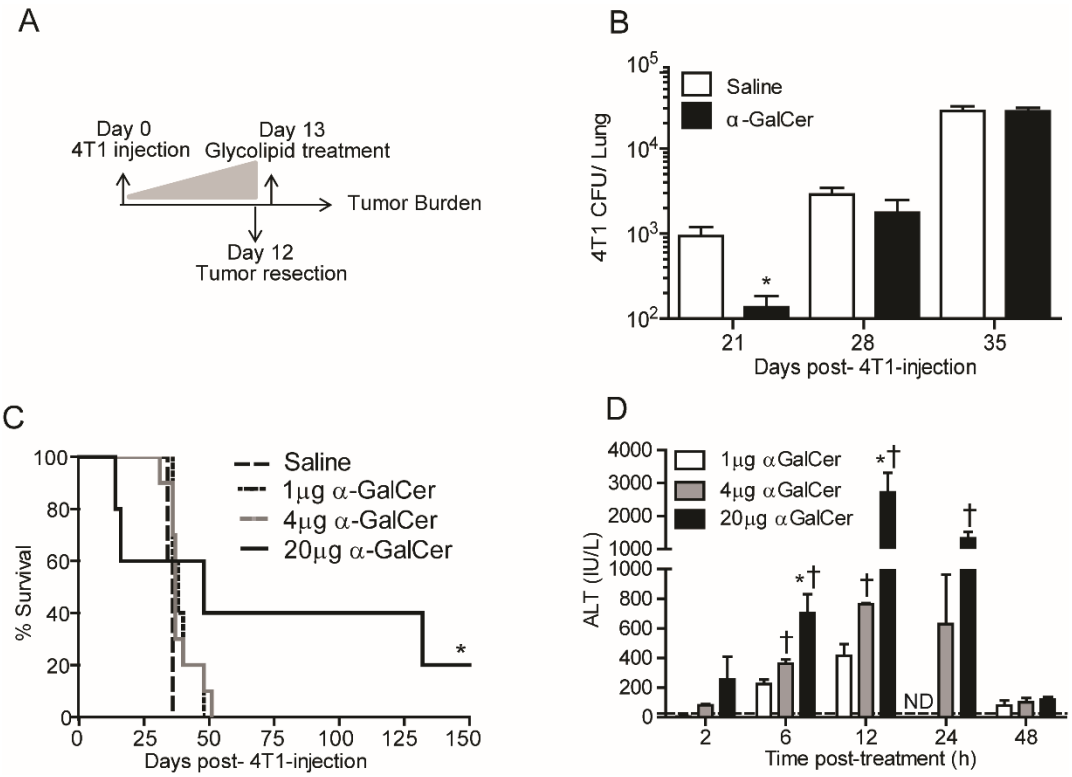

Appendix Figure 1: Treatment with free glycolipid following primary 4T1 tumor resection provides transient protection from lung metastases. (A) Schematic of the post-surgical NKT cell activation model. Mice were inoculated with $2x10^5$ 4T1 mammary carcinoma cells and primary tumors were resected on day 12. A single dose of free α-C-GalCer (i.p. 4 μg) was delivered on day 13. (B) Number of 4T1 CFU present in lung cell suspensions isolated at day 21, 28, or 35 after treatment with α-GalCer (i.p. 4 μg) (n = 7-12 per group). (C) Survival was assessed following treatment with (α-GalCer (i.p. 1 μg , 4 μg or 20 μg (n = 5-10 per group). * $p < 0.05$ compared to saline control. (D) Serum ALT levels were measured following administration of 1 μg, 4 μg or 20 μg a-GalCer (n = 3 per group). *$p < 0.05$ compared to 4 μg, †$p < 0.05$ compared to 1 μg. The dotted line indicates baseline ALT levels in naïve mice. B) and C) were generated by Daniel Clattenburg.

Copy right permission letters

NATURE PUBLISHING GROUP LICENSE
TERMS AND CONDITIONS

This is a License Agreement between Simon Gebremeskel ("You") and Nature Publishing Group ("Nature Publishing Group") provided by Copyright Clearance Center ("CCC"). The license consists of your order details, the terms and conditions provided by Nature Publishing Group, and the payment terms and conditions.

License Number	4205440666461
License date	Oct 10, 2017
Licensed Content Publisher	Nature Publishing Group
Licensed Content Publication	Nature Reviews Immunology
Licensed Content Title	|[alpha]|-Galactosylceramide therapy for autoimmune diseases: prospects and obstacles
Licensed Content Author	Luc Van Kaer
Licensed Content Date	Jan 1, 2005
Licensed Content Volume	5
Licensed Content Issue	1
Type of Use	reuse in a dissertation / thesis
Requestor type	academic/educational
Format	print and electronic
Portion	figures/tables/illustrations
Number of figures/tables/illustrations	1
High-res required	no
Figures	Figure 2
Author of this NPG article	no
Your reference number	
Title of your thesis /dissertation	DEVELOPING NATURAL KILLER T CELL BASED STRATEGIES OF TARGETING POST-SURGICAL BREAST CANCER METASTASIS
Expected completion date	Apr 2018
Estimated size (number of pages)	200
Requestor Location	Dalhousie University 5850 College St, Room 7C Halifax, NS B3H4R2 Canada Attn: Simon

TERMS AND CONDITIONS FOR PERMISSIONS

Nature Publishing Group hereby grants you a non-exclusive license to reproduce this material for this purpose, and for no other use, subject to the conditions below:

1. NPG warrants that it has, to the best of its knowledge, the rights to license reuse of this material. However, you should ensure that the material you are requesting is original to Nature Publishing Group and does not carry the copyright of another entity (as credited in the published version). If the credit line on any part of the material you have requested indicates that it was reprinted or adapted by NPG with permission from another source, then you should also seek permission from that source to reuse the material.

2. Permission granted free of charge for material in print is also usually granted for any electronic version of that work, provided that the material is incidental to the work as a whole and that the electronic version is essentially equivalent to, or substitutes for, the print version. Where print permission has been granted for a fee, separate permission must be obtained for any additional, electronic re-use (unless, as in the case of a full paper, this has already been accounted for during your initial request in the calculation of a print run).NB: In all cases, web-based use of full-text articles must be authorized separately through the 'Use on a Web Site' option when requesting permission.

3. Permission granted for a first edition does not apply to second and subsequent editions and for editions in other languages (except for signatories to the STM Permissions Guidelines, or where the first edition permission was granted for free).

4. Nature Publishing Group's permission must be acknowledged next to the figure, table or abstract in print. In electronic form, this acknowledgement must be visible at the same time as the figure/table/abstract, and must be hyperlinked to the journal's homepage.

5. The credit line should read:
   Reprinted by permission from Macmillan Publishers Ltd: [JOURNAL NAME] (reference citation), copyright (year of publication)
   For AOP papers, the credit line should read:
   Reprinted by permission from Macmillan Publishers Ltd: [JOURNAL NAME], advance online publication, day month year (doi: 10.1038/sj.[JOURNAL ACRONYM].XXXXX)

   Note: For republication from the *British Journal of Cancer,* the following credit lines apply.
   Reprinted by permission from Macmillan Publishers Ltd on behalf of Cancer Research UK: [JOURNAL NAME] (reference citation), copyright (year of publication)For AOP papers, the credit line should read:

Reprinted by permission from Macmillan Publishers Ltd on behalf of Cancer Research UK: [JOURNAL NAME], advance online publication, day month year (doi: 10.1038/sj.[JOURNAL ACRONYM].XXXXX)

6. Adaptations of single figures do not require NPG approval. However, the adaptation should be credited as follows:

   Adapted by permission from Macmillan Publishers Ltd: [JOURNAL NAME] (reference citation), copyright (year of publication)

   Note: For adaptation from the *British Journal of Cancer*, the following credit line applies.
   Adapted by permission from Macmillan Publishers Ltd on behalf of Cancer Research UK: [JOURNAL NAME] (reference citation), copyright (year of publication)

7. Translations of 401 words up to a whole article require NPG approval. Please visit http://www.macmillanmedicalcommunications.com for more information. Translations of up to a 400 words do not require NPG approval. The translation should be credited as follows:

   Translated by permission from Macmillan Publishers Ltd: [JOURNAL NAME] (reference citation), copyright (year of publication).

   Note: For translation from the *British Journal of Cancer*, the following credit line applies.
   Translated by permission from Macmillan Publishers Ltd on behalf of Cancer Research UK: [JOURNAL NAME] (reference citation), copyright (year of publication)

We are certain that all parties will benefit from this agreement and wish you the best in the use of this material. Thank you.

This Agreement between Dalhousie University -- Simon Gebremeskel ("You") and Elsevier ("Elsevier") consists of your license details and the terms and conditions provided by Elsevier and Copyright Clearance Center.

License Number	4205440089080
License date	Oct 10, 2017
Licensed Content Publisher	Elsevier
Licensed Content Publication	The Lancet
Licensed Content Title	Gene expression profiling in breast cancer: classification, prognostication, and prediction
Licensed Content Author	Jorge S Reis-Filho,Lajos Pusztai
Licensed Content Date	19–25 November 2011
Licensed Content Volume	378
Licensed Content Issue	9805
Licensed Content Pages	12
Start Page	1812
End Page	1823
Type of Use	reuse in a thesis/dissertation
Portion	figures/tables/illustrations
Number of figures/tables/illustrations	1
Format	both print and electronic
Are you the author of this Elsevier article?	No
Will you be translating?	No
Original figure numbers	Table 1
Title of your thesis/dissertation	DEVELOPING NATURAL KILLER T CELL BASED STRATEGIES OF TARGETING POST-SURGICAL BREAST CANCER METASTASIS
Expected completion date	Apr 2018
Estimated size (number of pages)	200

Requestor Location	Dalhousie University 5850 College St, Room 7C Halifax, NS B3H4R2 Canada Attn: Simon

INTRODUCTION

1. The publisher for this copyrighted material is Elsevier. By clicking "accept" in connection with completing this licensing transaction, you agree that the following terms and conditions apply to this transaction (along with the Billing and Payment terms and conditions established by Copyright Clearance Center, Inc. ("CCC"), at the time that you opened your Rightslink account and that are available at any time at http://myaccount.copyright.com).

GENERAL TERMS

2. Elsevier hereby grants you permission to reproduce the aforementioned material subject to the terms and conditions indicated.

3. Acknowledgement: If any part of the material to be used (for example, figures) has appeared in our publication with credit or acknowledgement to another source, permission must also be sought from that source. If such permission is not obtained then that material may not be included in your publication/copies. Suitable acknowledgement to the source must be made, either as a footnote or in a reference list at the end of your publication, as follows:

"Reprinted from Publication title, Vol /edition number, Author(s), Title of article / title of chapter, Pages No., Copyright (Year), with permission from Elsevier [OR APPLICABLE SOCIETY COPYRIGHT OWNER]." Also Lancet special credit - "Reprinted from The Lancet, Vol. number, Author(s), Title of article, Pages No., Copyright (Year), with permission from Elsevier."

4. Reproduction of this material is confined to the purpose and/or media for which permission is hereby given.

5. Altering/Modifying Material: Not Permitted. However figures and illustrations may be altered/adapted minimally to serve your work. Any other abbreviations, additions, deletions and/or any other alterations shall be made only with prior written authorization of Elsevier Ltd. (Please contact Elsevier at permissions@elsevier.com). No modifications can be made to any Lancet figures/tables and they must be reproduced in full.

6. If the permission fee for the requested use of our material is waived in this instance, please be advised that your future requests for Elsevier materials may attract a fee.

7. Reservation of Rights: Publisher reserves all rights not specifically granted in the combination of (i) the license details provided by you and accepted in the course of this licensing transaction, (ii) these terms and conditions and (iii) CCC's Billing and Payment terms and conditions.

8. License Contingent Upon Payment: While you may exercise the rights licensed immediately upon issuance of the license at the end of the licensing process for the

transaction, provided that you have disclosed complete and accurate details of your proposed use, no license is finally effective unless and until full payment is received from you (either by publisher or by CCC) as provided in CCC's Billing and Payment terms and conditions. If full payment is not received on a timely basis, then any license preliminarily granted shall be deemed automatically revoked and shall be void as if never granted. Further, in the event that you breach any of these terms and conditions or any of CCC's Billing and Payment terms and conditions, the license is automatically revoked and shall be void as if never granted. Use of materials as described in a revoked license, as well as any use of the materials beyond the scope of an unrevoked license, may constitute copyright infringement and publisher reserves the right to take any and all action to protect its copyright in the materials.

9. Warranties: Publisher makes no representations or warranties with respect to the licensed material.

10. Indemnity: You hereby indemnify and agree to hold harmless publisher and CCC, and their respective officers, directors, employees and agents, from and against any and all claims arising out of your use of the licensed material other than as specifically authorized pursuant to this license.

11. No Transfer of License: This license is personal to you and may not be sublicensed, assigned, or transferred by you to any other person without publisher's written permission.

12. No Amendment Except in Writing: This license may not be amended except in a writing signed by both parties (or, in the case of publisher, by CCC on publisher's behalf).

13. Objection to Contrary Terms: Publisher hereby objects to any terms contained in any purchase order, acknowledgment, check endorsement or other writing prepared by you, which terms are inconsistent with these terms and conditions or CCC's Billing and Payment terms and conditions. These terms and conditions, together with CCC's Billing and Payment terms and conditions (which are incorporated herein), comprise the entire agreement between you and publisher (and CCC) concerning this licensing transaction. In the event of any conflict between your obligations established by these terms and conditions and those established by CCC's Billing and Payment terms and conditions, these terms and conditions shall control.

14. Revocation: Elsevier or Copyright Clearance Center may deny the permissions described in this License at their sole discretion, for any reason or no reason, with a full refund payable to you. Notice of such denial will be made using the contact information provided by you. Failure to receive such notice will not alter or invalidate the denial. In no event will Elsevier or Copyright Clearance Center be responsible or liable for any costs, expenses or damage incurred by you as a result of a denial of your permission request, other than a refund of the amount(s) paid by you to Elsevier and/or Copyright Clearance Center for denied permissions.

LIMITED LICENSE

The following terms and conditions apply only to specific license types:

15. **Translation**: This permission is granted for non-exclusive world **English** rights only unless your license was granted for translation rights. If you licensed translation rights you may only translate this content into the languages you requested. A professional translator must perform all translations and reproduce the content word for word preserving the integrity of the article.

16. **Posting licensed content on any Website**: The following terms and conditions apply as follows: Licensing material from an Elsevier journal: All content posted to the web site must maintain the copyright information line on the bottom of each image; A hyper-text must be included to the Homepage of the journal from which you are licensing at http://www.sciencedirect.com/science/journal/xxxxx or the Elsevier homepage for books at http://www.elsevier.com; Central Storage: This license does not include permission for a scanned version of the material to be stored in a central repository such as that provided by Heron/XanEdu.

Licensing material from an Elsevier book: A hyper-text link must be included to the Elsevier homepage at http://www.elsevier.com . All content posted to the web site must maintain the copyright information line on the bottom of each image.

Posting licensed content on Electronic reserve: In addition to the above the following clauses are applicable: The web site must be password-protected and made available only to bona fide students registered on a relevant course. This permission is granted for 1 year only. You may obtain a new license for future website posting.

17. **For journal authors:** the following clauses are applicable in addition to the above:

Preprints:

A preprint is an author's own write-up of research results and analysis, it has not been peer-reviewed, nor has it had any other value added to it by a publisher (such as formatting, copyright, technical enhancement etc.).

Authors can share their preprints anywhere at any time. Preprints should not be added to or enhanced in any way in order to appear more like, or to substitute for, the final versions of articles however authors can update their preprints on arXiv or RePEc with their Accepted Author Manuscript (see below).

If accepted for publication, we encourage authors to link from the preprint to their formal publication via its DOI. Millions of researchers have access to the formal publications on ScienceDirect, and so links will help users to find, access, cite and use the best available

version. Please note that Cell Press, The Lancet and some society-owned have different preprint policies. Information on these policies is available on the journal homepage.

Accepted Author Manuscripts: An accepted author manuscript is the manuscript of an article that has been accepted for publication and which typically includes author-incorporated changes suggested during submission, peer review and editor-author communications.

Authors can share their accepted author manuscript:

- immediately
    - via their non-commercial person homepage or blog
    - by updating a preprint in arXiv or RePEc with the accepted manuscript
    - via their research institute or institutional repository for internal institutional uses or as part of an invitation-only research collaboration work-group
    - directly by providing copies to their students or to research collaborators for their personal use
    - for private scholarly sharing as part of an invitation-only work group on commercial sites with which Elsevier has an agreement
- After the embargo period
    - via non-commercial hosting platforms such as their institutional repository
    - via commercial sites with which Elsevier has an agreement

In all cases accepted manuscripts should:

- link to the formal publication via its DOI
- bear a CC-BY-NC-ND license - this is easy to do
- if aggregated with other manuscripts, for example in a repository or other site, be shared in alignment with our hosting policy not be added to or enhanced in any way to appear more like, or to substitute for, the published journal article.

Published journal article (JPA): A published journal article (PJA) is the definitive final record of published research that appears or will appear in the journal and embodies all value-adding publishing activities including peer review co-ordination, copy-editing, formatting, (if relevant) pagination and online enrichment.

Policies for sharing publishing journal articles differ for subscription and gold open access articles:

Subscription Articles: If you are an author, please share a link to your article rather than the full-text. Millions of researchers have access to the formal publications on ScienceDirect, and so links will help your users to find, access, cite, and use the best available version.

Theses and dissertations which contain embedded PJAs as part of the formal submission can be posted publicly by the awarding institution with DOI links back to the formal publications on ScienceDirect.

If you are affiliated with a library that subscribes to ScienceDirect you have additional private sharing rights for others' research accessed under that agreement. This includes use for classroom teaching and internal training at the institution (including use in course packs and courseware programs), and inclusion of the article for grant funding purposes.

Gold Open Access Articles: May be shared according to the author-selected end-user license and should contain a CrossMark logo, the end user license, and a DOI link to the formal publication on ScienceDirect.

Please refer to Elsevier's posting policy for further information.

18. **For book authors** the following clauses are applicable in addition to the above: Authors are permitted to place a brief summary of their work online only. You are not allowed to download and post the published electronic version of your chapter, nor may you scan the printed edition to create an electronic version. **Posting to a repository:** Authors are permitted to post a summary of their chapter only in their institution's repository.

19. **Thesis/Dissertation**: If your license is for use in a thesis/dissertation your thesis may be submitted to your institution in either print or electronic form. Should your thesis be published commercially, please reapply for permission. These requirements include permission for the Library and Archives of Canada to supply single copies, on demand, of the complete thesis and include permission for Proquest/UMI to supply single copies, on demand, of the complete thesis. Should your thesis be published commercially, please reapply for permission. Theses and dissertations which contain embedded PJAs as part of the formal submission can be posted publicly by the awarding institution with DOI links back to the formal publications on ScienceDirect.

Elsevier Open Access Terms and Conditions

You can publish open access with Elsevier in hundreds of open access journals or in nearly 2000 established subscription journals that support open access publishing. Permitted third party re-use of these open access articles is defined by the author's choice of Creative Commons user license. See our open access license policy for more information.

Terms & Conditions applicable to all Open Access articles published with Elsevier:

Any reuse of the article must not represent the author as endorsing the adaptation of the article nor should the article be modified in such a way as to damage the author's honour or reputation. If any changes have been made, such changes must be clearly indicated.

Gebremeskel S and Johnston B. 2015. Concepts and mechanisms underlying chemotherapy induced immunogenic cell death: impact on clinical studies and considerations for combined therapies. *Oncotarget.* 6(39):41600-19. doi: 10.18632/oncotarget.6113.

Gebremeskel S, Slauenwhite D, Johnston B. 2016. Reconstitution models to evaluate natural killer T cell function in tumor control. *Immunology and Cell biology*. 94(1):90-100. doi: 10.1038/icb.2015.67.

Gebremeskel S, Lobert L, Tanner K, Walker B, Oliphant B, Clarke L, Dellaire G, Johnston B. Combined chemotherapy and natural killer T cell immunotherapy enhances protection from breast cancer metastasis. *Cancer immunology research.* 5 (12):1086-1097.